ABSTRACT

A number of species begin to electrodeposit on Pt and Au in the range of potentials in which H_2O is thermodynamically stable, i.e., between the electrode potentials at which H_2 and O_2 are evolved. The resulting surface bonding energies may be accurately determined as a function of coverage. Critical literature surveys of six such systems (H on Pt, O species on Pt, O species on Au, Cu on Pt, Cu on Au and Pb on Au) show that although multiple bonding energies are a general feature of the electrodeposition of sub-monolayers of foreign species, no satisfactory explanation of their origin has been proposed.

Experimental studies of these six electrodeposition systems were carried out by the potentiodynamic sweep method using solutions of highly purified salts in water purified by a new catalytic pyro-distillation method. In each system, a more detailed resolution of the sub-monolayer bonding states was achieved than in any previously reported work. About six distinct sub-monolayer bonding energies were usually observed, each exceeding that for the subsequent bulk deposition. The kinetic reversibility of the electrodeposition was limited in most systems by steps in the reaction other than the Faradaic electron-transfer itself.

In particular, the hysteresis arising in the cyclic oxidation/reduction of noble metal surfaces is associated with the development of a stable surface "oxide" by a place-exchange mechanism. The bonding of the electrodeposited OH species is somewhat polar, and the resulting dipole-dipole repulsions are relieved by the field-assisted place-

exchange of some of the OH groups with the metal atoms to which they are bound, in such a way as to form a stable, "ionically bound", two-dimensional surface "oxide".

Data obtained from the individual electrodeposition systems have been used to develop a general classification of the nature of electrodeposits as a function of coverage according to various parameters of the species involved. A detailed discussion of surface bonding in terms of the transfer of charge at electrode/solution interfaces leads to a precise distinction between Faradaic electrodeposition (UPD and OPD), specific adsorption of ions and physical adsorption of ions.

The localized (non-metallic) bonding at the substrate surface, which gives rise to the general feature of multiple states of surface bonding, does not normally persist as the deposit thickens to more than one or two atomic layers. Thus, in general, the bonding of subsequently deposited atoms will be essentially metallic. On the other hand, when the deposit and substrate have widely differing electronegativities bulk surface compounds may be formed, e.g., oxides, intermetallic compounds.

It appears that the distinct states of surface bonding observed in the early stages of electrodeposition are generally related to the bonding of the deposited species in a succession of different bonding configurations stabilized by the influence of the applied metal/solution field on the surface electronic states of the substrate. Although present theoretical wave-mechanical treatments of surface bonding do not predict discontinuous changes in bond energy with increasing coverage,

there is much evidence that gases chemisorb in a series of geometrically different surface arrays which probably involve rearrangement of the surface atoms of the substrate, and it is thought that similar mechanisms apply in electrodeposition systems.

PREFACE

The purpose of scientific research and the nature of its benefits are much misunderstood. I therefore wish to preface this thesis by echoing some remarks of Michael Faraday to a meeting of the Royal Instititution, London on 6th May 1854*:

"Before entering the subject, I must make one distinction which, however it may appear to others, is to me of the utmost importance. High as man is placed above the creatures around him, there is a higher and far more exalted position within his view; and the ways are infinite in which he occupies his thoughts about the fears, or hopes, or expectations of a future life. I believe that the truth of the future cannot be brought to his knowledge by any exertion of his mental powers, however exalted they may be; that it is made known to him by teaching other than his own, and is received through simple belief of the testimony given. Let no one suppose for an instant that the self-education I am about to commend in respect of the things of this life, extends to any consideration of the hope set before us, as if man by reasoning could find out God. It would be improper here to enter upon this subject further than to claim an absolute distinction between religious and ordinary belief. I shall be reproached with the weakness of refusing to apply those mental operations which I think good in respect of high things to the very highest. I am content to bear the reproach. Yet in earthly matters I believe that 'since the creation of the world His invisible attributes,

---

*M. Faraday, "Researches in Chemistry and Physics", Taylor and Francis, London (1859).

His eternal power and divine nature, have been clearly seen, being understood through what has been made'*; and that I have never seen anything incompatible between those things of man which can be known by the spirit of man which is within him, and those higher things concerning his future which he cannot know by that spirit."

---

*St. Paul, Letter to the Romans, chapter 1, verse 20, (0057).

ACKNOWLEDGEMENTS

The author wishes to express his sincere thanks to:

His research director, Dr. B. E. Conway, for his invaluable guidance and countless personal discussions at all stages of the work.

Dr. H. Angerstein-Kozlowska, for expert advice about experimentation and many contributions to the evaluation of the results.

Mrs. G. Czartoryska, Dr. B. Dandapani, Dr. F. C. Ho, Mr. J. Klinger and Dr. B. Tilak, for permission to quote their unpublished results.

Dr. F. G. Will of the General Electric Co., Schenectady, N.Y., for supplying three single-crystal Pt electrodes.

Dr. P. B. Sewell of the National Research Council, Ottawa, for carrying out electron diffraction structural analysis of single-crystal surfaces, and for supplying a single-crystal Pt (100) disc.

Dr. J. W. Gadzuk of the Surface Chemistry Section, National Bureau of Standards, Washington, D.C., for helpful discussions about the relevance of the present data to present theoretical treatments of chemisorption.

The Sprague Electric Co., North Adams, Mass., for the award of the University of Ottawa Sprague Fellowship in 1970.

The National Research Council of Canada, for the award of a post-graduate scholarship during the years 1971-1974.

The University of Ottawa, for other financial support through Teaching Assistantships.

Above all, to my wife Lorna, whose self-sacrifice, patience and encouragement made this work possible.

TABLE OF CONTENTS

	Page
ABSTRACT	i
PREFACE	iv
ACKNOWLEDGEMENTS	vi
TABLE OF CONTENTS	vii
1. ELECTROCHEMICAL STUDIES IN THE SURFACE SCIENCE OF MONOLAYERS	
1.1 Phenomenology and methods	1
1.2 Information available from potentiodynamic current-potential profiles	5
1.3 Adsorption of H	7
1.3.1 Adsorption of H on Pt	7
1.3.1.1 Causes of multiple bonding states	11
1.3.2 Adsorption of H on Au	22
1.4 Adsorption of O species	23
1.4.1 Adsorption of O species on Pt	23
1.4.1.1 Introduction: nature of the "oxide" layer	23
1.4.1.2 Reversible adsorption at low coverages	25
1.4.1.3 Irreversible adsorption states: characteristics and kinetics	25
1.4.1.4 Oxidation mechanisms proposed	28
1.4.1.5 Effects of added anions	31
1.4.1.6 Effects of pH	32
1.4.1.7 Effects of crystallography of the Pt surface	33
1.4.1.8 Adsorption in excess of monolayer coverage	35
1.4.1.9 Pt dissolution and precipitation during cyclic adsorption-desorption	37
1.4.2 Adsorption of O species on Au	38
1.4.2.1 Introduction: nature of the "oxide" layer	38
1.4.2.2 Reversible adsorption of O species	39
1.4.2.3 Irreversible adsorption states: characteristics and kinetics	40

1.4.2.4 Oxidation mechanisms proposed. 43
1.4.2.5 Effects of added anions 44
1.4.2.6 Effects of pH 45
1.4.2.7 Effects of crystallography of the Au surface 46
1.4.2.8 Adsorption in excess of monolayer coverage 47
1.4.2.9 Au dissolution and precipitation during cyclic adsorption-desorption 47

1.5 Adsorption of Cu 49

1.5.1 Adsorption of Cu on Pt 49

1.5.1.1 Resolution of component processes 49
1.5.1.2 Causes of multiple states of adsorption 51
1.5.1.3 The state of the electrodeposited Cu 52
1.5.1.4 Kinetics and reversibility 55
1.5.1.5 The transition from UPD to bulk Cu deposition 56
1.5.1.6 Effects of added cations 57
1.5.1.7 Effects of anions and pH 58
1.5.1.8 Production of Cu^+ during cyclic adsorption-desorption 58

1.5.2 Adsorption of Cu on Au 61

1.5.2.1 The extent of UPD 61
1.5.2.2 Resolution of component processes 62
1.5.2.3 State of the deposit 63
1.5.2.4 Reaction mechanisms proposed 63
1.5.2.5 Kinetics and reversibility 64
1.5.2.6 Effects of competing adsorbates 65

1.6 Adsorption of Pb 65

1.6.1 Adsorption of Pb on Au 65

1.6.1.1 The extent of UPD 65
1.6.1.2 Resolution of component processes 67
1.6.1.3 The state of the deposit 68
1.6.1.4 Reaction mechanisms proposed 68
1.6.1.5 Kinetics and reversibility 70
1.6.1.6 Effects of crystallography of the Au surface 71
1.6.1.7 Effects of competing adsorbates 71
1.6.1.8 Surface rearrangement processes (alloy formation) 72

2. THE NATURE OF CHEMISORPTION ON METALS 73

2.1 Distinction between chemisorption and physical adsorption 73

2.2 Chemisorption treated as bonding to an isolated surface atom 76

2.2.1 Covalent bonding 76

2.2.2 Ionic bonding 78

2.2.3 Metallic bonding (classical treatment) 81

2.3 Chemisorption treated as bonding to a number of interacting substrate atoms 82

2.3.1 Introduction 82

2.3.1.1 Bonding in metals 82
2.3.1.2 Bonding on foreign atoms within alloys 85
2.3.1.3 Formation of surface states on bare metals 93

2.3.2 "One-orbital" wave-mechanical models of chemisorption 97

2.3.3 "Many orbital" wave mechanical models of chemisorption 102

2.3.3.1 Extensions of "one-orbital" models 103
2.3.3.2 Ligand field MO theories of chemisorption 107
2.3.3.3 "Giant molecule" treatments of chemisorption 111

2.4 Summary 112

3. SUMMARY OF AIMS OF THE PRESENT WORK 114

4. EXPERIMENTAL PROCEDURES 117

4.1 Electrodes 117

4.2 Electrolyte solutions 120

4.2.1 Acids 120
4.2.2 Salts 120
4.2.3 Water 121

4.3 Experimental cells 125

4.3.1 Cleaning procedures 126
4.3.2 Temperature control 126

4.4 Electrical circuitry 127

4.5 Estimation of electrode areas 128

5. THE ELECTRODEPOSITION OF H ON Pt 130

5.1 Results 130

5.1.1 Introduction 130
5.1.2 Effects of crystallography of the electrod surface 131

5.1.3 Small differences between anodic and cathodic current-potential profiles 133
5.1.4 Effects of pH 134
5.1.5 Variation of the UPD charge with temperature 138
5.1.6 Effects of adsorbed ions 141
5.1.7 Kinetics and reversibility 142

5.2 Preliminary discussion 145
5.2.1 Effects of specifically adsorbed ions 145
5.2.2 Effects of pH 149
5.2.3 The UPD charge and the H_2 evolution reaction 150
5.2.4 Occurrence of multiple bonding states 151

6. THE ELECTRODEPOSITION OF O SPECIES ON Pt 156

6.1 Results 156
6.1.1 Introduction 156
6.1.2 Effects of surface crystallography 158
6.1.3 Reversibility and hysteresis 159
6.1.4 Effects of specifically adsorbed ions and of pH 162
6.1.5 Reconstruction of the Pt surface 164
6.2 Preliminary discussion 166
6.2.1 Origin of multiple bonding energies in anodic deposition of O species 166
6.2.2 The secondary processes 171
6.2.3 Effects of anions and of pH 174
6.2.4 Dissolution-redeposition and surface reconstruction 177

7. ELECTRODEPOSITION OF O SPECIES ON Au 180

7.1 Results 180
7.1.1 General features of the current-potential profile 180
7.1.2 Calculation of the coverage by O species 181
7.1.3 Hysteresis in the current-potential profile 183
7.1.4 Effects of the presence of HSO_4^-, SO_4^{2-} and NO_3^- 188
7.2 Preliminary discussion 190
7.2.1 Origin of multiple anodic states 190
7.2.2 Place-exchange 192

7.2.3 Significance of the states resolved in the cathodic reduction of O species 196

7.2.3.1 Summary of reaction scheme for the surface oxidation and reduction processes 200

7.2.4 The coverage at which O_2 evolution begins 201

7.2.5 Influence of specifically adsorbed anions 204

8. THE ELECTRODEPOSITION OF Cu ON Pt 205

8.1 Results 205

8.1.1 Calculation of Cu coverages 205

8.1.2 General features of UPD of Cu 205

8.1.3 Cathodic processes 207

8.1.4 Deposition of bulk Cu 208

8.1.5 Anodic processes 208

8.1.6 Effects of specifically adsorbed anions 209

8.1.7 Relationship between deposition of Cu and states of co-deposited H 210

8.2 Preliminary discussion 211

8.2.1 The component processes 211

8.2.2 Relationship of the cathodic current-potential profile to kinetics of discharge of Cu^{2+} ions 212

8.2.3 Deposition at "coverages" exceeding $\theta_{Cu} = 1$ 215

8.2.4 Alloying 217

8.2.5 Effects of competing adsorbates on the bonding of Cu 218

8.2.6 Effects of electrodeposited Cu atoms on the bonding of H 218

9. THE ELECTRODEPOSITION OF Cu ON Au 220

9.1 Results 220

9.1.1 Determination of Cu coverage 220

9.1.2 General features of the potentiodynamic current-potential profile 220

9.1.3 The slow step in the discharge reaction 222

9.1.4 Effects of specifically adsorbed anions 225

9.2 Preliminary discussion 225

9.2.1 The mechanism of electrodeposition 225

9.2.2 Hysteresis and alloying 226

10. THE ELECTRODEPOSITION OF Pb ON Au 230

10.1 Results 230

10.1.1 Calculation of Pb coverages 230

10.1.2 General observations 231

10.1.3 Reversibility 232

10.1.4 The bonding state Pb_5 233

10.2 Preliminary discussion 234

10.2.1 Reversibility and place-exchange 234

10.2.2 Accurate measurement of Pb coverage 236

10.2.3 Epitaxy in Pb deposition 238

10.2.4 Significance of the chemisorption state Pb_5 242

11. GENERAL DISCUSSION 244

11.1 Common features of the electrodeposition systems studied 244

11.2 The origin and significance of multiple states of bonding in UPD 246

11.2.1 Intrinsic heterogeneity of substrate due to polycrystallinity 246

11.2.2 Desorption of anions or other adsorbates 247

11.2.3 Formation of a series of surface compounds similar to bulk compounds 248

11.2.3.1 Oxides 248

11.2.3.2 Intermetallics 249

11.2.4 Repulsive interactions between electro-deposited species 249

11.2.5 Modification of the electronic properties of the substrate associated with UPD 250

11.2.5.1 Localization of states for polar bonding 250

11.2.5.2 Ligand field effects; use of a series of hybrid bonding orbitals 251

11.2.5.3 Formation of surface superlattice arrays; reactive reconstruction of substrate surface 253

11.2.6 Summary 255

11.3 Significance of the similarity of current-potential profiles for UPD of different atoms at a single substrate 256

11.4 Modification of the UPD states by specific adsorption and by the UPD of other species 258

11.5 The distinction between Faradaic electrodeposition and specific adsorption 260

11.5.1 The electrical character of chemisorbed species at electrodes 260

11.5.2 Relationship between chemisorption of atoms and ions and ligand-metal interaction 264

11.5.3 Summary of characteristics of different types of surface bonding 265

11.6 Classification of the processes involved in Faradaic electrodeposition 268

11.6.1 Epitaxy in UPD 268

11.6.2 Significance of the coverage at which OPD begins 269

11.6.3 Processes following UPD 271

11.6.3.1 Place-exchange 271
11.6.3.2 Alloying 273

11.7 The usefulness of electrochemical data in the understanding of surface bonding 274

12. REFERENCES 275

CHAPTER 1

ELECTROCHEMICAL STUDIES IN THE SURFACE SCIENCE OF MONOLAYERS

1.1 Phenomenology and methods

This thesis is concerned with the resolution and significance of multiple states of chemisorption which are observed when $H^{\dagger}$, O, and metal species are electrodeposited on metal substrates. A fundamental understanding of the adsorption* mechanisms involved is of immediate relevance in electrochemistry and surface chemistry, and may be applied in catalysis, electrodeposition and corrosion-resistance.

The nature of a metal surface immersed in an electrolyte depends crictically on its electric potential and the solution composition. Under almost all conditions, the electrode has residing on its surface a layer of species from the solution, which may be physically adsorbed or chemisorbed. Chemisorption can lead to the formation of a surface phase either chemically or electrochemically; in the latter case electrons are produced or consumed in the reaction. The development of instrumentation, particularly in the last 20 years[1], has allowed much greater understanding of the thermodynamics, kinetics and mechanisms of electrode reactions, especially those reactions producing

---

†Chemical symbols will be used in this thesis simply as abbreviations, with no implication that the species is in an atomic state.

*The word "adsorbed" will be used to describe particles which are in any way bound to a surface without causing a disruption of the substrate lattice to form ordered structures with properties analogous to those of bulk compounds of the adsorbate and substrate elements. We shall be much concerned with the various mechanisms which can give rise to adsorption, and how adsorption can ultimately lead to the formation of ordered surface structures.

very thin surface layers.

The earliest electrochemical studies[2,3] were made by connecting two electrodes to the terminals of a battery and studying the effect of the passage of current on the solution. Although the charge passed could be measured with considerable accuracy[4] by means of coulometry, the lack of control of either potential or current at the (working) electrode prevented a thorough understanding of the processes taking place. Studies in which the reaction current was controlled were first carried out by Bowden and Rideal in 1928[5], using the so-called galvanostatic method. In its simplest form the galvanostat is a powerful battery connected to the electrodes through a resistance substantially greater than the cell resistance. The discharge of the battery is thus controlled by the external resistance, and the current is not affected by processes going on in the cell. The characteristic free energy of each reaction occurring at the electrode has a corresponding reversible electrode potential. Thus the shape of the potential-time curve from a galvanostatic experiment gives an indication of the succession of reactions occurring as the potential changes. Partial arrests in the curves correspond to the predominance of single reactions and/or a non-uniform double-layer capacitance[1].

Considerably better resolution of multiple electrode processes is possible by controlling the electrode potential[6-9] rather than the cell current, e.g., as in the case of passivation processes[10]. In many cases, surface reactions involve the formation of adsorbed intermediates which stifle the reaction after only very small amounts of charge have been passed, so that the steady-state currents are zero.

Such reactions are most conveniently studied by the potentiodynamic sweep method[11,12] where a controlling potentiostat sweeps the potential of the working electrode through a prearranged, time-dependent programme, and the resulting time- (and hence potential-) dependent currents are followed as a function of potential. Under conditions where continuous Faradaic surface reactions do not occur, diffusion-controlled currents, identified by their sensitivity to solution stirring, may generally be attributed to the reaction of solution impurities at the electrode surface. In the study of adsorption processes at electrodes, the concentration of reactants is usually kept sufficiently high to avoid the complications which arise from diffusion-controlled reaction rates.

Having chosen the experimental conditions to avoid bulk Faradaic processes, it is usually found that the electrode current passes through a series of maxima during a potential sweep. These current peaks show that the number of particles which may be adsorbed or desorbed in a reaction is limited; otherwise the current would increase exponentially with potential. The number of adsorption sites may be limited either by the available area of the electrode surface or because of electronic factors which limit the availability of bonding states. Both types of limitation will be discussed in detail as this thesis proceeds.

The sweep rate dependence of the current peak potentials gives a measure of the reversibility of the reactions, which may also be investigated by a.c. pseudocapacitance studies[13]. If it may be assumed that the reactions occur uniformly across the electrode surface, the amount of charge passed will give a measure of the surface coverage by the reacting species.

The relative merits of potentiostatic and galvanostatic methods in the study of surface reactions have been widely discussed[e.g.,1,14]. The potentiostat is particularly useful in that it allows the selective study of individual surface reactions according either to their reversible potentials, or to the overpotentials required for the passage of significant currents (10^{-5}—10^{-3} A cm^{-2}), and in that it can be used dynamically to give information about reaction kinetics[15] by means of relaxation studies.

The form in which potentiodynamic data are obtained is illustrated by Fig. 1 which is the current-potential profile for a Pt foil electrode cycled between 0.02 and 1.57 V* at a uniform rate of 0.05 V s^{-1}. Within the potential range 0.05 to 1.4 the currents decay rapidly to zero if the electrode potential is held constant, i.e., no continuous Faradaic surface processes occur. The currents observed are the sum of components from the Faradaic electrodeposition or electrodissolution of surface species (self-stifling reactions in this system) and the non-Faradaic double-layer charging currents which rearrange the ions and molecules in the interphase adjacent to the electrode surface so as to achieve the equilibrium configuration at the potential concerned.

As the electrode potential moves cathodically from 0.5 V, H is electrodeposited on the Pt with several distinct adsorption energies. As the sweep reaches potentials less positive than about 0.07 V, Faradaic currents (non-zero at constant potential) due to the electrolysis of the solution to form molecular H_2 are

*Unless otherwise stated, all potentials in this thesis are quoted in the European convention with respect to a reversible H^+/H_2 electrode in the same solution.

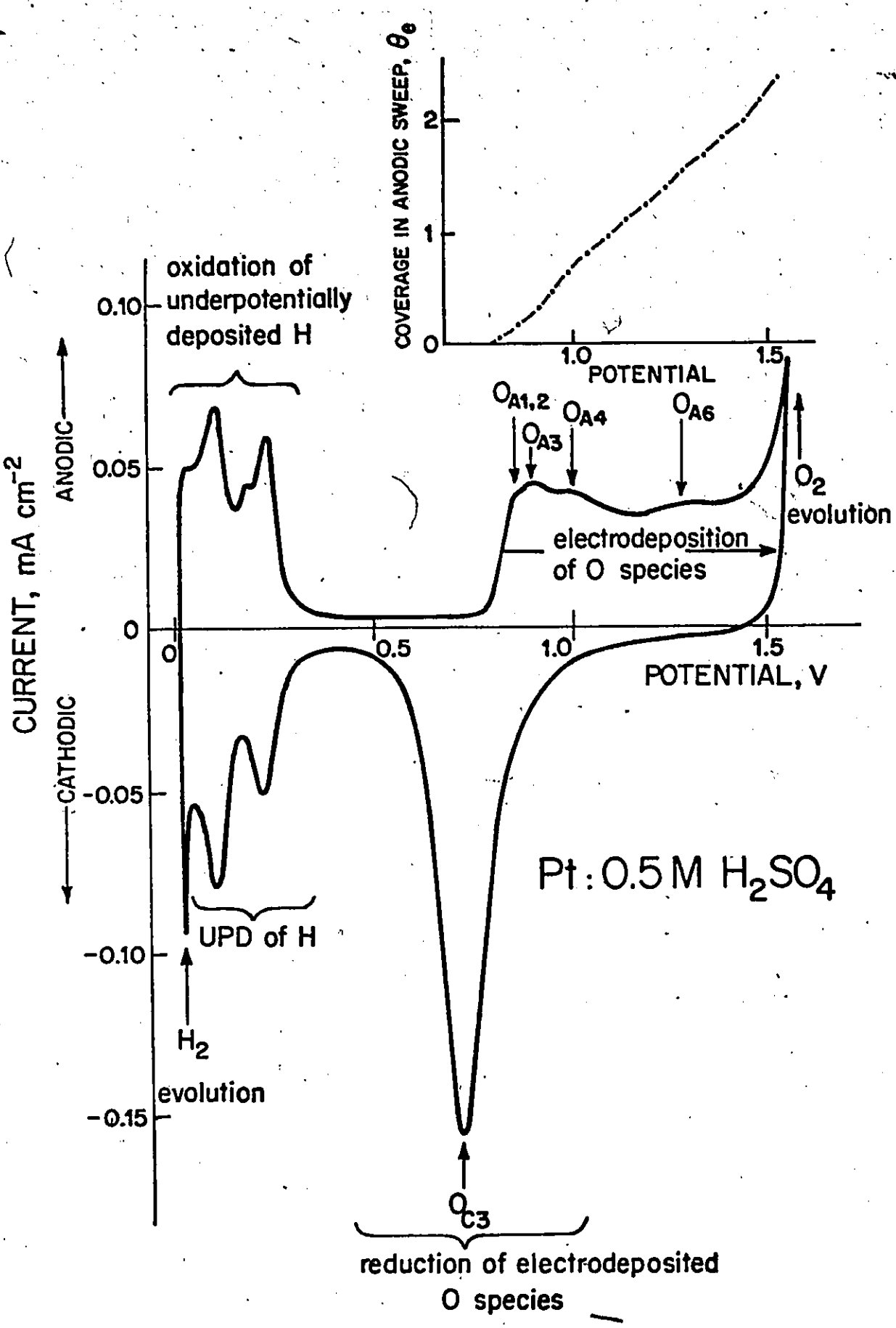

FIG. 1. TYPICAL POTENTIODYNAMIC CURRENT-POTENTIAL PROFILE AT Pt IN ACID SOLUTION ($s=0.05\ V\ s^{-1}$)

observed. After the potential sweep has reversed its direction, the adsorbed H is ionized from the surface, again in a series of distinct energies. There follows a potential region in which only the double-layer charging currents are seen, before the electrodeposition of O-containing species at a series of distinguishable energies, and the evolution of O_2. The electrodeposited O-species are all reduced from an apparently single bonding state after the reversal of the potential sweep at 1.57 V, leaving the Pt surface free of Faradaically adsorbed surface species before the commencement of the next potentiodynamic cycle.

The existence of multiple states of adsorption, such as those in Fig. 1, is now established in many systems. Early studies in this field were frequently irreproducible and conflicting, but the application of consistent high purity experimental conditions has produced major advances in the knowledge of the "spectra" of surface reaction energies. The type of information available from potentiodynamic sweep data will now be discussed as an introduction to reviews of the present state of knowledge in the adsorption systems chosen for study in this work. These detailed reviews will provide a basis for discussing the results obtained, and subsequently developing a more general model of adsorption on noble metal surfaces.

1.2 Information available from potentiodynamic current-voltage profiles

The number, size and shape of the peaks in current density-potential profiles obtained in potentiodynamic sweeps provide important information about the nature of the adsorption-desorption reactions occurring. If the supply of reactants is diffusion-limited the peak

currents will vary with the square root of the sweep rate; if there is no diffusion limitation the peak currents will be directly proportional to the sweep rate. This linear relationship is thus an identification of reversible Faradaic surface reactions.

A number of authors have calculated the current-potential profiles which would arise in simple reversible and irreversible surface reactions, and investigated the effects of various thermodynamic parameters of the systems concerned[16-23]. Unfortunately the main effort has been put into theoretical analyses of single-electron discharge processes leading to the formation of a single monolayer* of adsorbed species at the electrode. The electrochemical surface reactions of particular interest however generally exhibit several peaks in the current-potential profile at sub-monolayer coverages, and these usually overlap too much to allow accurate separation of the individual isotherms corresponding to the component adsorption processes. Current-potential profiles showing two peaks have been derived theoretically by Hale and Greef[19], but the empirical polynomial relating adsorption energy to coverage required to obtain the double peak is not based on any experimental parameters of adsorption systems.

The experiments described later in this thesis will show that when a current-potential profile can be separated into a sequence of adsorption isotherms, the reversibility of the successive processes may be judged from the shapes of the component peaks, and the extent of interactions between the adsorbed species from the half-widths of the

*The coverage of an adsorbed species will be expressed in this thesis in terms of the ratio of the number of adsorbed particles to the number of atoms in the electrode surface. Thus a coverage of $\theta = 1$ represents one monolayer of adsorbed species.

peaks. Isotherms involving interactions have been computed by the introduction of a parameter, g, in the adsorption equation[16]:

$$\frac{\theta}{(1-\theta)} \exp(g\theta) = Kc \exp(\frac{VF}{RT})$$

In the absence of interactions (i.e. under Langmuir conditions) the half-width corresponding to a reversible reaction is 90.6 mV[16,23]; if the reaction is irreversible it is 126 mV[23,24]. Repulsive interactions (g+ve) increase the half-width and attractive interactions decrease it, as shown in Fig. 2.

1.3 Adsorption of H

1.3.1 Adsorption of H on Pt

The first studies on the mechanisms of the electrodeposition of metals raised the question about a century ago of whether H at the metal surface, evidenced by the H_2 evolution reaction, was playing some part in the electrodeposition process. With the development of the galvanostatic method, Bowden and Rideal followed up earlier studies showing the electrodeposition began at potentials anodic to the bulk metal deposition potential[4,25], and began a series of studies on thin film electrodeposition with a study of H adsorption[26]. It is now a matter of history that the reactions of H at metal surfaces, in particular the H_2 evolution reaction, turned out to be of such interest to electrochemists that the mechanisms of thin film metal deposition were almost completely neglected for nearly 40 years, with the consequence that the technology of electroplating has developed largely on an empirical basis.

Knobel concluded in 1924 from the results of studies using galvanostatic pulses that adsorbed H on Pt was in an atomic state[27].

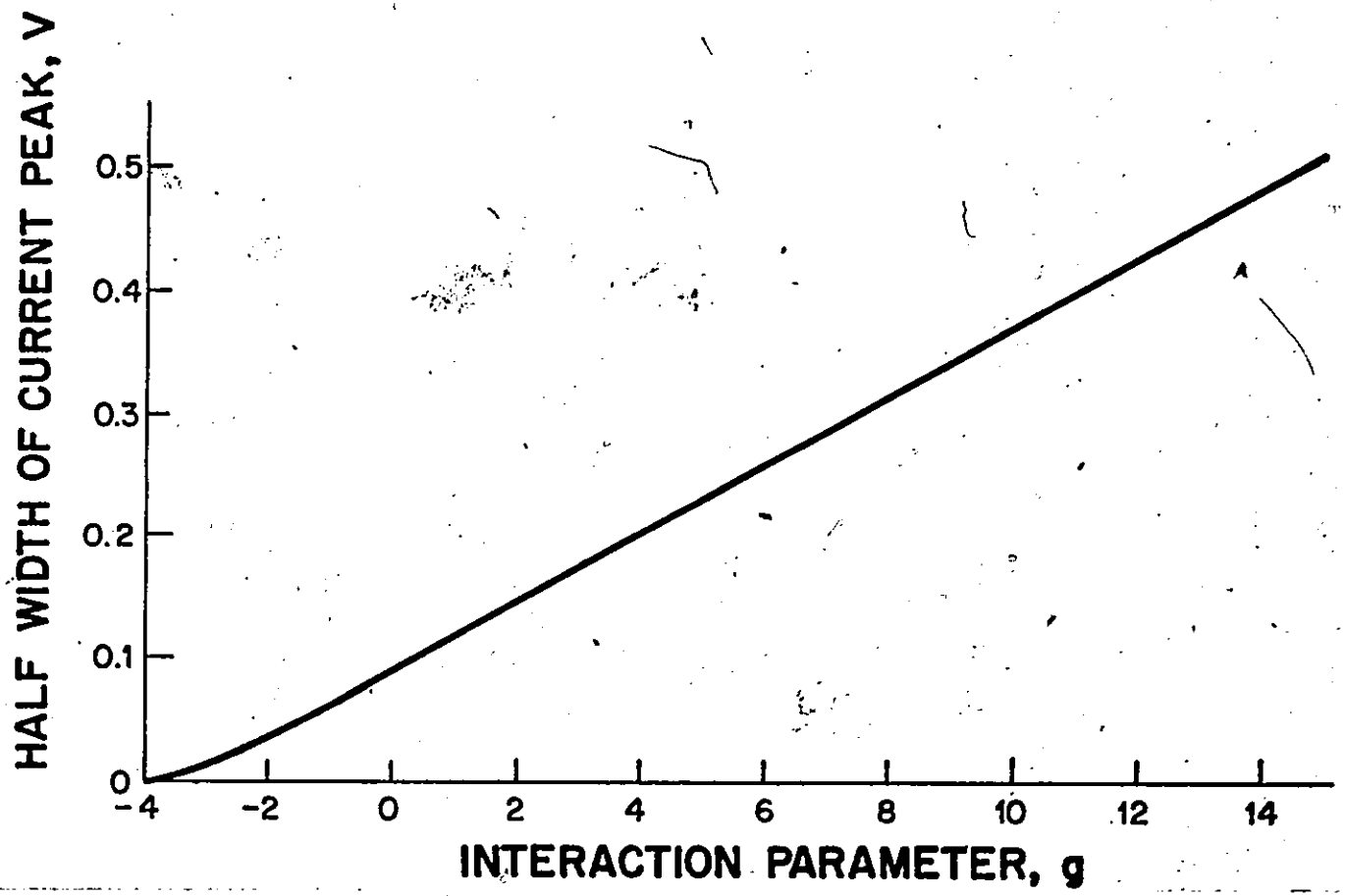

FIG. 2. DEPENDENCE OF HALF-WIDTH OF POTENTIODYNAMIC CURRENT PEAK FOR A REVERSIBLE ONE-ELECTRON SURFACE REACTION ON THE INTERACTION BETWEEN ADSORBED SPECIES

(This has more recently been confirmed by calorimetric studies of partial molar enthalpy[28]). Bowden then suggested[29] and later proved[30], see also 31 that on this basis the number of H atoms deposited at underpotential compared to the H_2 evolution potential would equal the number of Pt atoms in the surface of the electrode. His result has been verified by the use of BET techniques[32]. Thus the total charge passed in the underpotential deposition of H gives a useful in situ measurement of the actual surface area of a Pt electrode[33,34].

There is conflicting evidence as to whether the amount of H underpotentially deposited on Pt increases[35,36], decreases[37], or remains constant[38,39] with temperature. Decreases may simply be associated with the increased diffusion and adsorption of solution impurities at higher temperatures, while increases on Pt platinized at low temperature have been related to the existence of surface cracks and pores which would only become available for H adsorption at high temperatures and/or higher potentials[35,39]. Woods[40] has pointed out that lowering the temperature increases the potential range of underpotential deposition (UPD), allowing a more accurate measurement of the UPD charge independently of charge arising from H_2 evolution. His results agree well with surface area data obtained by pseudocapacitance measurements[41-43].

The increasing availability of sophisticated instrumentation in recent years has led to a flood of publications dealing with the adsorption of H on Pt[e.g.44-55]. The results obtained are however, frequently conflicting, largely because of insufficient control of the purity of the reagents[56-59], although it was noted as early as 1895 that "the amount of H absorbed (sic) by Pt is very largely influenced by slight traces of impurity, probably grease and other matter"[60].

A.c. studies of the pseudocapacitance associated with the deposition and removal of H[61,62], involving the method of Dolin and Ershler[13], show two maxima over a wide range of frequencies. In fact, even the early charging curves of Frumkin and Slygin[63] suggested that adsorbed H was ionized from Pt electrodes in two or three stages, but this aspect of the data was not discussed at the time. Polarographic[64] and potentiodynamic[12,38,65] studies have since confirmed that H is adsorbed and desorbed very rapidly with (at least) two distinct bonding energies, both in aqueous solutions and in molten salts[66]. These electrochemical data are confirmed by work function measurements[67] and field emission microscopy[68,69] showing (at least) two distinct adsorption states. Temperature-controlled desorption has resolved four states of adsorbed H on Pt, but two of these were reported to be molecular[70]. The results of Kubokawa, Takashima and Toyama[71] suggest that desorption from these two main bonding states into the gas phase requires activation energies of about 10 and 23 kcal mole^{-1}, respectively. The energy for the strongly bound state agrees well with the value obtained by U.H.V. calorimetry[72] (24.7 kcal mole^{-1}) and Trasatti's[73] theoretical value of 26 kcal mole^{-1}.

Two other adsorption states for H on Pt have been found in addition to the two dominant ones. Loučka and Weber[74] and subsequently other workers[52,75] noted the presence of a separate strongly-bound state at the lowest coverages, with a corresponding reversible potential of about 0.31 V. The existence of this peak is in fact visible in the earliest potentiodynamic sweep data[12]. There is also a small anodic peak with an energy between those of the main states, again visible in Will and Knorr's early data[12] but not discussed at that stage.

The finest resolution of multiple states of H adsorption has been obtained in gas phase adsorption studies on W[76]. Equilibrium isotherm measurements, flash desorption and LEED studies from a number of laboratories show a multiplicity of reproducible surface bonding energies. The selection of these energies observed varies slightly according to the crystallography of the substrate W, possibly because the adsorption energy depends on the local coordination of adsorbate particles by surface atoms.

The lack of resolution of the component states in H adsorption on Pt obtainable by galvanostatic methods hampered early attempts to fit the data to established isotherms. Bowden and Rideal[26], attempting to interpret the adsorption as a single process, suggested that the fall in heat of adsorption with coverage could be accounted for by the adsorbed species having a net dipole moment. When potentiostatic methods showed that two adsorption states were predominant in strong acid solutions, Breiter reported that both could be represented by Langmuir isotherms[77] c.f.[61]. His subsequent work showed that the Frumkin isotherm[78] would be a better fit for the data in the wider temperature range 273-343 K[79], since the heat of adsorption in both states fell more rapidly with increasing coverage than would be predicted by the Langmuir isotherm, i.e., there was an attractive interaction between adsorbate particles occupying the same state. More recently Bonnemay et al.[80] concluded that neither isotherm gave a satisfactory fit and that only an intrinsic heterogeneity model involving different adsorption energies at different crystal sites could explain the data.

1.3.1.1 Causes of multiple bonding states

The four types of mechanisms which have been suggested to account for multiple bonding states of H on Pt will now be reviewed.

(i) Adsorption of other species

Bagotskii et al.[81] concluded from the absence of the small peak between the two predominant H adsorption states in fast potentiodynamic sweeps that it appeared in the results of other workers as a result of the adsorption of "anions and other microimpurities". There is no doubt that competing adsorbates can change the adsorption characteristics of H on Pt, and the associated thermodynamic relationships have been developed by Frumkin and his co-workers[82-85]. To answer the question of whether competing adsorbates can create new adsorption states, the effects of anions, cations, neutral species and solution pH will now be discussed in turn.

(a) Effects of anions

The potential of zero charge of Pt lies within the potential region of H adsorption in acid solution, and depends not only on the pH but also on the anions present, changing from 0.18 V with $(Na^+)SO_4^{2-}$ and F^- to 0.14 V with Cl^-, 0.04 V with Br^- and $\sim$ -0.5 V with I^- [86]. The bonding of H at a given coverage is weakened by anions in the order $I^- > Br^- > Cl^- > SO_4^{2-} > ClO_4^- > OH$[65]. Early results suggested that halide ions could completely prevent the underpotential deposition of H[87,88], but careful experimentation by Bagotskii et al.[89] showed that only I^- decreases the amount of H deposited at underpotential. The other anions only decrease the bonding energy for H and its distribution

among the various states[89,90], since they reach zero coverage at potentials above 0.0 V[91,92]. In alkaline solutions however, where the potentials for H adsorption are more negative with respect to the p.z.c., even I^- is fully desorbed before the H_2 evolution potential is reached, so that a full monolayer of H may be deposited at underpotential[92]. Balashova and Kazarinov suggest that the state of adsorbed anions becomes more atomic and less ionic after long adsorption times or at higher potentials[86]. This is believed to be a result of chemisorption involving partial charge transfer[86]; a matter which will be discussed further later in the thesis.

(b) Effects of cations

Cations decrease the amount of H adsorbed on Pt at potentials near the p.z.c. in the order $Tl^+ > Ba^{2+} > Ca^{2+} > Cd^{2+}$, and this appears as a redistribution of bonding energies among the adsorbed H species. Higher concentrations of Tl^+ species however, reduce the total amount of H deposited at underpotential, and remove the resolution of the component energy states[94]. The Tl is thought to be adsorbed in a state "close to atomic"[94], and presumably acts simply by blocking the access of H species to the electrode. Matsuda and Notoya have suggested that alkali metal ions can also be adsorbed in the atomic state on Pt[95], and there is some evidence[96] that adsorbed cations are displaced by H at rates which increase with the bonding energy of the cation.

An intriguing practical application of the modification of the adsorption states of H on Pt by added cations has recently been reported by Sokoloskii and Anchevskaya[97]. These authors noted that the

triple bond in dimethylethynylcarbinol or the double bond in its reduction product could be selectively hydrogenated according to the proportion of "weakly" and "strongly" bound H on the Pt black catalyst, this ratio being controlled by the addition of alkali metal cations.

(c) Effects of pH

Breiter and Kennel[65] noted that the heat of adsorption of H at a given coverage increases with pH. This observation has been quantified by proton NMR relaxation studies showing that the H-Pt bond energy increases from about 4 kcal $mole^{-1}$ in 0.5 M H_2SO_4 to about 9 kcal $mole^{-1}$ in 0.5 M NaOH[98]. The only mechanistic interpretations of pH effects[92,99] have been in terms of the Frumkin model of H adsorption in two states of opposite dipole moment[82]. Increasing the pH was said to stabilize the strongly bound state (negative charge of H dipoles facing solution) in preference to the weakly bound state (positive charge outward).

The "spectrum" of bonding energies of H on Pt revealed by potentiodynamic studies is quite different in alkaline solutions to that in acids. Vielstich[100] was apparently the first to observe the decreased reversibility of H adsorption in the two predominant states observed in alkaline solutions. This irreversibility was confirmed by other data obtained at faster sweep rates[101-103]. At sweep rates of several volts per second and above the H is apparently deposited in a single energy state but desorbed in two distinct peaks.

(d) Effects of adsorbed neutral species

The amount of H which can be deposited at underpotential falls below a monolayer in the most concentrated H_2SO_4 solutions, probably because of surface blocking by adsorbed H_2SO_4 molecules[75]. Chemisorbed organic molecules can also reduce the U P D of H as well as change the distribution of bonding energies among the adsorbed species[104,105].

(e) Summary

There is no doubt that the coadsorption of other species can alter the bonding states available to H on Pt and in some cases reduce the amount that can be bound at underpotential. Although the adsorption of anions at potentials above the p.z.c. and cations below it could conceivably account for the two predominant adsorption states, there is no evidence of discontinuous desorption of competing adsorbates which could account for discontinuous adsorption of H in a series of distinct states.

(ii) Molecular H_2

The appearance of the small peak between the two predominant H desorption peaks in acid solution was ascribed by Breiter[106] partly to the oxidation of molecular H_2, as well as to the ionization of H diffusing up to the substrate surface after previous dissolution. Other authors have identified a very cathodic peak in the potentiodynamic profile with the oxidation of adsorbed molecular H_2[107,108] although the H_2 is more likely arriving at the electrode surface by diffusion from the solution. In molten salt solutions[66,109] the

formation and oxidation of molecular H_2 are thought to make major contributions to the currents in the H adsorption peaks. Although the cathodic evolution of molecular H_2 will clearly cause associated anodic currents from the oxidation of molecular H_2 diffusing back from the solution, forming new Faradaic current peaks or adding to those from the adsorption states; there is no real evidence that H adsorption states observed in the absence of continuous Faradaic currents owe their existence to the presence of molecular H_2.

(iii) Intrinsic heterogeneity:adsorption on different single-crystal planes

The idea that the multiple bonding states of H on Pt might simply arise from adsorption on a multiplicity of crystal planes lead Will[110] to compare the potentiodynamic current-potential profiles of the three principal index planes of Pt single-crystals. Although each crystal exhibited both main peaks and the small peak between them, Will maintained that each peak was associated with adsorption on one principal index plane. Bagotskii, Vassiliev and Pyshnograeva repeated and extended this work[81]. Evaluating similar data, they concluded that although the potentiodynamic sweep profile was slightly modified by the surface crystallography, the latter did not give rise to individual peaks.

The validity of all results obtained on "single-crystal" surfaces has been questioned by Biegler[111]. He suggested that the experimental method used (potentiodynamic sweeps) would itself dissolve and rearrange the surface (see Section 1.4.1), producing facets of other

crystallinities than that for which the crystal was cut. This may relate to Will's observation[110] that both the apparent electrode area and the relative peak heights changed as a freshly cut Pt face underwent cyclic voltammetry, although such an effect could also have been caused by the removal of impurities.

(iv) Intrinsic heterogeneity:other surface structural factors

Biegler[111] has suggested that the most strongly bound state of H adsorption, first reported by Loučka and Weber[74], arises from unidentified surface structural factors. He showed that the charge distribution amongst the other peaks was sensitive to the electrode pretreatment even under apparently "clean" conditions. There were significant differences between the current-potential profiles obtained on Pt wires and foils which he attributed to crystallographic differences arising from the metal-forming processes. Effects from cold-working the electrode, however, only persisted for three potentiodynamic cycles and were thought to relate to a crystallographically disturbed surface layer, removed by potential cycling. This confirmed the earlier work of Bagotskii, Vassiliev and Pyshnograeva[81] showing that neither preliminary cold work nor lattice defects developed during the experiment by twisting or stretching the Pt affect its adsorption properties. Thus although unsaturated valencies at surface defects may affect adsorption processes and may indeed create surface bonding sites of new energies, they exist in such relatively small numbers as to have a negligible effect on the overall process. Bagotskii et al.[81] concluded that the distribution of adsorption energies is determined not primarily by surface structural factors, but by the "electronic properties" of Pt.

(v) Intrinsic heterogeneity:local coordination of the adsorbate

There is a widespread assumption that the bond strength available at an adsorption site will increase with the number of unsaturated bonds in the surface of the substrate[68,76]. Thus adsorption between a group of surface atoms would be expected to be stronger than on top of a single atom. (The basis of such theories will be examined critically in Section 2.3). This model has been used to explain the strongly bound[70,112] and weakly bound[70,112,113] H species found in temperature-controlled desorption of H[70] and in IR studies[112,113].

Bond has proposed a model of adsorption on group VIII metals[114], based on the assumption that the positions of surface atomic orbitals may be calculated from bulk crystal theory, and that adsorption sites will occur where these orbitals overlap. The model has since been developed by Shopov et al.[115]. Bond pointed out the applicability of his model to the adsorption of H on Pt[116], and Weinberg and Merrill found that it would predict two chemisorbed and one physically adsorbed state for H on Pt(111)[117]. They concluded that the more weakly bound chemisorbed state corresponded to the adsorption of molecular H_2. Bronoël and Pesant tested Bond's theory by electrochemical experiments on single-crystal Pt[108]. Measuring adsorbed atomic H by a potentiodynamic sweep and supposedly "adsorbed molecular H_2" by a sweep after strong cathodic polarization they found reasonable agreement with the predicted values, and concluded that the adsorption of molecular H_2 was much slower than that of atomic H. These conclusions on the mechanism of H adsorption are probably erroneous, as the authors were almost certainly measuring the diffusion-controlled oxidation of cathodically-generated H_2, rather than the desorption of H_2.

The validity of Bond's and Shopov's assumption that emerging e_g orbitals provide adsorption sites is questioned by the work of Fassaert, Verbeek and Van der Avoird[118]. Their calculations, which involve all the 3d orbitals on a 13-atom cluster, show no indication that these particular orbitals play an important part in the bonding. On the contrary, the most important orbital for surface bonding was found to be that pointing perpendiculary out of the surface, which would not appear at all in Bond's model for the (111) plane. However, Fassaert et al.[118] returned to the general conclusion that the adsorption energy is primarily dependent on the local coordination of the adsorbate.

A variant on this type of mechanism suggests that the adsorbed species may move physically from one adsorption site to another of a different energy. For example, Podlovchenko and Petukhova[119] observed the small H desorption peak between the predominant states using smooth Pt electrodes, although their colleagues using platinized Pt did not, and concluded that the appearance of the peak was determined by structural factors in the electrode which controlled either the surface diffusion and "reorientation" of adsorbed H, or the partial dissolution of adsorbed H into the crystal[120]. There is conflicting evidence about the possibility of surface migration from one state to another. Norton and Richards[121] describe the weakly-bound state as a necessary precursor to the strongly-bound state, but Tsuchiya et al.[70] concluded from temperature-controlled desorption that the different states did not arise from surface migration of previously adsorbed species. Mechanisms involving the physical movement of adsorbed species between sites are difficult to justify thermodynamically, since the supply of <u>increasing</u>

"driving force", e.g., during a cathodic sweep, results in the adsorbate moving to a more weakly bound state.

Such direct experimental evidence as is available does not confirm the importance of local coordination. LEED studies of adsorption of H from the gas phase show that ordered structures only appear at high temperatures[122,123]. Direct observation by field desorption spectrometry suggests that H is adsorbed at random interstitial sites[124]. Similar results have been published very recently for the adsorption of W atoms on single crystal W[125], showing by FIM that the adsorbate atoms occupy the surface cavities above second- (normal lattice site) or third-layer atoms.

(vi) Induced heterogeneity:quantum-mechanical interactions via the electronic properties of the substrate

Stonehart[126] has proposed that the small H desorption peak between the two main states in acid solution arises from some unspecified interaction related to the coexistence of the two major species. It is difficult to see how such a state could arise from physical forces between the adsorbate particles, e.g., dipole-dipole attraction or repulsion, but quantum-mechanical treatments of H adsorption allow this possibility when the adsorption process itself modifies the substrate wave functions (Section 2.3).

Toya[127,128] has derived a simplified quantum-mechanical model which shows two stable adsorption states, but does not suggest that their stability will be restricted to certain ranges of coverage. The first, known as r-type adsorption, represents an adsorbed atom about 2.5 Å

above a substrate atom and having a negative polarization of about 2% of an electronic charge. The polar bond would account for the increasing work function at low adsorption coverages[67], and would lead to repulsive forces between nearby adsorbate species. The second, stronger adsorption, was called s-type. Here the H is treated as a proton lying in a crevice between surface metal atoms with its electron delocalized into the Pt conduction band. The associated dipole moment was calculated as 0.06 D, so s-type adsorption would decrease the Pt work function[67]. Toya's calculations are frequently regarded as further confirmation of the mechanism of H adsorption proposed by Frumkin and Slygin[63]. These authors made a thermodynamic analysis of the contributions of both the adsorbed H dipoles and the ions in the double-layer to the potential drop at the electrode surface. The ionic concentrations were measured directly[63,129,130] and it was concluded that the adsorbed H must increase the potential across the interface at low coverages and decrease it at high coverages[63]. This was thought to occur by the Pt-H dipoles having their negative ends face the solution at low coverage and face into the metal at high coverage. Frumkin and Slygin[63] also considered the two adsorption sites similar to those in Toya's model.

Another type of quantum-mechanical approach, derived by Zakharov et al.[131] showed four stable states of H adsorption, two atomic and two molecular. Although Tsuchiya et al.[70] found two atomic and two molecular adsorption states in gas phase adsorption experiments, their atomic states had dipoles of opposite sign as in Toya's model[127,128], while in Zakharov's treatment both atomic states are negatively charged, and no stable states exist above surface atoms.

Bewick and Tuxford[132] have used modulated specular reflectance spectroscopy within an electrochemical cell to measure the electrical changes in the surface accompanying adsorption. They concluded that the strongly-bound H was deep in crevices between surface Pt atoms (Toya's s-type[127,128]) with its electron in the conduction band, while the weakly-adsorbed H behaved more like an atom chemisorbed on top of the surface. If the strongly-adsorbed H does indeed inject its electron into the metal conduction band, induced heterogeneity could arise from the consequent changes in the electronic structure of the substrate (section 2.3).

(vii) Induced heterogeneity:restructuring of the substrate

Although it is only changes in the distribution of the various adsorption states, rather than their creation, that have been related to the adsorption-induced restructuring of Pt surfaces, it seems appropriate to discuss restructuring at this stage.

Small changes in the charge distribution between the bonding states occur as the potential of a Pt electrode is cycled[133]. Furuya and Motoo have interpreted this effect in terms of both the transfer of H atoms between bonding states and the rearrangement of the surface atoms[134], although similar effects were attributed to changes in HSO_4^- adsorption by Bagotskii et al.[89]. There is now direct evidence of Pt dissolution and re-precipitation during potential cycling from the work of Untereker and Bruckenstein[135] but no suggestion that the re-deposited atoms would form a new structure.

Continuous potential cycling has been found to alter both the appearance of the small anodic peak between the two major desorption peaks[40,134], and the distribution of adsorption energies on electrodes platinized at rather cathodic potentials[111,136]. Both have been related to a slow (logarithmic with time[134]) restructuring of the surface, and in support of such mechanisms is the surprising result from LEED studies of gas phase adsorption, that adsorption can itself reconstruct the surface of a Pt single-crystal[123,137]. If such a process were involved in electrochemical H adsorption, it would have to be entirely reversible, since the "spectrum" of bonding energies in successive adsorption-desorption cycles is exactly reproducible.

1.3.2 Adsorption of H on Au

Although multiple states of adsorption of H have been observed on Pt, Ir[46,138], and Rh[46,138,139], H does not adsorb on Au to any significant extent[139]. This makes it possible to characterize the surface composition of Pt-Au alloys by the amount of UPD of H on them[140-142]. Although the exchange current of the H^+/H_2 reaction is much lower on Au than on Pt, the couple remains reversible on Au electrodes at partial pressures from 1 down to 6×10^{-4} atmospheres[143].

The absence of UPD of H on Au suggests that the discharge and recombination processes involved in molecular H_2 evolution on Au do not occur on top of a Faradaically-discharged layer of H atoms, as seems to be the case on Pt. Gruneberg[144] has suggested that at the potentials of H_2 evolution on Au in 0.5 M H_2SO_4, reduction products of the H_2SO_4 itself may be observed.

1.4 Adsorption of O species

1.4.1 Adsorption of O species on Pt

1.4.1.1 Introduction: nature of the "oxide" layer

Questions as to the nature and bonding energy of anodically formed O-species on Pt are more complex than those about H on Pt. Although the cathodic deposition of adsorbed H gives way to H_2 evolution after the transfer of one electron per surface metal atom, the anodic deposition of O species can continue until at least two or three electrons have been transferred to each surface atom. Lack of agreement about the mechanism of oxidation has tended to preclude discussion of initial bonding states of O-species.

Two schools of thought have emerged concerning the nature of oxidized Pt surfaces. The first maintains that the Pt surface is covered by adsorbed O-containing species[13,45,63,130,145-161], rather than any definite oxide structure. Ershler[13,151-153] suggested that it was the surface field[63,130] arising from this adsorbed O which gave rise to the passivity of the Pt, and this theory has recently been taken up again by Burke and O'Meara[162]. It is based on work such as that of Nesterova and Frumkin[155] who found that polarization of Pt electrodes, or their prolonged contact with molecular O_2, formed less than a monolayer of adsorbed O.

The second school of thought proposes that electrochemically oxidized Pt surfaces are covered by a definite, chemically-bonded oxide structure[47,163-179]. Various oxides have been identified, usually by comparison with the bulk synthetic Pt oxides produced by Wöhler and Martin[180] and the equilibrium

potential measurements of Grübe[167] (PtO:0.9V; PtO_2:1.06V; PtO_3:1.5V; PtO_4 > 1.6V) which Lorentz and his co-workers [166,168,169] related to the lag points in their polarization discharge curves. The protective surface oxide has been reported as $Pt(OH)_2SO_4.3Pt(OH)_4.PtO_2$[164]; PtO[173,176,178,181], thought by some authors[176,178] to be formed from unstable precursors; PtO_2[165,171,182,183], identified by chemical analysis by Altmann and Busch[171], and by reflection electron diffraction by Shibata[184] as being "poorly crystalline"; a mixture of $PtO + PtO_2$, identified by film stripping and chemical analysis by Anson and Lingane[174]; PtO, later oxidized to PtO_2[172,175]; and $Pt(OH)_2$, later oxidized to PtO_2[177]. Other workers merely suggested that a "solid film" was produced[44,185] more than one monolayer thick[44].

It has been emphasized by Giner[45] and by Gilroy and Conway[186] that the identification of surface oxide structures by equating plateaux in charging curves with thermodynamic standard potentials requires the doubtful assumption that extremely thin layers on metal surfaces will have the same electrochemical properties as bulk oxide electrodes. Weil[187] has shown that the initial oxidation of Fe cannot be described in terms of a thickening bulk oxide, since the surface properties depend on the film thickness up to values of several tens of Å. Giner[45] argued that it would be more reasonable to regard the establishment of a "surface film of PtO" as the completion of a monolayer of PtO species, and Gilroy and Conway[186] suggested that since the stability range of oxides corresponding to PtOH, PtO and PtO_2 merged into one another, there was little value in relating formal mean valence states to bulk chemical compounds of these structures.

1.4.1.2 Reversible adsorption at low coverages

The initial adsorption of O species on to Pt from acid solutions (at potentials below about 0.9 V) has been shown by potentiodynamic studies[188,189] to be very reversible. Since these species could not be detected in early ellipsometric studies, Reddy, Genshaw and Bockris[190] concluded that the surface was covered by a chemisorbed layer of O. Although it has since been shown that ellipsometry can detect this type of film[191], it cannot be denied that many surface chemical properties of Pt change abruptly at about 0.95 V, e.g. the oxidation kinetics of H_2[192], C_2H_4[193] and other hydrocarbons[194] on Pt, the rate of increase of potential of Pt electrodes immersed in O_2-stirred $HClO_4$ solutions[162], and the coefficient of friction between two Pt electrodes. The latter decreases rapidly in the potential range 0.3-0.9 V, but begins to increase again at potentials above 1.0 V[195].

1.4.1.3 Irreversible adsorption states: characteristics and kinetics

When the anodic end-potential of a potentiodynamic sweep is increased to 1.1-1.2 V, the adsorption becomes irreversible, so the O species cannot be reduced from the Pt surface until the potential is substantially more cathodic than that at which adsorption occurred. This more cathodic reduction peak begins to dominate the cathodic sweep at higher coverages (see e.g. Fig. 1). The irreversibility of adsorption has often been interpreted as a time-dependent strengthening of the O-Pt bond[101,154,155,196], which can occur very rapidly (e.g. in 10^{-3} s)[101,197]. This "strengthening" is time-dependent, while the rate of discharge of O-

species is potential-dependent[197,198]. It will be shown below that the irreversibility probably relates to the stabilization of surface adsorbate structures by place-exchange processes rather than to the strengthening of individual Pt-O bonds facing outward from the metal surface. The inhibition of O species discharge increases with time at a given coverage, and this has been attributed[197] to either a fall in the surface potential or a discharge mechanism occurring on newly-produced active sites.

The ellipsometric parameters of Pt surfaces begin to change at potentials of about 1.1 v[199], i.e. when a charge has been passed equivalent to the discharge of one singly-charged anion per surface Pt atom. Continued oxidation of the surface can occur by a place-exchange mechanism, or further oxidation of the adsorbed species, or both. Schuldiner et al. have investigated the effects of the inaccessibility of the place-exchanged O species, which they refer to as "dermasorption"[200-202] (c.f. a similar earlier mechanism proposed by Kalish and Burshtein[203]).

The same essential features of the potentiodynamic oxidation and reduction of Pt surfaces (i.e. film formation and removal, stabilization of Pt-O structures) found in simple acid solutions are also observed in $KHSO_4$-Na_2SO_4 melts[204,205,606].

With increasing temperature, the amount of oxide formation detected by charging curves increases by 25% in the range 273-368 K[206]. The reduction potential sometimes moves cathodically with increasing temperature, since, although the higher temperatures accelerate the reduction process, they also accelerate the "bond strengthening" processes[206]. The earliest potentiodynamic studies of the initiation of irreversible oxidation behaviour[188,189] showed not only the reduction

peaks corresponding to the low-coverage, reversibly-adsorbed species and the more irreversible phase, but a third peak associated with the reduction of oxides formed at about 1.25 V (on which the authors did not comment).

The irreversibility of Pt oxidation also has other consequences. Hoar suggested in 1933[207] that it was this irreversibility which made it so difficult to achieve the theoretical potential[208,602] of the reversible O electrode (1.229 v) except at high temperatures in molten salts[209] where Pt oxides are unstable. Effects of Pt dissolution and impurity adsorption on the mixed potential observed have been reviewed by Rand and Woods[210]. The theoretical O electrode potential[211-213] and the open-circuit potential of Pt (0.46 V)[214] have recently been measured under unusually pure conditions.

Mathematical models of the incorporation of O into a Pt lattice have been reviewed recently by Stonehart et al[20] and Nadebaum and Fahidy[215]. Visscher and Devanathan[179] discussed the kinetics in terms of the thickening of $Pt(OH)_2$ films. The concluded that the Cabrera-Mott theory[216], involving the entry of metal ions into the film as the rate-determining step, provided a satisfactory quantitative explanation of the data. The oxidation rate is in fact logarithmic with time at constant potentials of up to 2.0 V[217]. Ord and Ho[218] and recently Damjanovic and co-workers[593,603,604] have proposed similar "high-field" mechanisms. The similarity in plots of reduction peak potential versus oxidation charge for Pt, platinized Pt and Rh, led Stonehart, Kozlowska and Conway[20] to suggest that a common oxidation mechanism may operate for all the noble metals although the kinetic parameters would differ from metal to metal.

1.4.1.4 Oxidation mechanisms proposed

Schuldiner et al[214] made steady-state potentiostatic measurements under conditions of extreme purity (impurity currents below about 10^{-9} A cm^{-2}), and concluded that the reactions

$$Pt + H_2O \rightarrow H^+ + Pt\text{-}OH_{ads} + e$$

and

$$Pt\text{-}OH_{ads} \rightarrow Pt\text{-}O_{ads} + e + H^+$$

were predominant in the potential ranges 0.5-0.75 V and 1.0-1.1 V respectively. Tarasevich and Bogdanovskaya[219], on the other hand, concluded that PtO was formed by the disproportionation of Pt-OH at potentials above 0.7 V, i.e. $2\ PtOH \rightarrow PtO + Pt + H_2O$. This would account for the formation of new adsorption sites[197] when electrodes are maintained at oxidizing potentials.

Vetter and Schultze[220] have proposed, on the basis of the pH dependence of oxidation current densities, that the first step in oxidation would be

$$H_2O_{aq} \rightarrow O^{2-}_{ads} + 2\ H^+_{aq}$$

or

$$H_2O_{aq} \rightarrow OH^-_{ads} + 2\ H^+_{aq} + e$$

The rate-determining step at all coverages would then be the place exchange of these adsorbed ions* with metal ions at the Pt surface. Tarasevich and Radyushkina[161] also proposed an oxidation mechanism involving the discharge of adsorbed OH^- radicals which were later oxidized to form a chemisorbed layer of O. In evaluating their results, they

*The postulation of O^{2-} or OH^- adsorbed ions seems unreasonable since the pH of the solution studied was <0.

assumed that the heat of adsorption of each species would change linearly with its coverage in a Temkin-type isotherm[224]. Tilak, Angerstein-Kozlowska and Conway later showed that anodic current-potential profiles showing four predominant peaks could be reproduced by the summation of four computer-generated Temkin isotherms. The speices adsorbed at the lowest coverages had a negligibly small interaction parameter, while those of the species adsorbed in successively higher ranges of coverage were successively higher. This work incidentally disproves both the mechanism of Vetter and Schultze[220], since the adsorption of O anions would involve a substantial interaction energy, and the models of Böld and Breiter[38,158] and Gilman[222], which fitted the data to a single Elovich[223]-Temkin[224] isotherm with an interaction parameter varying with potential because of supposed concurrent changes in the stoichiometry of the oxide.

The interaction parameter decreases with time at constant potential and Yuzhanina et al[198] have suggested that this indicates an increase in the degree of charge transfer from the chemisorbed species to the electrode "as the adsorption bond becomes stronger". Other indications that the interaction energy arises from surface dipoles are found in the work of Llopis and Colum[225] where an increase in the capacitance of Pt electrodes with oxidation is related to the existence of polar surface groups, and also in the increased work function of Pt[203,226] associated with surface oxidation, arising from the same negative dipoles of the adsorbed O species.

The results of Bagotskii and his co-workers[188,189], which first demonstrated the existence of three reduction peaks during the reduction of O species deposited at potentials up to about 1.3 V, were interpreted in terms of the adsorption of "at least two types of adsorbed O",

although the interaction parameter was thought to arise from intrinsic heterogeneity in the Pt surface[227,228] rather than induced heterogeneity caused by interactions between adsorbate species.

Other studies in this laboratory associated with the present work[229,230] have recently characterized these three states of O species. Kozlowska, Conway and Sharp[229] associated the initial reversible state of adsorption with the discharge of OH species at coverages too low for dipole-dipole interactions among the adsorbates to be significant. The two following states of electrodeposited species (not resolved separately in the reduction sweep), associated with increased interaction parameters[221], were related to the filling of successive arrays of mutually-repelling Pt-OH species, concurrent with place-exchange[231,232] in the surface to relax the dipole-dipole interactions by forming rearranged OHPt structures[190]. The most strongly bound form, shown by the most cathodic reduction peak, was associated with a two-dimensional PtO structure. The rapid processes which cause irreversibility later give way to much slower changes in the nature of the Pt-O species bond, which occur over much longer time periods[155,156]. Bowden, in fact, wrote in 1929 that "the formation of Pt oxide from adsorbed O is ..... a comparatively slow process compared with the rate at which O is being deposited",[182] and the recent studies of Stonehart, Kozlowska and Conway[20] confirm that the rate of discharge of the O species is greater than the rate of surface rearrangement until a full monolayer has been deposited. The place-exchange mechanism will of course consume no current[220], and accounts for the hysteresis[233-235] observed in the potentiodynamic results[20].

1.4.1.5 Effects of added anions and redeposition

Bowden suggested in 1929[182] that O adsorbed on Pt would have a dipole moment contributing to the interfacial potential difference. He calculated the dipole moment as 0.78 D. Frumkin[236], and more recently Petrii and Kotlov[99], have confirmed that Pt-O dipoles contribute to the potential at the electrode surface. The ionic charge in the double-layer thus decreases with increasing potential[236], i.e. the negative charge on adsorbed O species is sufficient to expel anions from the double-layer. The ionic double-layer charge does not increase until much higher anodic potentials are reached. Strongly bound anions increase the potentials at which O species begin to discharge on Pt[99]. In addition the adsorption of other species (e.g. Cl^- [159]) may produce soluble products, thereby attacking the anode surface.

Most anions, e.g. SO_4^{2-} [237,238], ClO_4^- [239], $H_2PO_4^-$ [240], Cl^- [241,242], Br^- [241,243] increase their coverage on Pt with positive potential until they are displaced by adsorbed O species. The more strongly adsorbed is the anion (the above list is in order of increasing bond strength), the smaller the interaction parameter is in its isotherm, i.e., the more "fully discharged" is its state on Pt[89]. The most strongly adsorbed species, e.g. I^- [241] remain on the Pt surface, blocking oxide formation, until their reversible oxidation potential is reached. Many anions show increased adsorption on Pt at potentials above 1.5 V, possibly as a result of their incorporation into the surface oxide film[91,244]. Khazova et al.[228] have shown that competition with other adsorbates can alter the distribution of the three distinguishable O species present on Pt electrodes.

1.4.1.6 Effects of pH

Butler and Armstrong[146], and later Vetter and Berndt[157], noted that the potential range of oxide formation moved cathodically by 0.059 V per pH unit increase. This was generally confirmed by potentiodynamic sweep data[158,217], although Tarasevich and Bogdanovskaya[219] showed that the main oxidation peak potential moved cathodically only to pH 7 and was then pH-independent. In basic solutions, a new oxidation peak was observed at potentials below 0.7 V. It moved cathodically with increasing pH in the range 7-14 and was quite reversible[100,102,219], moving only 0.03-0.04 V per decade of sweep rate in the range 0.05-10 V s^{-1} [219]. Potentiodynamic sweep data at higher pH's have also been recorded by other authors[12,100,103]. The increased coverage by O species at potentials below 0.8 V in basic solutions[51,102,129,219,245] was ascribed by Gilman[246] and Icenhower et al[51] to the adsorption of CO_2 from impurities in the reagent-grade KOH used to make up the solutions. The broadening and flattening of the reduction peak with increasing pH was related[51] to a catalytic reduction of PtO_2 to PtOH occurring only in acid solutions.

The reversible initial discharge of O species in KOH solutions occurs with anodic end-potentials of up to 0.8 V[100,102] (θ = 0.13[102]), but becomes increasingly irreversible with higher anodic end-potentials. Holding the potential of Pt at 0.8 V in 0.1 M NaOH increases the oxide coverage and moves its reduction potential cathodic to such an extent that the reduction of the initial reversible species is no longer apparent[247]. In acid solutions, the limiting coverage of the reversible species has been reported as θ = 0.15[102] and 0.27[229].

1.4.1.7 Effects of crystallography of the Pt surface

Bagotskii and his co-workers[248,249] studied the oxidation of single-crystal Pt surfaces in 0.5 M H_2SO_4. Although O species began to adsorb on (111) surfaces at lower potentials than on the other low-index planes, the rates of the oxidation and reduction processes became identical on all the substrates when referred to the unit atomic density in the electrode surface. The rate of anodic O_2 evolution, however, was higher on the more closely-packed planes, even when corrected for their higher atomic density[248]. Bagotskii et al.[248,249] concluded that the crystallography, geometry, and defect concentration of the electrode surface did not affect its oxidation. This experimental evidence rules out earlier speculations that surface reactions on Pt occur preferentially at "active sites", and shows rather that the distribution of adsorption energies is governed not primarily by surface structural factors, but by "the electronic properties of Pt"[249].

Biegler[111] disputes the validity of electrochemical data obtained on single-crystals since (a) atomically smooth Pt surfaces are known to facet in air due to the volatility of Pt oxides[250]; (b) potentiodynamic cycling causes Pt dissolution and surface roughening as discussed below and (c) various extremes of adsorption behaviour produced on polycrystalline Pt by different surface treatments[111] are not found in the single-crystal data. Certainly the optical micrographs associated with some single-crystal work[251] show that irregular, pitted and etched surfaces have been used. Biegler suggested that until new methods for surface preparation are devised, so-called "single-crystals" should at best be regarded as showing different distributions of low-

index planes, although he did conclude that the adsorption of OH and O species on Pt was a structure-sensitive process.

Since it has been established that Pt oxides formed by reaction with gas-phase O_2 are not electrochemically different from those formed anodically[245,252], some consideration will now be given to electron-optical studies of O adsorption on Pt. Tucker[253,254] has observed (2x2) and (3x3) two-dimensional O structures on Pt using LEED, with stable structures being formed at the following coverages: (111), 0.25 and 0.33, or possibly 0.5 and 0.67; (110), possibly 0.125; (100), 0.25, 0.33 and 0.5. The transformation from a (2x2) to a (3x3) surface structure generally requires surface mobility of the adsorbate. This mobility has been confirmed by coulometric studies of O adsorption from the gas phase at room temperature[255]. Tucker explained his data[253,254] on the basis that the adsorbates would not necessarily be held in the deepest parts of the crevices between surface Pt atoms.

There is conflicting evidence[122,256] on whether O chemisorbs on Pt (100) crystals. O has been found to chemisorb on stepped surfaces of Pt[257], although not on plane (111) surfaces, and Lang, Joyner and Somorjai[257] concluded that adsorption was favoured at step sites because of the increased coordination of atomic O available there. Somorjai has recently suggested that the adsorption process can itself lead to reconstruction of the crystal surface[258] so as to move Pt atoms from their initial sites to new positions stabilized as a result of interactions with the adsorbent.

1.4.1.8 Adsorption in excess of monolayer coverage

The thickening of "oxide monolayers" on Pt is thought to occur by the migration of ions in the surface layer under the influence of a high electric field[179,218]. It has become clear from a number of recent studies using a wide variety of techniques that the oxide formed on Pt at above 1.5-1.6 V (i.e. in excess of a monolayer of "PtO")[259] is essentially different from that formed at lower potentials[183,186,244,260-271]. A further new type of oxide appears at above 2.1-2.2 V[272-275] (cf. data on the oxidation of Pd[276] where reduction from 3 V shows two distinct peaks). O in oxides formed at 2.0 V exchanges very slowly, if at all, with the solution[277,278], but oxides formed at 1.8 V can be partially removed during washing[278]. ESCA analyses of Pt electrode surfaces anodized at various potentials[279], showed a predominance of chemisorbed O at 0.7 V. At 1.2 V, spectral peaks similar to those of PtO appeared, and at 2.2 V both PtO and PtO_2 were identified, in addition to the chemisorbed O. Evidence for the stability of Pt oxides in high-vacuum electron-optical equipment is found in recent Auger spectroscopy which showed that Pt anodized for 16h at about 80 mA cm^{-2} retained a stable PtO surface oxide under high vacuum[280].

Strong anodizing of Pt causes the evolution of molecular O_2 at the electrode surface. This reaction depends much more on the oxide coverage than the potential[220], and will not commence until the surface is covered by a monolayer of O species[281]. O^{18} tracer studies[282] have shown that the O adsorbed on Pt at above 1.2 V (i.e. that in excess of monolayer coverage) is directly involved in the anodic evolution of O_2, whereas the initial material adsorbed at 0.8 to 1.2 V is not.

The O species on Pt have been reported to reach limiting coverages measured as 2.66 electrons per atom[283] (e/a) (this value was later revised[284] to 2.05 e/a) and 2.68 e/a[285] on smooth Pt, and 2.08 e/a[284], 2.56 e/a[269] and 2.20 e/a[75] on platinized Pt. Visscher and Bleijlevens[75] have reported that the limiting coverage is decreased by very high concentrations of H_2SO_4, probably because the PtO layer is then covered by a strongly bound layer of H_2SO_4 molecules[74,286]. Decreasing limiting coverages at lower temperatures may also arise from anion adsorption. The formation of multilayers of oxide can be enhanced by mechanical roughening of the electrode[287] but does not normally occur below 295 K, even with long anodizations at 0.2 A cm^{-2} [288]. Some authors, however, have found no limiting oxide coverage[217], and this may relate to the continuous dissolution of O in Pt suggested by Hoare's bielectrode experiments[289].

Although the PtO layer itself reaches a limiting thickness, as shown rather conclusively by Tyurin and Volodin[269], who anodized specimens for over 5 weeks, higher potentials will produce Pt(IV) oxides[290], identified by X-ray diffraction[291] as well as by ESCA[279]. These arise at 2 V and above, coexisting with the Pt(II) oxides[292,293], and give a maximum thickness (measured by ellipsometry[275]) at 2.3 V. Pretreatment and memory effects have been investigated by Visscher and Bleijlevens[290]. At potentials above 1.8 V the electrode pseudocapacitance changes[294] and anions become strongly adsorbed. At the highest current densities in H_2SO_4 solutions the process goes over to sulphate oxidation[295], which impedes further oxide formation[290], and makes the state of the electrode very dependent on the composition of the solution[295].

1.4.1.9 Pt dissolution and precipitation during cyclic adsorption-desorption

The oxidation of Pt surfaces causes a slight dissolution of Pt[157,296], which is considerably increased if the electrode is cyclically oxidized and reduced. The dissolution of Pt at constant potential was noted 70 years ago[297]. It occurs even with polarizing currents as low as $1\text{-}2\times10^{-7}$ A cm^{-2} at 1.4 to 1.55 V[298]. The amount of Pt dissolved has been measured by radiometric[299] and colorimetric[300] analysis, and is consistent with the small excess of anodic over cathodic charge in potential cycling experiments to oxide-forming potentials[300]. It was known as early as 1839 that a.c. currents caused attack of the surface of Pt electrodes[301-303]. The excess charge required to oxidize a Pt surface over that to reduce it was ascribed in many early experiments to the production of a soluble O-containing species[176,304]; often specifically to H_2O_2[47,157] (as produced in the reduction of O_2[305]). In most cases, however, the real cause of the charge excess was the oxidation of impurities from the solution[246], as the equality of q_A and q_C in pure solutions is well established[12,158,160]. Ring-disc experiments have established that no H_2O_2 is produced[306,307], and Johnson, Napp and Bruckenstein[307] have identified Pt(II) as a product of the reduction (probably arising from reduction of PtO_2).

This dissolution increases the area of the electrodes[156,308,309] as well as their "activity"[182,310] (i.e. their ability to pass high currents in surface reactions). The increase in "activity" was ascribed by some authors[12,65,149] to a rearrangement of the surface layers of the electrode, and by others to the removal of surface impurities[246,311-313].

Shibata[270,314] and Biegler[308] have concluded that the surface attack on Pt is not due to the alternate dissolution and deposition of Pt metal but to the formation and reduction of surface oxides which weakens the surface bonding and rearranges or recrystallizes the surface structure[258]. Biegler[250] and Chao et al.[315] have demonstrated by electron micrographs that microroughening occurs when the anodic end-potential is sufficient to form more than the equivalent of one monolayer of PtO. At lower anodic end-potentials the cycling can in fact smoothen the electrode. Shibata[184] has used reflection electron diffraction to show that the reduction of multilayer Pt oxides causes platinization of the electrode surface, but with finer crystals than those found in conventional platinizing procedures. Finally the elegant experiments of Untereker and Bruckenstein[135] with a ring-disc electrode have confirmed that the roughening arises by a dissolution-redeposition mechanism (mainly involving Pt(II) species) caused by the potentiodynamic cycling.

1.4.2 Adsorption of O species on Au

1.4.2.1 Introduction: nature of the oxide layer

Most early studies of the anodic behaviour of Au were undertaken to answer the general question whether passivity arose from the formation of a crystalline barrier of reaction product or simply from the adsorption of a complete layer of polar species whose field prevented the access of further reactants. Au was a suitable metal for such studies, since the onset of passivation was obvious (particularly in HCl), and yet strong anodization produced visible surface films.

The passivating film was analyzed by a number of workers, and reported as: $Au(OH)_3$[316,317], (an extremely insoluble[317], n-type ionic conductor[318]); Au_2O_3 containing a little Au_2O[319] (Au_2O is unstable with respect to Au + Au_2O_3[320]); Au_2O[321], one[322] or perhaps two[323] molecules thick in acid solutions but probably only one molecule thick in alkali[322,323]; $Au_2O_3 \cdot 3H_2O$[324,325]; Au_2O_4[326], produced from Au_2O and AuO[175,327]; or $Au(OH)_3$ leading to AuO_2 which then breaks down to Au_2O_3 and O_2[318]. The "adsorption" school of thought postulated that passivation arose from the field of a sub-monolayer of adsorbed O atoms[328].

Over the years it has become accepted that Au_2O_3 is the passivating film: results such as the negative temperature coefficient of its formation[329] (the pre-passive species has a positive temperature coefficient), the fact that oxidized Au electrodes come to the equilibrium Au-Au_2O_3 potential[325,330,331] (1.362 V[332,333]), and radiotracer studies showing that the oxide is not hydrated[334] in acid solutions may be cited. The mechanism whereby the Au_2O_3 is formed is far less well understood.

1.4.2.2 Reversible adsorption of O species

Sirohi and Genshaw[335] showed by ellipsometry that only adsorbed species and not structured oxides were present on Au at potentials below 1.34 V in 0.5 M H_2SO_4 (below 0.2 V to S.C.E. in an NaOH solution of unspecified concentration). The first Faradaically-discharged deposits appear at about 1.27 V[148], although the double-layer capacitance begins to increase at about 0.8 V[331]. Potentiodynamic studies show that the first deposits are formed reversibly at low coverages at sweep rates of up to 10 V s^{-1} [336]. Their optical parameters are reversible with respect

to coverage up to $\theta = 0.44$[337]. The initially-deposited species has been reported as OH[330,338] or atomic O[148,339,340] in acid solutions, and as $\overline{OH}$[340] at higher pH.

1.4.2.3 Irreversible adsorption states: characteristics and kinetics

The initial oxidation of Au becomes irreversible even at low coverages if the adsorbed O species are left on the surface before the surface is reduced. As a result, the reduction peak potential in a potentiodynamic sweep is often several hundreds of millivolts more cathodic than the deposition potential. This hysteresis has been known for many years and was originally interpreted as a strengthening of the adsorption bond with time. Brummer[341] found that the "oxide" was much more difficult to reduce when the potential was held anodic before the reduction, particularly at lower anodic potentials, and that the extra oxide formed during holding increased with the holding potential. When more O species had been deposited at constant potential, the profile of the reduction sweep became taller and narrower, and its peak moved to a more cathodic potential.

The hysteresis in the oxidation of Au does not simply reflect an increase in the "bond strength" to the adsorbate, but rather a fundamental change in the state of the adsorbed layer. This is shown by the fact that anodes reduced from low oxidation potentials in fast potentiodynamic sweeps show a series of oxide-reduction reactions occurring at different potentials.

The earliest reports of multiple stages in reduction of O species on Au[327,329] probably relate only to the reduction of impurities

in addition to currents from the main reduction peak characterized by Brummer[341]. More recently Gruneberg[144] used potentiodynamic sweeps over a restricted potential range, and found that the oxide was reduced in two distinct peaks. The reduction profile was later resolved into three distinct peaks by Goldstein, Zalkind and Veselovskii[342], when stripping oxides formed at up to 1.35-1.45 V in $HClO_4$ solutions potentiodynamically at 100 V s^{-1} after ≤100 ms anodic holding. The reversibly adsorbed O species was reduced at 1.2-1.25 V in amounts which first increased with anodic holding and then decreased as adsorbates were simultaneously reduced from other bonding states. The second peak to appear was that of the "most strongly bound"* O species, reduced at 0.8-0.85 V. The "most strongly bound" form was produced from the "most weakly bound" form, since at the maximum rate of formation of the "most weakly bound" form (when its rate of formation was equal to its rate of disappearance) this rate was the same as the rate of production of the "most strongly bound" form. The coverage by the most strongly bound form increased rapidly with time to a maximum of about 0.1 monolayer, which was almost independent of the adsorption potential. With adsorption times longer than 10 ms, the main reduction peak appeared at 0.9-1.0 V, and quickly grew to dominate the reduction profile. With adsorption times >100 m s at 1.45 V only the main reduction peak appeared and the forms with weaker and stronger bonds could not be distinguished.

*"Weaker and stronger bonding" of O species and "time dependence of the bond strength" are frequently referred to in the literature. It seems preferable, however, to describe these effects in terms of increased or reduced stability of two-dimensional phases as the extent of place-exchange varies with time and potential.

Ferro, Calandra and Arvia[336] later obtained similar results in H_2SO_4 solutions but in addition resolved the reduction of the "most strongly bound" form (produced from the initial, reversibly-adsorbed species) into two peaks in 1 M $HClO_4$. These two peaks were still observed when the main reduction peak dominated the current-potential profile.

Multiple states are resolved in the adsorption of O species on Au[138,337] as well as in their desorption when fast potentiodynamic sweeps are used, but the corresponding arrests have not been observed in anodic charging curves[330,343]. The similarities in both the potentiodynamic sweep profiles and the optical properties of Au and Pt anodes led Conway et al.[337] to propose that the mechanism causing irreversibility in Au oxidation was a physical surface rearrangement following the initial electrochemical oxidation step. It was suggested that place-exchange and lateral rearrangement occurred progressively during the formation of surface oxide. A slow "unrearrangement" step, perhaps with a limiting rate, would then be required before the O species could be reduced at the electrode surface. Optical data collected in this study[337] showed that although the oxidation charge was reversible with respect to film thickness, the electrical properties of the film were not, confirming the existence of time-dependent rearrangement processes.

The oxidation rate of Au is experimentally logarithmic with time[335,341,344], with no discontinuity corresponding to monolayer coverage. It has been described in terms of Elovich[223] kinetics. The equilibrium film thickness increases linearly with potential[344].

1.4.2.4 Oxidation mechanisms proposed

Gruneberg[144], who was the first to observe twin desorption peaks, concluded that after oxidation to low coverages only, the surface species would be Au(OH), reduced in the more cathodic peak in the cathodic sweep. Higher adsorbate coverages were thought to be in a higher oxidation state and to be reduced in a two-stage mechanism, viz.

$$Au(OH)_3 + 2H^+ + 2e \rightarrow AuOH + 2H_2O$$

or

$$AuO(OH) + 2H^+ + 2e \rightarrow AuOH + 2H_2O$$

followed by

$$Au(OH) + H^+ + e \rightarrow Au + H_2O.$$

Goldstein et al.[342] suggested that the "bond strengthening" showed a further oxidation of the adsorbate, i.e.

$$Au + H_2O \rightarrow \underset{\text{reversibly adsorbed species}}{Au(OH)_{ads}} + H^+ + e \qquad \text{(fast)}$$

$$Au(OH)_{ads} \rightarrow \underset{\text{"most strongly bound" species}}{Au(O)_{ads}} + H^+ + e \qquad \text{(slow)}$$

They concluded that other forms of adsorbed O and surface oxides might be present at higher potentials. Laitinen and Chao[330] had previously suggested a similar mechanism scheme but with different kinetics and an explicit third stage:

$$Au + H_2O \rightarrow Au(OH) + H^+ + e$$

$$\underset{\text{"chemisorbed"}}{Au(OH)} \rightarrow AuO + H^+ + e \qquad \text{(fast)}$$

$$AuO + H_2O \rightarrow AuO(OH) + H^+ + e$$

The AuO(OH) species proposed has the same $Au_2O_3.H_2O$ formula suggested for the end product by other authors[326,343]. The fact that the multiple oxidation states of Au all merge into the state giving the main reduction peak even after short anodic holding times (which prevented many workers detecting the multiplicity of states[330,337]) suggests that the change in state of the first (Au(OH)) species is rapid, as proposed by Laitinen and Chao[330].

Some authors have proposed O^{2-} species as adsorbed intermediates in the oxidation[345] and reduction[343] of Au surfaces. (See footnote on page 28). According to Schultze and Vetter[345] the rate-determining step in Au oxidation is the incorporation of O^{2-} into the Au_2O_3 lattice (a "rearrangement" process). The main cathodic reduction peak is then attributed to reduction at the edges of patches[325,329] of Au_2O_3[345]. The early suggestion that the excess of Au oxidation charge over its reduction charge is due to H_2O_2 formation has been ruled out by Gruneberg[144], who studied the effects of added H_2O_2 on the potentiodynamic sweep profile. In pure solutions, the anodic and cathodic charges are equal[144,337], except for very small dissolution currents which will be discussed later.

1.4.2.5 Effects of added anions

Although the adsorption of cations on Au can be neglected[346,347] since the p.z.c. is at about 0.3 V[348], specifically adsorbed anions can have a major influence on the electrodeposition of O species. The specific adsorption of anions decreases in the order $I^- > Br^- > OH^- > Cl^- > SO_4^{2-} > ClO_4^- > F^-$ [347]. Thus for example O species begin to dis-

charge on Au about 0.1 V more anodically in H_2SO_4 solutions than in $HClO_4$ solutions[342], probably because of the difficulty of displacing the strongly adsorbed SO_4^{2-} from the Au surface. The same effect is observed when Na_2SO_4 is added to $HClO_4$ solutions[342]. This strong specific adsorption of SO_4^{2-} prevents the resolution of the multiple states of O species desorption[337,342] which may be seen in $HClO_4$ solutions.

Hamelin and Bellier[349] have studied the specific adsorption of Cl^- on Au single-crystal faces in the zone $[1\bar{1}0]$, using a slow potentiodynamic sweep modulated by a superimposed a.c. signal to measure the differential capacity of the electrode in unbuffered K_2SO_4 solutions. The current-potential and capacity-potential curves were not affected by the restructuring of the crystal surfaces[350] arising from the sweeps, and the Cl^- adsorption was apparently sensitive to the crystallinity of the substrate. However, other workers[351] using polycrystalline Au electrodes have not observed the fine structure of Cl^- adsorption states reported, and have ascribed capacitance maxima in the same potential region to the adsorption of O species.

1.4.2.6 Effects of pH

The potentials of Au oxidation move cathodically by 0.059 V per pH unit in both SO_4^{2-} solutions of constant ionic concentration[157], and in $HClO_4$ solutions[330,352].

1.4.2.7 Effects of crystallography of the Au surface

Early suggestions that adsorption on specific surface sites[148] would lead to the formation of an oxide continuous with the crystal lattice of the Au[338], have recently been investigated on single-crystal Au substrates. Sotto[353] showed that all three oxide reduction states could be resolved on each of the principal single-crystal faces, although in neutral solutions the resolution was improved at lower temperatures. She concluded that the three states represented Au(I), Au(II) and Au(III) oxides, could undergo transformations from state to state rather easily. Dickertmann, Schultze and Vetter[354], on the other hand, found only one potentiodynamic peak on the anodic side and one on the cathodic side at (100) and (111) electrodes, and concluded that Sotto's crystals may have shown a minor exposure of faces other than that for which they were cut. Since the difference according to crystallography in Dickertmann's work was only in oxidation and not reduction, the authors concluded that the oxide was not formed epitaxially and that its thickness was independent of the substrate lattice. The difference in oxidation rate of the different planes was therefore ascribed to either a difference in "electrosorption valence" (see Discussion in Section 1.5.1.3) or the difference in potential distribution at the crystal surfaces on account of their different p.z.c.[355]. Dickertmann et al.[354] concluded that a polycrystalline Au electrode would complete a monolayer of oxide on its (100) faces before the (111) faces were oxidized. Their results could alternatively be explained by the (111) crystal being dirty. The crystal surfaces were prepared by electropolishing in cyanide solutions, and an $Hg/HgSO_4$ reference electrode was apparently connected directly to the

small volume of solution on the working electrode surface by a capillary. Thus, the selective adsorption of CN^- or Hg could also have affected the results. Experience gained in the present work suggests this may have been the case.

1.4.2.8 Adsorption in excess of monolayer coverage

Early workers suggested that O_2 evolution began as soon as a monolayer of univalent ions had been discharged on the surface[148,150,322]. This charge is passed at a potential of 1.45 V in 1 M $HClO_4$[343] and H_2SO_4[356]. The mechanism of Au oxidation changes as the coverage exceeds that corresponding to a monolayer[353]. Ellipsometric[357] and reflectivity[358] data have shown that the surface films formed in excess of a monolayer differ from those formed in the potential range 1.2-1.4 V[344,357]. The "thicker" Au oxides are thought to have a definite phase structure[335] i.e. the adsorbed species and the surface Au atoms have rearranged themselves[148] to form an interpenetrating crystal lattice. This rearrangement may be facilitated by weakening of Au-Au bonds resulting from the formation of adsorption bonds[148].

1.4.2.9 Au dissolution and redeposition during cyclic adsorption-desorption

Anodic dissolution of Au has been known since 1806[359,360] and early work[361] showed that Au could be plated from an Au anode to a Pt cathode in H_2SO_4 solutions. Lehner[362] confirmed this work, and found that the process was rapid in concentrated acid or alkali and at high temperatures.

The current-potential profile on Au is changed in the oxidation

region when the anodic end-potential is raised to 2.0 V, although the original profile is recovered after several hours at lower potential[354]. The recrystallization of the electrode surface suggested by such results[354] has been studied by Chao, Costa and Tadjeddine[350]. Setting the current-reversal potentials to 0.4 and 1.9 V in 0.5 M H_2SO_4, they observed progressive surface facetting and grain-boundary attack, and concluded that the periodic oxidation weakened the bonding forces locating the surface atoms, so that they could diffuse to lower energy sites. Electron microscopic studies by Laitinen and Chao[330] showed that these surface changes do not occur at potentials below 1.65 V.

Rand and Woods[300] have analyzed solutions from potentiodynamic studies by atomic absorption spectroscopy and found that Au dissolves at a rate of 3.6 μC cm^{-2} per potentiodynamic cycle between 0.6 and 1.54 V. This dissolution has recently been characterized by Cadle and Bruckenstein[363] using the ring-disc method. They showed that Au dissolves in 0.2 M H_2SO_4 at potentials above 1.35 V during both oxidation and reduction sweeps. The amount of cathodically deposited Au was diffusion-controlled, and a function of the amount of Au oxide reduced. At potentials below 1.45 V (one monolayer), the predominant soluble Au species was Au(III), but beyond 1.45 V a significant amount of Au(I) was also produced. The ratio of soluble Au produced to surface oxide formed, decreased with increasingly anodic end-potentials. So also did the dissolution rate under potentiostatic conditions, particularly above 1.7 V[363], which corresponds closely to the potential at which the second monolayer of oxide is completed[357].

Moslavac, Lovreček and Radeka[364] have recently made an analysis of the kinetics of Au oxidation based on a model with simultaneous formation and dissolution of oxide.

1.5 Adsorption of Cu

1.5.1 Adsorption of Cu on Pt

While studying the nature of bonding, Oberbeck noted nearly 90 years ago that the surface properties of Cu deposits on Pt were independent of their thickness providing they were more than about 7 Å thick[4], see also [365]. Thinner layers, however, were found to be more strongly bound. The importance of this transition in the nature of the electrodeposition bond has been very largely neglected in subsequent work. Despite the consequent lack of understanding of the nature of the surface bond on metals, much useful data on metal deposition systems has accumulated in the intervening years, particularly as a result of the development of stripping voltammetry[366-371] for trace element analysis, and the use of galvanostatic and potentiodynamic methods (see Section 1.1).

1.5.1.1 Resolution of component processes

Early galvanostatic work by Bowles, in which the amount of Cu on the electrode surface could be independently measured by radiotracers, showed the existence of two predominant surface bonding energies in UPD. The lack of control of the electrode potential caused some problems arising from the production of Cu^+ ions, a matter which will be discussed separately in Section 1.5.1.8.

Tindall and Bruckenstein[372] subsequently used ring-disc electrodes

and the potentiodynamic sweep technique to improve the resolution of the component processes. Cu deposition occurred in three stages, which appeared in the reverse order in electrodissolution. If the potential was held constant at values corresponding to one of the first two processes (0.3 to 0.6 V), the current decayed rapidly to a residual value (presumably corresponding to the diffusion-controlled reduction of impurities). The authors concluded that these deposition processes corresponded only to the formation of Cu-Pt bonds. In contrast, when the potential was held at less than 0.18 V (in 10^{-5} M $CuSO_4$-0.2 M H_2SO_4) the currents increased to a limiting value, and visible deposits of Cu appeared on the cathode. As thicker and thicker Cu layers were removed potentiodynamically, only the most cathodic peak on the anodic sweep continued to increase. Cathodic processes occurring below 0.18 V, and the most cathodic peak on the anodic sweep, were ascribed to the formation and breaking of bulk Cu-Cu bonds. The other two anodic peaks corresponded to the oxidative dissolution of adsorbed Cu to Cu^{2+} ions, breaking Cu-Pt bonds.

A careful examination of the potentiodynamic current-potential profiles given by Tindall and Bruckenstein[372] and by Yoshida and coworkers[373,374] shows that the more anodic of the peaks associated with Cu-Pt bonds is resolved into two components, although this feature was not discussed by either group of authors. A similar current-potential profile was also obtained by Vassos and Mark[375] in studies of the electrodeposition of Cu on pyrolytic graphite (cf. the much poorer resolution of component processes on glassy carbon electrodes[376]).

1.5.1.2 Causes of multiple states of adsorption

The cause of the multiple peaks in the potentiodynamic electrodissolution of Cu monolayers has been discussed only in general and speculative terms. Tindall and Bruckenstein[372] excluded the possibility of their corresponding to a series of Cu-Pt intermetallics because of the similar spectrum of bonding states reported for Cu on pyrolytic graphite[375] where intermetallics cannot exist.

Several other groups of workers have simply speculated that the multiple bonding energies arise from Cu deposition at sites of "varying activity"[372,377,378], e.g. lattice defects, "crevasses" etc.[375]. The concept of "active sites" has however been fully investigated by Bagotskii and his co-workers[248,249] and ruled out as a possible cause of multiple bonding energies in favour of factors related to "the electrical properties of Pt" (see fuller discussion in Section 1.4.1.7).

Breiter[379], whose use of unpurified A.R. grade Cu salts was the probable cause of his only resolving two states in the desorption of a monolayer of Cu, noted that these two peaks were spread over a similar potential range to that for the desorption of a monolayer of H from Pt. He therefore concluded that the Cu was bonded at sites where the bonding was either "weak" or "strong" as in his model for the bonding of H on Pt[380]. This explanation was later taken up by other workers in Japan[373,374]. However, since the ratio of "weak" and "strong" bonding sites for Cu electrodeposited on Pt was different to that for H on Pt, Breiter suggested that the bonded species would have a specific effect on the surface bonding states in the sense of an induced effect[379]. Bowles, on the other hand, suggested that different bonding energies

would exist on the different crystal faces exposed by a Pt electrode[381], an explanation previously suggested by Will[110] on the basis of an interpretation of potentiodynamic studies of the deposition of H on Pt single-crystals.

1.5.1.3 The state of the electrodeposited Cu

In view of the present controversy as to whether electrodeposited metal species may be only partially discharged[382-385], the relevant data for the Cu on Pt system will now be reviewed in some detail.

It has normally been assumed on the basis of qualitative arguments that Cu would be discharged to the elemental state. An early exception to this was the suggestion by Degeiso and Rogers[368], on the basis of crystal lattice mismatch, that the initial deposits from halide solutions would be in the form of halide salts. However, ring-disc studies by Nekrasov and Berezina[377] showed experimentally that although Cu^{+} ions could be detected as an intermediate species in the reduction of Cu^{2+}, the deposit was in the form of Cu metal, in a "slightly activated state".

In 1970 Schultze published a paper[386] which introduced a new type of interpretation of electrodeposition data. Using rather poorly resolved galvanostatic data, he drew straight lines through plots of the charge passed at various potentials against $\log[Cu^{2+}]$, and derived the values of the potential by which certain charges had passed as a function of $\log[Cu^{2+}]$. Drawing straight lines through these graphs at constant charge (i.e. constant coverage), and overlooking the

systematic variation of the slopes with coverage, Schultze concluded that on the average the Cu surface species would be 73% discharged at coverages between $\theta = 0.3$ and 1.6. He then made a mathematical treatment of the kinetics and thermodynamics of Cu deposition based on the Temkin-type isotherm:

$$B\theta = RT \ln a_{Cu^{2+}} - z\gamma FE + \text{constant}$$

where $B = 11.3$ kcal mole^{-1}

θ = surface coverage by Cu species

z = 2 electrons per atom

γ = the fraction of the charge of an ion which is discharged as it adsorbs on the electrode surface, i.e. 0.73.

Schultze's conclusion that the desorption step is itself rate-determining is at variance with the accepted mechanism of the deposition of Cu metal on Cu (see Section 1.4.1.8) where the rate-determining step in dissolution is not the formation of Cu^{+} ions but the oxidation of Cu^{+} to Cu^{2+} ions.

Plots comparable to Schultze's, showing the potentials of the two main Cu desorption peaks (monolayer removal) and the small, more cathodic peak (partial second layer) as a function of $\log[Cu^{2+}]$, were subsequently published by Yoshida et al.[373,374]. Apart from the data corresponding to the removal of the last half-monolayer (where the Cu peaks overlap considerably and are difficult to resolve), it may be seen from Yoshida's data that the component peaks remain at constant overpotential to the reversible Cu/Cu^{2+} redox reaction with changing $[Cu^{+}]$. Schultze's plots, however, showed these overpotentials varying

with both $\log[Cu^{2+}]$ and coverage[386]. Yoshida et al. recorded their doubt that the Temkin isotherm proposed by Schultze could apply to coverages in excess of a monolayer.

In any case, direct experimental data is now available to show that the Cu deposit is fully discharged. Bowles reported this by comparing the deposition charge with the amount of radioactive Cu deposited[381], Cadle and Bruckenstein[387] correcting the earlier work of Napp and Bruckenstein[388], by ring-disc charge-balance studies. In addition, Vassos and Mark[375] showed that Cu deposition on graphite involving a charge corresponding to the complete discharge of a monolayer of Cu^{2+} ions, formed a uniform layer of Cu metal.

The reduction in the UPD of H on Pt corresponds to exactly half the charge involved in Cu deposition over a wide range of coverages[373,374 389,390]. This result cannot be explained in terms of a partially-discharged layer of Cu ions, since it is known that the saturation charge for H bonded to Pt corresponds closely to one electron passed per Pt surface atom[30-32].

Having established that the electrodeposited Cu is in a fully discharged state, it follows immediately that the charge measured in the two most anodic UPD peaks corresponds closely to the completion of a monolayer of deposited Cu[372-374,381,389,390].

The misleading results obtained by Schultze appear to have arisen for two reasons. Firstly he chose an experimental method (slow charging curves) which was insufficiently sensitive to resolve the component processes, and secondly he neglected to evaluate the effects of the dissolution of Cu as Cu^{+} ions by side reactions.

Horanyi[391] has very recently shown that the electrodeposition of Cu on Pt surfaces increases the adsorption of HSO_4^- ions. He explained this result in terms of the co-adsorption of specifically adsorbed HSO_4^- ions and partially discharged Cu^{2+} ions, but noted that the preferential adsorption of HSO_4^- on Cu metal rather than Pt metal would provide an alternative explanation.

1.5.1.4 Kinetics and reversibility

Byrnes and Rogers[392] suggested that Cu deposits on Pt at underpotential because of the contribution of the excess heat of adsorption of Cu on Pt (compared to Cu on Cu) to the activation energy of the discharge reaction. However, although the rate-determining step in the discharge reaction is known to be the reduction of Cu^{2+} to Cu^+ (see Section 1.5.1.8), there is no such agreement over the rate-determining step in the UPD of Cu on Pt. Rotating ring-disc studies have shown that the deposition rate is "almost entirely diffusion-controlled" when the Pt potential is stepped to 0.0 V in solutions containing 2×10^{-5} M Cu^{2+} [387] and 2×10^{-6} M Cu^{2+} [390]. Breiter[389] varied the stirring rate in 10^{-3} M Cu^{2+} solutions and found that the increase in deposition rate caused by stirring was less than could be accounted for by the consequent thinning of the diffusion layer. He concluded that both mass-transport and a slow discharge step were involved in the rate control. Schultze, as we have already discussed (Section 1.5.1.3), concluded from adsorption isotherms derived from charging curves that the rate was controlled by an adsorption reaction leading to a partially-discharged surface species.

Noting that the charge required to remove the "strongly bound"

Cu was independent of the galvanostatic current used to remove it in the range 20 mA to 2A, Breiter[389] concluded that the dissolution of Cu in Pt (alloying) is negligible when the Cu is deposited from 10^{-3} M $CuSO_4$ - 0.5 M H_2SO_4 solutions by holding the potential at 0.3 V for up to 2400 s. Tindall and Bruckenstein[372,393] also failed to find any evidence for solid solution or alloy formation between Cu and Pt, although they noted that the electrodeposition of Cu on Pt from $HClO_4$ solutions was highly irreversible[393].

1.5.1.5 The transition from UPD to bulk Cu deposition

Some fine electron microprobe analysis by Vassos and Mark[375] showed that when the equivalent of one monolayer of Cu had been deposited on a graphite surface, the Cu was uniformly distributed across the surface. Deposits thick enough to show the bulk Cu dissolution peak when anodically desorbed were associated with the appearance of local aggregates of Cu up to several μm thick. These growths were far apart and lay on top of a Cu film one or two monolayers thick, when the total Cu deposit would have been sufficient to form a film 5-6 layers thick had it been uniform. Since the Cu did not accumulate in surface imperfections such as scratches, this work gives additional proof that large bonding energy differences do not exist between surface sites.

The mechanism of bulk growth via local thickening was also deduced by Breiter[379] as an explanation of the small peak in the anodic potentiodynamic sweep occurring after the removal of the bulk Cu layers but before the oxidation of the remaining monolayer of Cu[373,374,379]. First the local overgrowths would be oxidatively dissolved, then the

remaining few local patches of Cu with properties intermediate between the bulk and the monolayer, and then finally the monolayer of the most strongly bound Cu. Breiter[379] suggested that an alternative mechanism, of "weak adsorption of Cu atoms in a second layer on top of the monolayer", would be expected to make the height of the "second layer" peak more concentration-dependent than was observed.

Direct experimental evidence of the transition from monolayer to bulk deposition is also available from the recent in situ RHEED studies of Horng and Vook[394]. Using very smooth Ag(111) substrates, they found that at room temperature Cu formed very uniform deposits up to thicknesses of about two monolayers, beyond which discontinuous and local Cu overgrowths were formed (cf. Oberbeck's result in 1887 that films thicker than 6.9-7.3 Å behaved as bulk Cu[4]). The lattice parameters of Cu overgrowths of less than 6 Å thick were larger than that of bulk Cu, probably because they were strained by the larger lattice of the Pt substrate.

1.5.1.6 Effects of added cations

The influence of foreign ions in the electrolyte has received little attention, despite its fundamental importance with regard to electroplating technology. The effects of various added cations during galvanostatic electroplating were studied by Mikhailov[395]. His observation that the plating potentials at first fell relative to a Cu metal reference electrode for about a minute and then rose to an equilibrium value several minutes later, is direct evidence of the transition from bonding influenced by the substrate (UPD) to bulk electrodeposition, although the author did not apparently understand it as such. The

added cations affected this equilibrium plating potential by tens of millivolts, although the effects decreased with increasing temperature so that at 348 K Cu deposited from all the solutions at about 0.07 V.- It was assumed that the electrodeposition energy would include that spent on desorbing competing cations to make way for Cu, and this desorption energy was found to increase with the charge/radius ratio of metal cations in the series K^+ to Be^{++}. The mechanism was thought to involve either the displacement of specifically adsorbed foreign cations or an interaction of the hydration shells of these cations with "polarized Cu atoms" (see Section 1.5.1.3).

1.5.1.7 Effects of anions and pH

Degeiso and Rogers[368] used stripping voltammetry to study the equilibrium underpotential coverage of Cu on Pt cathodes as a function of the anions present and the pH. The underpotential for Cu deposition was reduced by anions in the order $Cl^- > Br^- > SO_4^{2-} > ClO_4^-$, although the anion effects were found to be much smaller than those of pH. Increasing the pH in $HClO_4$ solutions reduced the underpotential for Cu deposition, and also increased the production of Cu^+, described by the authors as a "sorption loss".

1.5.1.8 Production of Cu^+ during cyclic adsorption-desorption

Cu^+ ions produced during the electrodeposition of Cu will not all be reoxidized during the next anodic sweep, as some will have diffused away from the electrode in the meantime. In this case, the anodic charge will be less than the corresponding cathodic charge in cyclic voltammetry

measurements. Experimental evidence of the production of soluble species was first recorded in 1903 when LeBlanc and Schick[396] found that the application of a slowly-alternating potential to two Cu electrodes in a solution of a Cu salt caused both electrodes to lose weight continuously.

Since the production of soluble species can complicate the understanding of the bonding processes between Cu and Pt, a brief review of the processes involved will now be given.

The electrodeposition of Cu from Cu^{2+} solutions is one of the most widely studied metal discharge reactions. Early data on the equilibria involved are summarized by Pourbaix[397]. More recently, studies have been made by Hillson[398], Bockris and co-workers[399-401], Bertocci[402], Eichkorn, Fischer and co-workers[403,404], and Albaya and Lorenz[405]. The minimum ratio of the exchange current densities for the Cu^{2+}/Cu and Cu^{+}/Cu couples is always less than 0.001, so the species normally in equilibrium with the surface will be Cu^{+} [399,405]. If the electrode surface has an unusually low dislocation density, the surface diffusion of adsorbed species may take over as the rate-determining step[400]. The $Cu^{+} + e \rightleftharpoons Cu$ reaction has an increasing influence on the rate at high Cu concentrations[400,401]. The deposition characteristics depend on the surface crystallography of single-crystal Cu substrates[404], and crystallization overpotentials have been measured[403].

The fact that the amount of metal removed is apparently less than the amount of metal deposited was interpreted in early cyclic voltammetry experiments[e.g.396] as "sorption losses" (irreversible alloying) or "varying current efficiencies". Nekrasov and Berezina[377], using a ring-disc electrode system, detected small amounts of an

oxidizable species (Cu^+) during the electrodeposition of Cu on amalgamated Au, which were too large to be simply the products of solution equilibria between Cu^{2+}, Cu^+ and Cu. This confirmed the two-stage reduction model for Cu deposition found in the work of Stackelberg and Freyhold[406]. Nekrasov and Berezina found that the reduction of Cu^+ was reversible, as reported by Mattson and Bockris[399] but that the Cu metal was deposited in a slightly activated state, because of crystallization overpotentials.[377]

The controversy about whether Faraday's laws were "really obeyed" was not finally resolved until quantitative data on the production of Cu^+ ions was published by Tindall and Bruckenstein in 1968[372, 393]. The potential range in which Cu^+ was produced by reduction was about 0.25 to 0.1 V[372,377]. Tindall and Bruckenstein concluded that the amount of Cu^+ formed in reduction was neither controlled solely by the thermodynamics of the $Cu^{2+}/\ Cu^+/\ Cu$ equilibria[377], nor solely by the slowness of reducing Cu^+. The amount of Cu^+ depended in a complex fashion on the electrode history, the potential and the thickness of Cu electrodeposited. Cu^+ was not detected as a stable intermediate in electroreduction unless more than 500 $\mu C\ cm^{-2}$ of Cu had been deposited (about one monolayer) and appreciable amounts of Cu^+ were not found until twice this much had been deposited. The conclusions of earlier work by Johnson, Napp and Bruckenstein[407], in which it was suggested that Cu^+ species were adsorbed during the reduction of Cu^{2+} in HCl solutions, were later revised by Cadle and Bruckenstein[387]. The latter authors used a ring-disc electrode system to show that the number of electrons transferred in electrodeposition is not one but two. Such

Cu^+ ions as are produced are not deposited and Cu is only bonded to the Pt in a fully discharged state.

Bowles[381] made an elegant demonstration of the formation of Cu^+ by using radiotracer measurements of the amount of Cu deposited to calculate a charge-potential curve, on the assumption that two electrons were always passed in electrodeposition, and then subtracting these charges from those derived from his experimental pseudocapacitance data. The resulting peak was related to the one-electron process. Indeed it had a half-width of about 0.094 V, close to the theoretical value of 0.091 V[16,23] for a reversible, one-electron process (Fig. 2).

Cu^+ ions may also be produced in the chemical stripping of Cu from Pt electrodes by an open-circuit reaction with Cu^{2+} ions[408,409]. The equilibration of this process was found to take about 30 min in a solution of 4×10^{-4} M $CuSO_4$ + 0.2 M H_2SO_4, although the rate of Cu^+ formation depended on the thickness of the Cu metal deposit unless the latter was more than about 100 atoms thick[408].

1.5.2 Adsorption of Cu on Au

1.5.2.1 The extent of UPD

Cu deposits from concentrated solutions (1 or 2 M $CuSO_4$ - 0.5 M H_2SO_4) in a single broad UPD peak[410,411]. The subsequent electrodeposition is according to a Tafel relationship similar to that obtained on a Cu metal electrode in the same solution[410]. In dilute solutions of Cu^{2+}, however, the potential range of UPD is apparently sensitive to the potentiodynamic sweep rate. Takamura, Sato and Takamura[412] found a broad constant-current plateau at potentials cathodic to the initial

deposition peak when using a sweep rate of 0.114 V s^{-1} in 3 x 10^{-3} M $Cu(ClO_4)_2$ - 1 M $HClO_4$ solutions. At a sweep rate of only 2 mV s^{-1}, Schmidt, Beutler and Lorenz[413] found bulk Cu deposition initiated at more anodic potentials in both $HClO_4$ and Na_2SO_4 solutions. A second broad current peak was observed, more cathodic than the first, and the total UPD charge was about 450 μC cm^{-2}, i.e. approximately one monolayer. It may be that the Nernst potential was depressed in the work of Takamura et al.[412] because of a partial diffusion-control of the reaction rate at the sweep rate and Cu concentration investigated. Schmidt et al.[413] used a four-electrode cell in which Cu precipitated from the small volume of solution was immediately made up by a generator electrode system. Bulk deposition of Cu was, however, almost eliminated when the Cu concentration was reduced from 3.6 x 10^{-6} M to 2.7 x 10^{-6} M.

1.5.2.2 Resolution of component processes

Less resolution of component processes has been previously achieved in the adsorption of Cu on Au than in any other system involved in the present studies. The two adsorption peaks found by Schmidt, Beutler and Lorenz[413] in slow potentiodynamic sweeps at low Cu^{2+} concentration show no substructure in $HClO_4$ solutions, although their profiles are not typical of single-process isotherms, with or without interaction forces. In Na_2SO_4, however, there is some evidence that both the predominant deposition peaks may be the sum of two components.

In the experiments of Takamura et al.[412], the anodic current-potential profile showed a tall and narrow peak apparently superimposed on the more reversible low-coverage deposition process. The corresponding

measurements of surface reflectivity were definitely irreversible with respect to potential although their reversibility with respect to charge (coverage) was not discussed. Some substructure is evident in the reflectivity-potential plots but this may simply show the non-linearity of charge with potential.

It should be noted that no previous workers studying the adsorption of Cu on Au have described any purification techniques used to ensure the absence of impurities added with the Cu salts.

1.5.2.3 State of the deposit

Schmidt, Beutler and Lorenz[413] used the four-electrode chamber cell developed by Schmidt and Gygax[414] to compare the amount of Cu deposited out of the solution with the charge passed at the Au electrode. This showed that the adsorbed Cu was in a fully-discharged state since an average of 2.05 ± 0.1 electrons were supplied to deposit each Cu atom. Takamura et al.[412] also concluded that the Cu deposit was fully discharged from a qualitative assessment of their specular reflectivity data.

1.5.2.4 Reaction mechanisms proposed

Raducanu and Lorenz[410] concluded from the sweep-rate dependence of the Cu deposition rate that the discharge occurred in two consecutive one-electron stages, as in the model proposed by Bockris and co-workers[399-401], i.e.

$$Cu^{2+} + e \rightleftharpoons Cu^{+} \qquad \text{(slow)}$$

$$Cu^{+} + e \rightleftharpoons Cu \qquad \text{(fast)}$$

Lorenz, Moumtzis and Schmidt have suggested that UPD occurs

over a wide range of potentials because different adsorption sites on the Au offer a wide range of bonding energies[412]. They quoted studies of H deposition on Pt by Will and Knorr[12] and Breiter[106] as evidence for the same feature.

In later work[415,416], Lorenz and his co-workers describe the UPD peak observed at high Cu^{2+} concentrations as a "sorption peak of Cu^{2+} ions", and relate their findings to the partial discharge mechanism of Schultze discussed in Section 1.5.1.3. This is quite unwarranted in view of the quantitative proof by Schmidt and Gygax[414] that the Cu on the Au surface is in a fully discharged state.

Lorenz, Moumtzis and Schmidt[411] made a potentiodynamic study of Cu electrodeposition on Au in a potential range involving considerable bulk Cu deposition. They found that the anodic charge always exceeded the cathodic charge because of additional currents arising from the oxidation of Cu^{+} produced by chemical stripping of bulk Cu deposits[408] at potentials cathodic to the Cu/Cu^{+} redox equilibrium (see Section 1.5.1.8). The difference between the anodic and cathodic charge was greater at slow sweep rates, since bulk Cu then remained on the electrode longer, allowing more Cu^{+} ions to be produced in the chemical stripping reaction. The charge passed in the UPD peak at low coverage was in excess of that required to deposit a monolayer of Cu from Cu^{2+}, particularly during the anodic sweep, and this discrepancy was related to the formation of Cu^{+} as a stable intermediate in the reduction process.

1.5.2.5 Kinetics and reversibility

The kinetics and reversibility of Cu deposition on Au have apparently never been studied systematically. The symmetry of the

anodic and cathodic potentiodynamic current-voltage profiles at sweep rates below about 1 $V\,s^{-1}$ [411] suggests that the processes involved are moderately reversible provided that thick deposits of bulk Cu are not laid down.

The most recent publication of Lorenz et al.[416] contains the puzzling statement that "a mathematical treatment of the experimental results obtained by cyclic voltammetry under semi-infinite diffusion conditions[417] (relatively high Cu^{2+} concentration in the electrolyte and low scanning rates) showed that the diffusion of Cu^{+} ions from the electrode surface into the bulk of the solution can be considered as the rate-determining step".

1.5.2.6 Effects of competing adsorbates

Raducanu and Lorenz[410] studied the effects of adding surface-active molecules (β-naphthoquinoline and dibenzyl sulphoxide) to the electrolyte. The amount of Cu deposited at underpotential was reduced by these additions and the deposition became more irreversible. This was explained in terms of a simple surface-blocking mechanism where the presence of the surfactant prevented access of Cu to the adsorption sites.

1.6 Adsorption of Pb

1.6.1 Adsorption of Pb on Au

1.6.1.1 The extent of underpotential deposition

Pring reported in 1913[25] that the rates of electrochemical surface reactions on thin Pb electrodeposits differed from those on thick deposits and Pb metal electrodes. The existence of such effects

in the electrodeposition of Pb itself was shown when Coche[418] found that measurable amounts of Pb could be deposited on Au at potentials anodic to the Nernst potential of Pb.

The first systematic study of the initial electrodeposition of Pb was made by Mills and Willis[419] in 1953. Making slow charging curves in alkaline $Pb(Ac)_2$ solutions, they found that 500 $\mu C\ cm^{-2}$ of Pb was deposited, in two distinct waves, before the reversible deposition potential was reached. In view of the roughening of their electrodes caused by a preparative etch, they concluded that this pre-bulk deposit was rather less than a complete monolayer. After the formation of the initial underpotential deposit, the potential rose briefly as bulk deposition commenced and then fell back to a constant value as visibly thick Pb deposits were laid down. This evidence of a crystallization overvoltage prompted the authors to suggest that the UPD would form a deposit of uniform thickness, but that at the Nernst potential, deposition would only occur at discrete Pb crystallites.

Schmidt, Moser and Riesen[420] investigated the adsorption of Pb on Au by means of slow potentiodynamic sweeps. The amount of UPD in 10^{-3} M Pb^{2+} solutions was thought to represent a coverage of more than one monolayer.

Schmidt and Gygax[421] used a new type of four-electrode cell[414] in later investigations. A generator electrode made of the metal to be deposited was potentiostatted so as to continuously replenish the solution to a preset concentration as the deposition proceeded. The current in this generator circuit gave a continuous measure of the precipitation rate, which could be compared with the discharge rate expressed by the current at the working electrode. The charge in the

underpotential deposit varied from 0.42 to 0.465 mC cm^{-2} according to the pH of the solution and the other ions present.

In summary, estimates of the charge involved in the UPD of Pb on Au are as follows, in order of publication: Mills and Willis[419], 500 μC cm^{-2}; Schmidt and Gygax[421], 420-465 μC cm^{-2}; Takamura, Takamura, Nippe and Yeager[358], 400 μC cm^{-2}; Schmidt and Wüthrich[422], 374 μC cm^{-2}; Adzic, Yeager and Cahan[423], 300 μC cm^{-2}; and Takamura and Sakamoto[424], 450 μC cm^{-2}. Values obtained with single-crystal substrates[423] were lower, 225-250 μC cm^{-2}, perhaps because the surfaces were smoother.

1.6.1.2 Resolution of component processes

The current-potential profiles of Schmidt and Gygax[421] showed two UPD peaks. The more cathodic of these had a much narrower half-width than the other. More recently, several groups of workers have resolved the UPD into four or five distinct peaks[412,422-424]. One of these peaks, at about 0.05 V, corresponds to a charge-passage of about 80 μC cm^{-2} [423] yet has a half-width of only 0.01[423] or 0.02 V[422]. It will be referred to[423] as the "spike" peak.

Schmidt and Wüthrich[422] suggested that the thermodynamics of Pb deposition corresponded to Langmuir- or Freundlich-type isotherms. Adžić, Yeager and Cahan[423] however, noted that the "first deposition peak" was too wide to correspond to a Langmuir isotherm, and the "spike" peak too narrow. It has since been shown[424] that the "first deposition peak" considered by Adžić et al.[423] is the sum of two component peaks.

Vicente and Bruckenstein[425] observed that plots of the amount of Pb deposited as a function of time at constant potential

consisted of two linear sections separated by a discontinuity occurring after the passage of about 247 μC cm^{-2}. Ellipsometric[412] and resistivity[605] studies show discontinuities in the electrical properties of the Pb film at similar coverages (230 μC cm^{-2}[412] and ~200 μC cm^{-2}[605], respectively).

1.6.1.3 The state of the deposit

Schmidt and Wüthrich[422] used their four-electrode cell to compare the charge consumed in deposition at the working electrode with that produced by Pb dissolution at the generator electrode. They concluded that the electrodeposited Pb could retain no more than 5% of its charge in the ionic state. Vi cente and Bruckenstein[425] confirmed the metallic nature of the underpotential deposit using a ring-disc electrode system. By comparing the ring and disc currents in a desorption sweep they showed that if Pb^{2+} were adsorbed on the electrode, it could cover no more than 3% of the surface.

Despite the experimental evidence that the Pb deposits are in a fully discharged condition, Adžić, Yeager and Cahan[423] interpreted the deposition at potentials anodic to the "spike" in terms of specific adsorption of partially discharged Pb^{2+} ions, and the spike itself as an abrupt surface phase-transition leading to the formation of a metallic layer.

1.6.1.4 Reaction mechanisms proposed

Because of the evidence for the metallic nature of Pb electrodeposits, the chemical reaction is not in question. However, as with H, the cause of the multiple adsorption states of Pb has not been established.

Schmidt and Wüthrich[422] fitted the data to various isotherms. Unfortunately they worked from charge-potential plots rather than their well-resolved current-potential data. Isotherms were constructed on the erroneous assumption that only two consecutive deposition waves occurred, and are therefore of no consequence.

The potentiodynamic data of Vi cente and Bruckenstein[425] also resolved the UPD into only two component processes. The authors suggested that the low-coverage peak (occurring at potentials anodic to the "spike") represented the completion of a close-packed square lattice monolayer of Pb having the same area as the electrode, since the experimental charge involved (247 $\mu C\ cm^{-2}$) was close to the theoretical value for such a model (260 $\mu C\ cm^{-2}$). This would imply an absence of localized bonding forces, since the adsorbed Pb atoms would be in very many different geometrical relationships with substrate atoms. It would also imply that bulk Pb is not formed (i.e., the Nernst potential is not reached) until the average deposit thickness reaches 1.5 atoms, a similar value to that found for Cu on Pt. Takamura, Watanabe and Takamura[426] have extended this theory by suggesting that every peak on the current-potential profile indicates the existence of a different type of adsorbed phase. The factors accounting for the differences were not discussed.

Adžić, Yeager and Cahan[423], on the other hand, suggested that the different peaks arise from the different crystallographic faces exposed by the electrode. Potential-cycling of single-crystal Au electrodes was thought to cause the development of other low-index planes on the surface, and an evaporated polycrystalline surface was thought to characterize the equilibrium distribution of crystal faces in the surface.

The specular reflectance of an Au electrode changes considerably as small quantities of Pb are deposited on it, although the sign of the change depends on the wavelength of the incident light[358]. The reflectance change is linear with the deposition charge[412] except for a discontinuity at the "spike" peak[423], which led Takamura, Sato and Takamura[412] to suggest that the "spike" peak corresponded to the adsorption and desorption of a different type of adsorbed Pb from that deposited at higher potentials. Unfortunately reflectance data give no information about the nature of the Pb-Au bond[412,423] although it is possible to conclude that the electronic properties of the Pb change abruptly at the potential of the "spike". Preliminary ESCA studies of the Pb monolayer[423] showed that its properties were different from those of bulk Pb (cf. Pring's observation in 1913[25]), but similar to those of bulk Pb having an oxidized surface.

1.6.1.5 Kinetics and reversibility

The similarity between the anodic and cathodic current-potential profiles in Pb deposition makes it quite clear that the adsorption and desorption reactions are rapid[424]. Lorenz, Hermann, Wüthrich and Hilbert[416] fitted the adsorption data to a kinetic model where surface diffusion to various types of adsorption sites was rate-controlling, and charge-transfer only occurred at steps on the electrode surface. Using curve-fitting methods, they found that the exchange-current density of the adsorption process was several A cm^{-2}, i.e., about four orders of magnitude higher than for Cu on Au.

1.6.1.6 Effects of crystallography of the Au surface

Adžić, Yeager and Cahan[423] studied the UPD of Pb on single-crystal Au substrates. The occurrence and potentials of various current peaks were dependent on the surface crystallography and, on the (110) and (111) surfaces, the potentiodynamic profile was dominated by a single peak. The authors suggested that an anodic pretreatment process might have exposed other surface crystallographies by micro-roughening the electrodes (see also Section 1.4.2.9) and in addition, the current-potential profiles published showed overall residual currents, differing from crystal to crystal, which cast some doubt on the reliability of the work.

1.6.1.7 Effects of competing adsorbates

The UPD of Pb is shifted to more cathodic potentials by anions in the order $Br^- > Cl^- > CH_3COO^- > NO_3^-$ [420]. The addition of NaCl to $HClO_4$ solutions also displaced the Pb deposition reaction to more cathodic potentials[425]. In Cl^- and CH_3COO^- solutions, the $PbCl^+$ [425] and $(CH_3COO)_xPb^{2-x}$ [422] species will first undergo decomplexation before deposition occurs. The addition of aliphatic amines to the solution once again moved the deposition potentials cathodically, the effect increasing with the number of C atoms in primary amines[424]. This specific adsorption of amines redistributed the Pb amongst the spectrum of bonding states, although the total UPD charge was hardly altered.

The solution pH does not affect the UPD charge[421], but the pH-dependence of the individual peak potentials cannot be gauged from the data available.

1.6.1.8 Surface rearrangement processes (alloy formation)

The unusual reversibility of the adsorption of Pb on Au shows that irreversible surface rearrangement processes, such as those found in the adsorption of O species on Pt and Au, do not normally occur. The existence of much slower rearrangement processes has, however, been established by the detection of surface alloy formation.

Conrad reported in 1903[427] that the rest potentials of noble metal electrodes covered by thin layers of Pb became gradually more anodic with time of immersion in an electrolyte. He explained this effect in terms of a slow reaction forming surface alloys. Schmidt and Gygax[421] observed new anodic desorption peaks in potentiodynamic studies when bulk Pb deposits were left on Au. They subsequently correlated the appearance of these new peaks with the detection of the intermetallic compounds $AuPb_2$ and $AuPb_3$ by X-ray diffraction[428] cf.[605]

Schmidt and Wüthrich[422] later showed that alloy formation did not occur as long as the coverage of Pb was kept below a monolayer. After holding the potential of an Au electrode just anodic to the Nernst potential for 10h, only the dissolution peaks corresponding to the monolayer were observed in an anodic sweep. The Pb deposition current decayed rapidly to zero if the potential sweep was stopped above the Nernst potential. Thus it was established that the UPD is reversible and that alloying does not occur without the presence of Pb phase nuclei.

CHAPTER 2

THE NATURE OF CHEMISORPTION ON METALS

2.1 Distinction between chemisorption and physical adsorption

Chemisorption occurs when a species interacts sufficiently strongly with a substrate to cause its electronic orbitals to overlap those of the surface and form a chemical bond. In physical adsorption the interaction is so weak that the electronic structure of neither phase is appreciably altered. Although theoretical models of physical adsorption treat the adsorbate and adsorbent as thermodynamically separate phases, experimental results suggest that adsorption always causes some electronic perturbation.

The attractive forces in physical adsorption can arise from interactions between dipoles, or between dipoles and induced dipoles, or from quantum-mechanical London dispersion forces produced by the response of polarizable electrons to the instantaneous dipoles created by nearby electrons. The forces involved are weak and non-directional, and generally vary slightly but continuously with coverage[429]. Thus the distinct bonding energies occurring in chemisorption systems over limited ranges of coverage are not observed.

In the simplest model of physical adsorption, the adsorbate particles are assumed to be mobile on the surface in the sub-monolayer range of coverage. In this so-called Henry's law behaviour, the log of the coverage is proportional to the chemical potential of the adsorbate at the surface, measured either as an electrode potential or as the

logarithm of a gas pressure. At high coverages, Henry's law is no longer obeyed, since the mobility of the adsorbates is restricted by their finite size and mutual interaction. Transitions from mobile to localized adsorption may also be induced by lowering the temperature of a system which obeys Henry's law[430]. The arrangement and mobility of adsorbates on surfaces has been studied by LEED (e.g.[431,432]), but the changes in mobility do not correspond well to theoretical expectations[433].

The general physical adsorption isotherm of Hill[434] and de Boer[435] treats the adsorbate as a two-dimensional Van der Waals gas film, mobile on a substrate, but in equilibrium with a bulk gas phase. This isotherm has been refined and widely applied by Pierotti and Thomas[436,437].

Two possible causes of the experimental variation in heat of adsorption with coverage have been postulated: (a) intrinsically heterogeneous adsorption sites on the adsorbent surface, and (b) induced heterogeneity arising from lateral interactions between adsorbed species. Models involving physical adsorption on heterogeneous surfaces have recently been reviewed by Sams[429]. Sinanoglu and Pitzer[438] found that the Lennard-Jones (6:12) potential function describing the interaction of two particles in free space[439] required an additional repulsive potential term proportional to r^{-3} to describe the interaction of two particles adsorbed on the same substrate. The resulting isotherm agreed well with experimental heat of adsorption data[440]. Pierotti[436] and Müller[441] have considered the perturbation of the surface arising from the presence of the adsorbate. Although this makes their treatments strictly outside the area of physical adsorption, the consideration of dispersion force interactions and a polarization potential due to

interaction with the surface electric field[437], and the perturbation of the double-layer at the bare metal surface[442] by adsorbates[441] have given useful results. The change in substrate work function caused by adsorption, evaluated by FEM, was found to decrease with increasing work function and/or with increasing packing density of the metal surface lattice[441].

In contrast to physical adsorption, the formation of real bonds in chemisorption processes produces new chemical compounds at the surface. It should be noted that chemisorption bonds are much more difficult to characterize than molecular bonds because (i) the state of surface atoms is not really understood; (ii) it seems that in chemisorption the adsorbate is often bonded to more than one atom in the adsorbent surface; (iii) this multiplicity of bonding and the interactions between adsorbate particles can alter the energetics of the surface with respect to the bonding of further adsorbate particles.

Theories of the nature of the chemisorption bond will now be reviewed in roughly the same order in which they were proposed. Section 2.2 deals with theories based on the formation of diatomic molecules through pairwise bonding between a single adsorbate species and a single adsorbent atom. Covalent, ionic and metallic bonding will be considered in treatments which are essentially classical, i.e. do not allow for interactions between the adsorbent atom involved in the bonding and other atoms in the adsorbent. Section 2.3 considers treatments in which a full quantum-mechanical description of the chemisorption bond has been attempted. The consequences of crystal-field splitting on the

location of bonding sites will also be discussed. It will be argued later in this thesis that electrochemical techniques allow a more convenient sub-division of chemisorption into Faradaic electrodeposition or specific adsorption, according to whether the adsorption involves a net charge transfer, or is merely a redistribution of charge at the interface.

2.2 Chemisorption treated as bonding to an isolated substrate atom

Early theories of surface bonding postulated that the adsorbate would react with a single atom in a surface. The bond would be analogous to that in a diatomic molecule, and was assumed not to affect the properties of any other atoms in the substrate. In extreme cases, such a bond could be completely covalent or completely ionic.

2.2.1 Covalent bonding

Pauling estimated the covalent bond energies of heteronuclear diatomic molecules in 1932[443] by averaging the bond energies of the corresponding homonuclear molecules and adding a term to allow for polarity in the bond arising from the difference in electronegativity of the component atoms. Eley used the same approach to estimate the energies of covalent adsorption bonds[444]. Assuming that surface bonds in a metal substrate (M) would not be broken during, e.g. H adsorption, Eley estimated the covalent M-H adsorption bond strength as the difference between the M-M and H-H bond (in H_2) energies, plus the electronegativity difference term. The M-M bond energy may be taken as 1/6 of the heat of sublimation, but Eley's estimates of the electronegativities (from

zero-coverage dipole moments calculated from Mignolet's surface potential data[445] by Malone's relationship[446]) lead to estimates of M-H bond energies which differed widely and randomly from experimental data[447]. Better estimates of the adsorption energies of H on transition metals were obtained by Stevenson[448] by estimating the electronegativity of the adsorbate as the average of its ionization potential and electron affinity, and that of the metal as an empirical fraction of its work function. Stevenson's estimates of the bond energies of H on noble metals were poor, and those for the adsorption of other gases were unsatisfactory. More recent calculations based on Eley's equation have met with no more success[447].

Dowden has proposed a bond-orbital model of chemisorption based on the valence-bond theory[449], where an intermediate state of chemisorption, using d-orbitals only, lies between physical adsorption and full chemisorption using dsp hybrid bonds. The transfer of an adsorbate from this intermediate state to the final state would require little activation energy on a transition metal, but more on a non-transition metal substrate.

Theories of covalent chemisorption have usually been tested by their applicability to the adsorption of gases and organic molecules on metal substrates. However, even systems chosen to avoid complicating factors frequently exhibit a multiplicity of chemisorption bond energies at different coverages, which cannot be explained by simple models involving a covalent bond to a single surface atom. For example, flash desorption studies[450,451] show that CO chemisorbs on W in states having two different bond energies, and that the more strongly bound state can

be resolved into three sub-states. The explanation suggested[450,451] is that the multiple states of the strongly bound species relate to adsorption on different crystal planes of the substrate (intrinsic heterogeneity effect), and that the weakly bound species is CO adsorbed on single sites which have become isolated after a random 2-site adsorption into strongly bound states. The adsorption of larger organic molecules studied in research on catalysis[e.g.447,452] can likewise only be understood in semi-empirical terms.

2.2.2 Ionic bonding

A particle ionically bonded to an electrode carries a charge which attracts it to the metal because the electrode surface carries a net charge of opposite sign. Since the charge on a non-metal cannot be conveniently varied, classical treatments involving ionic bonds in surface diatoms have not been widely applied to such systems. Sophisticated analyses of adsorption on non-metals have, however, been developed in terms of band structure and surface states[447,453,454], but these are outside the scope of the present work.

A simple classical estimate of the strength of an ionic chemisorption bond is given by the difference of the ionization potential of the adsorbate (I) and the work function of the metal (ϕ), plus the attractive (image) energy between the ion and the metal surface, i.e.

$$-\Delta U = [-I + \phi + \frac{q^2}{4r}]$$

where q is the charge on the ion and r its equilibrium distance from the surface. For the chemisorption of a negative ion

$$-\Delta U = [-\phi + A + \frac{q^2}{4r}]$$

where A is the electron affinity of the adsorbate. The last term in both equations is the classical image potential, and r is usually taken as the radius of the ion.

Since numerical estimates of heats of adsorption based on this type of theory are in poor agreement with experimental data for the adsorption of O, N and H on metals which are neither of the alkali nor alkaline-earth series[447], it is probable that local ionic bonds are not formed in these chemisorption systems. Much better agreement has been found with the experimental heats of adsorption of alkali metals on W[455], and successful wave-mechanical treatments of these systems in terms of ionic bonding, where interaction effects between substrate atoms are included, will be discussed later in Section 2.3.3. Poor agreement with experimental data usually casts doubt on the applicability of the simple classical ionic bonding model[456]. The chief sources of error probably arise because the model takes no account of: (a) electronic interactions between substrate atoms, (b) non-integer charge on the adsorbate (see discussion in Section 1.5.1.3), (c) the effects of adsorption on the substrate work function[457], and (d) the extent to which the image potential formula is valid at distances comparable with the lattice spacing of the substrate.

The fraction of ionic character (f_i) in an adsorption bond may also be calculated from Higuchi, Ree and Eyring's quantum-mechanical model of chemisorption as the formation of diatomic surface molecules[457,458].

f_i is defined by

$$\mu = f_i \, e \, r$$

where μ is the dipole moment of the bond, e the electronic charge, and f_i is calculated from

$$\frac{1}{f_i} = 1 + \frac{(\Delta U - \Delta U_i)}{(\Delta U - \Delta U_c)}$$

where ΔU is the chemisorption bond energy, and ΔU_i and ΔU_c are the energies of purely ionic and covalent bonds respectively. Heats of adsorption calculated from semi-empirical estimates of ΔU_i and ΔU_c agreed satisfactorily with experimental data for the adsorption of Na, K, Cs, Sr and Ba on W, and for H, O, N, and CO on a range of metals. The adsorption of alkali metals on W was found to be entirely ionic. This was confirmed by Levine and Gyftopoulos[459] who reviewed data for the adsorption of a wide variety of metals on W, and by Schmidt and Gomer[460], who studied the adsorption of K on the (110) surface of W single-crystals. However, a controversy has arisen about whether the ionic bonds involved are localized in the substrate, or delocalized (metallic but polar). Utsugi and Gomer[461] have suggested that the broadening of the s level in Cs arising from adsorption will make part of the s "band" lie below the W Fermi level, so that the two metals will share conduction electrons. Other authors consider that the formation of non-metallic surface compounds in adsorption "demetallizes" the surface atoms involved, so that surface atoms will no longer exhibit identical collective properties. The quantitative perturbation of the properties[462]

of the substrate metal is calculable by quantum-mechanical methods, and will be discussed in Section 2.3.3.

The Higuchi, Ree and Eyring model[457,458] suggested that Ba-W and Sr-W bonds are mostly ionic with some covalent character (f_i = 0.97 for Ba and 0.67 for Sr). Adsorption bonds in the gas-metal systems (e.g. Pt-H) are covalent with only a small amount of ionic character (f_i = 0.02 to 0.09). This is consistent with the electrochemical behaviour of H on Pt already discussed in Section 1.3.1, and the surface potential measurements of Collins and Blott[463] for H on W.

The extent to which the chemisorption bond between O and transition metal surfaces is ionic is not clear. The change in surface potential which occurs in O chemisorption has been taken to show that the O is in an atomic state[464], although this interpretation is not unequivocal[465]. In any case, the interpretation of surface potential data is called into question by the possibility of place-exchange in the surface even at low coverages by O species (see Section 1.4).

2.2.3 Metallic bonding (classical treatment)

A simple classical theory of the adsorption of a metal on a substrate of another metal was recently put forward by Gerischer, Kolb and Przasnyski[466,467]. On the basis that the work function of the adsorbate (ϕ_A) may be taken as a measure of the A-A bond strength, and that the energy required to discharge an A^+ ion on the substrate S would be $\phi_S - \phi_A$, they plotted the differences of the potential for the deposition of approximate monolayers of A on S and that for the

reversible deposition reaction of A on A versus ($\phi_S - \phi_A$). The linearity of plots of data from a large number of metal systems confirmed their assumption that the adsorbate is deposited in an entirely discharged state. In some ways this linearity is surprising since no account was taken of lattice energy terms.

2.3 Chemisorption treated as bonding to a number of interacting substrate atoms

2.3.1 Introduction

Doubts about the physical reality of surface diatomic models of chemisorption and the generally poor agreement between their predictions and experimental data have prompted a number of recent attempts to formulate a complete quantum-mechanical model of the interaction between an adsorbate and a real metal adsorbent. A review of these approaches will now be introduced by a summary of our knowledge of delocalized bonding in metals and alloys.

2.3.1.1 Bonding in metals

The metallic bond results from an attractive interaction between delocalized electrons and a lattice of positively charged metal ions. These cohesive forces are opposed by the mutual repulsion of the free electrons and by local repulsion between adjacent metal ions. The delocalized nature of the bonding makes many properties of metals and alloys rather insensitive to their structural geometry, e.g. the cohesion of metals varies little with ordering or solidification.

It was Drude[468] who first proposed that atoms in metals are

positively ionized, and held together by their interaction with the delocalized electrons, which they have lost and are now "free" to move throughout the crystal. Both Drude[468] and Lorentz[469], who soon added further developments to the theory, assumed that the electric field within the metal crystal would be homogeneous and that the conduction electrons would obey the Maxwell-Boltzmann statistics developed for the kinetic theory of gases. After Pauli's proposal of quantum (Fermi-Dirac) statistics[470], and experiments[471-473] which confirmed the wave nature of electrons proposed by de Broglie[474], Sommerfeld modified the model so that the electrons moved in quantized states in a uniform potential[475].

Bloch[476] then calculated the effects of the periodic electrostatic field established by the lattice of metal ions on the wave equations for the delocalized electrons. Bloch's replacement of uniform potential fields within crystals by structure-sensitive fields made a basis for the development of the molecular orbital (MO) theory by Hund, Mulliken, Lennard-Jones and others. It also had the important implication that the electronic energy E would not be a continuous function of the wave number k ($k = \frac{2\pi}{\lambda} = 2\pi\frac{mV}{h}$; $E = \frac{mv^2}{2} = \frac{h^2k^2}{8\pi^2m}$), but would contain "gaps" of forbidden energies.

Making the assumption that the perturbing lattice potential would be weak, Brillouin[477] derived the allowed ranges of electronic energies. He illustrated them by drawing polyhedra in k-space (Brillouin zones) to illustrate the limits of the continuous energy functions. Since the perturbing field was weak, the electrons were "nearly free" within the lattice, and apart from the energy gaps represented by the

surfaces of successive polyhedra, the overall dependence of E on k remained close to the parabola of Sommerfeld's model[475]. In monovalent metals, the valence electrons will half-fill the first zone, and all take part in the conductivity process, giving a situation close to that of a free-electron model. In divalent metals, the first zone is exactly filled by the two electrons per atom. Conductivity can then only arise from band overlap in the electronic states, or spillover of electrons across narrow gaps between one zone face and the next zone. This leads to the important conclusion that a detailed knowledge of the intersection of the Fermi surface with the Brillouin zones of the crystal is required to characterize the conduction electrons in a metal. The crystal structure itself imposes directional constraints on general properties such as the valence-electron-to-atom ratio and the density of states at the Fermi surface.

This theory of "nearly-free" electrons provided a basis for discussion of the relative stability of alternative structures in metals and alloys[478,479] and of the occurrence of intermetallic compounds[480,481]. As more refined wave functions were developed[482-484] to allow for a constant weak field between the atoms (electrons free), and an atomic potential function (strong field) near the atom cores, it became clear that the success of the original model had been largely fortuitous[485].

The original approaches to the band theory assumed that the electrons did not interact with one another, and that they filled all possible energy states up to the Fermi level but none above it. The resulting Fermi surface was a sphere centered on the origin in reciprocal space. More recent "many-particle" calculations, which recognize

electron-electron interactions, show that the edge of the Fermi surface is somewhat diffuse[486-488] and that it is distorted outward as it nears zone boundaries[489]. The topology of the Fermi surface has been studied by the anomalous skin effect,[485,490] and the de Haas-van Alphen magnetic susceptibility effect.[485]

Some information on the actual electrons involved in bonding inside pure noble metals is given by Brooks' detailed quantum-mechanical calculations of the cohesive energy of Cu, Ag, and Au.[491] In order to obtain agreement with experimental values, it was necessary to include interaction terms arising from the overlap of the inner shells of the metal ions which occurs at their equilibrium separation. Mott[492] subsequently suggested that the overlap term probably arose from d-shell electrons, since the correction was least for Ag, whose single valence and lack of colour imply that its d-electrons are more strongly bound than those of Cu or Au. The d-electrons would then contribute to the cohesion by hybridization of the 3d band with the 4s and 4p electrons.

2.3.1.2 Bonding of foreign atoms within alloys

Before discussing the nature of bonding of foreign species at metal surfaces, it will be useful to consider the perturbation of the collective bonds in a metal arising from the introduction of foreign (alloying) elements into the lattice. Since chemisorption bonds also are generally delocalized to a greater or lesser extent (Section 2.3.3), the electronic perturbations of the substrate caused by alloying will be similar in principle to those caused by adsorption. In addition, adsorption will itself lead to alloying in cases where the substrate

atoms bond more strongly to adsorbate species than to one another, and where the other properties of the system allow the adsorbates to dissolve so as to maximize their coordination by substrate atoms.

In some alloys, the foreign atoms are dispersed at random throughout the host lattice, either substituted for host atoms or in the interstices between them. In others, interactions between the atoms may either aggregate the foreign species into local clusters, or disperse them into ordered superlattices.

In view of the many complications arising from the bonding of unlike metal atoms, it is not surprising that theoretical analyses of bonding developed for pure metals have not been extended to general models applicable to alloy systems. Some progress has been made, but the main advances have arisen from detailed structural studies of alloy systems and careful discussion of the empirical rules which have emerged, largely from the work of Hume-Rothery and his co-workers[481,493].

Interstitial solid solutions are only found when the diameter of the alloying atom is <2 Å. The extent of substitutional solid solubility is mainly limited by three factors: (i) the crystal form of the foreign element, (ii) the relative sizes of the two atoms, and (iii) the electronegativity difference of the two elements.

Substitutional solid solution does not occur to any appreciable extent when the two metals are from different crystal systems. It is also very limited if the atomic diameters differ by more than about 15%, apparently because the host lattice can only tolerate a limited strain energy. When this strain energy is exceeded, at a certain concentration

of the alloying element which will depend on its size, the host lattice may take up another structure having greater interatomic distances, or the foreign atoms may space themselves out symmetrically and form a superlattice to minimize the strain energy,[494,495] or they may be rejected by the host lattice and form local aggregates. Similar superlattices arise from size factor considerations in a wide range of alloy systems[496] (e.g. Laves phases, Zintl compounds and sigma phases).

The substitutional solid solubility of a foreign atom is also limited when its electronegativity differs considerably from that of its host. In this case, pairwise interaction between the unlike metal atoms gives rise to partially ionic local bonds. Analyses of the extent of localized bonding in alloys have important consequences in chemisorption, since any localization of conduction electrons will change the density of states at the Fermi surface. This will be discussed in detail in Section 2.3.3.

When a metal is alloyed with another metal having a very different electronegativity, the two components may locally form "intermetallic" compounds. These contain the different atoms in whole-number ratios and obey normal valency laws. However, their conductivity and reflectivity are often as great as those of metals and they are frequently stable over significant composition ranges, so their bonding cannot be entirely covalent. The formation of intermetallic compounds within a bulk alloy may be compared with the formation of surface compounds when a metal reacts with a strongly electronegative non-metal, e.g. O, S, Cl. In the latter case also the bond is predominantly covalent but with a certain degree of delocalization. In both situations, it is the

electronegativity difference which causes the formation of a compound rather than of a random solid solution.

Attempts to relate the limit of solid solubility arising from the electronegativity difference factor to the local bond energy between the two components[496] have met with little success. This may simply relate to the inaccuracy of the data available. Electronegativity values often vary with the method of measurement, e.g., standard electrode potential, heat of formation of a halogen bond, work function, or ionization potential. In addition, most heat of formation data are derived from the half-cell potentials of non-characterized alloy surfaces.[497,498]

Solid solubility is also restricted in the composition ranges in which "electron compounds" are found. The relationship between the composition and stability of such structures has provided a continuing challenge to the theoretical understanding of bonding in alloys. Hume-Rothery was the first to note that many isostructural metal compounds had identical ratios of valence electrons to atoms; either 21/14, 21/13 or 21/12[481,499]. These "electron compounds" are generally formed between atoms of similar size, although the tolerance for mismatch is greater than that in primary solid solutions. They exist over wide compositional ratios about the exact electron/atom ratios in both binary and ternary alloy systems, and both ordered and random solutions (probably containing short-range order) are found. A theoretical basis for their stability was first sought in the 1930's[478,479,500] in terms of the compositional dependence of the intersection of the Fermi surface with the faces of the Brillouin zones.

The simplest model of the effects of alloying elements in perturbing the electronic structure of their host involves merely the expansion or contraction of a spherical Fermi surface as the electron concentration is increased or decreased. The band structure of the host metal is assumed to be "rigid", i.e., changes in electron concentration only fill or empty pre-existing electron states characteristic of the unalloyed host lattice[501]. If the Fermi surface lies well inside the first Brillouin zone, the relationship between the electronic energy E and the number of electrons with that energy, N(E), i.e., the so-called density of states function, is parabolic as in Sommerfeld's model for pure metals[475]. As the electron concentration is increased, the distortion of the Fermi surface as the Brillouin zone faces are reached[489], and the subsequent filling of states corresponding to the corners of the zone, give a maximum in the density of states at the Fermi surface, $N(E_F)$, as the Fermi surface just touches the nearest faces of the first Brillouin zone[478]. If an alloy system contains various possible phases, one may conclude in general terms that the most stable phase at any given composition will be that having the lowest Fermi energy, i.e., that structure whose density of states function deviates most above the Sommerfeld parabola[475] due to the outward distortion of the Fermi surface as it meets the Brillouin zone faces[489] when filled by the total number of electrons present. If, for example, the density of states function for primary solid solution falls below the parabola as "corner sites" are being filled in the Brillouin zone, one would expect that primary solid solutions of the foreign atoms would become less stable than other phases at that composition. Jones[478] and the other early workers found

surprisingly good agreement between the results of this approach and experimental data for limits of solid solubility. A recent NMR study[502] of long-range oscillations of electronic density around foreign atoms in a metal suggested that there is also a minimum in the total electronic energy ($\int_0^{E_F} E.N_E dE$) as the corner sites in the Brillouin zone are being filled.

Jones simple criterion for the limit of solid solubility[478] has more recently been disproved by experimental evidence that the Fermi surface touches the {111} faces of the first Brillouin zone even in unalloyed noble metals[490,495,503,504]. As an alternative, Hume-Rothery and Roaf[505] have suggested that the solid solutions become unstable due to a fall in $N(E_F)$ as the Fermi surface touches the square {200} faces of the Brillouin zone. This would seem to explain the stability of electron compounds. It may be, however, that the transitions in stability are not abrupt at all, and that a steep fall in the density of states at the Fermi surface is an oversimplified criterion for the breakdown in stability of a phase.

The electronic perturbation caused by foreign atoms in a metal lattice cannot generally be studied by the methods developed for pure metals because, unless either a superlattice or an intermetallic compound is formed, considerable effects arise from electron scattering[504]. The sparse and indirect evidence available[496,504], e.g., based on the acoustic attenuation of very high intensity pulsed magnetic fields and the positron annihilation effect, does suggest however, that reasoning based on the intersection of Fermi surfaces and Brillouin zones may also be applied to alloys, and that the electron/atom ratio has a very important influence on alloying behaviour.

Unfortunately however, the very basic question of the extent to which the conduction electrons of the solute will enter the conduction band of the alloy remains largely unanswered[492,506,507]. Since the electron concentration in an alloy can be reduced by the formation of new localized states near the solute atoms (effectively leaving them incompletely ionized, with a polar bond to the surrounding metal atoms[506]), or increased by hybridization of the d electrons with s states, other parameters relating to some "effective electron/atom ratio" have been proposed[508,509].

In primary solid solutions where the electron concentration is increased by alloying (e.g., in alloys of noble metals with polyvalent solutes), the calculations of Friedel[506] and Flinn[510] predict the occurrence of short-range order. Long-range order is expected when the solute concentration exceeds about 25%, as for example in Cu_3Au. These theories have not, unfortunately, received thorough experimental scrutiny.

A significant new approach to the band structure of noble metals and their alloys was proposed by Cohen and Heine[484] in 1958. It has become known as the "soft band" model and has proved particularly useful in assessing the effects of alloying on the solvent metal band structure. Cohen and Heine assumed that the energy states corresponding to the centres of Brillouin zone faces were either s-like or p-like in character, and that the band gap could be expressed as the energy difference between the s and p states ($E_s \sim E_p$). They then introduced a distortion parameter (d_{sp}) which measured the distortion of the Fermi surface from a sphere by the amount by which the energy at the zone

face was depressed below the free electron parabola:

$$d_{sp} = \frac{\frac{1}{2}(E_s - E_p)}{\frac{1}{2}(E_s + E_p) - E_F}$$

When $|d_{sp}| \geq 1$, either E_s or E_p is depressed below E_F, so the Fermi surface bulges outwards and touches the zone faces. (Note that Gadzuk and Plummer[511] have derived a similar distortion parameter ($R(\varepsilon)$) in the interpretation of adsorption data obtained by FEM). Since, in an alloy, the terms E_s and E_p are averaged values, the dissolution of foreign atoms in a noble metal will immediately affect the shape of the Fermi surface by altering the distortion parameter, as well as by affecting the band gap. The assessment of the quantitative effects of solute elements on the band structures of noble metals is extremely difficult in view of the complexity of the possible effects of d-band hybridization[484] on the interaction of the Fermi surface and the Brillouin zones.

The inconclusiveness of the present theories may be illustrated by their application to Au-based alloys. The soft band model[484] predicts an increase in the band gaps as a result of alloying Au, and experimental results[512] show that the change in band gap is indeed smallest with those solutes which show the greatest primary solid solubility (i.e., interact least strongly with the Au). Au-Al alloys are an exception, but this may be due to the d-band lying above the Fermi level, which would give an effect opposing the increase in the band gap. The lower limits of primary solid solubility in Au than in alloys based on Cu or Ag had been explained in terms of a greater-than-unity valence for Au[513,514], relative size effects[515], and in terms of electronegativity

differences[516]. All three approaches could explain the unusual structures of dilute alloys based on Au, but seem inadequate to explain the more normal γ and ε phases found in higher alloys. The soft band model[484] is more successful. It predicts the increase in band gap and increased distortion of the Fermi surface on alloying, which could account for the peculiarities of the dilute α, β and ξ phases. Since the higher alloys contain more "solute" than Au, their band structure should depend more on the solute, and Au-, Ag-, and Cu-based alloys would be expected to behave similarly, as is confirmed experimentally[512].

Thus, theoretical analyses of the relative stability of different structures in noble metal alloy systems are almost always tentative. It may, however, be generally concluded that size effects are present in all metallic solid solutions, and that systematic changes in physical properties often relate to specific interactions between the Fermi surface and the Brillouin zone over the range of electron/atom ratios involved.

2.3.1.3 Formation of surface states on bare metals

The above descriptions of electronic energies within metallic structures do not necessarily apply to the electronic states at their surfaces where the field of the positive ion lattice is inhomogeneous and discontinuous. "Free" electrons may be localized at the surface in two types of surface states. "Intrinsic" surface states arise on bare metal surfaces simply as a consequence of the interruption of the lattice, while "extrinsic" states are caused by the application of an external field at the surface, e.g. due to an adsorbate. Intrinsic states will

be discussed in this section and extrinsic states in Sections 2.3.2 and 2.3.3.

Tamm[517] first pointed out that intrinsic surface states would exist on the end of a one-dimensional atomic chain having one electron per atom moving in a field of δ-functions centered on each atom but with a finite potential at the end of the chain. Assuming that the electrons could tunnel through the potential barriers, Tamm found that a new eigenstate was localized at the "surface" (end atom), with an energy outside the bands of states existing in the chain, and that there were as many intrinsic states as band gaps in the chain.

Other mathematical approaches to Tamm states[518-520] subsequently showed that they would occur in pairs in finite atomic chains with closely-spaced levels as long as the chain was not too short[518]. Using the "nearly-free" electron approximation instead of Tamm's δ-functions, Maue[519] showed that the pairs of surface states arose from the localization of states which would be in the upper and lower band, respectively, of an infinite atomic chain.

The theory of Tamm states was generalized by Goodwin[521] in both the "nearly-free" and "tight-binding" approximations of a finite atomic chain. Despite the refinement of the models, Goodwin pointed out that the bulk states of real metals were insufficiently well understood to predict the consequent surface states which would exist within the band gaps. Neglecting electronic spin, the number of surface states would equal the number of surface atoms, so Tamm states would only be expected to have measurable effects in surface phenomena (e.g. photo-

emission and conductivity[519]), or in cases where for some reason there are few bulk conduction states (e.g. on semiconductors[522,523] or insulators[447]).

The nearly-free electron model involving a periodic potential without edge effects at the end atoms, described by Maue[519] and Goodwin[521], was approached in another way by Shockley[524]. He conceptually formed an atomic chain by reducing the interatomic distances from infinity to their equilibrium values. As this was done, the electron levels in the chain broadened into bands which subsequently overlapped. When this overlap occurred, a pair of states became localized at the "surface", having closely-spaced energy levels between the original bands. Shockley states are a general feature of three-dimensional crystals as well as the one-dimensional atomic chains originally considered. Since they arise from band overlap, they will always be unoccupied in monovalent metals, where the first Brillouin zone is only half filled. Tamm states, on the other hand (large lattice constant and uncrossed bands in Shockley's model; tight-binding case for Goodwin), will lie just above each energy band whether or not the bands have crossed.

Artmann[525] refined Goodwin's analysis, taking into account factors such as lattice vibrations, and verified Shockley's suggestion that the conductivity of semiconductors was largely due to the formation of surface states. The same may also be true with metals, to some extent, as evidenced by the anomalous skin effect[526]. Koutecky[527] has derived a very general quantum-mechanical model of energy states in crystals which gives Tamm and Shockley surface states in particular cases. Tamm states are localized near the surface when the potential gradient is considerable.

Shockley states arise from the unsaturated ("dangling") bonds which would protrude from the surface if the crystal lattice were interrupted but the crystal field maintained right up to the surface. Koutecký also found a third type of surface state, localized at the second atom from the "surface" (end of the chain), and with an energy level within the band gap. He called this a Shockley subsurface state.

The occurrence of surface states has thus been studied either by solving the Schrödinger equation for a periodic potential function of preconceived shape, or by choosing atomic orbitals, e.g. the H s-orbital[528], Wannier functions[527,529], Green's functions[530] or Bloch functions[476], and then using an LCAO-MO method to find solutions. Other approaches, such as the free electron network theory[462], and the Madelung potential method[531], have been used much more rarely.

The application of all these methods to real metal surfaces is extremely complex. The delocalization of electrons and the overlapping of bands aggravate the problem of calculating Shockley states, which is difficult to treat in elementary cases by the simplest LCAO approximation. Although Tamm states involve real surface potentials such as might be involved in chemisorption, and may be calculated by LCAO-MO methods, the overlap of electronic orbitals among neighbouring substrate atoms is completely neglected in their evaluation.

With respect to the theoretical analysis of the chemisorption bond, the most useful calculations so far are those which attempt to evaluate the density of states function at crystal surfaces[532-534]. As with many problems in electron band theory, the calculation may be

approached in two ways, by emphasizing either the "nearly-free" nature of the electrons far from the atomic cores, or the "tight-binding" situation close to the cores. Lang[534] has reviewed calculations using the first method, evaluating the electron-electron interactions in a homogeneous ("jellium") charge background, and then adding the perturbing effects of the discrete lattice charges by means of pseudopotentials[535]. The density of states function for a transition metal surface has been evaluated in the tight-binding approximation by Haydock and co-workers[532, 533]. They showed that not only the populations but also the energies of the main levels in the d-band differed according to the crystal system, the low-index surface chosen and the coordination of any particular atom in the surface.

2.3.2 "One-orbital" wave-mechanical models of chemisorption

The treatment of chemisorption bonding in Section 2.2 regards the adsorbate as one half of a surface diatomic molecule, unaffected by the bonding of the other half (the surface metal atom) to the rest of the metal. While this may be applicable to entirely localized ionic bonding, a more general model must allow the adsorption bond to be delocalized. In the extreme case, the adsorbate must be able to interact with every atom in the substrate, as in electroplating. The simplest approach to such a model is achieved by modifying the methods used to investigate surface states. The atom on the end of the chain, or one in an array, is replaced by an atom having the electrical properties of the adsorbate, and the effect of the resulting perturbation of the crystal field on the wave functions is calculated, usually by LCAO methods.

In the simplest case, the adsorbate is bonded on the end of a linear chain of atoms, each having only one electronic orbital, which only overlaps that of its nearest neighbour. As a chain of n atoms is built up, a band of states will be formed, represented by the (n-1) real roots of the wave equation[528]. If the remaining root is real, its associated energy state will also fall in the band, so all the states in the atomic chain will be delocalized. If, on the other hand, the remaining root is imaginary, it will represent a state outside the band, i.e., the state will be localized at the adsorbate atom, as in the ionic adsorption models considered in Section 2.2.

More specifically, Grimley[528] has shown that adsorption at the end of a chain of atoms with s-type orbitals gives two types of solution to the wave equation:

If the potential field of the adsorbate atom is varied so that it attracts electrons more and more strongly from the chain, the band states will first fall in energy, and then a Tamm state known as a P state will separate from the bottom of the band as a localized level. Finally, as the potential of the adsorbate atom becomes infinitely positive, the wave function for the P state degenerates to the atomic orbital it had in the isolated state, and the delocalized wave function has zero amplitude at the adsorbate. In this extreme case, adsorption could only be ionic.

In the converse situation, as the adsorbate becomes increasingly electropositive, the bond energy increases and then a type N state separates at the top of the band. Its energy will increase until

once again the adsorbate orbital has degenerated to its original atomic state and no longer overlaps with the wave functions of the band states. These results persist in three dimensions except that states localized at atoms on the ends of chains become bands of states localized at the crystal surface. The type N states are bonding states and the type P states antibonding in a manner analogous to that of states in diatomic molecules where the same terminology is applied.

Shockley states will persist after chemisorption only if the adsorption bond arising from the partial saturation of the free surface valencies is weaker than the self-bonding in the substrate. If the chemisorption bond is of comparable strength to the self-bonding, a Tamm state will always be formed. Koutecký[527] has therefore suggested that Shockley states may be expected in catalysis, and Tamm states in strong chemisorption where there is the possibility of surface compound formation. Thus, the models discussed in Section 2.2 regarding chemisorption as the formation of a diatomic molecule will all involve Tamm states[536].

Grimley's analysis of adsorption at the end of a chain of one-electron atoms[528] indicates that the bonding will be covalent if there is an equal probability of finding the Tamm state electron on the adsorbate as in the substrate. If the electron becomes localized on either the adsorbate or the end atom of the crystal, the many-centre covalent bond will become a molecular orbital surrounding only the adsorbate and the end atom, in a two-centre covalent bond. Since the conditions for true covalency are rather stringent, the bond is much more likely to be polar, but ionic bonds may also be two-centered or

many-centered. If the potential field of the adsorbate brings the bond energy to a value within the occupied band of states, the bonding will become a general delocalized interaction between the adsorbate and all the "conduction" electrons, described by Grimley as "metallic-like", and similar in many ways to the bonding within alloys discussed in Section 2.3.1.2. Five other types of bonding can arise on the end of a "one orbital" atomic chain[537] with up to two N or P states localized at the adsorbate.

Davison and Koutecký[538] have modified these theories to deal with adsorption on the end of a chain of alternate elements, in a treatment which may perhaps be used by future workers as a basis for the analysis of the situation in which very strong adsorbate-substrate bonds lead to alloying. They found that the electron energies in the chain lay in two bands separated by a gap characteristic of the pair of species involved, and that chemisorption states could lie anywhere between the extreme energies of the two bands.

Although chemisorption can, in general, produce as many localized states as the sum of the number of orbitals on the adsorbate, the number of adsorbent atoms perturbed by the bonding, and the number of bands of states in the substrate, a maximum of only two localized states is predicted by one-orbital treatments of adsorption on both one-dimensional atomic chains and three-dimensional lattices. These will be associated not only with the adsorbate, but also with as many of the substrate atoms as are perturbed by the adsorption. In the case of a three-dimensional substrate, there is a minimum of one localized state with the one-orbital treatment.[537]

The complexities of calculations on semi-infinite models prompted Blyholder and Coulson[539] to calculate chemisorption states on short finite chains and small, two-dimensional arrays. Replacing the basic Hückel MO treatment[521,528,540,541] by a more refined SCF-LCAO-MO calculation, they showed that the more manageable smaller models predicted essentially the same states as semi-infinite models. Adsorption above a corner atom was stronger than above one in the middle of an edge, and the main contributions in these two cases were concluded to be unsaturated valence bonds and localized states respectively. Heats of adsorption on these small atomic arrays depended to a great extent on the localized states involved.

Einstein[542] has recently extended the one-electron, tight-binding model of a simple cubic lattice to include the effects of adding a new energy level at the surface to represent an adsorbate. The resulting density of states functions for substrate atoms adjacent to the adsorbate showed features comparable to those of photo-electron spectra of W covered by a variety of adsorbates[543].

The first particles to adsorb on a surface can bond in doubly-occupied localized (Tamm) states which are essentially identical. As the coverage increases, however, their bonding states will split to give a pair of even states below the original level and a pair of odd states above it[528]. If the bonding originally produced a P state, the interaction will force the odd P state higher until it either becomes a delocalized state in the substrate band, or appears as an N state above the band. Similar reasoning may be applied to predict reversed effects if the isolated adsorbate formed an N state. Thus, as more

adsorbate particles bond to the surface, the energy of the bonding states (N) decreases and that of the antibonding states (P) increases. Although this result was derived from a one-orbital tight-binding model[528], it points the way to a mechanism for the frequently-observed fall in heats of adsorption with increasing coverage.

It must be emphasized that these effects do not arise from any direct interaction between adsorbed species; the resonance integral between adjacent adsorbates is taken as zero at all coverages. Their interaction occurs only through the broadening of the surface state bands arising from the splitting of the original local bonding states.

Koutecky's SCF-MO model[544] predicts that when the adsorbate-adsorbate distance becomes comparable with the separation of atoms in the substrate surface (so that they have a finite overlap integral), the diatomic adsorbed complex will be more stable than the separately adsorbed species. This may account for activation barriers in dissociative chemisorption.

2.3.3 "Many-orbital" wave-mechanical models of chemisorption

A realistic model of a metal substrate must consider the effects of the existence of more than one electronic orbital per atom, and nearly-free electrons in overlapping bands. Adsorption on such substrates has been treated by three methods: (i) modification of "one-orbital" theories to allow for overlapping conduction bands in the substrate; (ii) ligand field investigations of the spatial distribution of bonding orbitals to allow calculation of bonding energies at specific adsorption sites; (iii) evaluation of the adsorbate-plus-adsorbent system as a single giant molecule.

2.3.3.1 Extensions of "one-orbital" models

The one-orbital models have been extended in two ways, to account for the two limiting cases which can arise in chemisorption. In the case of weak, delocalized bonding, an analysis is made of the consequent perturbation of the substrate wave functions. In the strong-bonding case, where localized surface states form a molecular-type "surface compound", corrections are again made for the interaction with the substrate, but these are assumed to be so weak that the surface state itself is unaltered. Since experimental chemisorption bond energies are of the same order of magnitude as metallic bonds and the dissociation energies of simple diatomic molecules, systems approximating to both cases will be expected to arise in practise.

Models using the Lennard-Jones[439] or Morse[545] potentials with summed pairwise interactions give no specific information about the perturbation of a substrate by a weakly-bonded adsorbate. Yet on the other hand, extensions of LCAO-MO treatments to consider multiple orbitals on the substrate atoms are usually so complex that their conclusions can only be qualitative or empirical.

It is often difficult to justify the surface compound formation model for the interpretation of IR spectroscopic data of gas adsorption on metal substrates. Real metals have so many overlapping bands of bulk states that it is unlikely that the chemisorption bond energy could fall outside all of them and form a localized surface state so as to justify the interpretation of the adsorption spectrum in terms of an isolated surface compound[546]. However, the practical

usefulness of such interpretations is itself evidence that the d orbitals of substrate surface atoms often do couple more strongly with the adsorbate than with adjacent metal atoms and that adsorption merely shifts and broadens the corresponding energy bands in the metal. Without the presence of the underlying metal, the bond would be localized and have a discrete energy, but since this energy lies within a delocalized band of the bulk substrate it becomes a "virtual" level[546]. The chemisorption may thus be analyzed in two stages. In the first the virtual levels are approximated by a surface compound model, and in the second the resulting broadening and shifting of the bulk bands are estimated. Clearly the surface compound model is only justified if the coupling between the virtual states and the delocalized bands of the bulk substrate is rather small.

Grimley illustrated the surface compound model by its applicability to the adsorption of CO on Ni[546], since the bonding in this system is known to be weak* and hence probably localized in Shockley states, and recent band structure calculations are available for Ni.

---

*CO can adsorb on Ni in a number of configurations[547] e.g.,

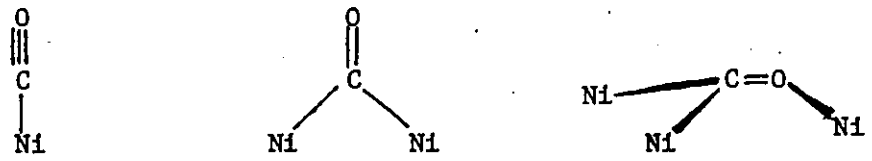

Grimley[546], following Blyholder[548], made calculations only on the first of these three surface compounds, but although the recent work of Doyen and Ertl[549] suggests that the overlap integrals will be little altered if the CO is bonded to a Pt atom off its axis, explicit calculations are not available for CO adsorbed in the bridged forms.

The Ni Fermi level is about 10 eV above the highest normally occupied level (5σ) in CO, and about 12 eV below the lowest normally vacant level (2π). Grimley's many-orbital analysis of the surface molecule showed that chemisorption would remove 0.21 electron from the Ni atom and donate 0.28 electron to the CO. This would raise the 5σ and 2π orbitals of the CO and lower the $d\sigma$ and $d\pi$ orbitals of the Ni. The coupling of the surface molecule to the bulk Ni substrate through the broad sp band, which contains the d band, converts the calculated discrete levels into virtual levels and rearranges the electron distribution slightly, so as to raise the energy of the surface compound and slightly weaken the chemisorption bond. The value of 2.67 eV calculated for the surface compound is therefore too high. The experimental value for the Ni-CO bond is 1.82 eV[550].

Jansen[551] has argued that the spherical nature of transition metal d electron orbitals shown by neutron diffraction experiments makes it doubtful that adsorption will occur on top of a single surface atom using a directed orbital controlled by crystal-field splitting. He therefore proposed a three-centre model of the surface compound, where the adsorbate bonds to two adjacent substrate atoms, but unfortunately did not evaluate the effects of coupling to the bulk metal substrate. Van der Avoird made calculations on four-particle systems[118] (e.g. bridged H_2 on Pt) and later calculated the adsorption energy of H on the principal index faces of a 13 atom cluster of Ni (with metallic properties)[118]. The chemisorption energy was found to decrease with the local coordination of the adsorbate (see Section 2.3.3.2).

A particularly successful application of the surface compound

model has appeared in the treatment of chemisorption of alkali metal atoms on W[600]. Gadzuk[601] used Newns'[566] modification of the Anderson SCF-MO theory (developed for electronic states in alloys) in both tight-binding and free electron models, and verified Newns' deduction that dramatic changes in the density of states function of the surface compound can result from small changes in the parameters of the chemisorption system. Gadzuk suggested that many of the features of electron spectra arose from "virtual surface molecules" where strong adsorption had modified the conduction band of the substrate[601].

The work of Rand and Woods[552] on the electrodeposition of H and O species on noble metal alloys implies that these chemisorption bonds are localized but not restricted to one substrate atom. Their results suggest that homogeneous alloys show averaged properties of their components, whereas alloys where local surface ensembles of one type of atom may be expected to arise from a miscibility gap, show the properties of both components simultaneously. It would therefore seem reasonable to analyze electrochemical chemisorption on noble metals in terms of surface compound models.

The implication that both localized and delocalized bonding are involved in real chemisorption systems revives an intriguing suggestion first made by Grimley[528] on the basis of a one-orbital analysis. If adsorption in a certain system could only occur by localized bonding, and if the field at the adsorbate surface was insufficient to completely localize one surface state per surface atom, then the saturation coverage in chemisorption would occur at considerably less than a monolayer. Grimley[528] suggested that such a

mechanism could account for the low saturation coverage of N on transition metals[553]. Grimley's derivation was based on the modification of Tamm states by the perturbation of bulk states arising from further adsorption, but the same saturation effect could presumably occur with weak chemisorption in Shockley states where the adsorbate field progressively delocalized the surface states. We shall discuss this hypothesis later with regard to sub-monolayer coverage limits in chemisorption states resulting from electrodeposition on noble metals.

2.3.3.2 Ligand field MO theories of chemisorption

The problem of locating the sites on a crystal surface where adsorption will be favoured has also been approached by ligand field theory, a composite of crystal field theory and MO theory.

Crystal field theory examines the reduction or elimination of degeneracy in the five degenerate 3d orbitals of transition metal cations as they are placed in an electric field[554]. If the field has octahedral symmetry, the d_{xy}, d_{yz} and d_{zx} orbitals degenerate into a more stable group designated t_{2g} and the $d_{x^2-y^2}$ and d_{z^2} orbitals degenerate into a less stable group designated e_g. In a tetrahedral or cubic field the order of the split d levels is inverted; d_{xy} d_{yz} and d_{zx} become less stable as the degenerate t_2 level, and $d_{x^2-y^2}$ and d_{z^2} become more stable as the e level.

Comparable results are obtained when molecular orbital theory is applied to σ bonds. When a metal ion is octahedrally coordinated by ligands, the two molecular orbitals bonding the ligand form split pairs designated a_{1g} for the 4s interactions, t_{1u} for the 4p, and e_g

for the d_{z^2} and $d_{x^2-y^2}$. The d_{xy}, d_{xz} and d_{yz} orbitals do not interact, and degenerate to the t_{2g} level. The effects of non-octahedral fields are harder to evaluate by MO theory. When the ligand has π orbitals, the three p orbitals may be involved in bonding, as well as the d_{xy}, d_{xz} and d_{yz}.

Chemisorption on real metals involves both crystal field effects, which establish the directions and energies of the surface wave functions, and also a degree of covalency in bonding which is best treated by MO theory. Ligand field theory combines the two effects evaluated independently.

When the energy gap between e_g and t_{2g} levels is small, the five d orbitals will be filled one by one before any electrons are paired, but, if the gap is large, the lower levels will be filled by paired electrons before the upper levels are occupied. The relative stability of different coordinations of an adsorbate particle by substrate atoms may be measured by the ligand field stabilization energy (the energies by which the electrons in split levels have fallen from their original degenerate states weighted by the number of electrons in each level). In octahedral coordination, the filling of levels according to the strong ligand field model ($e_g >> t_{2g}$) will lead to states as stable as or more stable than those arising from the weak ligand field model ($e_g \sim t_{2g}$) according to the number of d electrons filling these levels. Thus, the relative stability of octahedral and tetrahedral coordination is controlled by the number of d electrons in the metal. Dowden and Wells[555,556] have therefore suggested that the relative efficiency of catalysts is related to their ability to

stabilize certain reactive adsorption configurations. Haber and Stone[557] calculated the stability of O^{2-} anions on the principal crystal faces of NiO, assuming that sufficient adsorption would occur to octahedrally coordinate the Ni^{2+}, and found that by far the greatest stabilization would occur on (110) faces, and that its magnitude was close to the observed heat of adsorption at low coverages.

Shvets and Kazansky[558] investigated the adsorption of O^{2-} radicals on a series of transition metals by esr and concluded that the adsorption behaviour was sensitive to the coordination of the adsorbate (i.e. the crystal form of the metal). Metal valency effects, however, complicated the analysis of the coordination effect.

On the assumption that electron bands will arise as a result of molecular orbital overlap under the directional influence of the crystal field, Trost[559] has calculated the orbital construction and the stabilization energies of the transition metals. On this basis he was able to predict the crystal structures of all except Mn and Fe.

Bond[114] has extended the crystal field models of Trost[559], Goodenough[560] and Dowden[561] to provide a simple picture of the emergence of surface molecular orbitals on transition metals. He assumed that Shockley-type unsaturated valencies (see Section 2.3.1.3) would exist at the surface in the same configurations as in the bulk under the influence of the crystal field. By sketching the emergent e_g (bonding) and t_{2g} (non-bonding) orbitals he predicted the sites where adsorption could take place on the principal index faces. For example, H could bond on an f.c.c. metal by overlapping its s orbital with (i) an e_g

orbital above a (100) surface atom; (ii) five e_g orbitals in the octahedral "hole" on (100); (iii) two e_g orbitals at a bridging site on (110), or (iv) three e_g orbitals in a "hole" on (111). Bond's model has been developed by Shopov et al.[115] and by Carra and Ugo[562]. It has been applied to the adsorption of H on Pt[108,116,117] (see Section 1.1.2) and to that of CO, O and CO_2 on (111) surfaces of Pt and Ni[563]. It must, however, be emphasized that Bond's is a Shockley-type model and can only apply where weak adsorption merely saturates pre-existing dangling valence bonds. If the adsorption is strong, the surface potentials involved in forming Tamm states will perturb the crystal field and invalidate the calculation of surface bond directions from the symmetry of the bulk crystal field. The results of Rand and Woods[552], described above, showing that the chemisorption bonds formed after electrodeposition at noble metals are neither fully localized nor fully delocalized, cast doubt on the applicability of Bond's model to the systems of interest in the present work.

By calculating the interaction and crystal field splitting between orbitals of neighbouring atoms in metal crystals, Goodenough[560] has calculated semi-empirical density of states curves for various metals. Such data could be extremely important in the development of quantitative theories of adsorption. Quantitative models of surface states can perhaps be developed from a knowledge of the bulk density of states, and the actual chemisorption orbitals estimated through ligand field interactions of adsorbate and substrate. Kelly[564] has recently extended earlier calculations of the surface density of states of transition metals[532,533] to an examination of the interaction of an

adsorbate with a group of neighbouring substrate atoms in or just beneath the surface. The resulting bond is a group orbital (c.f. the surface compound model) depending not only on the electronic properties of the adsorbate and substrate but also on the configuration of the bonding site. Calculations of the density of states curve appropriate to the adsorption of H at various sites on b.c.c. and f.c.c. principal index planes[564] showed such a strong coupling of the substrate atoms involved in the "surface complex" with those in the bulk substrate that Kelly doubted the validity of this type of model. The coupling was even independent of the bond energy between the adsorbate and the substrate atom group, to a first approximation.

2.3.3.3 "Giant molecule" treatments of chemisorption

In the most realistic theoretical treatments of chemisorption, the adsorbate-adsorbent system is regarded as a single giant molecule. Full consideration may then be given to local interactions within the molecule (e.g. the adsorption bond and the localization of surface states). The resulting computations are unfortunately so complex that simplifying assumptions often bring the conclusions into question. Only the adsorption of H on metals has been treated by this method.

Grimley[565] has analyzed the system in terms of one-orbital functions. Newns[566] extended the treatment to a many-orbital model with a tight-binding approximation of the d-band to predict the relative chemisorption energies of H on a series of transition metal substrates. The corresponding calculated values of the charge on the adsorbed H were only consistent with surface potential data if it was assumed that

the H would be adsorbed in concave surface declevities, as suggested earlier by Culver, Pritchard and Tomkins[567].

Toya and Horiuti[127,128] also concluded that H could adsorb in concave surface declevities. They called this s-type chemisorption, and suggested that the H's electron would be delocalized and the bonding essentially metallic. Another solution to their calculation showed (r-type) adsorption sites about 2.5 Å directly above surface metal atoms. Here the H was slightly negatively charged and the authors predicted that the positive dipole moment would decrease the work function with increasing coverage.

Giant molecule models may also be analyzed as bulk metals having surface alloying. Adsorption produces long-range oscillations in the density of states of the substrate[568] which decay with distance from the adsorbate just as those around a foreign atom in an alloy[506,569]. Qualitatively similar oscillations were found when Lang and Kohn[569] analyzed a nearly-free-electron model using a uniform background potential ("jellium") to simulate the substrate. Work function data calculated using a jellium model[570] are apparently in qualitative agreement with experimental data from W surfaces as a function of the coverage of chemisorbed alkali metal atoms[571].

2.4 Summary

The central difficulty in the theoretical analysis of chemisorption is that of finding an expression which will realistically describe the potential function within a metal, yet be amenable to the multiple calculations of the interactions of wave functions which must

be made. The surface complex model appears promising for those systems where the bonding is strong and localized, but the conflict between the data of Rand and Woods and the calculations of Kelly forbid a definite conclusion as to the applicability of this model to electrodeposition systems. It could hardly be expected to apply to the bonding of metals to metals, but might be applicable to the chemisorption of O species on Pt or Au. The most sophisticated treatments of the chemisorption bond are the giant molecule treatments of H adsorption, but even they only present qualitative conclusions.

Despite the fact that these theoretical approaches lag so far behind experimental techniques in their ability to predict the "fine structure" of adsorption states, even qualitatively, they contain a number of useful pointers as to the likely causes of that fine structure which will be discussed in more detail in Section 11.2.

CHAPTER 3

SUMMARY OF AIMS OF THE PRESENT WORK

The foregoing chapters have shown that there is at present very little correlation between experimental data and theoretical treatments of surface bonding on metals. Experimental results have frequently been reported in descriptive terms only, and not discussed in terms of mechanisms on an atomic scale.

It has nevertheless been shown that in many systems sub-monolayer electrodeposition proceeds in distinct successive stages, each having a characteristic bonding energy exceeding that of the bulk deposit. The finest resolution of the "spectra" of bonding states has been achieved in electrochemical (potentiodynamic) studies of the discharge of ions at noble metal surfaces. Accurate measurement of the currents involved in the discharge process and the potentials at which they flow allows the coverage of the deposited species to be calculated to within about 2% of a monolayer, and the relative bonding energies of the various states to within about 500 cal. The discharge reaction only occurs at vacant surface sites where bonding can occur, unlike OPD reactions which proceed at rates independent of the coverage of material previously deposited. The kinetic limitations of UPD (e.g. the activation energy) relate both to the mechanism of discharging the ion and to that of its subsequent bonding.

It is the purpose of the work described in this thesis to characterize the kinetic and thermodynamic behaviour of multiple

states of chemisorption occurring when submonolayer amounts of various species are electrodeposited on Pt and Au under a variety of conditions. The relationship between bonding energy and coverage will be examined critically in order to establish the origin of the multiple states of bonding. The physical nature of the bonding will be discussed in terms of both the decreasing influence of the nature of the substrate as the bonding changes from UPD to OPD, and the possibility of place-exchange between deposited species and substrate atoms, leading to random or ordered solid solutions in the electrode surface.

The foregoing review of adsorption has shown that the following specific issues must be resolved:

(i) Experimental techniques must be improved until the currents recorded only relate to the electrodeposition process of interest. Impurity currents passed at the same potentials must thus be reduced to a minimal level.

[The rigour of this criterion may be illustrated as follows: In the field of organic chemistry a moderately highly purified compound would be perhaps 99.9% pure. In a 10^{-3} M solution this would represent one impurity in 10^{5} parts on a volume basis and this could produce a discharge current of about 0.01 mA cm^{-2}. The peak currents associated with surface bonding in these studies were as low as 1 μA cm^{-2} so if the impurity currents were even 10% of the discharge currents in this (the worst) case, the initial reagents would have to be 99.9995% pure.]

(ii) The origin of multiple states of chemisorption must be established. In what way are the bonding states characteristic of the deposit, the substrate and the solution? Is the heterogeneity intrinsic or extrinsic?

(iii) The reasons for the transition from UPD to OPD must be established by a comparison between electrodeposition data from a number of systems. Of particular interest is the nature of the electrode surface at the reversible deposition potential of the deposited species in its "bulk" form.

(iv) Place-exchange, and the equivalent process of surface alloying, have been shown to occur in some electrodeposition systems. They require a more general characterization so that their cause and extent may be analyzed. Why, for example, does electrodeposition lead to the formation of bulk electrodeposits in some systems, while in others the deposit dissolves in the substrate almost as fast as it is discharged, e.g. H in Pd and Hg in Au?

(v) Ultimately a general model of chemisorption must be developed which will take account of the mass of experimental evidence which has accumulated for a wide variety of systems, so that quantitative correlations with the theoretical analyses of surface bonding may be sought.

CHAPTER 4

EXPERIMENTAL PROCEDURES

4.1 Electrodes

Working electrodes were made from wire of 99.999% purity, Johnson Matthey "Thermopure" Pt, and "Grade 1" Au. Lengths of these wires, usually 0.38 mm in diameter (0.015") were first degreased overnight in refluxing acetone in a Soxhlet extractor. A droplet of (Pb-free) soft-glass was then melted on to the wire and sealed into the thin-walled end of a soft-glass tube, leaving between 2 and 10 mm of wire protruding beyond the end of the tube. The soft glass had been previously cleaned in fresh concentrated H_2SO_4 and rinsed with pyro-distilled water (see Section 4.2.3), and the degreased wire was only touched with cleaned platinum forceps. The completed electrodes were washed in fresh concentrated H_2SO_4 and stored in pyro-distilled water. In some cases, the electrical contact to the working electrode was made via a length of 20 gauge Cu wire spot-welded to the Pt at least 5 cm above the seal. No other sealants or contact material (e.g. the Picien wax and Wood's metal previously used in this laboratory) were used, to avoid the risk of contaminating other electrodes and the cell walls if the working electrode seal failed. Large area working electrodes were prepared by spot-welding Pt or Au sheet (Johnson Matthey "Apparatus grade pure Pt" or "Grade 1" Au - 99.999% pure), usually about 8 mm square, to the exposed wire.

This method of preparing electrodes is easier than that of sealing Pt wires in Pyrex bulbs under H_2 atmosphere[664,665] previously used in this laboratory and was shown to give identical results in cyclic voltammetry experiments.

Three Pt single crystals cut from 5 mm dia. rod to expose the (100), (110) and (111) faces were given for this study by Dr. F. G. Will (G.E., Schenectady, New York, U.S.A.). Results obtained with them in earlier work may be seen in the literature[110,253,254]. Their soft-glass mounts did not provide a complete solution seal and were therefore dissolved away in HF. After some experimentation it was found that they could be satisfactorily sealed in Araldite epoxy, stirred till it had almost set and then painted onto the sides of the crystal. A jet of purified N_2 was blown on the experimental face of the electrode while the epoxy hardened. Araldite coatings prepared in this way were chemically stable in acid solution (e.g. 0.5 M H_2SO_4) for periods of up to two weeks, after which they were removed by dissolution in pyridine. When Pt wires were mounted in epoxy in this way, the resolution of bonding states which could be achieved was never quite as good as with electrodes sealed in soft glass.

Another Pt (100) single crystal, prepared and characterized by Dr. P. B. Sewell (National Research Council, Ottawa), was used unmounted, supported on a short Pt wire sealed in soft glass and spot-welded to the side of the single-crystal disc. The single-crystal faces then represented 85-90% of the area of Pt immersed in the solution

Counter electrodes were large foils (about 1 cm x 1 cm) of the same metal as the working electrode, prepared in a similar manner. [The use of Pt counter electrodes with Au working electrodes in preliminary experiments caused the Au electrode to behave somewhat like a Pt-Au alloy, presumably because Pt was dissolved at the counter electrode and electrodeposited at the working electrode (cf. references 135,300)].

The reversible hydrogen reference electrodes consisted of tightly-folded layers of woven Pt wire gauze (Johnson Matthey "Apparatus grade pure Pt") spot-welded to 0.51 mm diameter (0.02") Pt wire sealed in glass in the usual way. These electrodes were platinized according to the procedure recommended by Feltham and Spiro[572], and checked against similar electrodes from time to time to detect the appearance of any potential drift. The H_2 (99.95% pure in the cylinder) supply for the reference electrode was purified in a standard system[583]: $MgClO_4$, molecular sieve, palladized asbestos at 620K, and activated charcoal traps.

The high currents passed in surface processes during potentiodynamic sweeps at rates over about 0.5 V s^{-1} can introduce a resistance overpotential arising from the iR drop between the working electrode and the Luggin capillary of the Pt/H_2 reference electrode. The errors which can arise from this iR drop were avoided by using the potential of a short (2-5 mm) Pt or Au wire, placed within 1 mm of the working electrode as the reference potential when using sweep rates exceeding 0.2 V s^{-1}. The potential of this "floating" reference electrode remained constant to

within ±2 mV over periods of many minutes. The potential scale of current-potential curves was calibrated from the sweep reversal potentials, which were always measured against an external Pt/H_2 reference electrode.

4.2.1 Acid and base solutions

The purest commercially available H_2SO_4 and $HClO_4$ (B.D.H. AristaR grade) were used to make up solutions without further purification. The limits of impurity as supplied are quoted as well below 1 ppm, and "dirt" in the solution was very rarely traced to the acid supply.

The starting material for NaOH solutions was Fisher certified reagent grade NaOH pellets. These were dissolved and filtered in boiling pyrodistilled water and then recrystallized at least five successive times. The solution which remained after recrystallization was decanted off.

pH measurements were made with a Radiometer 4c pH meter, using a Radiometer 6200B glass electrode and a Radiometer K100 calomel electrode.

4.2.2 Salts

Salts were prepared from the following starting materials: Fisher ACS grade Na_2SO_4; Fisher certified reagent grade $MgSO_4$; B.D.H. AnalaR grade $CuSO_4$; Alfa-Ventron Corp. stock no. 22115 $Cu(ClO_4)_2.6H_2O$; Baker reagent grade $HgSO_4$ (used in very dilute solution without further

purification); Fisher certified reagent grade $Pb(NO_3)_2$. Solutions of these salts were filtered and recrystallized not less than four successive times.

4.2.3 Water

During 1971, solutions made from distilled city water, distilled again from alkaline $KMnO_4$, began to give stray impurity currents at Pt, with selective blocking of currents from the surface reactions of O and H species. Problems connected with water purity also began to appear at about this time in a number of other laboratories in the Ottawa area. The nature of the new impurity could not be established, but a new method[573] (patent pending) was developed in the course of the present work to remove it by catalytic pyrodistillation.

The purification is based on a patented process[574] for making potable water from urine in spacecraft by passing impure steam over Pt gauze screens at 1370K under partial vacuum, but with an air bleed. A somewhat similar system was developed by Criddle[575], in which the impure steam reacted with O_2 at high temperature in an alumina tube containing no catalyst.

The apparatus developed in the present work is shown schematically in Fig. 3. A batch of about 1.5 ℓ of doubly-distilled water is boiled in the flask on the left and mixed with purified O_2 entering the flask at about 1 ml s^{-1}. The steam rises through an 18 mm diameter silica tube and is heated to 1070K as it passes through 40

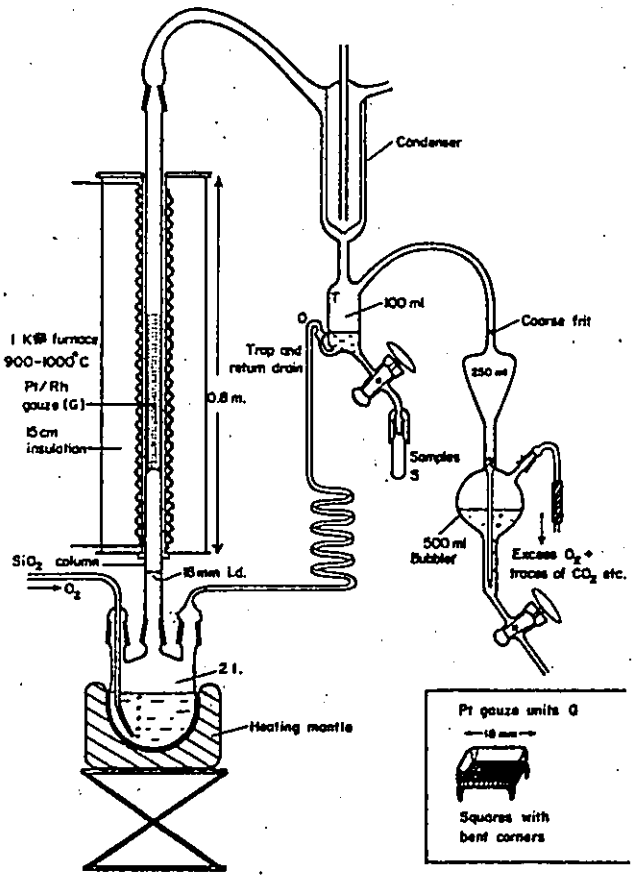

FIG. 3. APPARATUS FOR THE PYRODISTILLATION OF WATER

closely packed 90% Pt-10% Rh woven gauze baffles (G). The temperature is lower than that used by Konikoff[574], since hydrothermal distillation of the catalyst[576,577] begins to increase at temperatures above 800 K[578], leading to the appearance of dark deposits in the cooler tubing beyond the furnace. After passing over the catalyst, the steam is condensed in the trap T, from which about 100 ml of purified water overflows back to the boiling flask through the Soxhlet siphon O about every half-hour. Since, with this distillation rate, the steam passes over the catalyst in 1-2 s, the water is allowed to recirculate at least 4 times around the apparatus (total time about 48h) before being distilled from the trap into a further conventional distillation stage, introduced to remove any traces of Pt or Rh species arising from volatile oxidation products of the catalyst. To eliminate contamination from airborne dust, the apparatus was enclosed in a large fireproof box. Ground glass joints, which can harbour impurities[575], were eliminated as much as possible. Those which were essential were inverted (cone below, socket above) or covered as shown in Fig. 2.

This process, based on the destructive oxidation of impurities to gaseous oxidation products (e.g. CO_2, NO_2), is thought to be essentially superior to others recently developed elsewhere based on the <u>adsorption</u> of impurities on activated charcoal[579] or on platinized Pt sponge potentiostatted at 0.005-0.350 V[580]. Adsorption methods involve the difficulty of maintaining the adsorbent material in an ultrapure condition, and the assumption that new impurities appearing in the water supply will still be removed by the same adsorbent. The removal of residual impurities by the present apparatus

is evidenced by the fact that the waste gases decrease the pH in the exit bubbler to 4-5 during a period of 3-4 months, after which the water there is replaced.

Using catalytically pyrodistilled water and AristaR grade acid, potentiodynamic pre-electrolysis involving high anodic potentials (e.g. reference 581) was not necessary to obtain the "clean" oxidation-reduction profile on Pt and Au. The "clean" profile was normally achieved on Pt after about 10 cycles (typically 0.07 to 1.32 V) in a new solution, but under optimum conditions was obtained on the second cycle after the electrode had been left on open-circuit for many hours in a deaerated solution[582]. This result incidentally eliminates the objection that the structure of the current-potential profile for Pt in aqueous solution is an artefact arising from multiple potential cycles.

A large number of experiments were made in 1971 with impure solutions, and the experience gained from them, has been made the basis of the following general principles for diagnosing the cause of impurity effects in current-potential profiles at Pt.

(i) Stirring the solution "spoils" the profile: reactive impurities in the solution reaching the working electrode under diffusion control.

(ii) Stirring the solution "improves" the profile: impurities leaking from inside the electrode tube because of a poor glass/metal seal.

(iii) The profile is "dirty" but largely unaffected by

stirring: strongly adsorbed impurities on the electrode.

(iv) The profile is "dirty", largely unaffected by stirring, but improves with potentiodynamic cycling: surface impurities on the electrode slowly removable by oxidation or reduction.

(v) Peak currents do not increase linearly with sweep rate (sweep rates < 1 V s^{-1}): reactive impurities in solution.

(vi) An overall slant or shift in the profile with respect to the zero-current line: either a very dirty electrode or an electronic artefact arising in the control circuitry (e.g. in some cases from the combination of a Hewlett-Packard 60 Hz filter unit and the Tektronix 564B oscilloscope).

On the basis of this work, the following criteria were established to confirm the purity of a Pt electrode-solution system:

(i) Absence of any effects of stirring on the i-V profile.

(ii) Maintenance of the resolution of the multiple H and O peaks and the shape of the profile down to sweep rates at least as low as 0.005 V s^{-1}.

(iii) Equality of anodic and cathodic charge in the potentiodynamic sweep.

(iv) Constancy of the H deposition and removal charge to within 5% of its original value for at least 1 h while the potential range used excludes the O-species deposition region.

(v) Absence of any slant of the profile about the zero line.

4.3 Experimental cells

The three different types of cell used in this work are shown schematically in Fig. 4. Cell (a) was used for rapid testing of successive solutions. Solutions could easily be drained through the large stopcock and the reference electrode side-arm and washed out through the N_2 entry. Cell (b) was designed for the study of temperature effects so that the reference electrode would always be at the same temperature as the working electrode. Cell (c) was developed to achieve the ultimate experimental purity. It had been found that substantially "cleaner" results could be obtained by simplifying the cell design and removing all ground-glass joints in contact with the solution. The impurity levels were reduced, probably because of the ease of cleaning the cell, and in addition the cell was easier to use.

Solutions were deoxygenated by a slow stream of N_2 bubbled from the bottom of the working electrode compartment so as to avoid dead spaces. The N_2 gas (99.99% pure, as supplied in cylinders) was purified in a conventional gas train[583] consisting of: molecular sieve (BDH type 4A), $Mg(ClO_4)_2$, Cu turnings at 350°C (periodically regenerated by purified H_2), and then through 3 traps cooled by liquid N_2, two of these containing activated charcoal, and finally a pre-saturator containing pyrodistilled water. When a freshly prepared solution was used, the last traces of O_2 were expelled about 20 mins after N_2 bubbling was started.

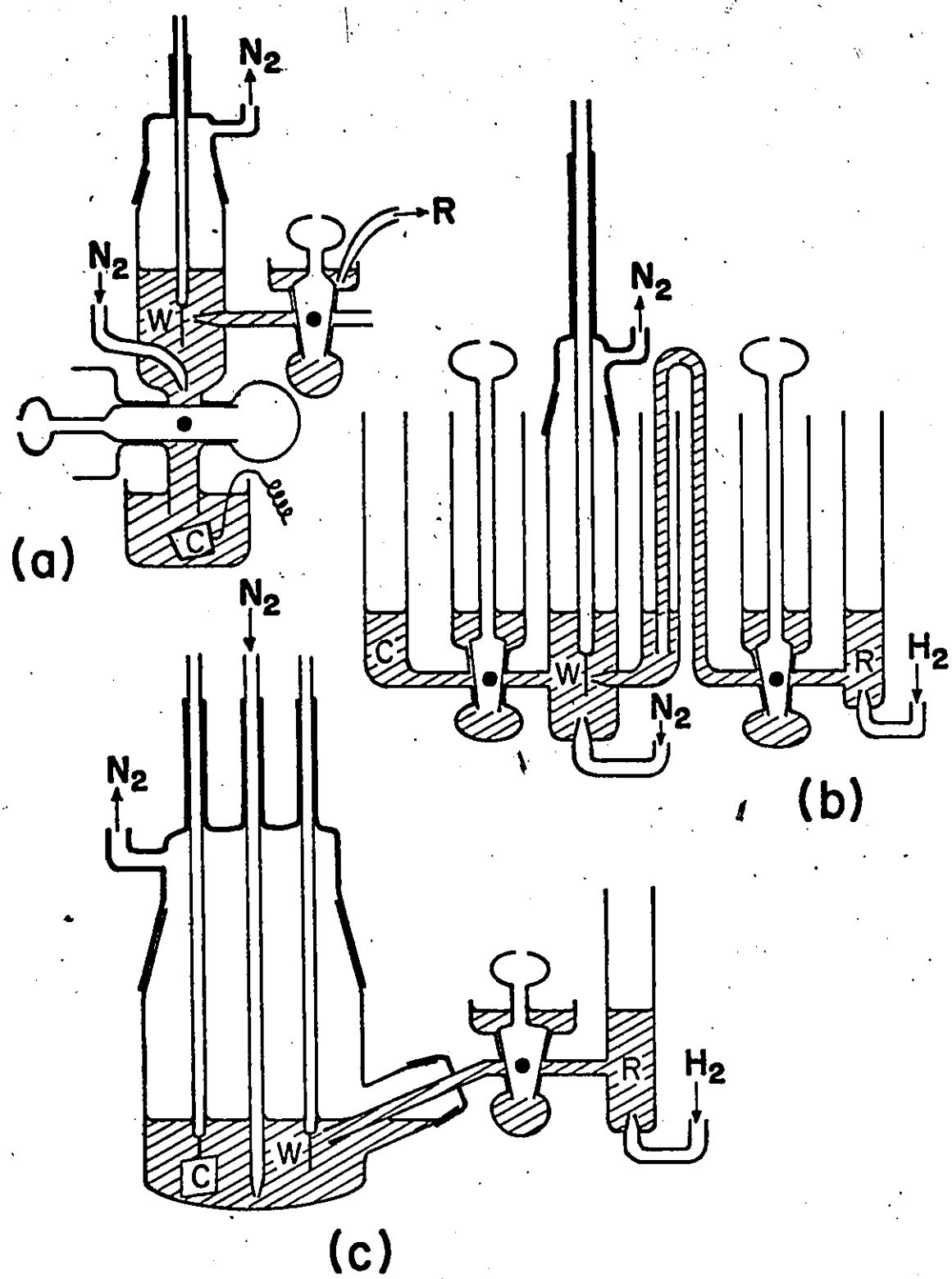

FIG. 4. SCHEMATIC DESIGNS OF EXPERIMENTAL CELLS

4.3.1 Cleaning procedures

Glass apparatus being used for the first time was soaked (inside and out) overnight in fresh concentrated CrO_3 - H_2SO_4 solution. This was thoroughly rinsed away with doubly distilled water and replaced with fresh concentrated H_2SO_4 (Baker analyzed reagent grade). Before starting an experiment, the H_2SO_4 was poured away and the cell immediately rinsed all through about 4 times with very hot pyrodistilled water taken from the 2 ℓ boiling flask illustrated on the lower left of Fig. 3. The cell was then filled with hot pyrodistilled water and left to stand for about 20 mins. After this it was rinsed with the experimental solution, left full for about 10 mins and finally refilled with the experimental solution.

After an experiment, the solution was poured out and the cell immediately refilled with fresh concentrated H_2SO_4. The electrodes were not normally removed between experiments. No other solutions entered the cell except fresh concentrated H_2SO_4, pyrodistilled water and the experimental solutions. Identical cleaning procedures were applied to the ancilliary glassware used for preparing salts or solutions.

4.3.2 Temperature control

Effects of the solution temperature were studied by immersing either cell (b) or the central compartment of cell (c) into a 10 ℓ water bath where the temperature was controlled to ±2 K by crushed ice or by a Haake E52 circulating water heater. When using cell (c),

the reference electrode was outside the water bath. It remained at room temperature except in experiments at the highest temperatures (e.g. over 360 K, when it rose to about 10 K above room temperature).

The progress of the solution temperature towards a value pre-set in the water bath was visible from changes in the potentiodynamic sweep profile. The absence of time effects in the profile was found to be the most sensitive measure of the reaction temperature control.

4.4 Electrical circuitry

The basic electrical circuit used in this work is shown in Fig. 5. The potential of the working electrode was controlled by a Wenking No. 6288 potentiostat according to the programme set by a function generator. (Servomex LF 141, Tacussel GSTP2 and Tacussel GSATP function generators were used interchangeably, according to the complexity of the cyclic programme required). The potential of the working electrode was measured by connecting it to the Pt/H_2 reference electrode through a Tektronix Type O operational amplifier acting as a very high impedance 1:1 amplifier. Currents passed at the working electrode were measured as potentials across a Leeds and Northrup 4755 decade resistance box inserted into the counter electrode circuit. The current-potential profile could be recorded on a Hewlett-Packard 2D-2AM X-Y recorder, a Polaroid camera on a Tektronix 564B storage oscilloscope or a 35 mm camera on a Tektronix 502 dual beam oscilloscope. Continuous readout of the working electrode potential was available on

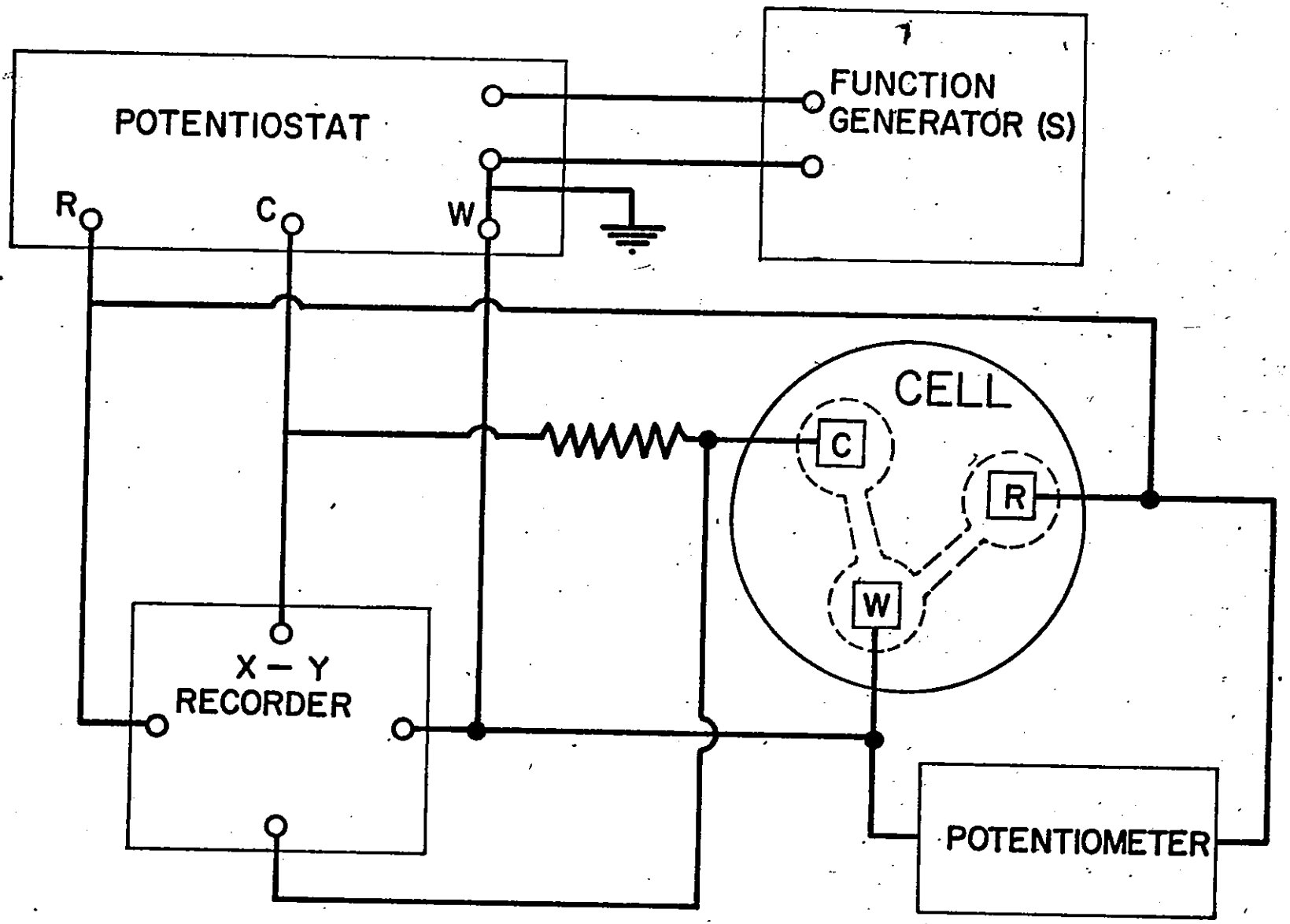

FIG. 5. ELECTRICAL CIRCUITRY EMPLOYED IN POTENTIODYNAMIC SWEEP STUDIES

a Dana 4300 digital multimeter. The circuit was grounded from a single point (the working electrode) directly to an incoming fire hydrant through a 0.6 cm diameter Cu pipe.

In other experiments, slow linear potential sweeps applied to the working electrode were modulated by a high frequency a.c. symmetrical sawtooth signal of small amplitude. Variation of the a.c. frequency (i.e. of the linear sweep rate of the small amplitude sawtooth) enabled the reversibility of the deposition processes to be studied with regard to all surface bonding states occurring within the potential range involved. The modulation sawtooth signal, generated by the Servomix LF 141, was added to the slow overall sweep from the Tacussel GSTP2 in another Tektronix type O operational amplifier, and the combined signal then supplied to the potentiostat. The rate of the slow carrier sweep was maintained at least two orders of magnitude lower than the modulation rate so that the currents added by the slow sweep were always less than 1% of those arising from the modulation.

4.5 Estimation of electrode areas

In view of the widely scattered values of surface roughness factor reported in the literature, no estimates of electrode areas were made in terms of their apparent geometrical area. Pt electrode areas were calculated as follows (see also discussion in Section 1.3.1): The total anodic H removal charge was calculated by graphical integration (weighing fine paper: accuracy ±1%) after setting the cathodic limit to the saddle point between H deposition and H_2 evolution. Double-layer charging currents were subtracted on the basis that they

would be the same on the H covered surface as on bare Pt. Assuming that the charge measured to the saddle point in the cathodic curve corresponds exactly to the deposition of a monolayer of H [34], the real surface area of Pt electrodes was calculated on the basis that the charge required to oxidize a monolayer of H from polycrystalline Pt is 220 μC per real cm^2 [584] of the surface.

The corresponding charge required to discharge a singly-charged ion on every surface atom on a polycrystalline Au electrode (200 μC cm^{-2}) was obtained by multiplying this figure by the ratio of the squares of the radii of Au and Pt. The estimation of the real area of Au electrodes is, however, much more difficult, as the internal standard of the H charge is absent. In most cases the area was calculated in 0.5 M H_2SO_4 according to the criterion of Michri, Pschenichnikov and Burshtein[585]. These authors found that the charge involved in the discharge of O-species at potentials below the saddle point occurring immediately before O_2 evolution corresponded to a charge of 400 μC cm^{-2} of real surface area as measured by B.E.T., over a wide range of temperatures and sweep rate. The problems involved in the accurate determination of Au electrode areas will be discussed in detail in Section 7.1.2.

CHAPTER 5

THE ELECTRODEPOSITION OF H ON Pt

5.1 Results

5.1.1 Introduction

Previous work, reviewed in Section 1.3.1, has established that the electrodeposition of H on Pt is an unusually fast reaction. It takes place as follows:

$$Pt + H_3O^+ + e \rightarrow PtH + H_2O \quad \text{in acid solutions}$$

or

$$Pt + H_2O + e \rightarrow PtH + OH^- \quad \text{in alkaline solutions.}$$

It has been shown that, at room temperature, the number of H atoms which may be electrodeposited on a Pt electrode before significant H_2 evolution occurs, equals the number of Pt atoms in the electrode surface[29-32]. The reversibility of the overall electrodeposition-electrodissolution cycle for H and the consequent lack of hysteresis in the potentiodynamic current-potential curve (Fig. 6), prove that slow post-electrochemical processes such as diffusion of atoms in the electrode surface are absent, and that dissolution of H into the bulk Pt lattice is negligible. Thus, the reaction kinetics are determined only by the rate of charge transfer at the electrode surface. The absence of complicating reactions makes the system particularly suitable for a study of the factors governing the appearance of different states of electrodeposited atoms on an electrode surface. Previous workers have shown that H electrodeposited on Pt is bound

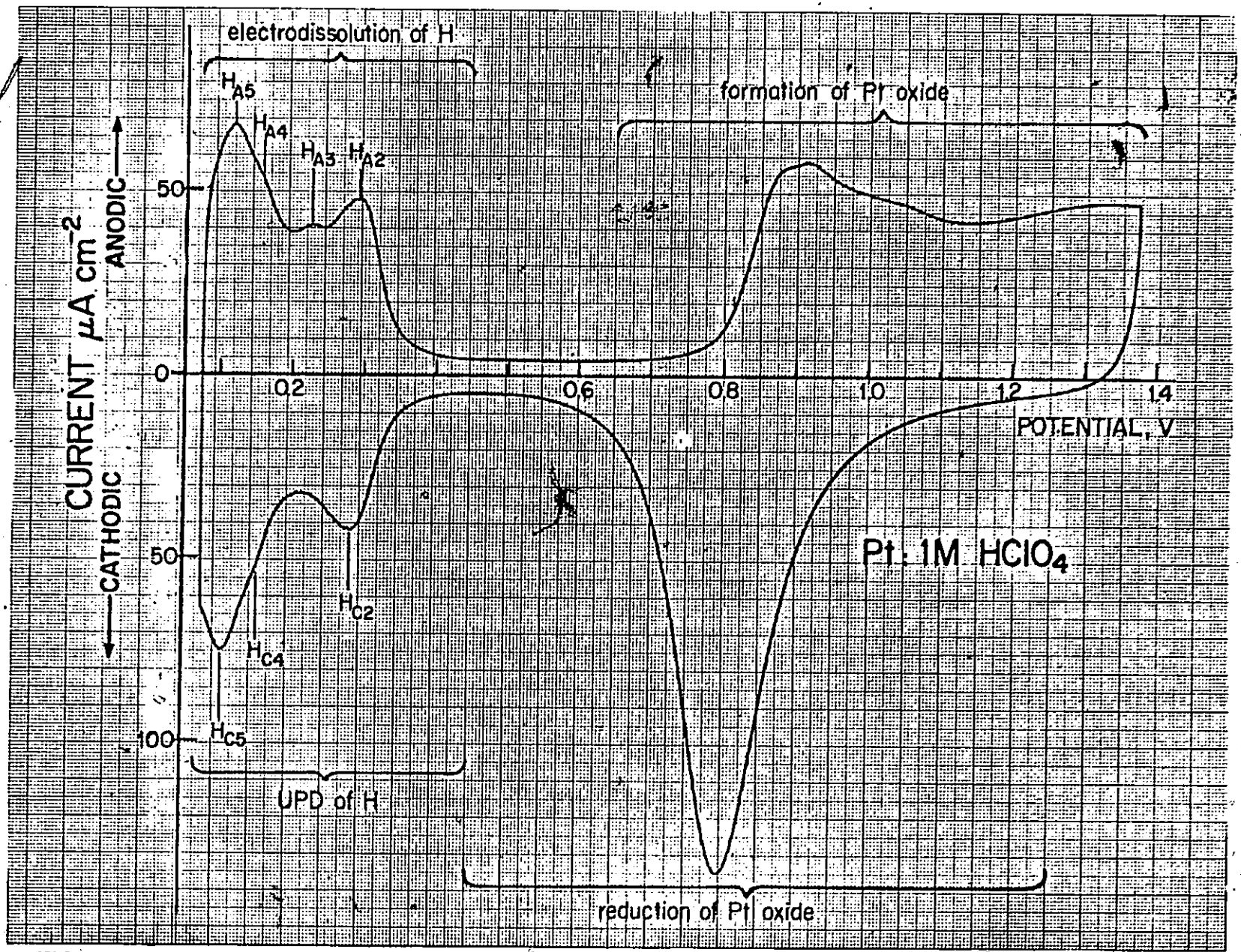

FIG 6 POTENTIODYNAMIC CURRENT-POTENTIAL PROFILE AT Pt IN 1 M $HClO_4$ AT 0.05 V s^{-1}

in at least two atomic states, which have different bonding energies, (Section 1.3.1).

The use of the rigorous purification techniques described in Chapter 4 has led to considerable improvement in the resolution of the different states of surface bonding of H at Pt. In fact, an important finding in the present work is that at least five bonding states are involved in the deposition of a monolayer of H on Pt. A typical current-potential curve obtained at Pt (in 1M $HClO_4$) is shown in Fig. 6. The electrodeposition of H occurs at underpotential, i.e., at potentials less negative than that for H_2 evolution (cf. Fig. 1). Under the conditions of Fig. 6, three overlapping current maxima are resolved in the cathodic sweep, and four in the anodic sweep. The corresponding states of surface bonding of the electrodeposited H are numbered in order of increasing H coverage, with the subscript A or C according to whether the anodic (electrodissolution of H) or cathodic (electrodeposition of H) is described. Not all the current peaks are, however, resolved under any given set of experimental conditions. When a composite peak is produced by the overlapping of two components, the designations of both components are included, e.g., $H_{A4,5}$.

5.1.2 Effects of crystallography of the electrode surface

In order to investigate Will's suggestion[110] that the multiple states of deposited H described above relate simply to the existence of different bond energies on different crystal planes exposed by a polycrystalline Pt substrate (see Section 1.3.1.1.(ii)), a number of experiments were carried out with single-crystal electrodes. It is

clear, however, from experiments in 0.1M H_2SO_4 (Fig. 7*) that although the distribution of the electrodeposited H among the bonding states depends on the surface crystallography, the same states appear, with the same bonding energies at single-crystal surfaces as at the polycrystalline ones. Similar results are obtained at higher pH, where four anodic peaks are clearly resolved (Fig. 8). To simplify the presentation of these results, data for the Pt (110) crystal have been omitted. They were in all cases intermediate in shape between those for the (100) and (111) single crystals, as shown, for example by Fig. 33 in Chapter 6.

[The surface crystallography of the three Pt single-crystal electrodes obtained from Dr. Will was characterized, using reflection electron diffraction, by Dr. P. B. Sewell at the National Research Council Laboratories in Ottawa, after the completion of a long series of experiments involving tens of thousands of potential cycles to a variety of anodic potentials. During this time the current-potential profiles had become progressively similar, and Dr. Sewell confirmed that the surfaces had become largely polycrystalline, although with a predominance of (110) orientations on all the crystals. The only results using these crystals which will be quoted here are therefore those from the first experiments when they satisfied the criteria for "cleanliness" but were distinctively different. The Pt (100) single-crystal used for the data in Fig. 7 however, was separately prepared

---

*In Fig. 7 and others without a scale of current density, current-potential profiles have been superimposed from electrodes which have different surface areas. The curves have not been normalized to a common current density scale because of the errors that would be introduced by redrawing.

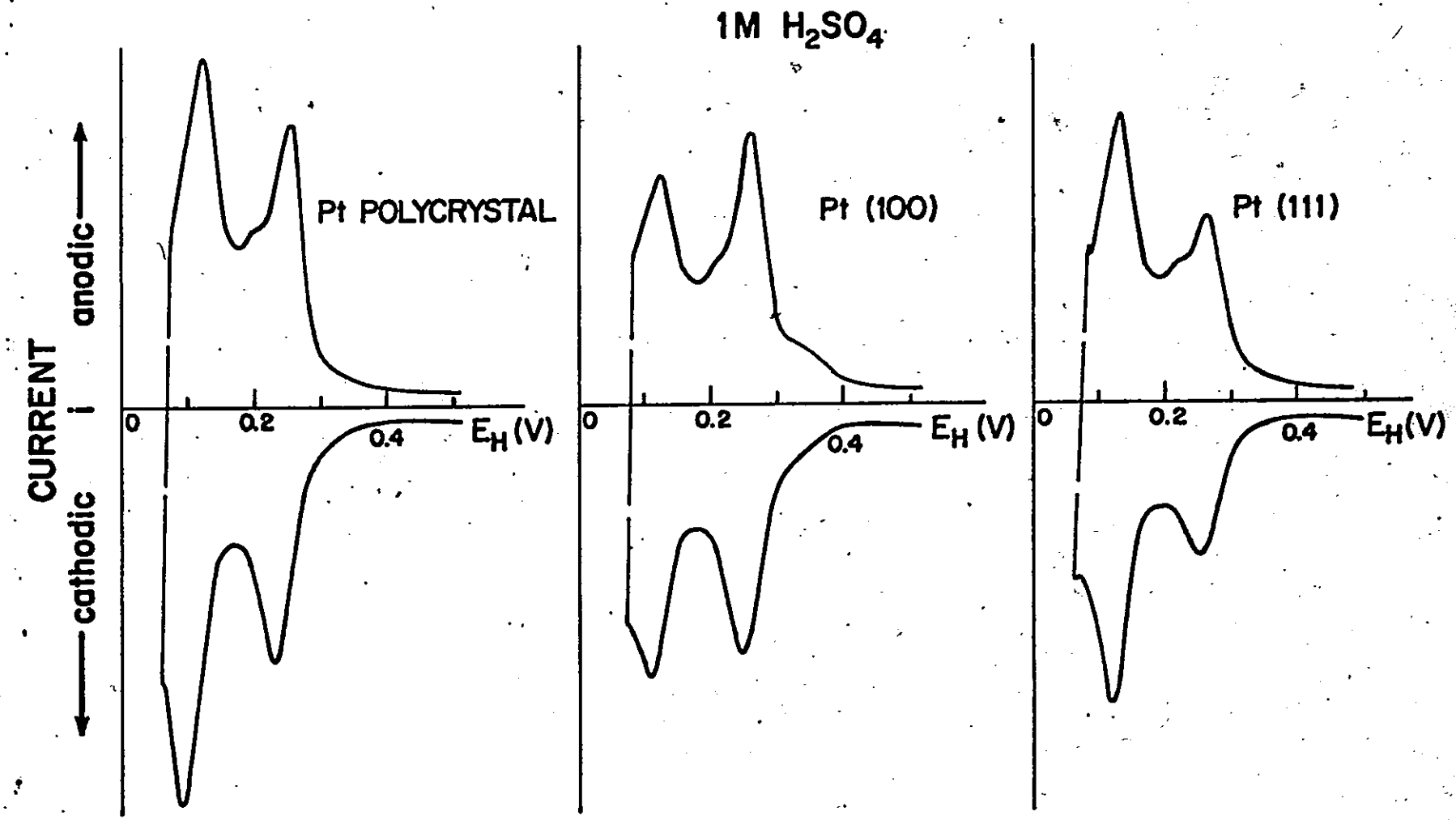

FIG 7 COMPARISON OF POTENTIODYNAMIC CURRENT-POTENTIALS AT SINGLE-CRYSTAL AND POLY-CRYSTALLINE Pt ELECTRODES IN 1M H_2SO_4 ($s=0.05\ V\ s^{-1}$)

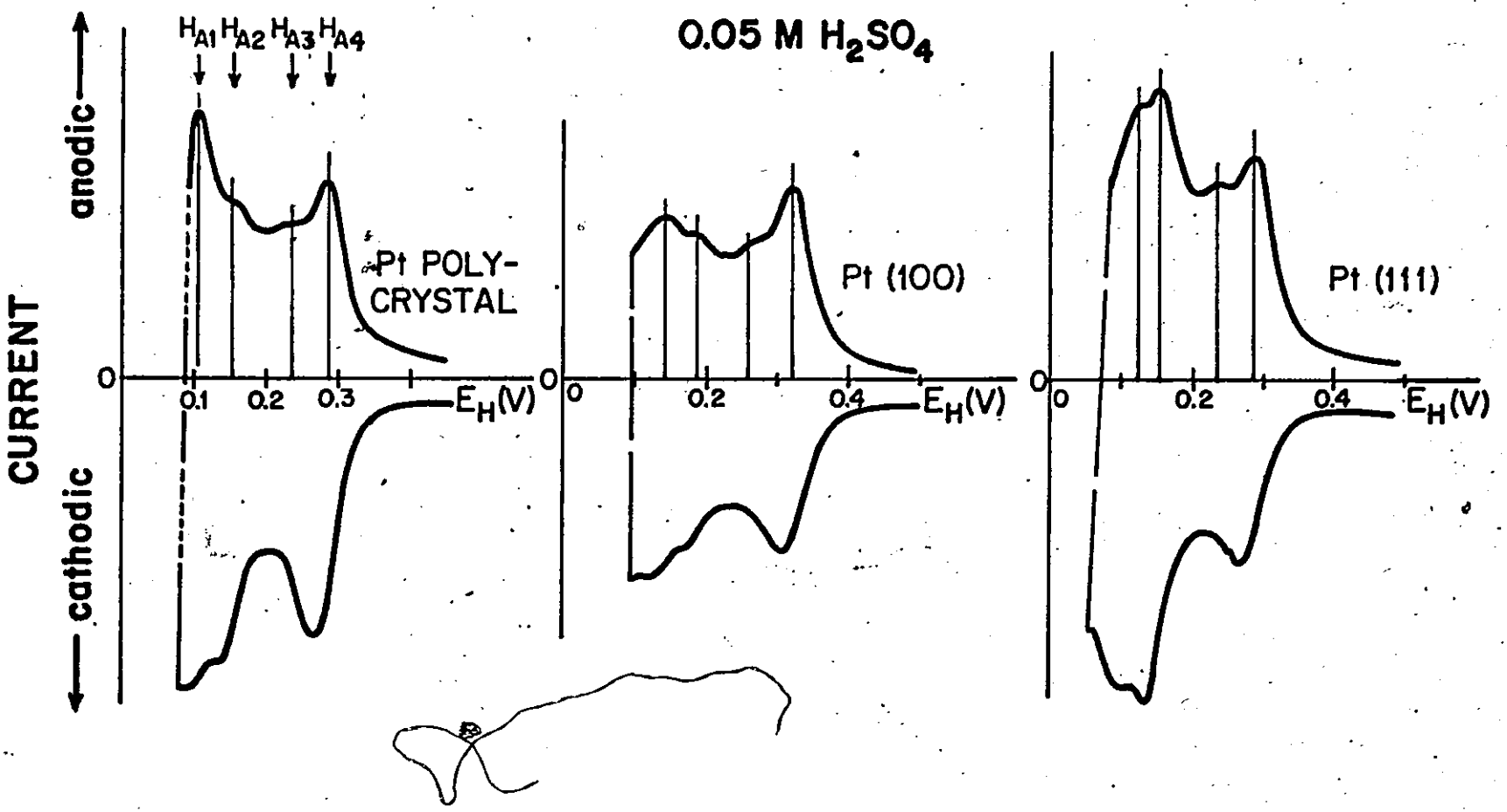

FIG 8 COMPARISON OF POTENTIODYNAMIC CURRENT-POTENTIAL PROFILES AT SINGLE-CRYSTAL AND POLYCRYSTALLINE Pt ELECTRODES IN 0.05 M H_2SO_4 (s= 0.1 V s^{-1})

at the National Research Council Laboratories and characterized by Dr. Sewell immediately before and after the experiment. No surface crystalline imperfections were present, and although some surface facetting might have been caused by the potential sweeps (line-broadening in the electron-diffraction pattern), it was on too fine a scale to be characterized.]

5.1.3 Small differences between anodic and cathodic current-potential profiles

Although the current-potential profiles representing the discharge and ionization of H on Pt are almost entirely symmetrical about the zero current line, a closer scrutiny shows the existence of small but significant differences. Since these small differences are used to identify the current peaks when the profile differs from that of Fig. 6, they will be described at this stage.

In almost every solution examined, more H seemed to be ionized from the more strongly bound states (e.g. H_{A2} at low pH) than was discharged into it in the previous cathodic sweep. Conversely, less H was ionized from the more weakly bound states (e.g. $H_{A4,5}$ at low pH) than had been discharged into them.

In H_2SO_4 and in concentrated $HClO_4$ solutions, another difference between the cathodic and anodic current-potential profiles is clearly visible. If either (i) the cathodic reversal potential is less positive than that of the H_{C4} peak (Fig. 9) or (ii) the anodic reversal potential is above that required to initiate surface oxidation (Figs. 10,11) the proportion of the electrodeposited H oxidized from the H_{A3} state is increased. This increases the currents in peak H_{A3} in the anodic

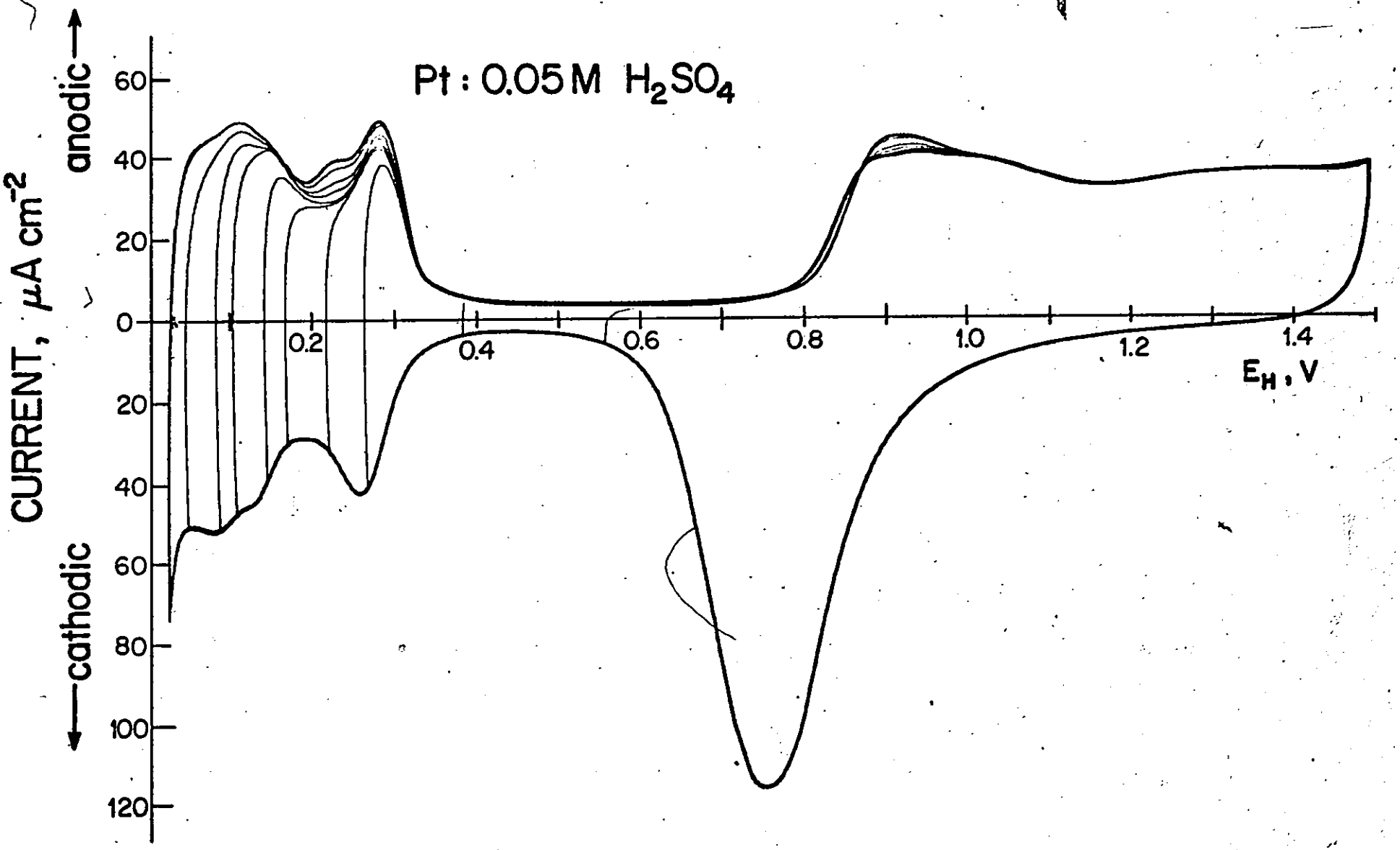

FIG 9 POTENTIODYNAMIC CURRENT-POTENTIAL PROFILES AT Pt INVOLVING A SERIES OF CATHODIC END-POTENTIALS ($s = 0.05\ V\ s^{-1}$)

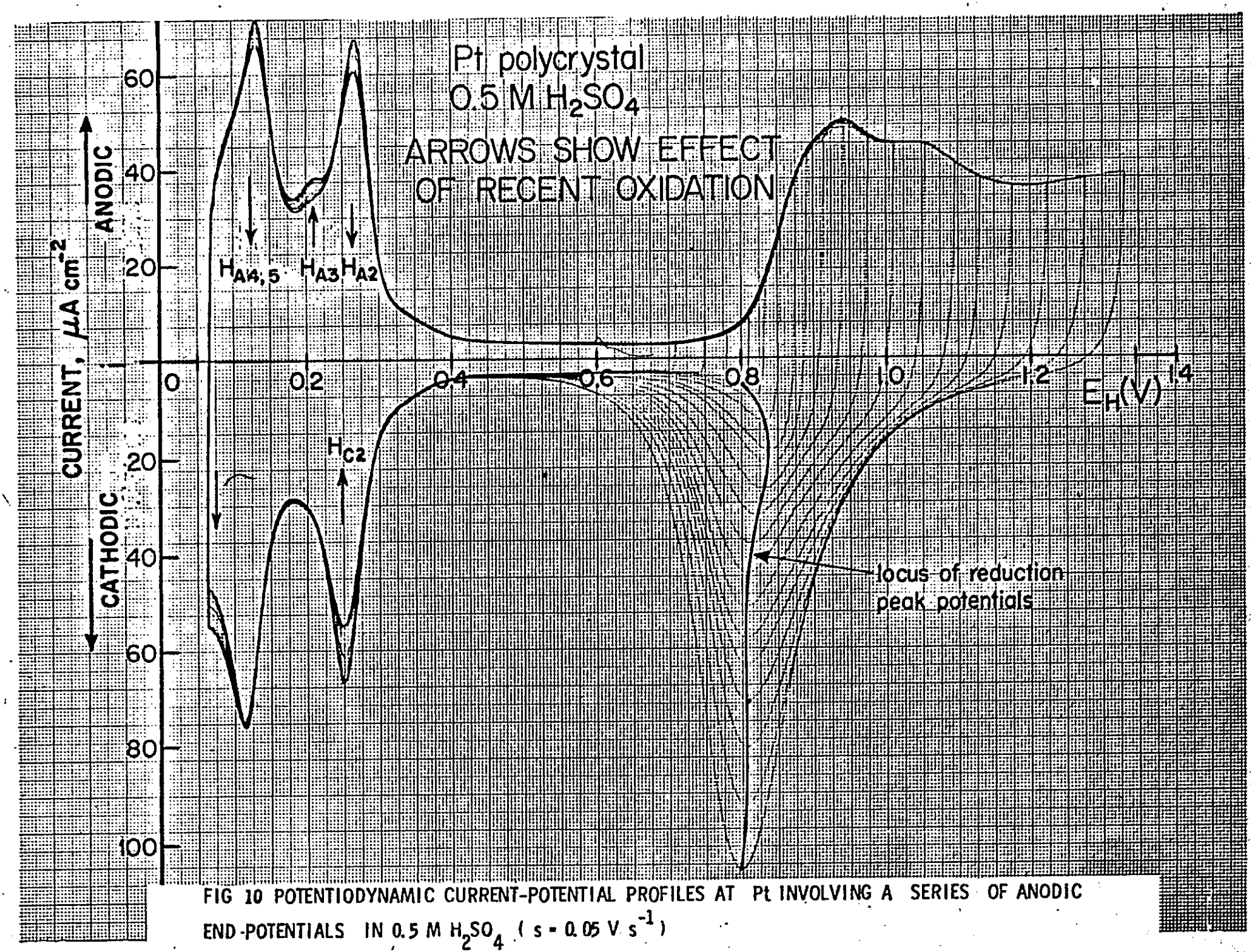

FIG 10 POTENTIODYNAMIC CURRENT-POTENTIAL PROFILES AT Pt INVOLVING A SERIES OF ANODIC END-POTENTIALS IN 0.5 M H_2SO_4 ($s = 0.05\ V\ s^{-1}$)

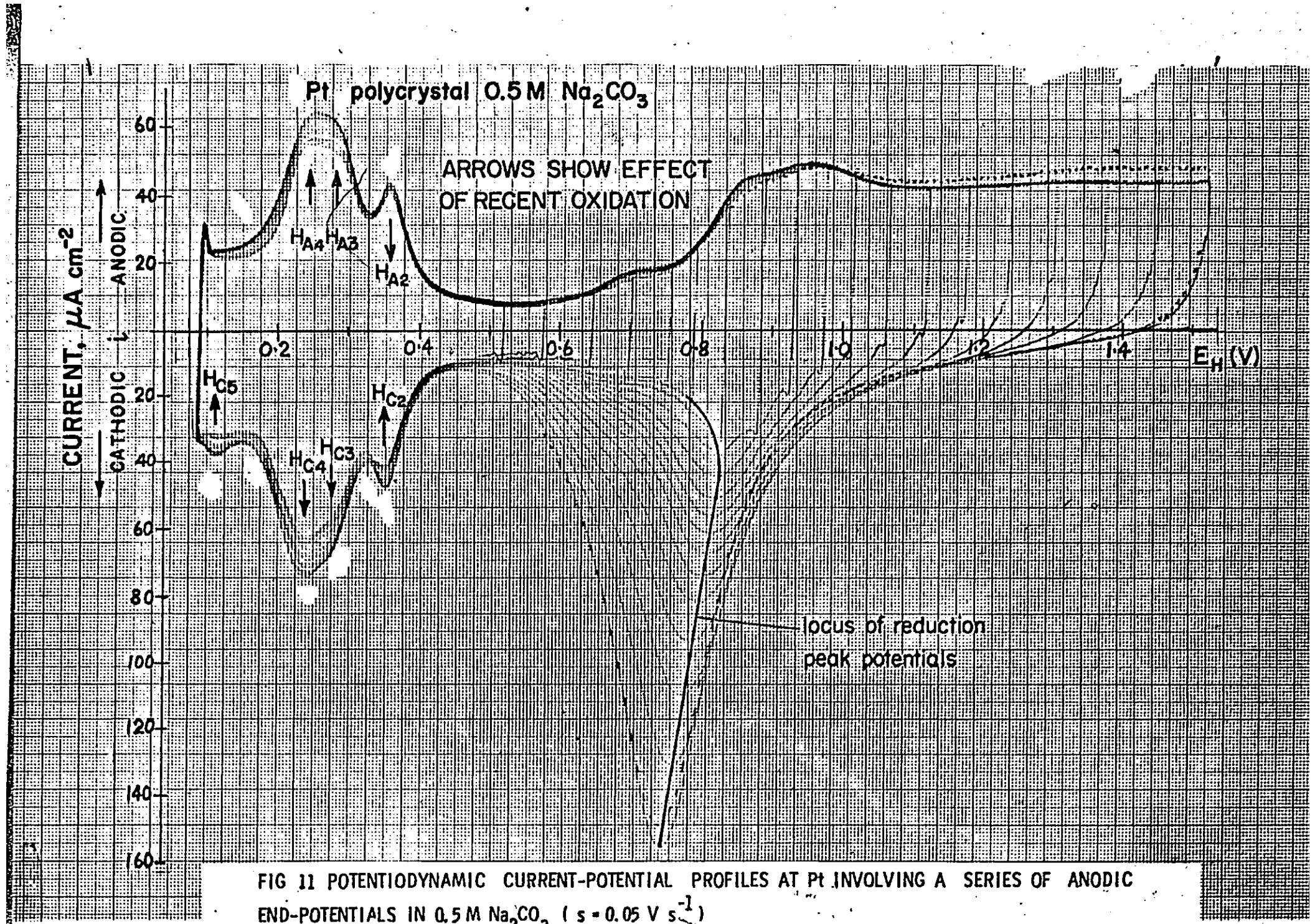

FIG 11 POTENTIODYNAMIC CURRENT-POTENTIAL PROFILES AT Pt INVOLVING A SERIES OF ANODIC END-POTENTIALS IN 0.5 M Na_2CO_3 ($s = 0.05\ V\ s^{-1}$)

sweep. The corresponding peak (H_{C3}) in the cathodic sweep (Fig.12) is not resolved in H_2SO_4 or concentrated $HClO_4$ solutions (Fig. 13). The charge in the H_{A3} peak is also increased when the sweep is interrupted at a potential between that of the $H_{C4,5}$ peak and that for H_2 evolution before the anodic sweep is commenced (Fig. 14). When this type of potential hold is employed, the H_{A3} peak remains resolved even at sweep rates above 0.2 V s^{-1}.

5.1.4 Effects of pH

Current-potential profiles recorded in alkaline solutions differ from those in acid in that (i) the electrodeposition of H appears to begin at more positive potentials (measured with respect to a Pt/H_2 electrode in the same solution) and (ii) the H atoms occupy a different distribution among the monolayer bonding states. The first effect arises at least partly because, in alkaline solutions, the oxide reduction reaction extends to the H deposition potentials, as will be discussed in more detail in connection with Table 1, below. The second effect appears to be related to the changing coverages of specifically adsorbed ions and water molecules as the p.z.c. of Pt moves to more positive potentials (measured with respect to a Pt/H_2 electrode in the same solution) with increasing pH, as will be discussed in Section 5.2.2.

The unusual behaviour of the H_{A3} peak mentioned above facilitates the designation of the peaks in alkaline solutions. The anodic current-potential curve in acid solutions shows no peak or shoulder corresponding to the electrodissolution of H from the H_{A3} state unless the sweep extends to potentials less positive than those of the H_{C4}

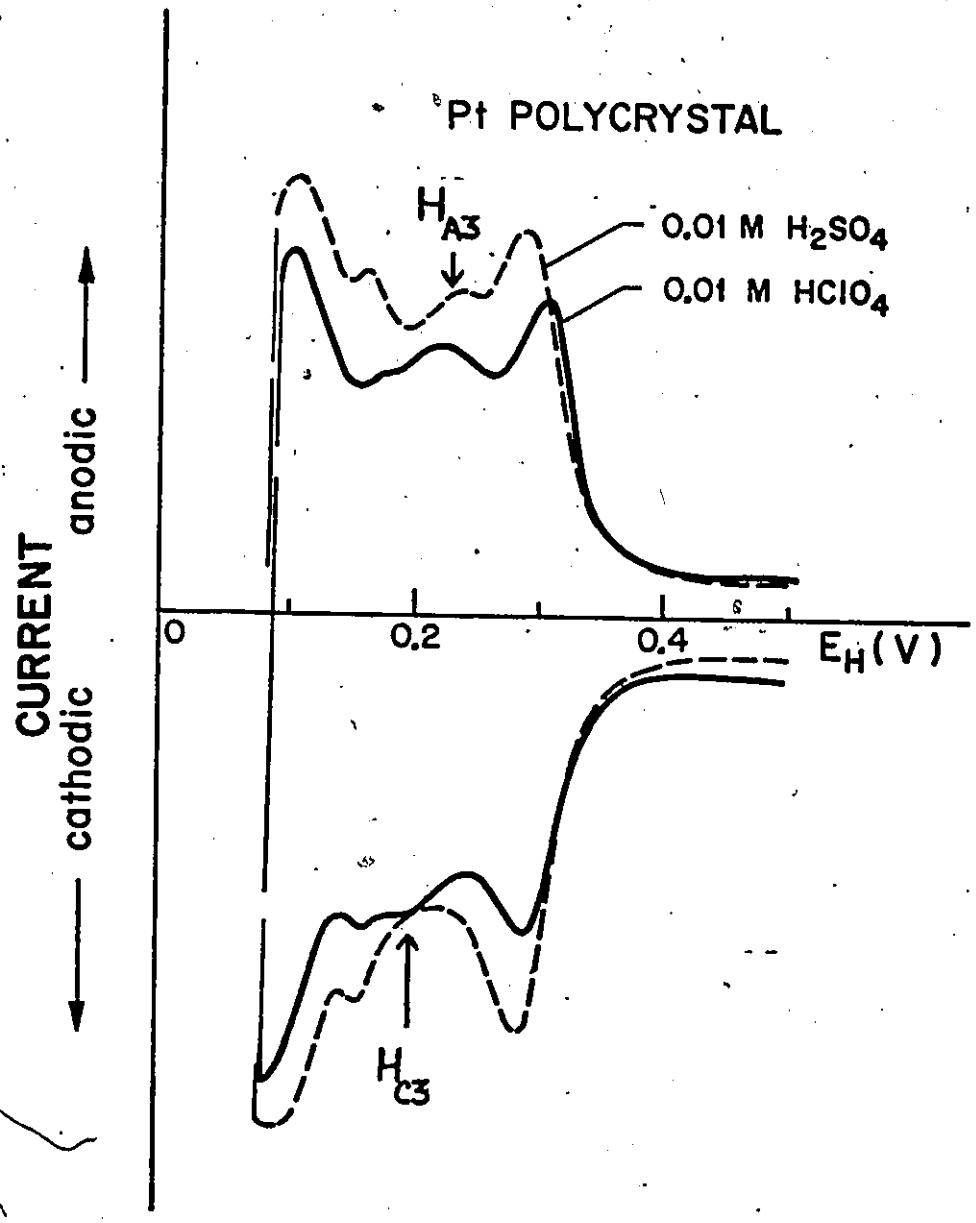

FIG 12 COMPARISON OF POTENTIODYNAMIC CURRENT-POTENTIAL PROFILES AT Pt IN 0.01 M H_2SO_4 AND 0.01 M $HClO_4$ ($s = 0.05\ V\ s^{-1}$)

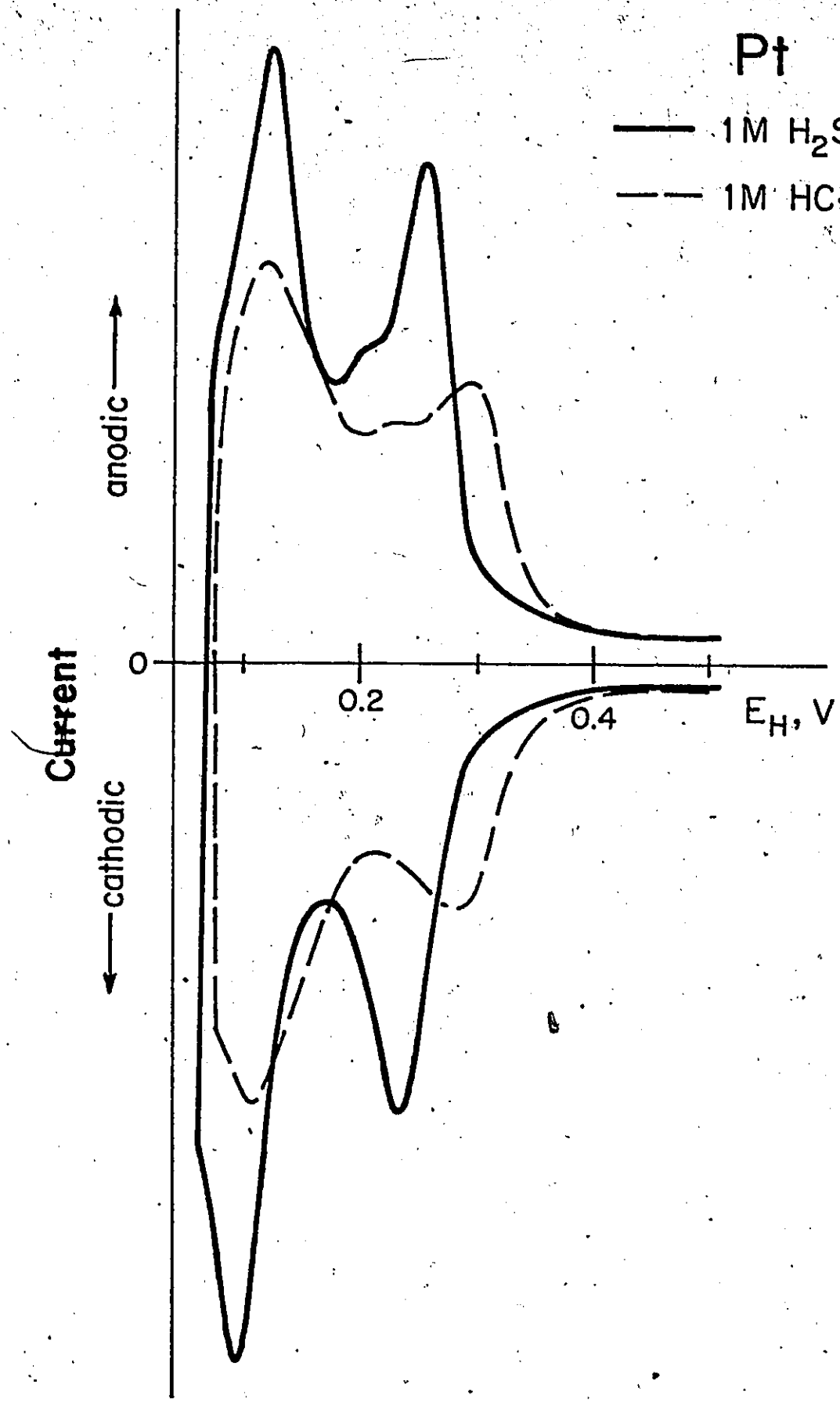

FIG 13 COMPARISON OF POTENTIODYNAMIC CURRENT-POTENTIAL PROFILES AT Pt IN 1 M H_2SO_4 AND 1 M $HClO_4$ ($s = 0.05\ V\ s^{-1}$)

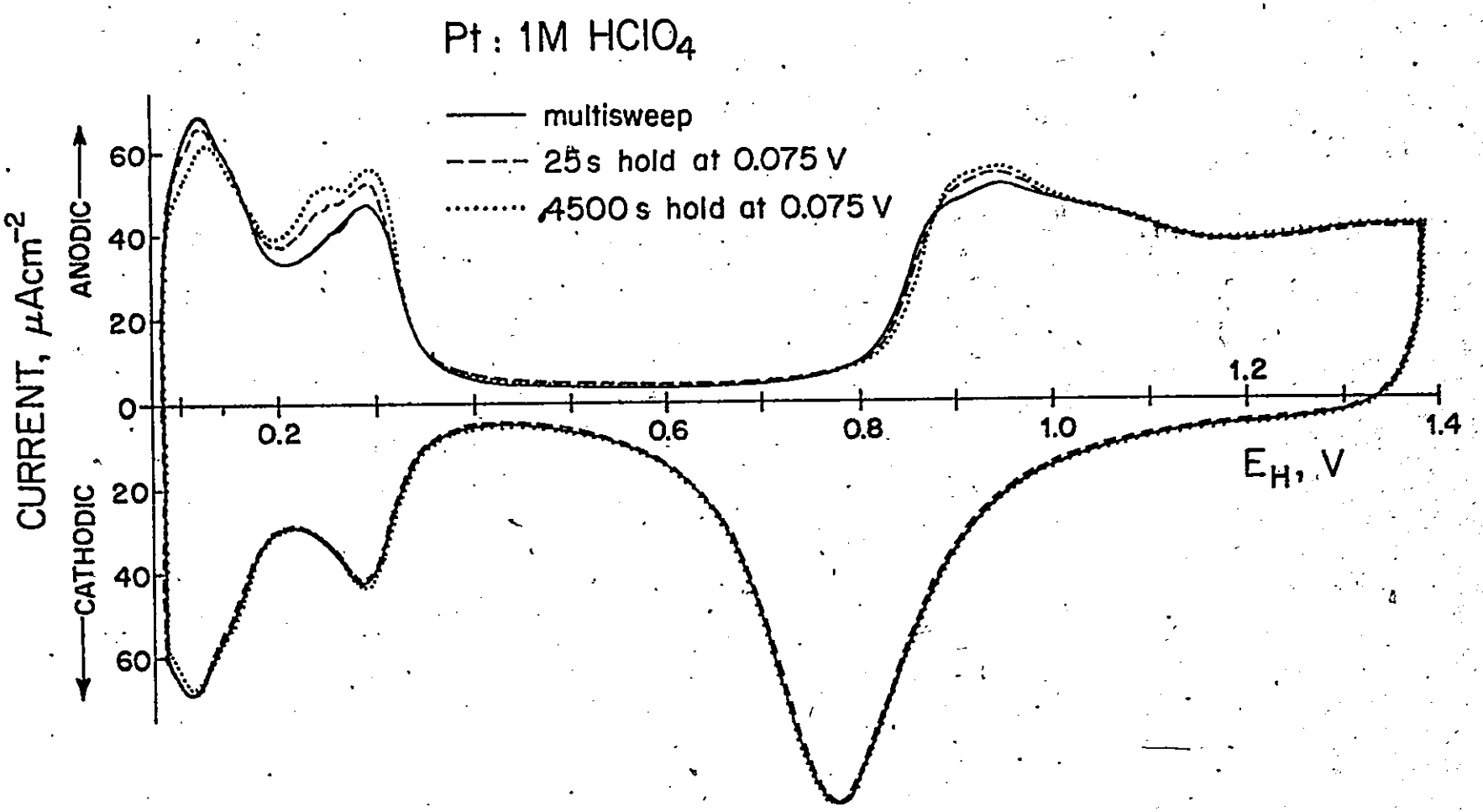

FIG 14 EFFECTS OF INTERRUPTING A POTENTIAL SWEEP AT 0.075 V ON THE SUBSEQUENT CURRENT-POTENTIAL PROFILE AT Pt (T = 274 K s = 0.05 V s^{-1})

peak (Fig. 9). In addition, smaller currents in the H_{A3} peak are associated with smaller currents in the H_{A2} peak, i.e., the bond energies of the H_{A3} state must extend to values nearly as strong as the strongest in the H_{A2} state whether or not the H_{A3} peak is resolved in the anodic sweep. Similar behaviour is observed in alkaline solutions when sweeps from a succession of cathodic end-potentials are compared (Fig. 15). This identifies the predominant duplex peak observed at high pH as H_{A4}, H_{A3}, rather than as H_{A5}, H_{A4} as might appear at first sight. Once again, the H_{A3} state is seen to involve bonding energies as strong as those of the H_2 state. Even when the H_{A4} and H_{A3} peaks overlap to such an extent that their separate resolution is lost (e.g.at high pH in NaOH), the presence of the H_{A3} peak within the composite $H_{A3,4}$ peak can still be demonstrated by varying the cathodic end-potential.

The greatest resolution of the current-potential curve in alkaline solutions is obtained in dilute Na_2CO_3 (Fig. 16), probably because such solutions may be prepared with a high degree of purity. Impurities in NaOH were always found more difficult to remove, even though five successive recrystallizations were employed. It is to be noted that two peaks are resolved at potentials below those of the H_{C4} state in dilute Na_2CO_3 (Fig. 16), so that the cathodic sweep shows five distinct submonolayer peaks, although H_{C1} is not resolved.

Figure 17 shows the relationship between the peak potentials and the pH of the solution for a wide variety of solution compositions. The potentials were measured to a Pt/H_2 electrode in the individual solution concerned. Since there is appreciable uncertainty in

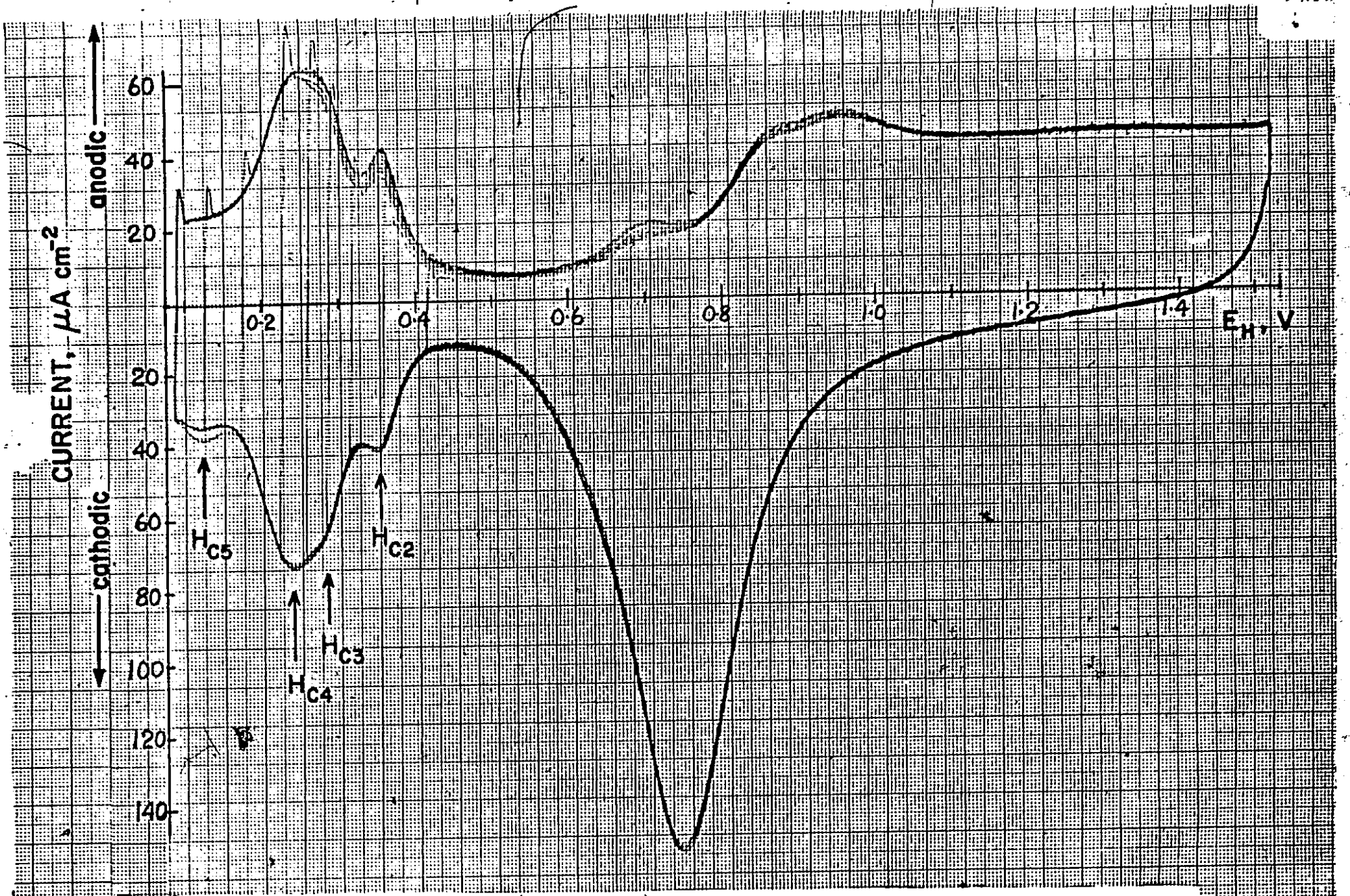

FIG 15 POTENTIODYNAMIC CURRENT-POTENTIAL PROFILES AT Pt INVOLVING A SERIES OF CATHODIC END-POTENTIALS IN 0.5 M Na_2CO_3 (pH 11.2) AT 0.05 V s^{-1})

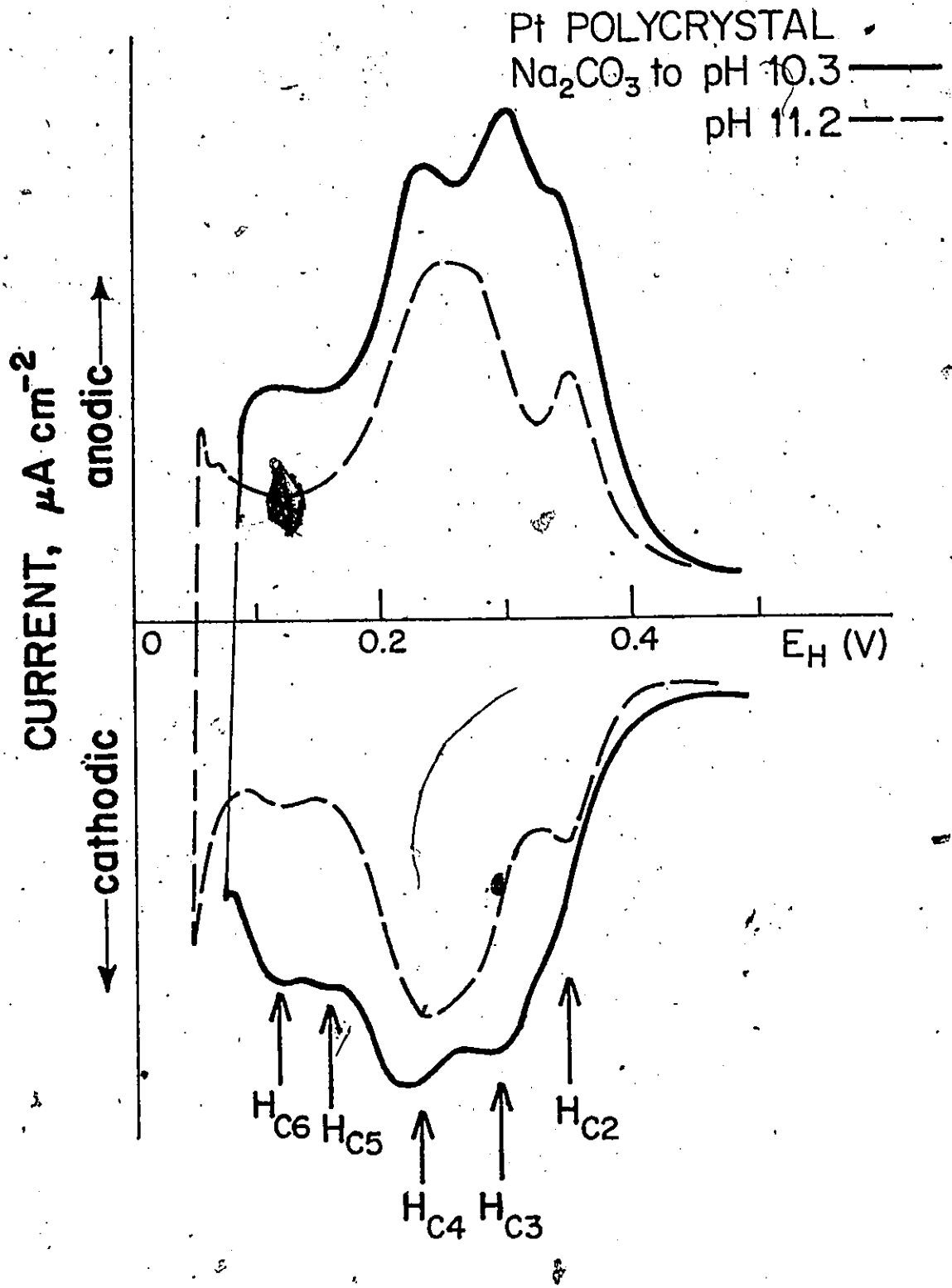

FIG 16 POTENTIODYNAMIC CURRENT-POTENTIAL PROFILES AT Pt IN Na_2CO_3 SOLUTIONS ($s = 0.05\ V\ s^{-1}$)

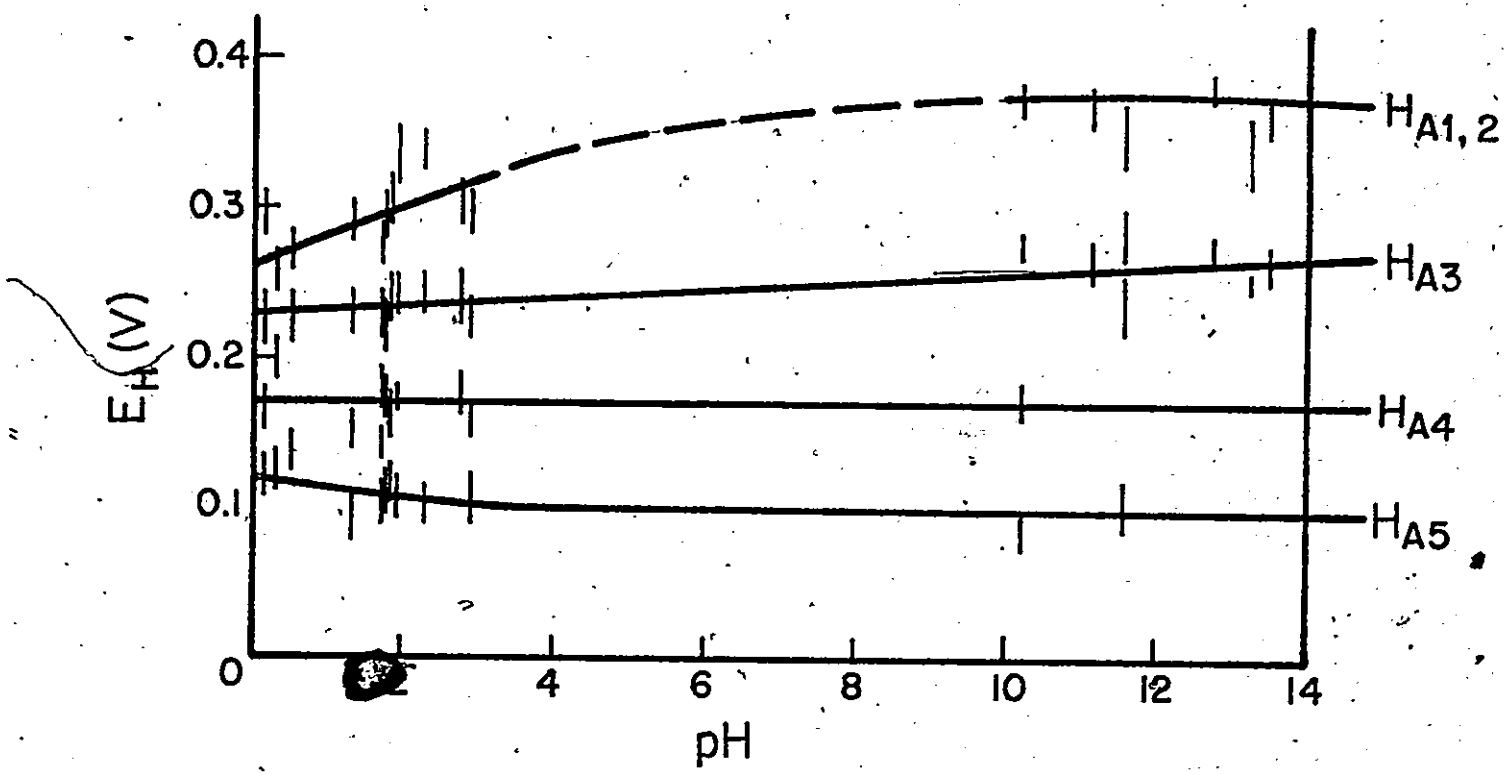

FIG 17 pH DEPENDENCE OF THE POTENTIALS OF THE ANODIC H PEAKS ($s = 0.05\ V\ s^{-1}$).

determining the potential of a component peak in a series of overlapping peaks, estimated error bands have been drawn around the apparent peak potentials. The low pH end of this diagram is shown in detail in Fig. 18. Peaks H_{A3} and H_{A4} have almost the same pH dependence as the Pt/H_2 electrode in the range 0-3. The potential of H_{A5} approaches that of H_{A4} at low pH in sulphate* solutions but not in $HClO_4$, probably because of effects of specifically adsorbed anions. Although the ratio of HSO_4^- to SO_4^{2-} ions in the solution will increase as the pH falls, data are not available to show whether the predominantly adsorbed anion correspondingly changes from SO_4^{2-} to HSO_4^-**. The extrapolation of the trends in anodic peak potentials measured in acid solutions to the values measured in alkaline solutions (Fig. 17) confirms the designation of the peaks in the current-potential profile at high pH which was deduced above.

Figure 19 shows a comparison of current-potential profiles obtained over a wide range of pH in solutions having a constant (0.5M) sulphate concentration. All these experiments were carried out with a single Pt electrode, and at a sweep rate of 0.05 V s^{-1}. Anodic and cathodic charge data obtained after subtracting double-layer charging currents (as described in Section 4.5) are shown in Table 1. Q_{H_A} and Q_{H_C} denote the anodic and cathodic H charge passed at potentials above 0.05V; $Q_{A_{tot}}$ and $Q_{C_{tot}}$ are the total charge passed in the anodic and

---

*The expression "sulphate" solutions will be used to describe those containing either H_2SO_4 or Na_2SO_4 without implying that the predominant ion is HSO_4^- or SO_4^{2-} (as controlled by the pH).

**A concentration of even 10^{-8}M in the 200 ml of solution used would be sufficient to provide a monolayer of adsorbed ions on 1 cm^2 of electrode surface under equilibrium conditions if the adsorption bond were strong enough.

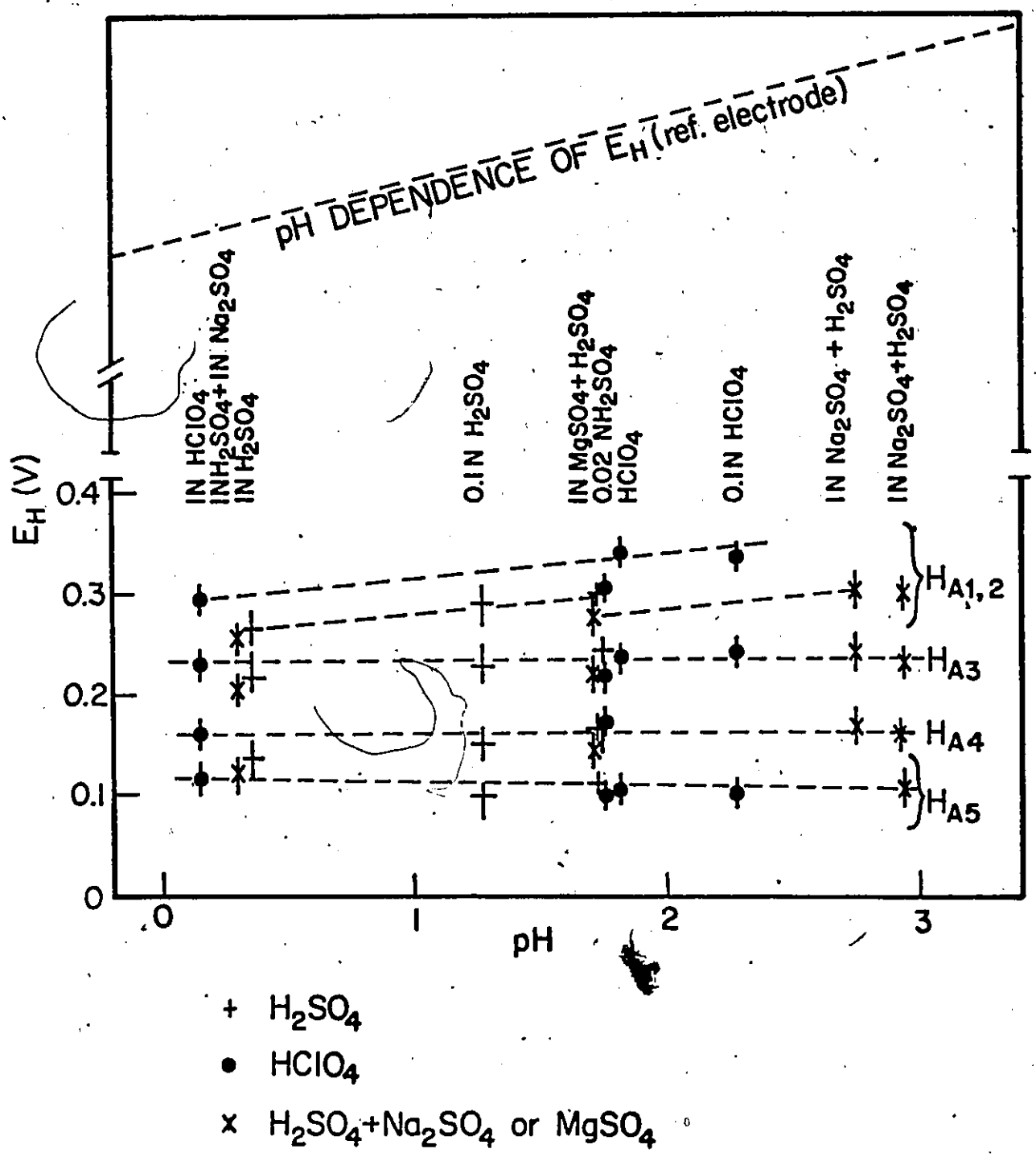

FIG 18 pH DEPENDENCE OF THE POTENTIALS OF THE ANODIC H PEAKS IN ACID SOLUTIONS ($s = 0.05\ V\ s^{-1}$)

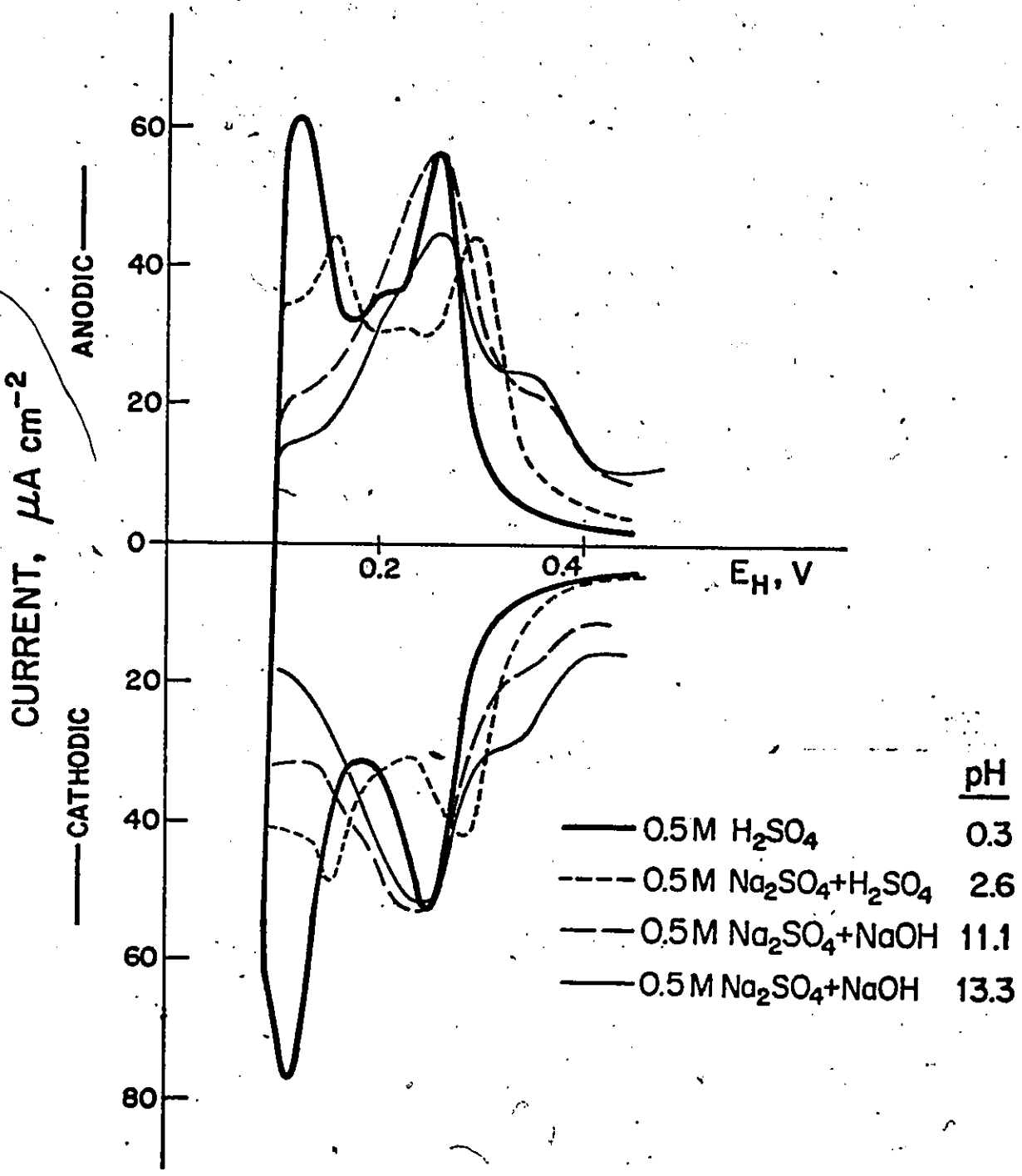

FIG 19 EFFECTS OF SOLUTION pH ON THE POTENTIODYNAMIC CURRENT-POTENTIAL PROFILE FOR THE UPD OF H AT Pt ($s = 0.05\ V\ s^{-1}$)

TABLE 1

Balance of anodic and cathodic charges (μC)* involved in electrodeposition of H and O on Pt as a function of pH in 0.5 M sulphate solutions

pH	Solution	Q_{H_A}	Q_{H_C}	$Q_{A_{tot}}$	$Q_{C_{tot}}$	$\frac{Q_{H_C} - Q_{H_A}}{Q_{H_C}}$	$\frac{Q_{C_{tot}} - Q_{A_{tot}}}{Q_{C_{tot}}}$
0.3	0.5 M H_2SO_4	56.7	60.5	191.5	192.9	6.3%	0.7%
2.6	0.5 M Na_2SO_4 + H_2SO_4	58.9	61.4	182.5	185.8	4.2%	1.8%
11.1	0.5 M Na_2SO_4 + NaOH	65.3	69.1	222.6	215.7	5.5%	-3.2%
12.8	0.5 M Na_2SO_4 + NaOH	58.4	62.6	179.1	178.7	6.7%	-0.3%
13.5	0.5 M Na_2SO_4 + NaOH	55.3	67.9	184.0	179.0	18.6%	-2.7%

*Actual charges are given for one particular Pt electrode. The reading error is about ±2%.

Thus, at room temperature, the charge involved in the UPD of H on Pt does not vary with the pH of the solution (when measured at 0.02 - 0.05 V s^{-1}).

5.1.5 Variation of the UPD charge with temperature

It has been generally accepted that exactly a monolayer of H atoms is deposited on Pt before H_2 evolution begins[29-32], and the UPD charge can therefore be used as a measure of the real surface area of the electrode[33,34]. However, the present data show that the UPD charge (measured as the H oxidation charge when the cathodic limit is adjusted to the saddle point before H_2 evolution in the cathodic sweep, see page 128) falls substantially as the temperature is raised (Fig. 20(a)) in H_2SO_4 solutions ranging from 5M to 0.0025M. As the temperature is raised, Faradaic H_2 evolution currents become significant at progressively more positive potentials (i.e., the potential of the saddle point corresponding to the onset of significant H_2 evolution becomes more positive; Fig. 20(b)). The electrode potentials were measured with respect to a Pt/H_2 reference in the same solution and at the same temperature. The potential scales thus obtained are designated E_{H_T} in the graphical data.

It is not clear why the saddle point in the current-potential curve moves to less-positive potentials and the UPD charge falls substantially in the data obtained at 366K in H_2SO_4 solutions of 0.05M and above. This may result from the combined effects of anion adsorption on the H_2 evolution kinetics and the energy of adsorption of H. Alternatively, it may simply be an artefact due to the increased

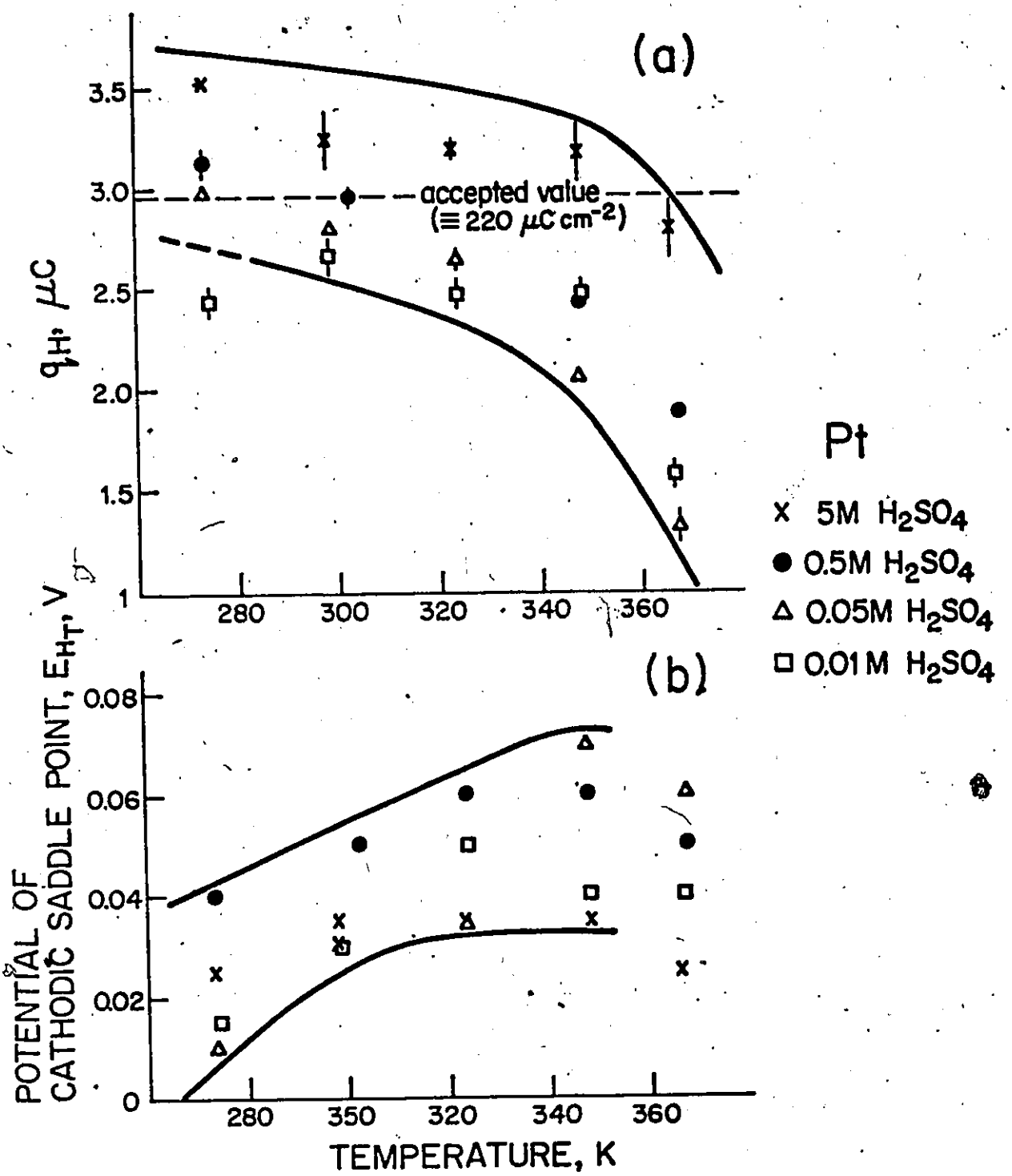

FIG 20 EFFECT OF SOLUTION TEMPERATURE ON (a) CHARGE ASSOCIATED WITH THE UPD OF H AND (b) POTENTIAL OF SADDLE-POINT PRECEEDING H_2 EVOLUTION IN THE POTENTIODYNAMIC CURRENT-POTENTIAL PROFILE ($s = 0.05\ V\ s^{-1}$)

ability of impurities to diffuse to the electrode in the nearly-boiling solution and adsorb so as to reduce the reactive area of the electrode.

These results suggest that the major factor causing variations in the measured value of q_H is neither the temperature nor the pH of the solution, but the limit of measurement imposed by the potential of the H^+/H_2 equilibrium under the experimental conditions. This may be further illustrated by a comparison of current-potential profiles obtained at a series of different temperatures. Figure 21(a) shows a series of sweeps in 0.5M H_2SO_4, all taken to the same cathodic end-potential (0.07V) measured with respect to a Pt/H_2 electrode in the same solution at the temperature of the experiment. This end-potential arises more and more within the potential range of the H_5 peaks as the temperature is raised. The sweeps in Fig. 21(b), in 0.01M H_2SO_4, are similar except that the cathodic end-potential was chosen at each temperature so that just a little H_2 would be evolved in the sweep, as shown by the increased anodic currents as the sweep changed direction. The peak potentials (measured with respect to a Pt/H_2 electrode in the same solution at the same temperature) move much less with temperature in dilute H_2SO_4 than in concentrated H_2SO_4, although the H_2 evolution currents at the potentials of the H_{C5} peak still increase markedly with temperature, as expected kinetically.

It appears from Fig. 21 that the variations in the current-potential profile with temperature arise because of shifts in the relative potentials of peaks, each associated with a <u>fixed</u> charge, rather than from <u>changes</u> in the charge of peaks, each occurring at a fixed potential. There are also differences in the profile connected

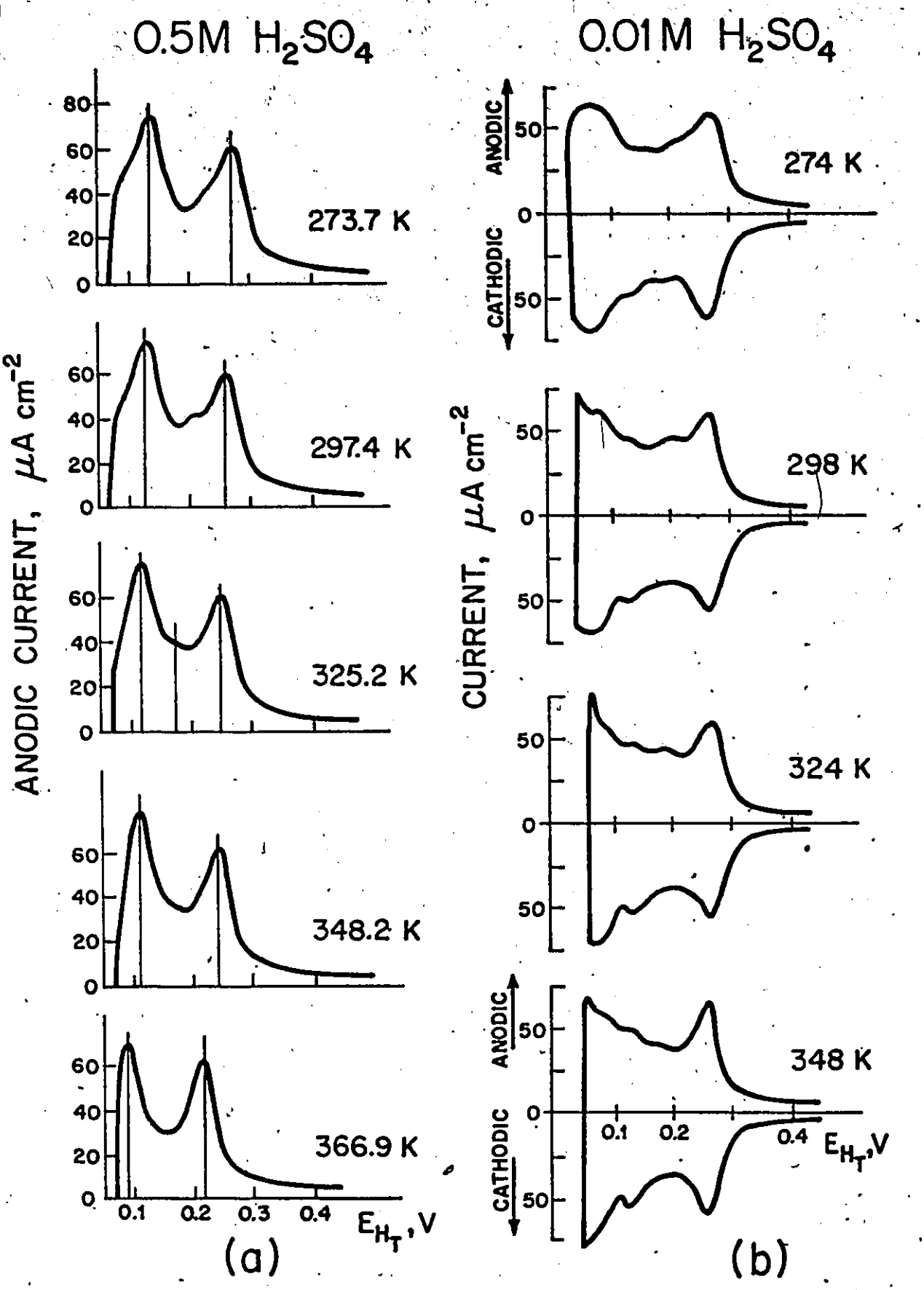

FIG 21 EFFECTS OF TEMPERATURE ON THE POTENTIODYNAMIC UPD OF H AT Pt IN (a) 0.5 M H_2SO_4 (b) 0.01 M H_2SO_4 ($s = 0.05\ V\ s^{-1}$)

with the concentration of H_2SO_4 in the solution, as follows: In 5M H_2SO_4, the H_1 state is resolved at temperatures of up to about 340K (Fig. 22), but peaks H_4 and H_5, and H_2 and H_3 are inseparably merged. In 0.5M H_2SO_4 (Fig. 21) the H_1 state is resolved only at 274K. The H_{A3} state starts with a potential comparable with that of the H_{A2} state at 274K, but becomes relatively less strongly bound as the temperature is raised, until its potential merges with that of the $H_{4,5}$ states at about 360K (Fig. 21). The energy of the H_{A3} state undergoes a similar change with respect to temperature in 1M $HClO_4$ solutions. In dilute H_2SO_4, the H_{A1} peak is not resolved even at 274K, and H_{A5} is not resolved at the higher temperatures because the H_2 evolution reaction occurs at a relatively more positive potential (Fig. 21).

Since it would appear that changes in the current-potential profile with the reaction temperature must depend either on ionic adsorption effects or on differences between the entropies associated with electrodeposition into the various states of surface bonding, and no quantitative adsorption data for ions are available at elevated temperatures, an attempt was made to compare the entropies. Figure 23 shows the anodic peak potentials corrected* to the values which would

*The absolute temperature coefficient of the Pt/H_2 electrode was calculated as follows:

The equilibrium potential, E, of the reaction

$$H^+ + e \rightleftarrows 1/2\ H_2$$

is given by

$$E = E^\circ\ (= 0, \text{ by definition}) + \frac{RT}{F} \ln a_{H^+}$$

To evaluate $\frac{dE}{dT}$, we calculate ΔS° for the reaction from

$$\Delta S^\circ = S^\circ_{H_2} - \overline{S}^\circ_{H^+} - S^\circ_e$$

Substituting the best numerical estimates for $\overline{S}^\circ_{H^+}$ and S°_e and the well-known value for $S^\circ_{H_2}$ gives

$$\Delta S^\circ = \frac{31}{2} - (-4.5) = +20 \text{ e.u.}$$

The positive sign of ΔS° will reduce ΔG° for the reaction at higher temperatures (since $\Delta G^\circ = \Delta H^\circ - T\Delta S^\circ$), pushing the equilibrium to the right, and therefore raising the potential by consuming electrons. Quantitatively,

$$\Delta S^\circ = zF\left(\frac{dE^\circ}{dT}\right)$$

so that

$$\frac{dE^\circ}{dT} = \frac{+20 \times 4.18}{96{,}500} = +0.84 \text{ mV K}^{-1}$$

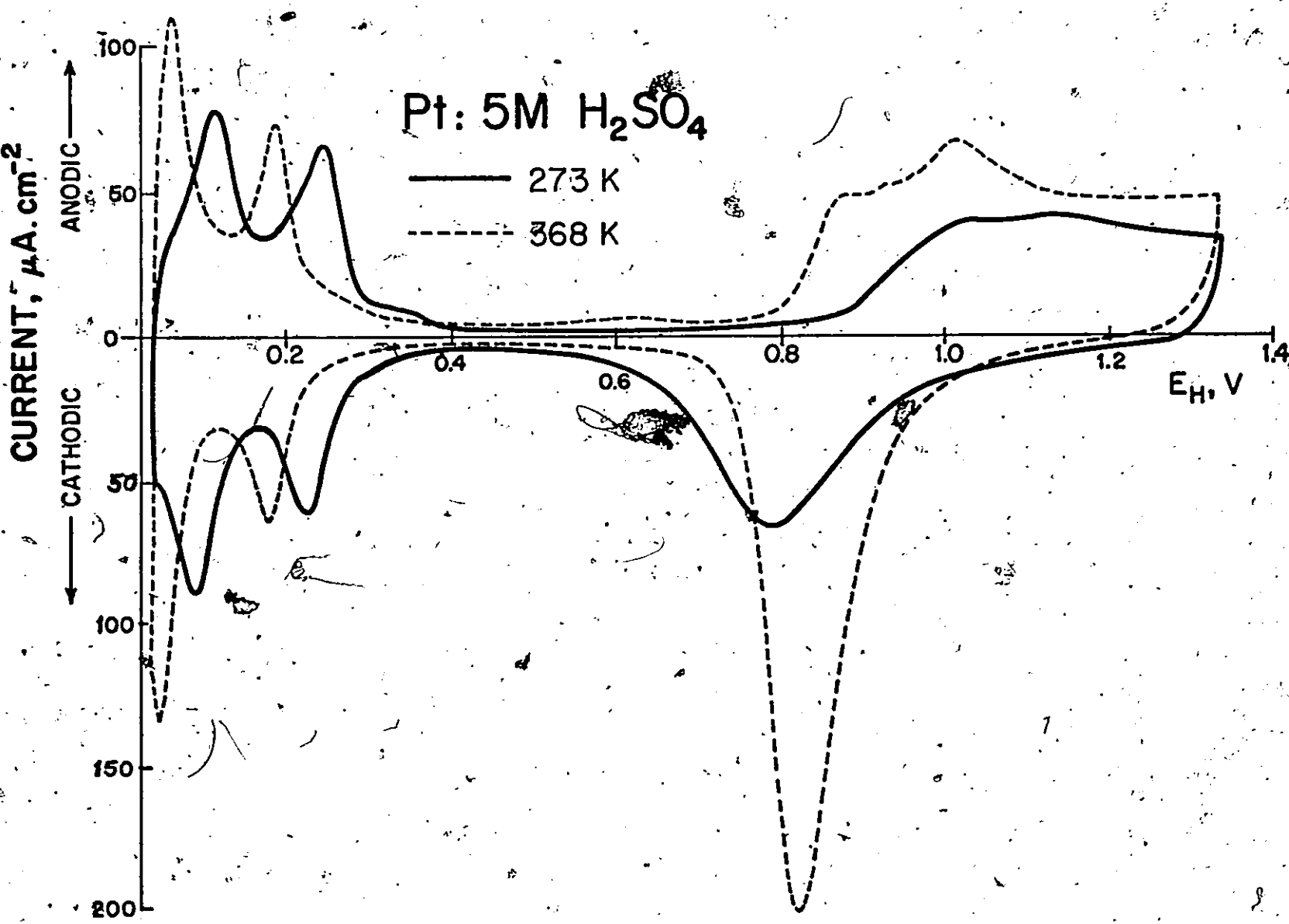

FIG 22 POTENTIODYNAMIC CURRENT-POTENTIAL PROFILES AT Pt IN 5 M H_2SO_4 AT 273 AND 368 K
(s = 0.05 V s^{-1})

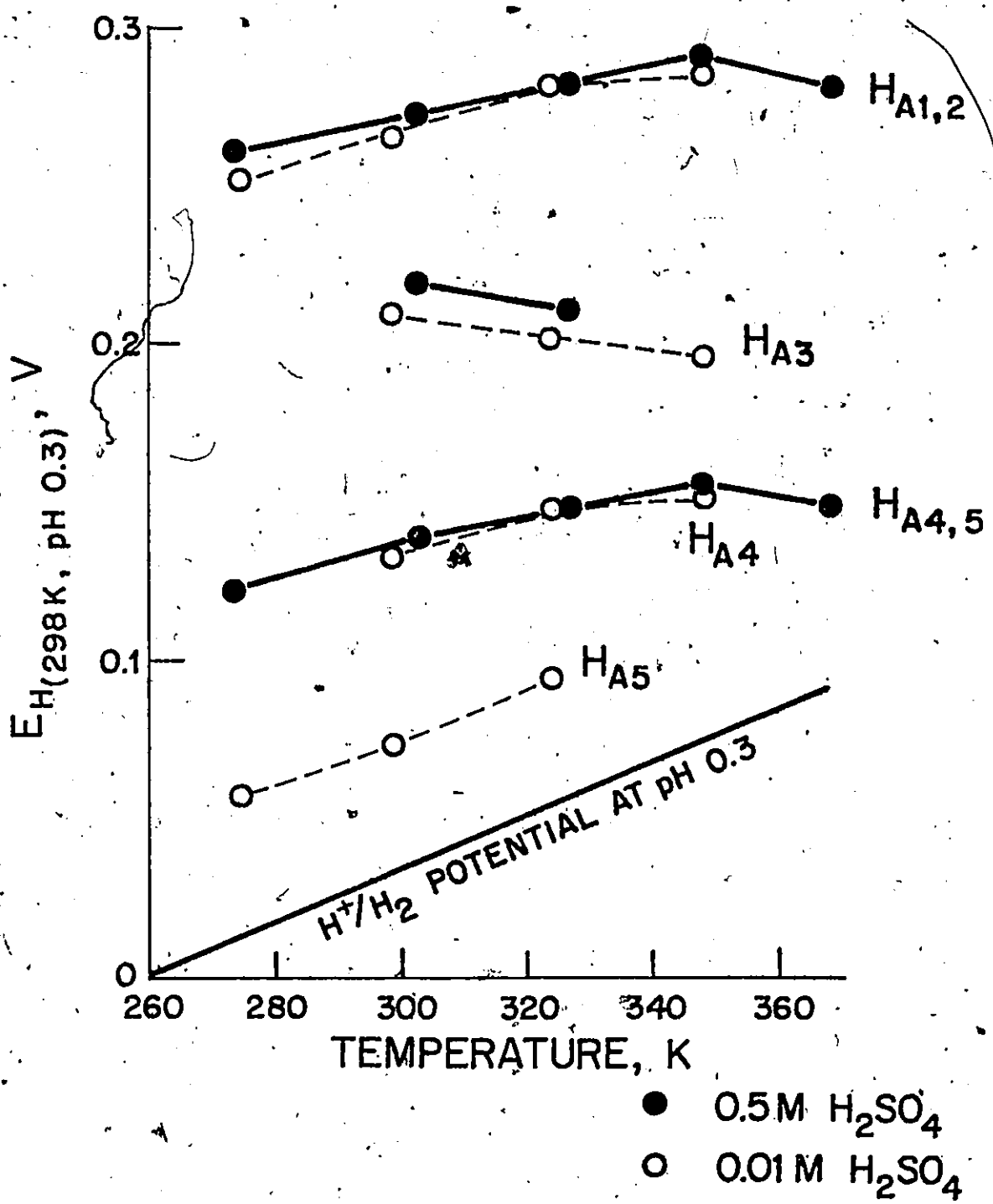

FIG 23 TEMPERATURE DEPENDENCE OF H PEAK POTENTIALS (EXPRESSED w.r.t. A Pt/H_2 ELECTRODE IN 0.5 M H_2SO_4 AT 298 K)

have been measured with reference to a Pt/H_2 electrode at pH 0.3 (0. 5M H_2SO_4)/at constant temperature of 298K. The shift of the H_{A3} peak relative to H_{A4} and H_{A5} evidently arises because the entropy* associated with deposition in the H_{A3} state is small and maybe even negative, whereas that associated with H_{A2}, H_{A4} and H_{A5} is apparently positive. The uncertainty arising from the estimation of the potentials of the overlapping component peaks prohibits any accurate numerical estimation of the entropies for deposition in the corresponding states.

The fact that the Pt surface need not be covered by a monolayer of H atoms before H_2 evolution commences was confirmed by experiments in H_2SO_4 - $HgSO_4$ solutions at room temperature. Progressive electrodeposition of Hg was found to reduce the H deposition charge ultimately to 5% of its original value without changing the potential for significant rates of H_2 evolution (i.e., within the accuracy of ±8 mV, the potential of the saddle point in the cathodic curve occurring before H_2 evolution was independent of the Hg coverage). Of course, H_2 evolves on many metals while the coverage of electrodeposited H is well below a monolayer. On Au, for instance, the coverage of H is less than 0.02 when H_2 evolution begins[139]**.

5.1.6 Effects of adsorbed ions

In order to study the electrodeposition of H with the least perturbation from adsorbed ions, the only anions added were HSO_4^-, SO_4^{2-}, and ClO_4^-, and the only cations Na^+, Mg^{2+} and H^+. The current-potential curve in dilute H_2SO_4 is similar to that in dilute $HClO_4$ (Fig. 12). However, the addition of sulphate ions to these dilute solutions has

*Part of the temperature dependence of H peak potentials will be due to temperature-dependent anion adsorption effects (see below). Corresponding entropy contributions will then be involved.

**Thus it is the thermodynamic free energy of the overall process $2H^+ + 2e \rightarrow H_2$ that determines the potential for H_2 evolution and not H coverage, though this may affect the kinetics of H_2 evolution.

three distinct effects on the electrodeposition and oxidation of H: (i) it reduces the underpotential of deposition in the $H_{1,2}$ (and possibly the H_3) state, (ii) it causes the H_4 and H_5 peaks to merge into the composite $H_{4,5}$ peak, and (iii) it increases the aspect-ratio of peaks $H_{1,2}$ and $H_{4,5}$. That these effects arise from the specific adsorption of HSO_4^- or SO_4^{2-} ions rather than from concurrent pH changes is shown by the fact that adding Na_2SO_4 or $MgSO_4$ to dilute H_2SO_4 makes the current-potential curve become more like that in 0.5M H_2SO_4 (Fig. 24). Small differences in the current-potential curve at potentials negative to the p.z.c. of Pt (about 0.18 V at pH 0.3)[586] may be related to the nature of the cations present.

In alkaline solutions, the addition of Na_2SO_4 produces no significant changes in the current-potential profile. This is consistent with the extrapolation of presently available p.z.c. data[586], which suggests that in alkaline solutions the p.z.c. of Pt will be considerably more positive than the potentials of the UPD of H.

5.1.7 Kinetics and reversibility

It has already been pointed out that the discharge and oxidation of H on Pt are fast reactions in comparison with other electrochemical deposition processes. The asymmetry of the current-potential profile resulting from the onset of irreversibility shows (Fig. 25) that although the electrodeposition of H is essentially reversible at 10 V s^{-1} in 0.5M H_2SO_4, it is clearly irreversible at 100 V s^{-1}, although iR losses in the solution cause some distortion in the profile for the faster sweeps. Despite this increased distortion

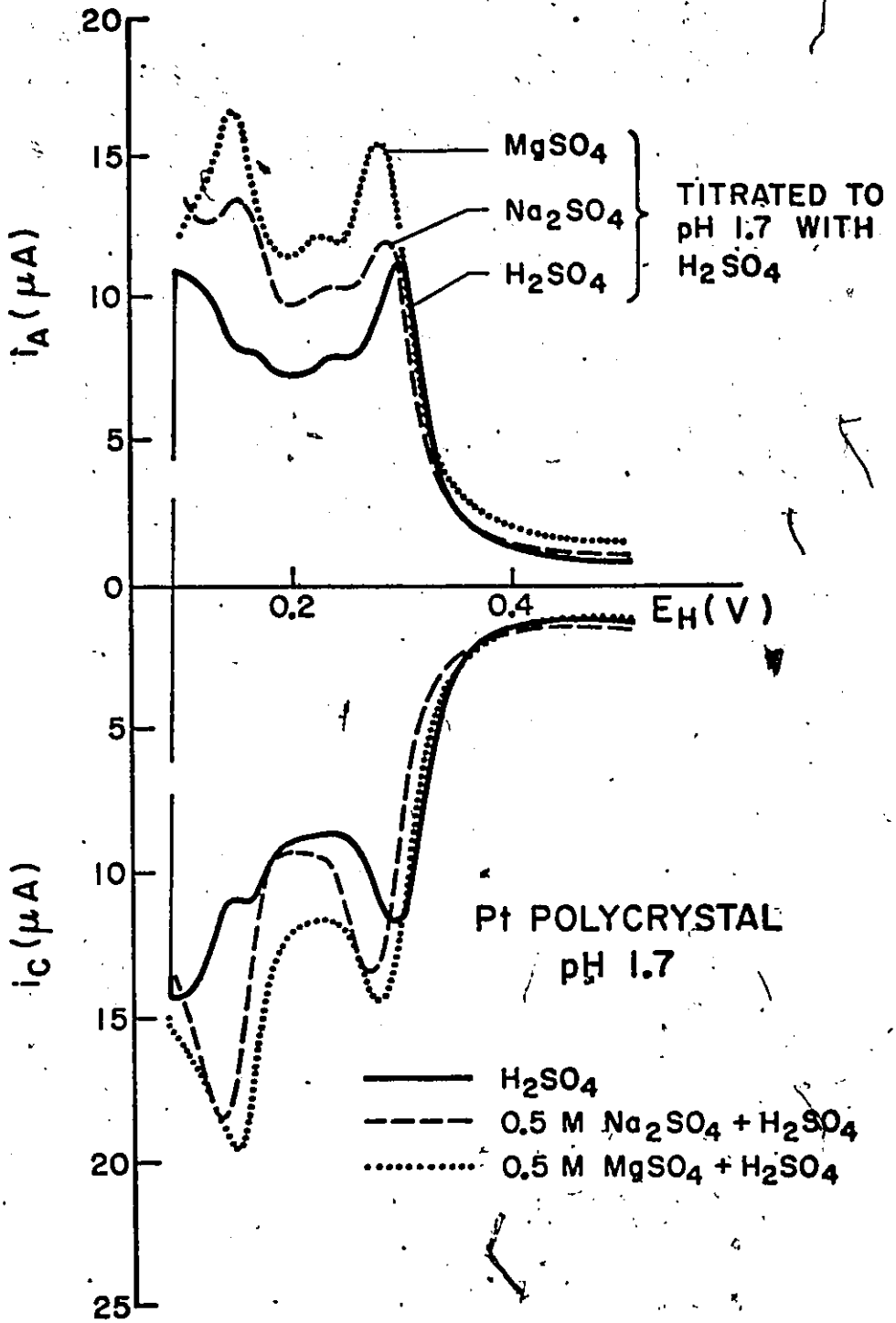

FIG 24 EFFECTS OF Na_2SO_4 AND $MgSO_4$ ADDITIONS ON THE UPD OF H AT pH 1.7 ($s = 0.05\ V\ s^{-1}$)

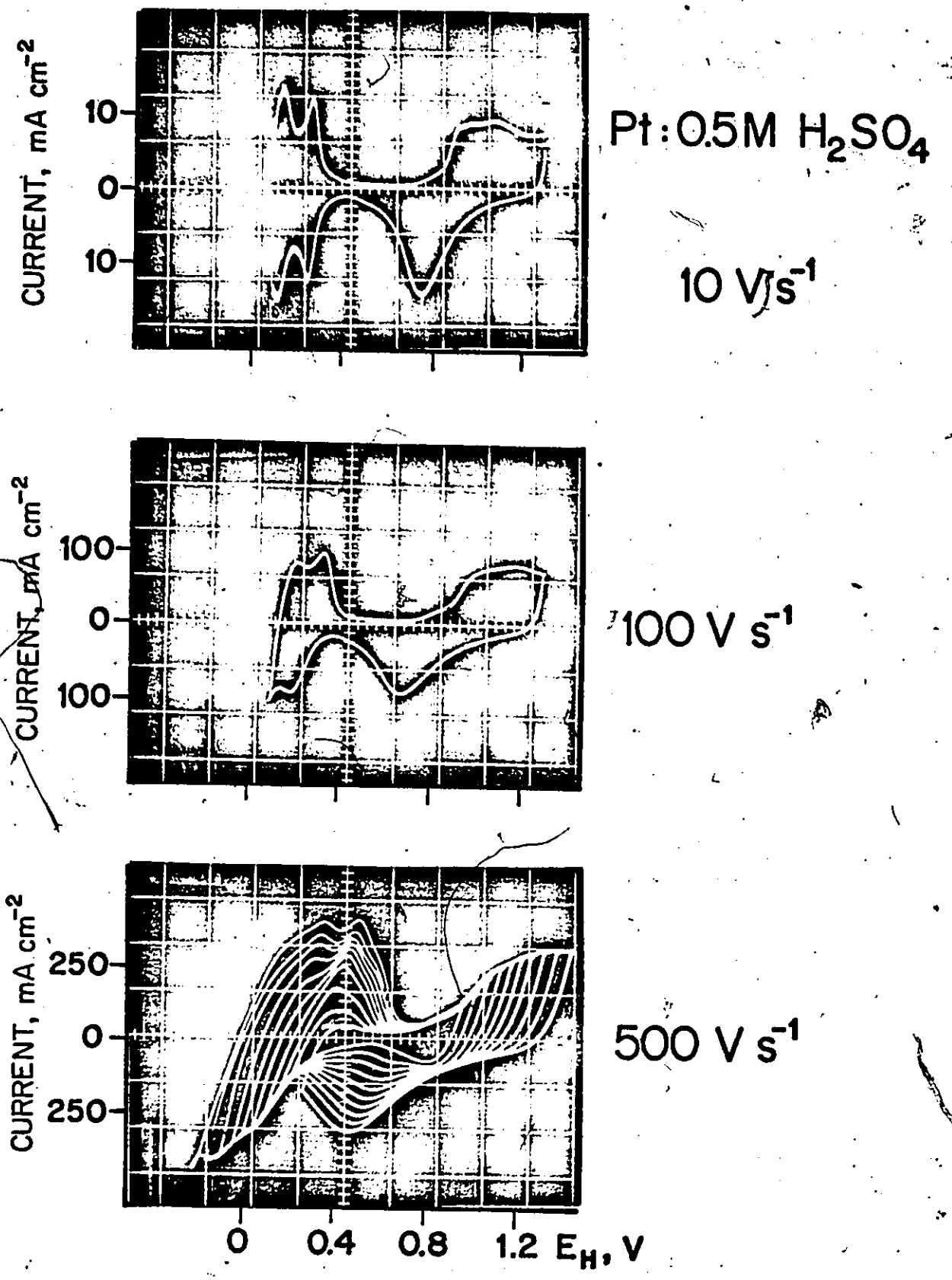

FIG 25 IRREVERSIBILITY IN THE UPD OF H AT Pt AT HIGH SWEEP RATES

at higher sweep rates, at least three states of H are still resolved in the anodic profile at even 500 V s^{-1}. (Fig. 25 shows a series of current-potential profiles at this sweep rate over a limited potential range which is successively shifted to less-positive potentials). In alkaline solutions, the current-potential profile becomes asymmetrical (Fig. 26) at sweep rates about an order of magnitude lower than in acid (Fig. 25). The electrodeposition of H becomes so irreversible at higher sweep rates in alkaline solutions (Fig. 27) that the anodic H peaks become superimposed on other oxidation peaks. This leads to a complex situation in which different types of species present on the surface may react together; e.g., in an <u>overall</u> anodic process such as:

$$Pt\text{-}H + H_2O \rightarrow Pt\text{-}OH + 2H^+ + 2e$$

Figure 28 shows a typical example of the dependence of the peak potentials on the sweep rate. At sweep rates above about 1 V s^{-1}, the electrodeposition currents begin to exceed the exchange current, the processes become irreversible and the peak potentials increase (by about 0.11 V $decade^{-1}$ of sweep rate). At a lower temperature (274K), the anodic peaks become irreversible at 0.2 V s^{-1} and the shift per decade is 0.09 V. The combination of a series of such plots for different solutions (Fig. 29) shows very clearly the increasing irreversibility of H adsorption with increasing pH. More recent work in this laboratory, involving the use of an automatic iR compensator, shows that this trend continues as the pH is lowered below 0.3. In 5M H_2SO_4, the onset of irreversibility occurs at about 100 V s^{-1}[582]. The rate constant of the electrodeposition reaction (k_o) may be calculated

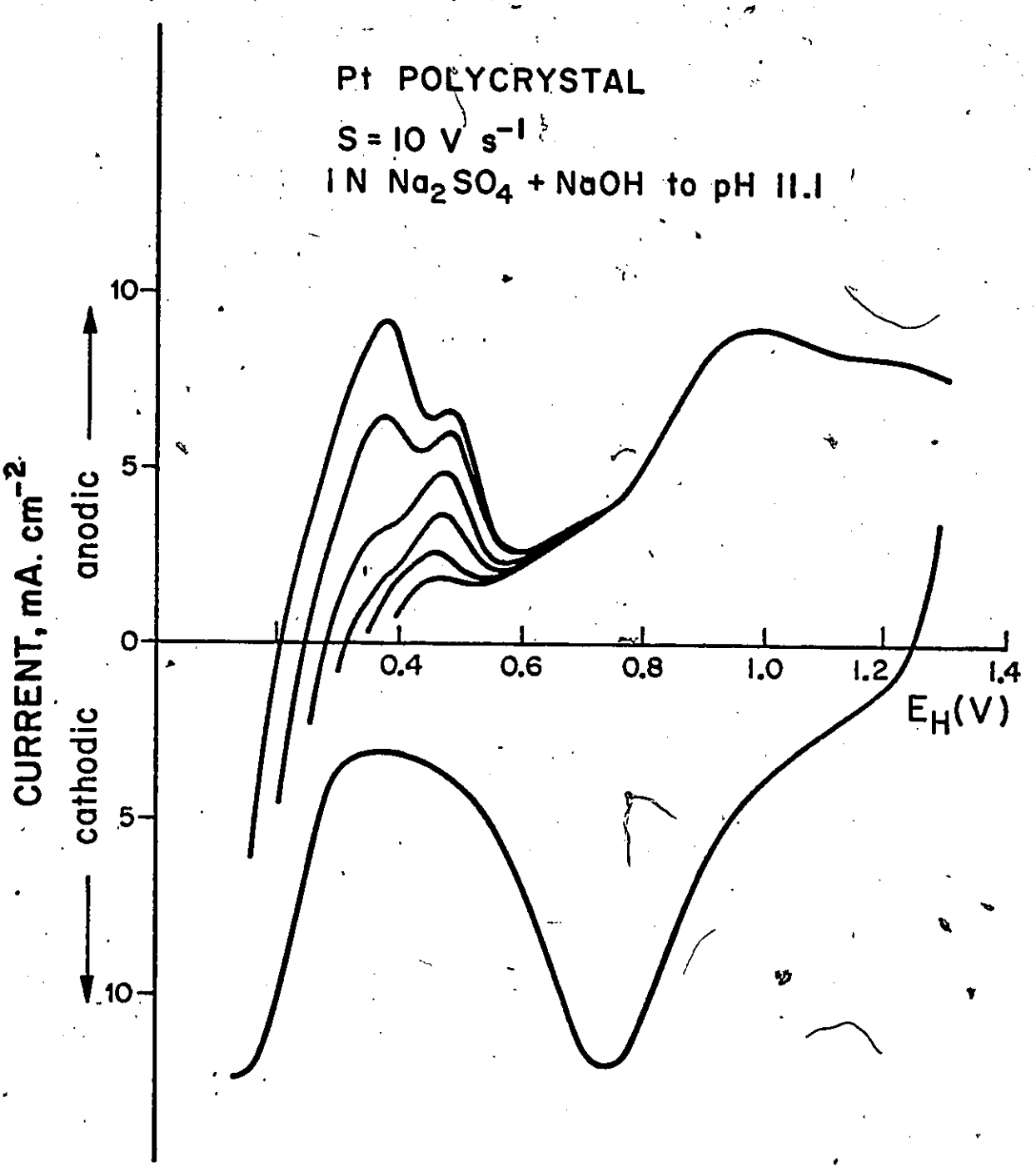

FIG 26 IRREVERSIBLE UPD OF H AT Pt AT 10 V s^{-1} IN ALKALINE SOLUTION SHOWN BY SWEEPS WITH DIFFERENT CATHODIC END-POTENTIALS

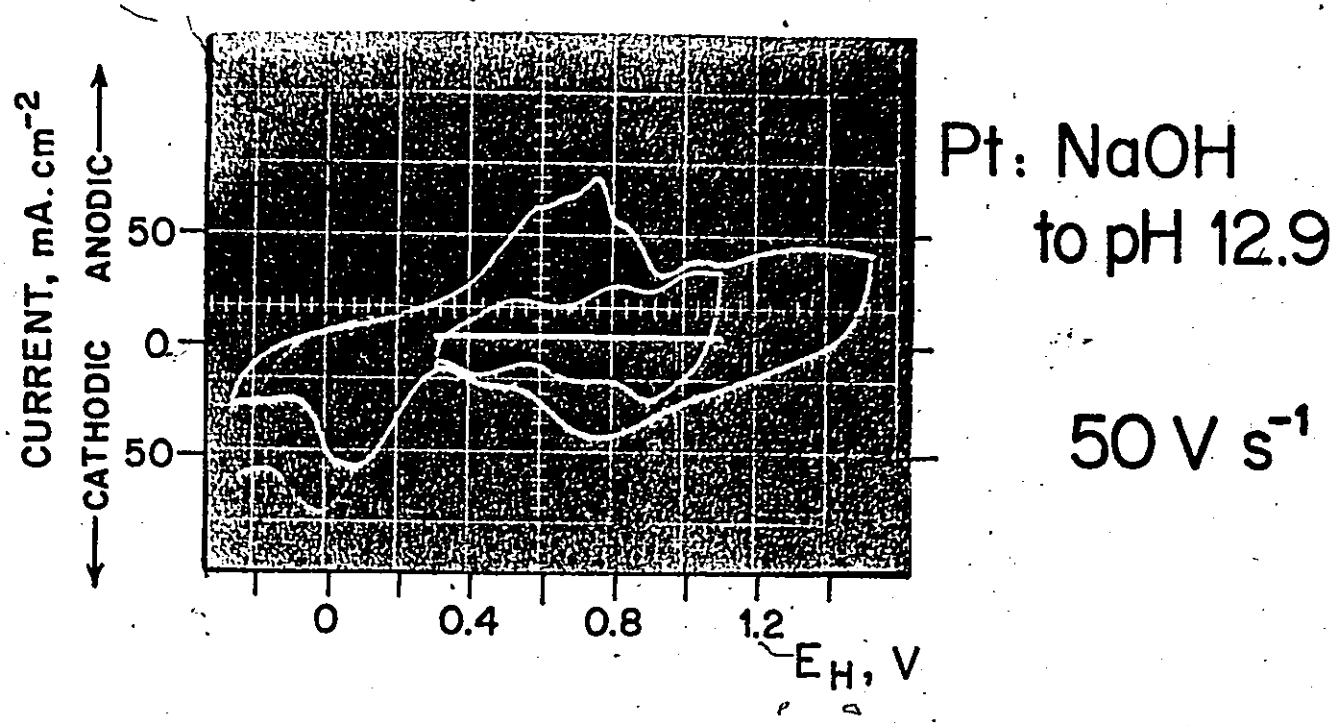

FIG 27 POTENTIODYNAMIC CURRENT-POTENTIAL PROFILES AT Pt AT 50 V s^{-1} SHOWING THE SUPERIMPOSITION OF CURRENTS FROM THE UPD OF H AND O SPECIES

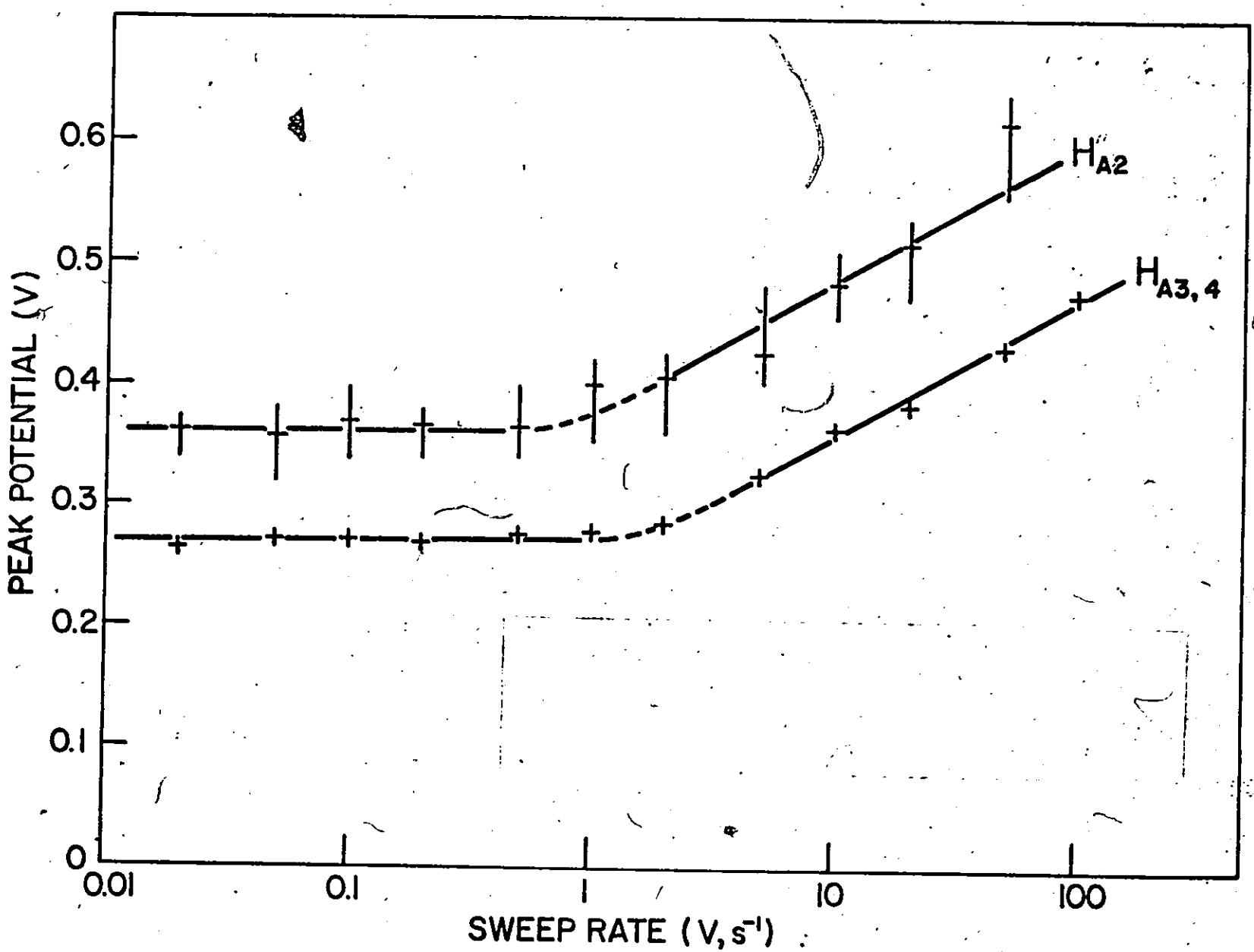

FIG 28 ANODIC H PEAK POTENTIALS AS A FUNCTION OF ANODIC SWEEP RATE AT pH 11.1

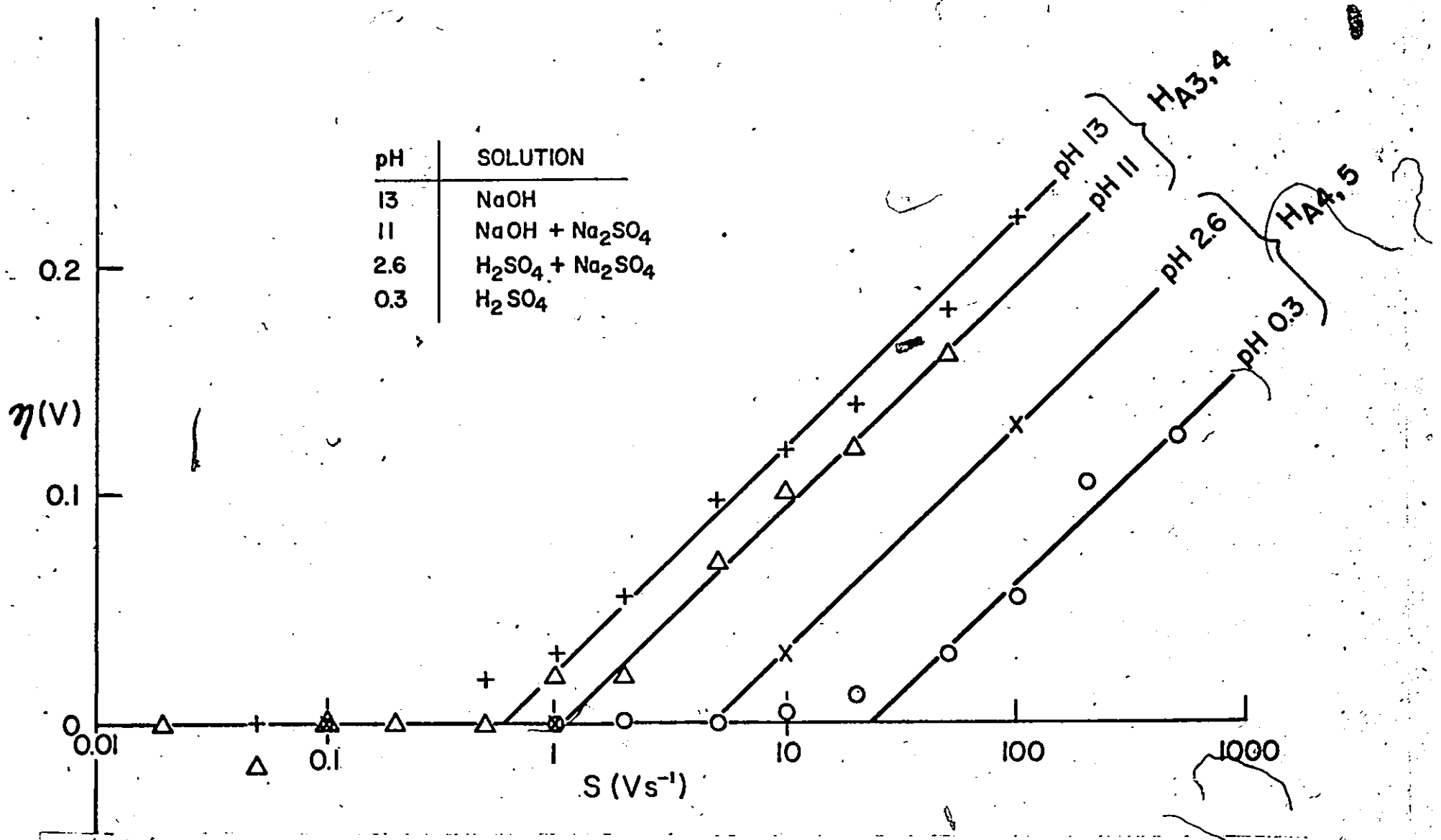

FIG 29 SHIFT OF ANODIC PEAK POTENTIAES WITH LOG (SWEEP RATE) SHOWING TRANSITION FROM REVERSIBLE TO IRREVERSIBLE BEHAVIOUR WITH INCREASING SWEEP RATE AT VARIOUS pHs

directly from the value of the sweep rate (s_o) at which the electrodeposition current begins to exceed the exchange current since, from the Butler-Volmer equation, $s_o = k_o \frac{2RT}{F}$ for a one-electron reaction with a β-factor of 1/2 at low overpotentials. The calculated rate constants are:

pH	-0.7	0.3	2.6	11	13
k_o (s^{-1})	1935	445	94	20	11

The rate constant increases almost linearly with the activity of H_3O^+ ions in acid solutions, but this dependence is much less strong in alkaline solutions where the predominant reactants are H_2O molecules.

The relative reversibility of H deposition into the various states was assessed by a comparison of the current envelope obtained from a slow potential sweep modulated by a triangular function of low amplitude, and the current-potential curve obtained at a linear sweep rate equal to that in the triangular modulation. Figure 30 shows typical results for acid and alkaline solutions in the range of sweep rates where electrodeposition is becoming irreversible. These graphs were made by superimposing data obtained from linear sweeps, modulated sweeps carried cathodically, and modulated sweeps carried anodically. The dotted lines show the envelope of the currents passed when the slow carrier sweep was moving in the same direction as the unmodulated sweep. Such comparisons of the relative peak heights of the reversible components, as may be made from these data, suggest that the reversibility of deposition in the various states is rather similar. This confirms the finding in Fig. 28 that the differences between the exchange currents for H deposition in the various states are relatively small.

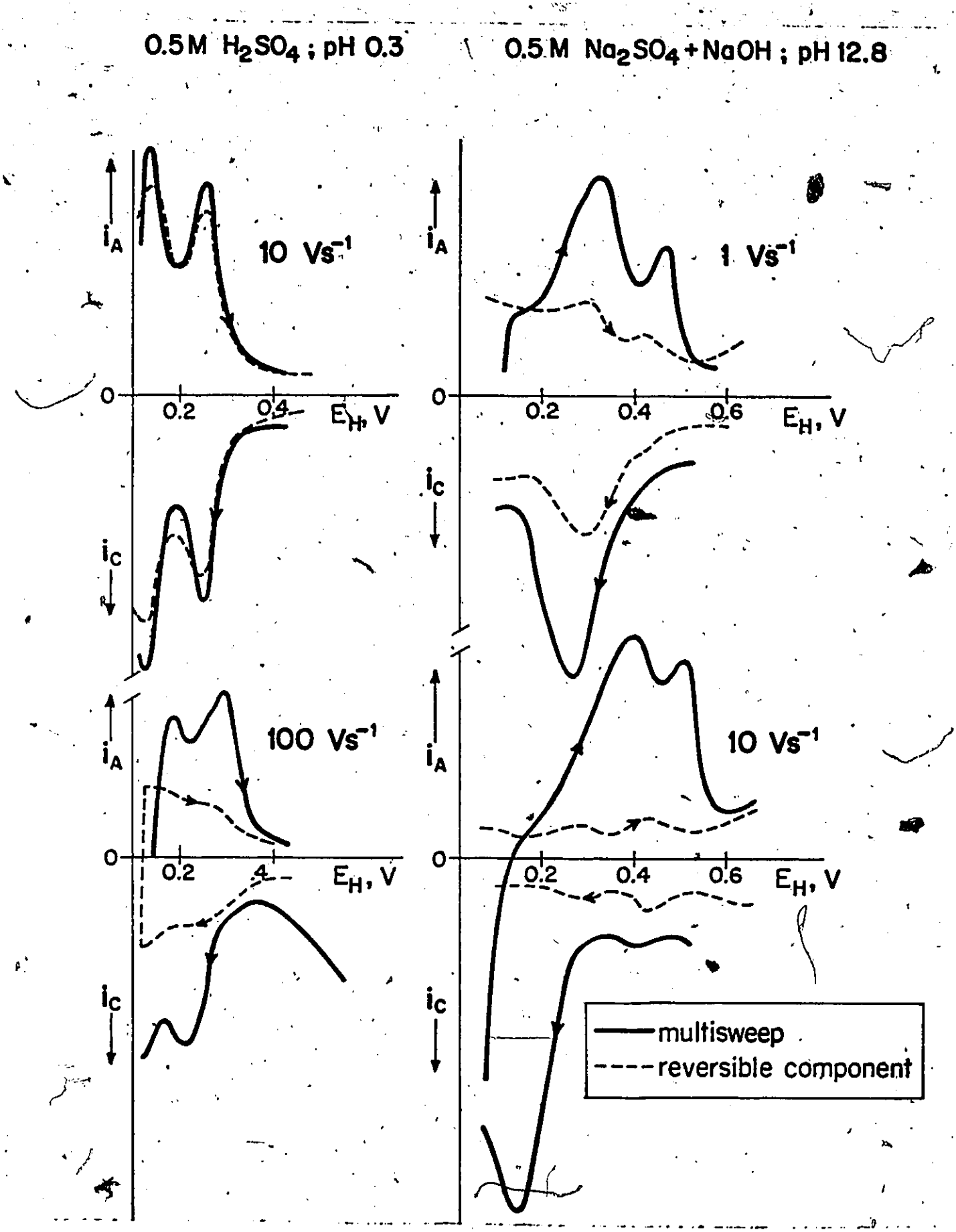

FIG 30 THE REVERSIBLE COMPONENTS OF THE CURRENTS ASSOCIATED WITH THE UPD OF H IN ACID AND ALKALINE SOLUTIONS

5.2 Preliminary discussion

None of the variables studied in the experiments reported above either leads to the formation of new bonding states for H or to the elimination of states which would otherwise exist. However, the changes in the bonding energy and coverage of the states which have been observed may in many cases be related to changes in the composition of the double layer at the Pt/solution interface. These effects will be examined as an introduction to the discussion of the cause of the multiple states of bonding.

5.2.1 Effects of specifically adsorbed ions

Only the effects of weakly bound anions were studied in the present work. Earlier investigators have shown that halide ions, which are strongly bound, not only reduce the range of underpotentials over which electrodeposition of H occurs on Pt, but also change the distribution of H among the various bonding states (Section 1.3.1.1.(i)(a)).

The present results show that the effects of HSO_4^-, ClO_4^- and SO_4^{2-} ions are, in many ways, similar to those of the halide ions, although much smaller in magnitude. The energy required to displace HSO_4^- or ClO_4^- ions reduces the potential at which deposition occurs in the low-coverage states. However, when the anions are desorbed during the cathodic sweep, the Pt surface becomes exposed at a potential at which an overpotential exists for the surface deposition reaction at the prevailing coverage. This increases the apparent coverage in the more weakly bound states. However, the extra charge which is passed at less-positive potentials is thought to relate to deposition in the

states which would normally be filled at more positive potentials. It is thus proposed that the states in which electrodeposited atoms are bound depend primarily on the coverage rather than the potential at which they are deposited.

The small differences between the current-potential curves for the electrodeposition and oxidation of H at Pt at sweep rates between about 0.01 and 0.2 V s^{-1} appear to be related to the time- and potential-dependent desorption of anions. At very slow sweep rates, the coverages of all adsorbed ions will be at their equilibrium values at all potentials, regardless of the sweep direction. At very fast sweep rates, in a potential range including that of oxide formation, the coverages will be low and will not change significantly during the sweep. (In the specific adsorption of SO_4^{2-} ions, for example, it can take many minutes for the anion coverage to reach its full equilibrium value[587]). However, at intermediate sweep rates, the coverage of specifically adsorbed anions will always be lower in the anodic than in the cathodic sweep. Although it is clear that ionic effects will diminish with the sweep rate (assuming that the sweep range is sufficient to oxidize the Pt surface, thus completing the desorption of anions), and will be less in the anodic sweep than in the cathodic sweep, the sweep rate which will maximize the resolution of the individual states in the oxidation of H while minimizing the effects of specifically adsorbed ions cannot be predicted. The apparent coverage in the states measured in the anodic sweep will vary with the sweep rate because the sweep rate will control the coverage of specifically adsorbed ions as a function of potential (assuming that

the sweep range is sufficient to oxidize the Pt surface). In addition, the extent to which the H peaks overlap in the anodic sweep will depend on the temperature, since the standard reversible potentials of the individual peaks have different temperature coefficients.

The difference in the apparent charge in the cathodic and anodic H_3 peaks is particularly interesting. Holding the electrode potential at 0.075 V, which reduces the coverage of anions, increases the charge in the H_{A3} peak (Fig. 14). Conversely, a potential hold at 0.4 V, which will increase the anion coverage, reduces the charge in H_{A3} (Fig. 31). However, even when the H_{A3} peak is thus diminished, the saddle point between $H_{A1,2}$ and $H_{A4,5}$ seems too high to be accounted for by the sum of currents from these two peaks. It appears, therefore, that the time effects on the charge in the H_3 state relate to only a small proportion of the H adsorbed in that state. The H_3 state is not "created" by holding the potential to allow HSO_4^- to desorb; rather, the equilibrium distribution under such conditions allows more H to be accommodated in the H_3 state and less in the $H_{4,5}$ and H_2 states than is the case under continuous potentiodynamic cycling conditions. It will be noted that the $H_{A1,2}$ peak current increases with both reductions in the anion coverage (Fig. 14) and increases in the anion coverage (Fig. 31). This anomaly is not at present understood. Possibly the increase in $H_{1,2}$ currents after holding at 0.4 V arises from increased deposition in the H_{C1} state which more than compensates for the decreased deposition in H_{C2}. (The H_1 peaks are normally only resolved in continuous cycling in solutions containing high concentrations of HSO_4^- ions[52,74,75]).

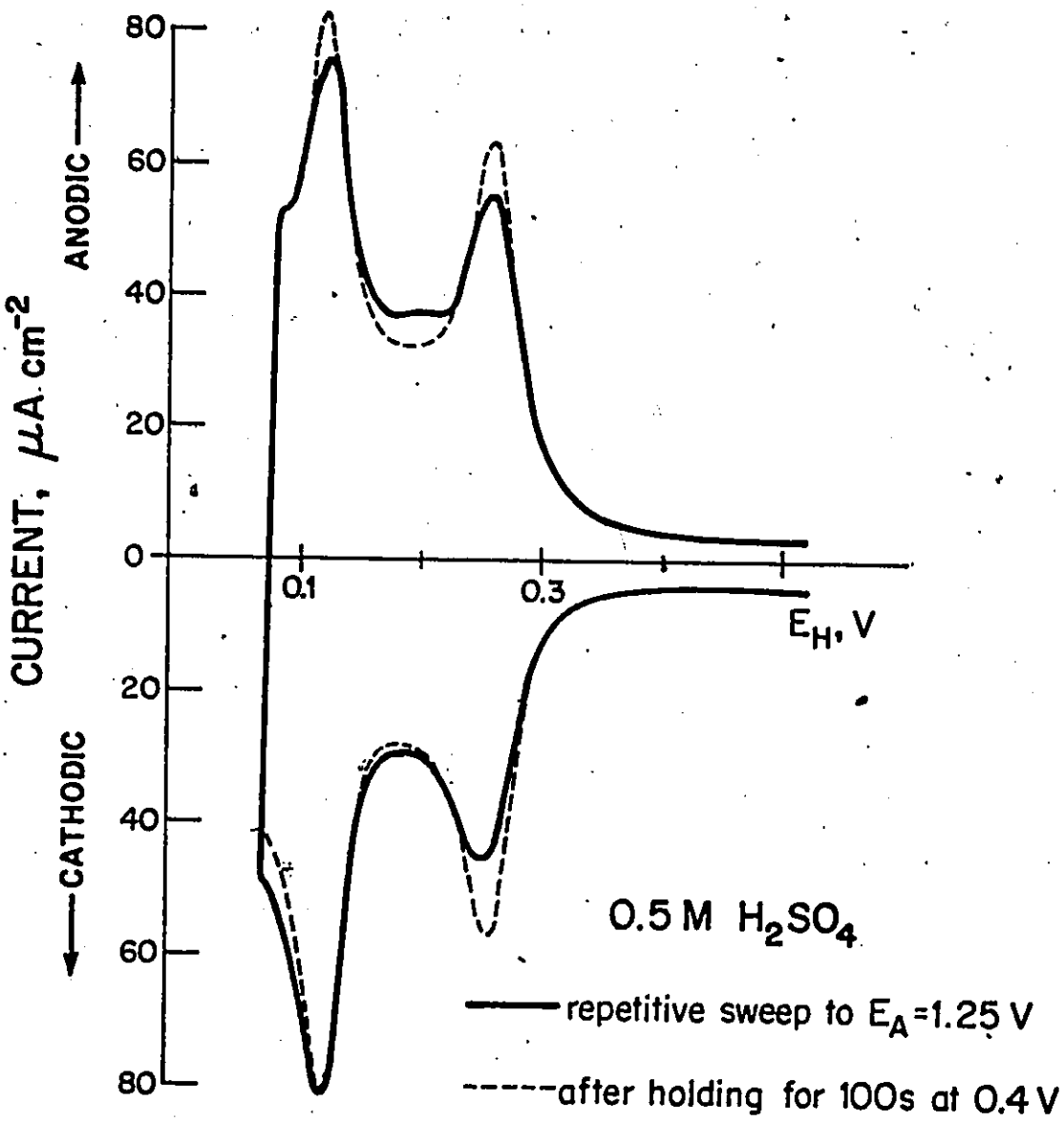

FIG 31 POTENTIODYNAMIC UPD OF H SHOWING THE EFFECT OF INTERRUPTING THE CATHODIC SWEEP FOR 100 s AT 0.4 V ($s = 0.05\ V\ s^{-1}$)

Incidentally, the fact that changes in the ionic composition neither "create" nor "destroy" individual bonding states of H on Pt disproves the suggestion implicit in the work of Schuldiner and Warner[607] that multiple bonding states arise (in the deposition of O species on Pt, at least) from the discontinuous removal of competing adsorbates.

The variation in the distribution of electrodeposited H atoms among the bonding states with the crystallography of the surface in acid solutions (Figs. 7 and 8) may also be partly caused by specifically adsorbed ions. The small differences in the current-potential profile which relate to the crystallography diminish still further as the concentrations of HSO_4^-, ClO_4^- and SO_4^{2-} ions are reduced. It is known that surface electronic properties (e.g. work function[442]) vary with the lattice plane exposed, so it is to be expected that the coverage by specifically adsorbed anions will also depend on the plane exposed. Thus the bonding states of H will be affected not only directly by the electronic properties of the surface plane, but also indirectly by the consequent changes in the specific adsorption of ions and in the p.z.c.

In acid solutions, the p.z.c. of Pt lies between the potentials of the predominant $H_{1,2}$ and $H_{4,5}$ peaks[586]. The original Frumkin model of H adsorption in <u>two</u> states of opposite dipole moment[82] is now clearly inadequate as a basis for the explanation of the behaviour of H on Pt, not only because more peaks have been resolved by the use of the potentiodynamic sweep method, but also because the same peaks occur at similar potentials in alkaline solutions, where the p.z.c. arises at (relatively) more positive values[586].

The fact that ClO_4^- ions affect the electrodeposition of H at potentials below the p.z.c. of Pt very much less than do HSO_4^- (Section 5.1.6) is consistent with earlier studies showing that the equilibrium coverage of ClO_4^- ions on Pt[239] is only about half that of HSO_4^- ions[86,237,238]. HSO_4^- ions suppress the electrodeposition in the H_4 state to the extent that it is no longer resolved in 0.5 M H_2SO_4 solutions, and produce the familiar composite $H_{4,5}$ peak, whereas the H_4 state is clearly resolved in 1M $HClO_4$ solutions.

The effects of Na^+ and Mg^{2+} cations on the UPD of H are much smaller than those of the anions described above. This is consistent with radiotracer data showing that Na^+ ions are only very weakly adsorbed at Pt[86,588,589]. Thus the small magnitude of the effects of Na^+ and Mg^{2+}, which are only significant at potentials less positive than that of the p.z.c., may relate simply to the low coverages of these cations.

5.2.2 Effects of pH

It has been shown that although the H peak potentials have the same pH dependence as that of the reversible Pt/H_2 electrode in the same solution, and although the total UPD charge is independent of pH, the coverages of H in the individual states are not, and also that the rate constants for the deposition and ionization reactions become smaller with increasing pH. The changes in the energies and relative coverages of the bonding states with increasing pH are thought to arise from reductions in the specific adsorption of anions at the H deposition potentials as the p.z.c. moves to (relatively) more positive potentials[586].

Thus, the spectrum of states of bonding of H at Pt will be most clearly resolved in solutions of high pH or low concentrations of acid, in which ionic effects are minimized. In addition, as Woods[40] has pointed out, the superposition of currents from H_2 evolution on the H peaks at high coverage may be minimized by reducing the temperature, but this enhances anion adsorption effects.

The decreasing rate constant of the H deposition reaction with increasing pH almost certainly arises from the concurrent change in the deposition mechanism. In acid solutions, the deposition will proceed *via* the discharge reaction:

$$Pt + H_3O^+ + e \rightarrow Pt\text{-}H + H_2O$$

In alkali, on the other hand, the current for this reaction is diffusion-limited and very small, so the only significant reaction is

$$Pt + H_2O + e \rightarrow Pt\text{-}H + OH^-$$

which evidently is more irreversible. A similar difference in kinetics arises in the H_2 evolution reaction from acid and alkaline solutions.

5.2.3 The UPD charge and the H_2 evolution reaction

The fact that H_2 may be evolved at Pt electrodes which are not covered by a full monolayer of H atoms, suggests the following tentative mechanism for H_2 evolution. As the electrode potential becomes less positive and the H coverage increases, the bonding energy of electrodeposited H falls. A coverage is finally reached when the Pt-H bond energy has fallen to a value of half the dissociation energy of H_2. This coverage will depend on the temperature *via* the relative

entropy changes associated with the UPD of H and the $2Pt\text{-}H \rightarrow H_2 + Pt$ reaction. At this stage, H may be deposited from H_2 on to a Pt-H species with zero free energy change, i.e. the underpotential of deposition is zero. The Pt-H bond, however, is not sufficiently strong to hold the second H atom which has been deposited, so an H_2 molecule breaks away from the electrode surface, exposing the surface Pt atom at an overpotential for H deposition. Another H atom will therefore be immediately deposited on the bare metal and the reaction cycle will continue.

Since the H deposition and H_2 evolution reactions observed in cyclic voltammetry can evidently occur independently, great care must be exercised in the interpretation of the temperature dependence of the UPD charge. For example, Breiter's deduction of heats of adsorption from the temperature dependence of the maximum measurable H coverage[77,79] now appears to have no basis. The recent work of Woods[40] shows that lowering the temperature substantially reduces the H_2 evolution currents at the potentials of the H_5 peaks, allowing the (monolayer) H deposition charge to be measured more accurately. Low temperature measurements of the UPD charge probably provide the most accurate basis for the measurement of the real areas of Pt electrodes.

5.2.4 Occurrence of multiple bonding states

The increased resolution of potentiodynamic data resulting from the use of carefully purified water and other reagents shows that, at room temperature, a monolayer of H is discharged at underpotential on Pt, even at single crystallographic planes, in at least five states having distinctly different energies. This multiplicity of states of

bonding does not depend on the composition of the solution at the electrode surface nor on the crystallography of the electrode surface, although both these factors modify the bonding energy for individual states and the apparent distribution of H among the states available.

H is deposited on Pt over a range of underpotentials of about 0.35 V. Since both the atomic H deposited and the molecular H_2 evolved originate from a common species (H_3O^+ or H_2O, according to the pH), this shows that the (free) energies of bonding differ by up to 8.1 kcal mol^{-1}. This range of energies is comparable with that found in gas/solid adsorption studies, e.g. Tsuchiya et al[70] used the thermal desorption technique to measure activation energies* for the adsorption of H from four bonding states on Pt as 2.8, 0.9, 0.4 and 2.1 kcal mol^{-1}, while Kubokawa et al[71] measured the activation energies* for desorption from two predominant bonding states as 10 and 23 kcal mol^{-1}. (The latter data are in better agreement with the value for the strongly bound state obtained theoretically[73] and by U.H.V. calorimetry[72] than the former.).

Since the five or six electrodeposition states are neither created nor eliminated by changes in the metal structure and the composition of the double layer, it must be concluded that <u>at least five bonding states</u> exist under <u>all</u> experimental conditions, but that any given state can only be detected in a potentiodynamic sweep when the standard free energy of deposition in that state differs sufficiently

*Since the activation energy required to adsorb H on Pt from the gas phase is almost zero, the activation energy of desorption is almost equal to the desorption energy. It is thus permissible, in this case to make a comparison of what are essentially kinetic and thermodynamic parameters.

from those of the states of neighbouring energy, and when the coverage in that state is sufficiently high. If the currents from adjacent peaks are additive to any great extent, the overall profile may not reflect the multiplicity of component peaks. This is illustrated by recent work in this laboratory[24] in which a computer-generated current-potential curve was developed to simulate the familiar three peaks in the oxidation of H in 0.5M H_2SO_4 by the superposition of isotherms representing four adsorption energies. The main features of the experimental curve were quite well reproduced by component states having coverages θ_H = 0.3, 0.2, 0.2, 0.3 and standard reversible potential separations of 0.03, 0.09 and 0.08 V, or coverages θ_H = 0.3, 0.15, 0.20, 0.35 and separations 0.04, 0.08, 0.08 V. However, when the appropriate distribution of peak currents was obtained from this summation of Langmuir isotherms, the spread of underpotentials was appreciably greater than that measured experimentally. This was corrected by applying an attractive (Temkin) interaction parameter of g = -1 in the relation

$$\frac{\theta}{1-\theta} \exp(g\theta) = K_{C_{H^+}} \exp\left(\frac{VF}{RT}\right)^{16} \qquad (1)$$

for each of the component isotherms. An experimental basis for the existence of such attractive interactions between electrodeposited H atoms is provided by the narrowness of peaks $H_{1,2}$ and H_5 (about 0.045 and 0.08 V, respectively) under conditions where the adsorption of solution species during 30 h potential cycling between 0.05 and 0.7 V had redistributed almost all the charge into these two peaks[590]. (The total charge associated with the UPD of H did not fall by more than 7% during the course of this experiment, suggesting that the solution may

have been unusually pure.). Similar results have since been reported by Woods[40]. It is perhaps possible that the attractive interactions arise from electrostatic forces between the partial positive charge on Pt-H dipoles and adjacent specifically adsorbed anions.

The limited understanding of the UPD of H on Pt by previous workers mainly relates to their having studied a very limited range of solution compositions and temperatures - almost always 0.5 M H_2SO_4, 298K. The publication of other results involving the addition of unpurified reagents (e.g. references 52, 107) has left the false impression that the best resolution of the component reactions is obtained in concentrated H_2SO_4 solutions. In such solutions, the energies of the bonding states overlap to such an extent that only two (or three) peaks are observed in the potentiodynamic sweep profile. Thus, previously developed electrochemical models for the electrodeposition of H on Pt describe the formation of two species having different bond polarity[82], and sometimes a third state supposed to arise from their mutual interaction[126]. The present results require a new type of model to account for the occurrence of at least five states of bonding of electrodeposited H. The reasoning above has shown that the discreteness of the bonding energies must arise as a consequence of the electronic factors in bond formation, rather than from any external environmental factors. Presently available quantum-mechanical models of H adsorption only account for two states of atomic H[127,128], or two atomic states and two molecular states[131]. Since the present work shows that multiple submonolayer states of bonding of electrodeposited species are a general feature of surface bonding on noble metals, the development of a general model of electro-

deposition involving discrete bonding energies will be postponed until a general discussion of all the reaction systems studied is given in Chapter 11.

CHAPTER 6

THE ELECTRODEPOSITION OF O SPECIES AT Pt

6.1 Results

6.1.1 Introduction

Earlier work, including the previously published results of this study[229], has established the following characteristics of the oxidation of Pt in 0.5 M H_2SO_4:

(i) The discharge of O species begins at an underpotential of about 0.4 V below the reversible O_2 potential (1.23 V), and the coverage* reaches $\theta_e = 1$ at about 1.1 V (in 0.5 M H_2SO_4 with a sweep rate of 0.05 V s^{-1}). Significant currents appear from the evolution of O_2 at about 1.5 V, when the coverage is about $\theta_e = 2$. In purified solutions[573], the current-potential profile generally shows four anodic current peaks, but apparently only one cathodic peak, as shown earlier in Fig. 1. Other peaks, which will be discussed later, may be resolved by changing the sweep rate, temperature, and pH; the designations of the peaks shown in Fig. 1 were established after evaluating all the data, and by comparison with the oxidation of Au, at which better resolution is obtainable.

---

*Coverages will be expressed in terms of the quantity θ_e, i.e. the number of electrons passed in oxidation or reduction per atom in the Pt surface. This measurement will be used because of the uncertainty whether the deposited "O" species is OH or O. The total charge transferred when one electron is passed at each surface atom is measured by the charge, Q_H, required to oxidize the total amount of H which can be deposited on Pt at underpotential at room temperature. The coverage is then calculated as

$$\theta_e = \frac{q_{ox}}{Q_H}$$

where q_{ox} is the charge passed in oxidizing or reducing the Pt surface.

(ii) The potentials of the anodic peaks do not vary with the sweep rate below 1 V s^{-1}, indicating that the deposition processes are rapid under such conditions.

(iii) The fact that the cathodic current-potential profile is entirely different from the anodic profile (Fig. 1) shows that, although the electrodeposition of O species is a fast step, the discharged species are in a metastable state. Under normal conditions, the deposit rapidly reaches a more stable state, from which it is reduced in the following cathodic sweep. The pathway of the reduction reaction is clearly not merely the reverse of the discharge reaction. Otherwise the overall oxidation-reduction reaction would be reversible (as with H on Pt), and the current-potential curve would be symmetrical about the zero-current axis except at high sweep rates, when kinetic effects arise in the oxidation and reduction. The hysteresis[234,235] which results from the secondary processes following the discharge step produces a distinctly different current-potential profile from that arising from kinetic irreversibility[229]. If, by maintaining the electrode at an oxidizing potential for a long time, the secondary processes are allowed to equilibrate the state of the deposit, the reduction peak becomes narrower, suggesting that the deposited species now behave somewhat like a bulk compound, with substantial attractive interactions[229]. However, if the deposited species are not given time to reach equilibrium, various stages of the secondary processes may be resolved in the cathodic profile[188,189,229], which would otherwise appear as a single peak.

(iv) The rate of oxidation of Pt falls logarithmically with time at constant potential[20,176,186,217]. In part of this study previously

reported[230] it was found that on resuming an anodic sweep (0.05 V s^{-1}, 0.5 M H_2SO_4) interrupted at an oxidizing potential, the anodic currents were initially lower than those obtained without the hold, but rose to equal them at higher potentials (Fig. 32). When the interrupted sweep was extended to sufficiently anodic potentials for the anodic current to reach the "uninterrupted value", the subsequent cathodic curves became identical. The result of this experiment is most important. It not only disproves the early suggestion that secondary processes would produce new sites for the discharge of O species[197], but also eliminates disproportionation reactions (e.g. 2 PtOH → PtO + Pt + H_2O followed by Pt + H_2O → PtOH + H^+ + e)[219], and surface diffusion of discharged O species to form islands, as possible mechanisms of the secondary processes[229].

6.1.2 Effects of surface crystallography

The oxidation behaviour of Pt (100), (110) and (111) single-crystal surfaces was found to be very similar to that of polycrystalline Pt described above. Each crystal showed the characteristic multiple-peak, current-potential profile (Fig. 33), with only minor variations in the anodic peak potentials and the charge associated with each peak. [This suggests that Somorjai's finding that O_2 does not chemisorb on Pt (100) surfaces at low pressures[122] may relate either to the presence of surface impurities or to effects of surface crystallography on the activation energy of the dissociation reaction in adsorption from the gas phase]. The reduction peak potential was even less sensitive to the surface crystallography than the anodic peak potentials. Figure 33 shows the

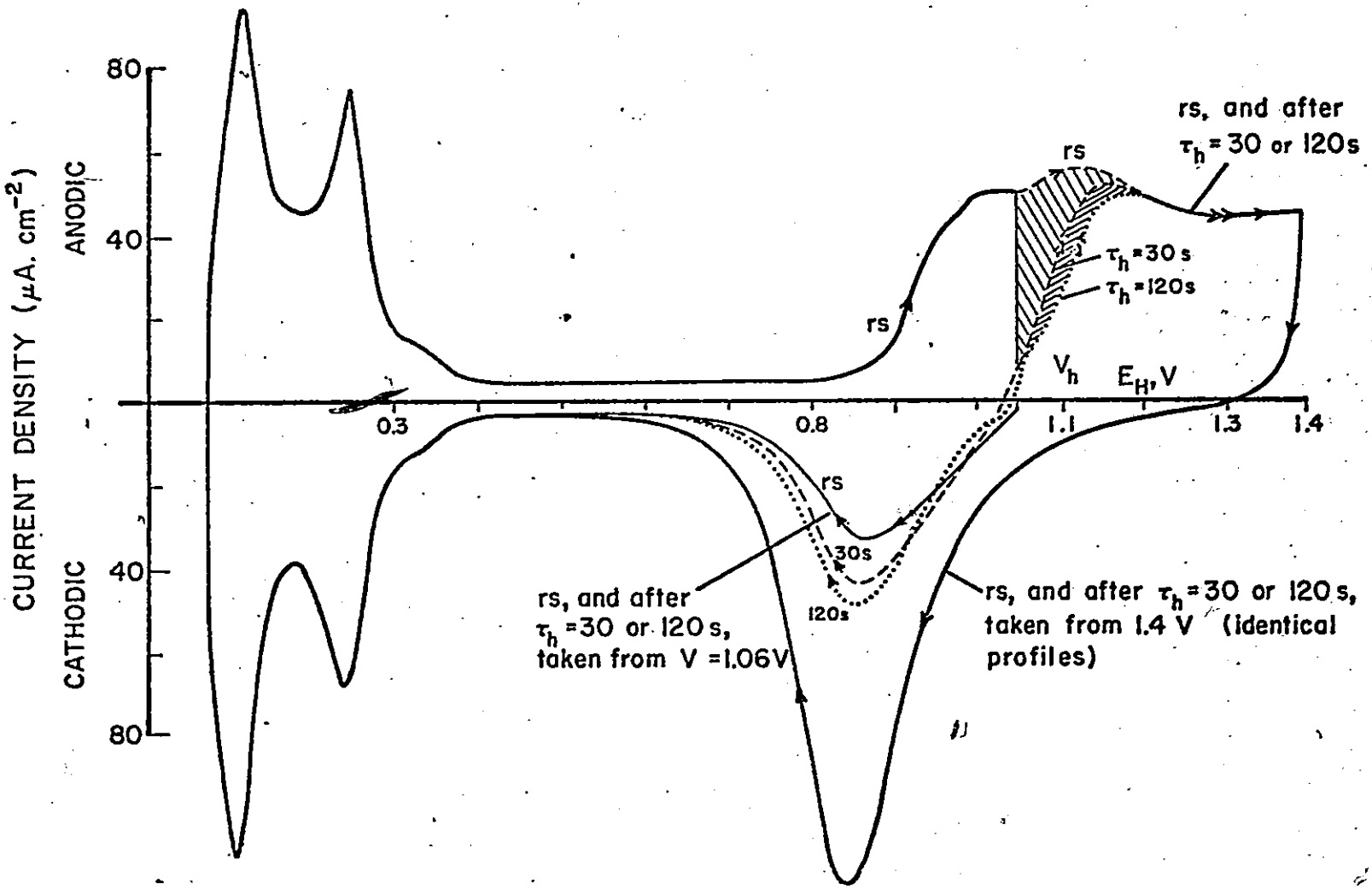

FIG 32 POTENTIODYNAMIC ANODIC AND CATHODIC CURRENT-POTENTIAL PROFILES AFTER HOLDING A Pt ELECTRODE AT 1.06 V IN 0.5 M H_2SO_4 FOR DIFFERENT TIMES r_s = REPETITIVE SWEEP; τ_h = HOLDING TIME

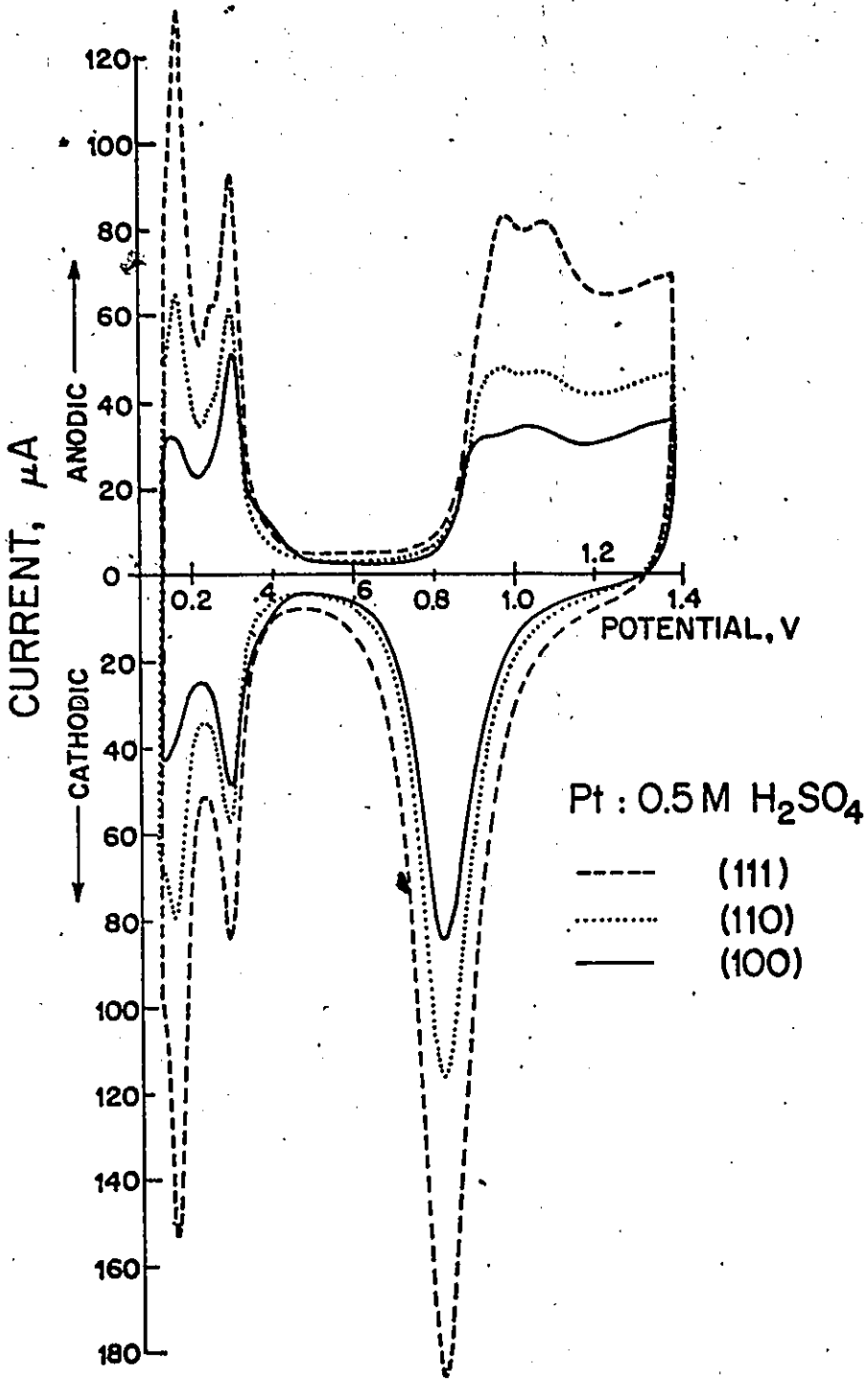

FIG 33 COMPARISON OF POTENTIODYNAMIC CURRENT-POTENTIAL PROFILES AT DIFFERENT SINGLE-CRYSTAL SURFACES OF Pt IN 0.5 M H_2SO_4 ($s = 0.05\ V\ s^{-1}$)

full potential range of the current-potential profile to emphasize the fact that the crystallography of the Pt surface affects the electrodeposition of O species much less than that of H.

6.1.3 Reversibility and hysteresis

The potentials of the anodic peaks $O_{A1,2}$ and O_{A3} (Fig. 1) do not depend on the sweep rate below s = 1 V s^{-1} (Figs. 34 and 35), showing that deposition in the metastable anodic states is reversible under these conditions. This reversibility is confirmed by the fact that the pseudocapacitance[16] (i_p/s) of the anodic sweep peaks is independent of the sweep rate (below 1 V s^{-1}) in all solutions at all temperatures. Representative results for the predominant peaks in dilute and concentrated acid solutions are shown in Fig. 36. As the sweep rate is increased, the peaks shift to more positive potentials as the deposition becomes kinetically irreversible. The processes corresponding to the $O_{A1,2}$ and O_{A3} peaks are much slower in acid than in alkaline solutions; the rate constants for the respective processes are about 43 and 41 s^{-1} in 0.5 M H_2SO_4, but are probably both in excess of 1000 s^{-1} in 0.05 M NaOH*. The increased rates in alkaline solutions suggest that the electrodeposition occurs directly from OH^- ions at high pH.

---

*These values were calculated from the sweep rate (S_o) at which the Tafel line joining the peak potentials from higher sweep rates intersects the line joining the constant peak potential values measured at slow sweep rates (Figs. 34 and 35), using the relationship (p. 143): $S_o = k_o \frac{2RT}{nF}$. The deposition was assumed to be a one-electron reaction having a standard free energy independent of coverage (i.e. g = 0) and a Tafel slope of 0.120 V $decade^{-1}$. The experimental Tafel slopes measured from Fig. 34 agree quite well with this assumption, being: O_{A1}, 0.115 V $decade^{-1}$; O_{A2}, 0.142 V $decade^{-1}$; O_{A3}, 0.143 V $decade^{-1}$; and O_{A4}, 0.118 V $decade^{-1}$.

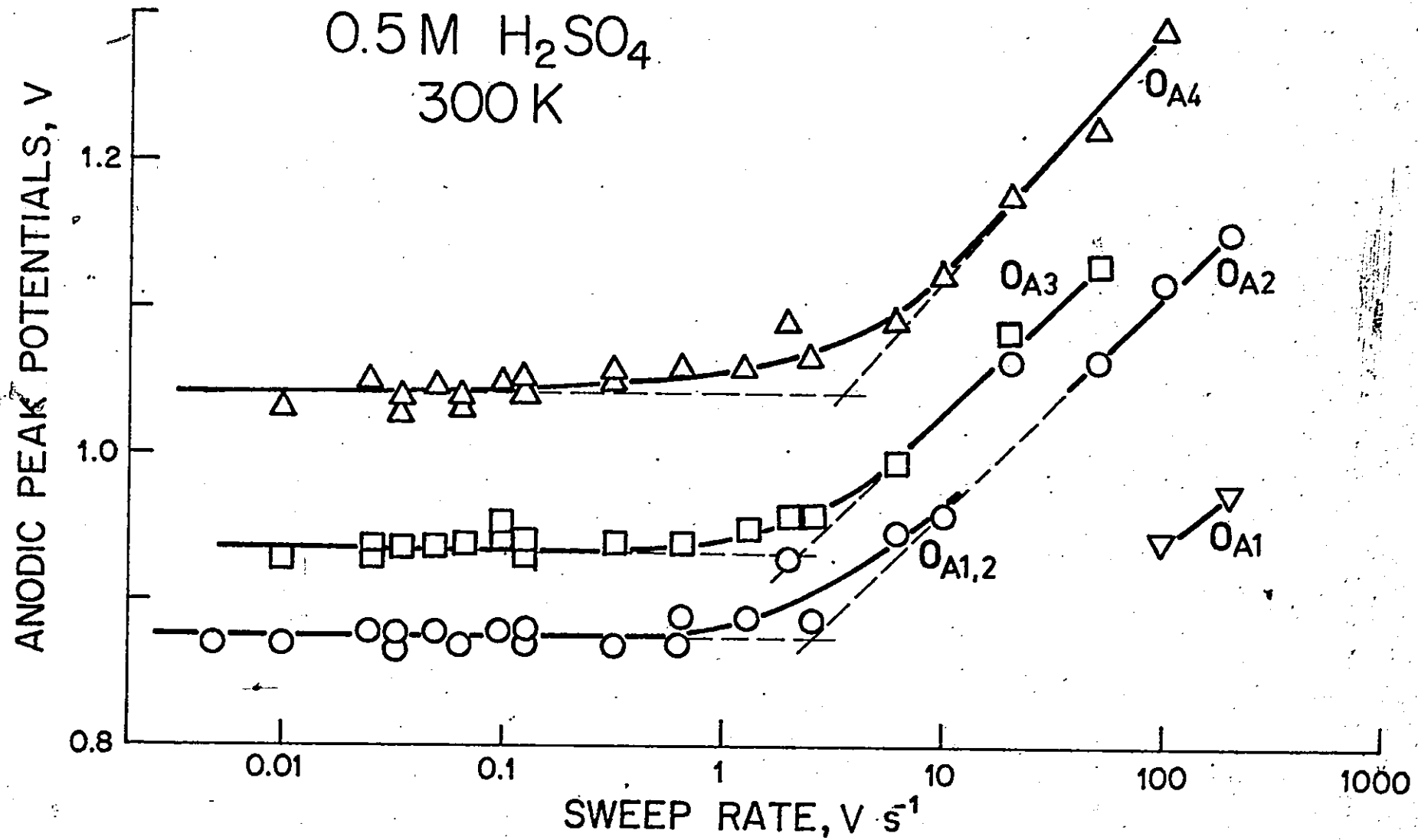

FIG 34 OXIDATION PEAK POTENTIALS AT Pt AS A FUNCTION OF SWEEP RATE IN 0.5 M H_2SO_4

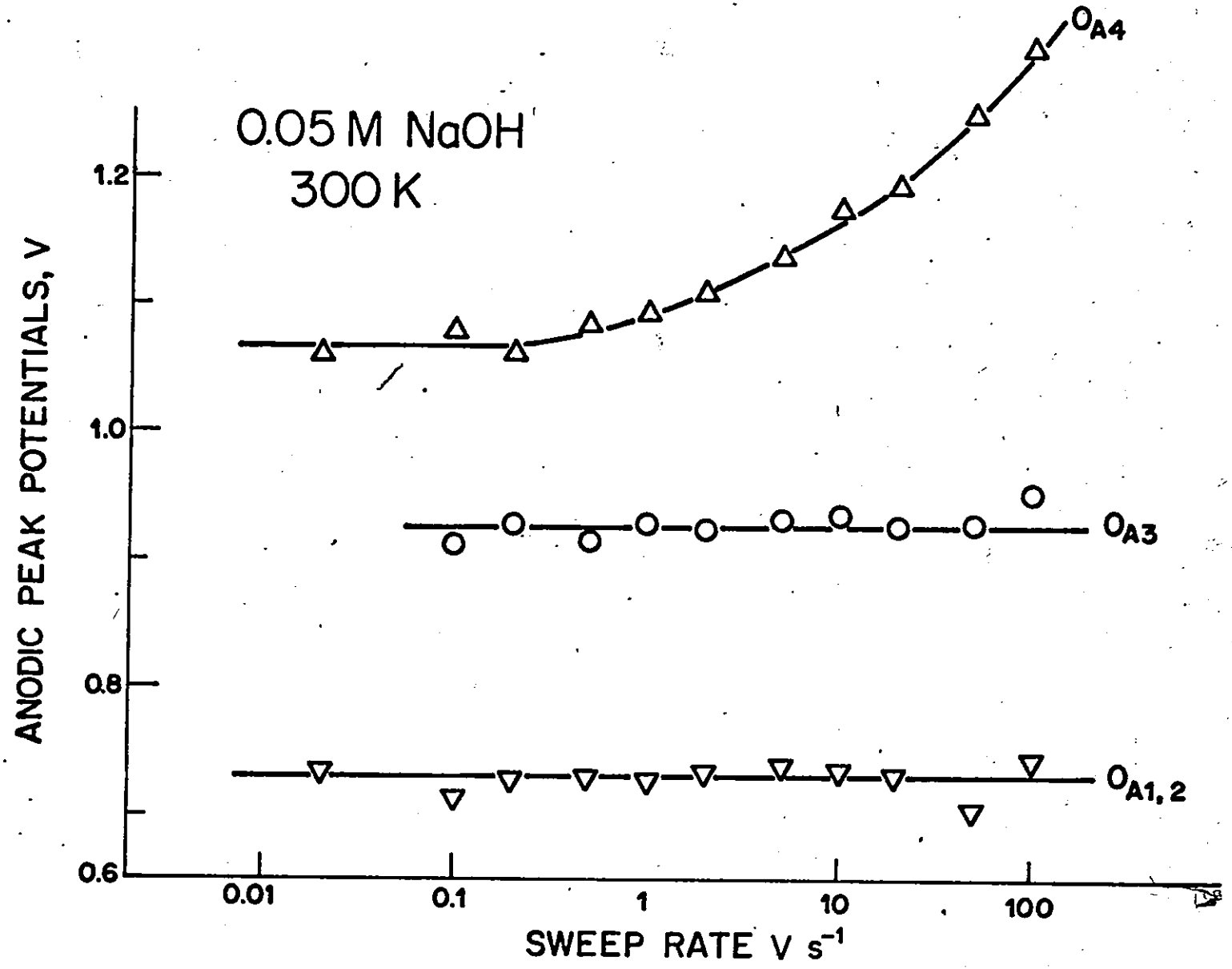

FIG 35 OXIDATION PEAK POTENTIALS AT Pt AS A FUNCTION OF SWEEP RATE IN 0.05 M NaOH

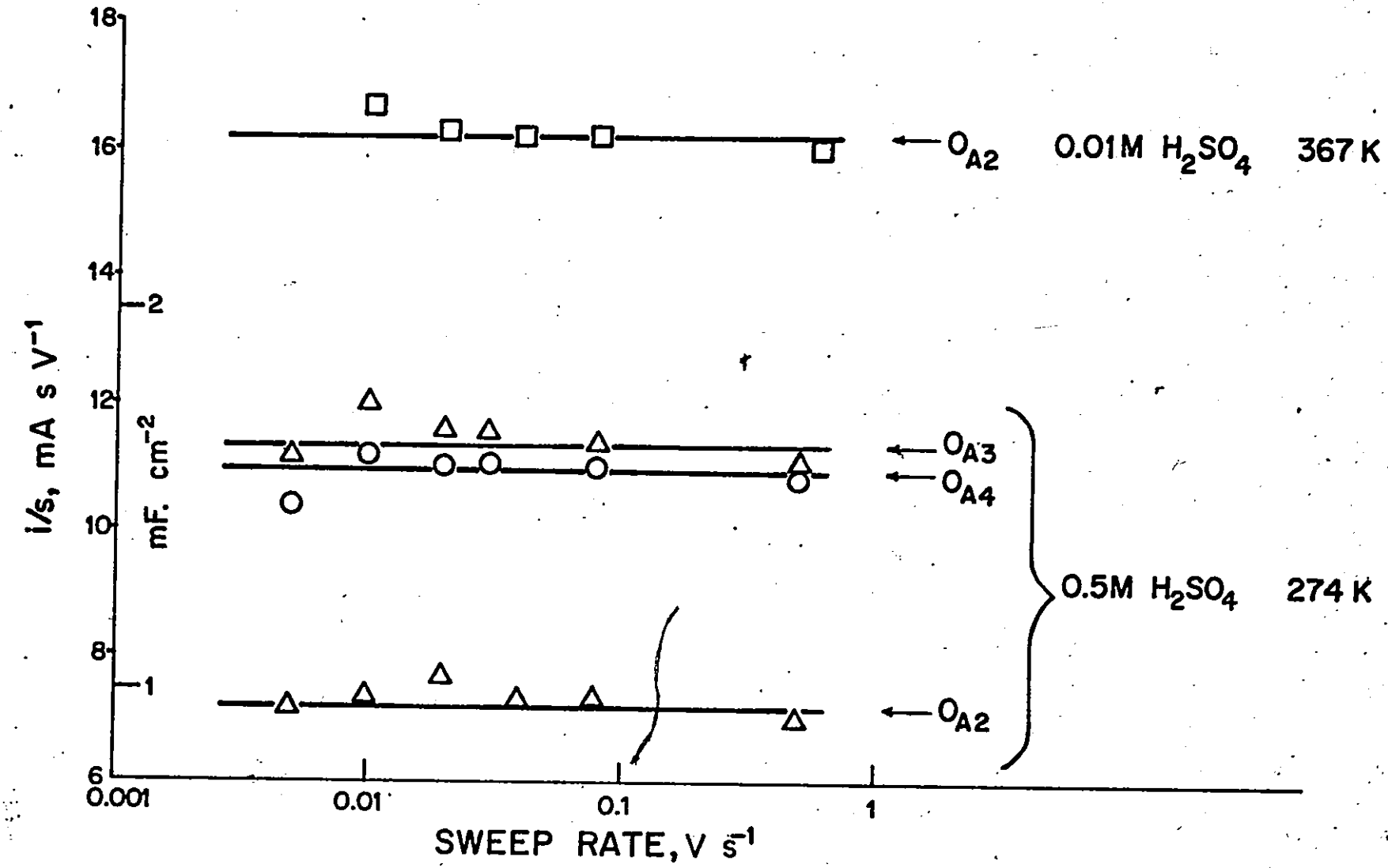

FIG 36 PSEUDOCAPACITANCE ASSOCIATED WITH CURRENT PEAKS IN THE ANODIC OXIDATION OF Pt AS A FUNCTION OF SWEEP RATE

The hysteresis in the overall oxidation-reduction cycle shows that the reduction reaction occurs *via* a different pathway to that of the (fast) oxidation reaction. Thus, when the direction of an anodic sweep is reversed, only such discharged O species as have not undergone the secondary process (i.e. that remain in the metastable state in which they were deposited) will be reduced at the potentials at which they were deposited. Hysteresis arises as the remaining (transformed) material is reduced. This feature was studied quantitatively by superimposing a rapidly alternating triangular modulation of small potential amplitude on a slow linear potential sweep acting as a carrier signal (see Section 4.4). The currents resulting from the modulated sweep measure only the component of the oxidation/reduction current which is reversible at the potential and time involved. Thus, at a given sweep rate, the currents from the modulated sweep will become less than those from a linear sweep at the same rate as the modulation (Figs. 37 and 38) when and if the deposition/reduction begins to be irreversible. This type of quantitative comparison becomes inapplicable at higher coverages, since the slow rate of the carrier sweep in the modulation experiment allows more time for species deposited at lower coverages to reach equilibrium bonding configurations than in the course of a fast multisweep. Thus deposition during a modulated sweep is carried out on a more equilibrated film than in the case of a multisweep at the equivalent linear sweep rate. This leads to differences between the response of the electrode to anodically- and cathodically-carried modulations as seen in Fig. 38. Thus, for example, the reversible component corresponding to deposition in the

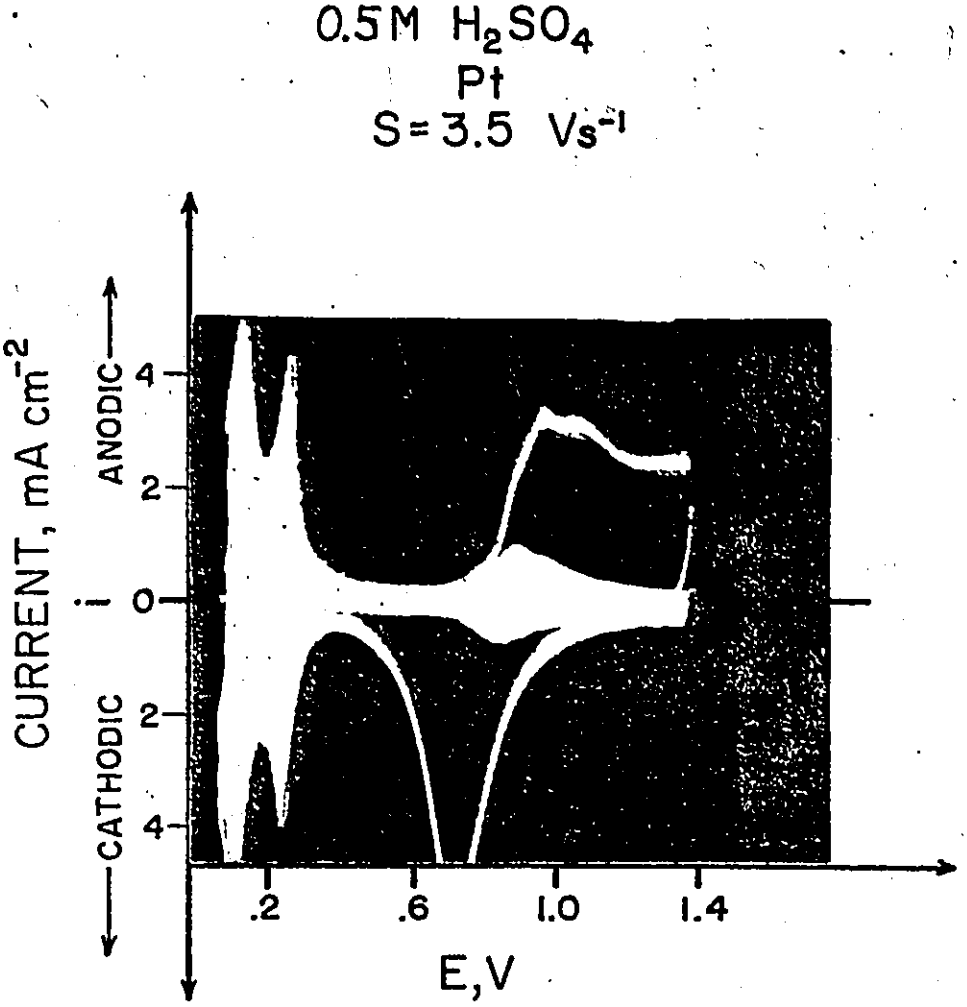

FIG 37 COMPARISON OF POTENTIODYNAMIC CURRENT-PROFILE AT Pt IN 0.5 M H_2SO_4 AT 3.5 V s^{-1} (outer line) WITH THAT OBTAINED BY SUPERIMPOSING A 3.5 V s^{-1} TRIANGULAR MODULATION ON A SLOW SWEEP (solid white portion)

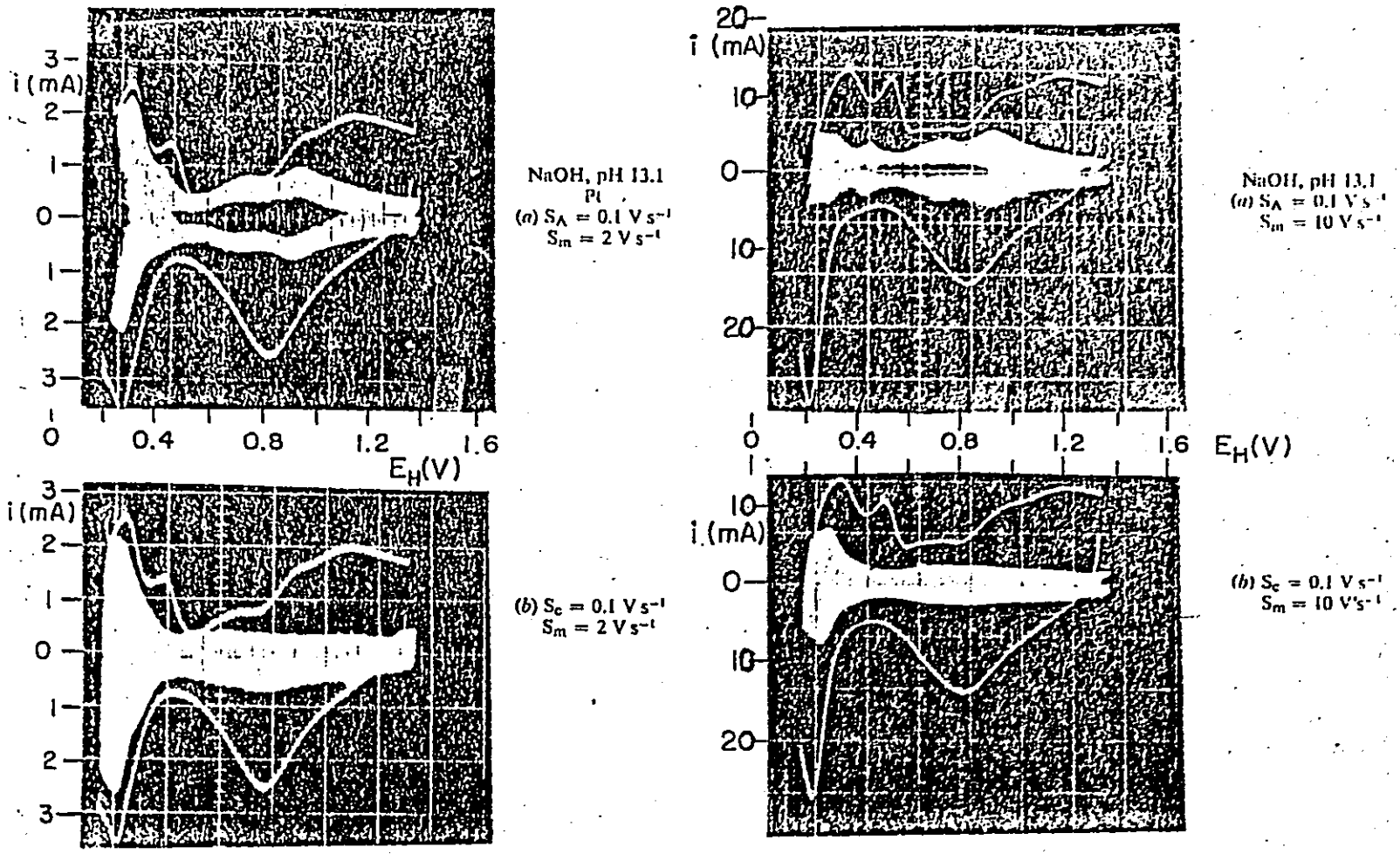

FIG 38 COMPARISON OF POTENTIODYNAMIC CURRENT-POTENTIAL PROFILES AT Pt IN NaOH AT pH 13.1 (outer lines) WITH THOSE OBTAINED BY SUPERIMPOSING TRIANGULAR MODULATIONS HAVING THE SAME LINEAR SWEEP RATE ON A SLOW SWEEP (solid white portion)

state O_{A1} does not appear when the alternating modulation is carried on a cathodic sweep, because the "stabilized" O species cannot be reduced at this potential, so there is no free surface on which the (reversible) O_{A1} reaction can occur. Modulated sweeps in 0.5 M H_2SO_4 (Fig. 37) confirm the earlier conclusion from Figs. 34 and 35 that the $O_{A1,2}$ and O_{A3} processes are much less reversible in acid than in alkaline solutions.

The secondary processes not only cause hysteresis in the overall oxidation-reduction process; they also allow deposition to continue at constant potentials at which the surface would otherwise have attained a constant equilibrium coverage. The continuing deposition at constant potential obeys a logarithmic rate law with respect to time[20,176,186,217], even at the lowest coverages (Fig. 39), and on single-crystal surfaces, despite the fact that the electrodeposition into the metastable states in the anodic sweep before the potential hold occurred at rates lower than the exchange current. Similar continuing deposition at constant potential was observed in alkaline solutions even within the potential range of the O_{A1} peak. No detectable oxidation processes occurred, however, during similar interruptions of the potential sweep at less positive potentials, i.e. within the anodic "double-layer" region.

The fact that the potential of the reduction peak varies considerably according to the coverage of O species attained at the reversal potential (Figs. 10 and 11) gives strong evidence that this peak is the sum of a number of component peaks. This was confirmed by detailed studies of the composite peak potential as a function of

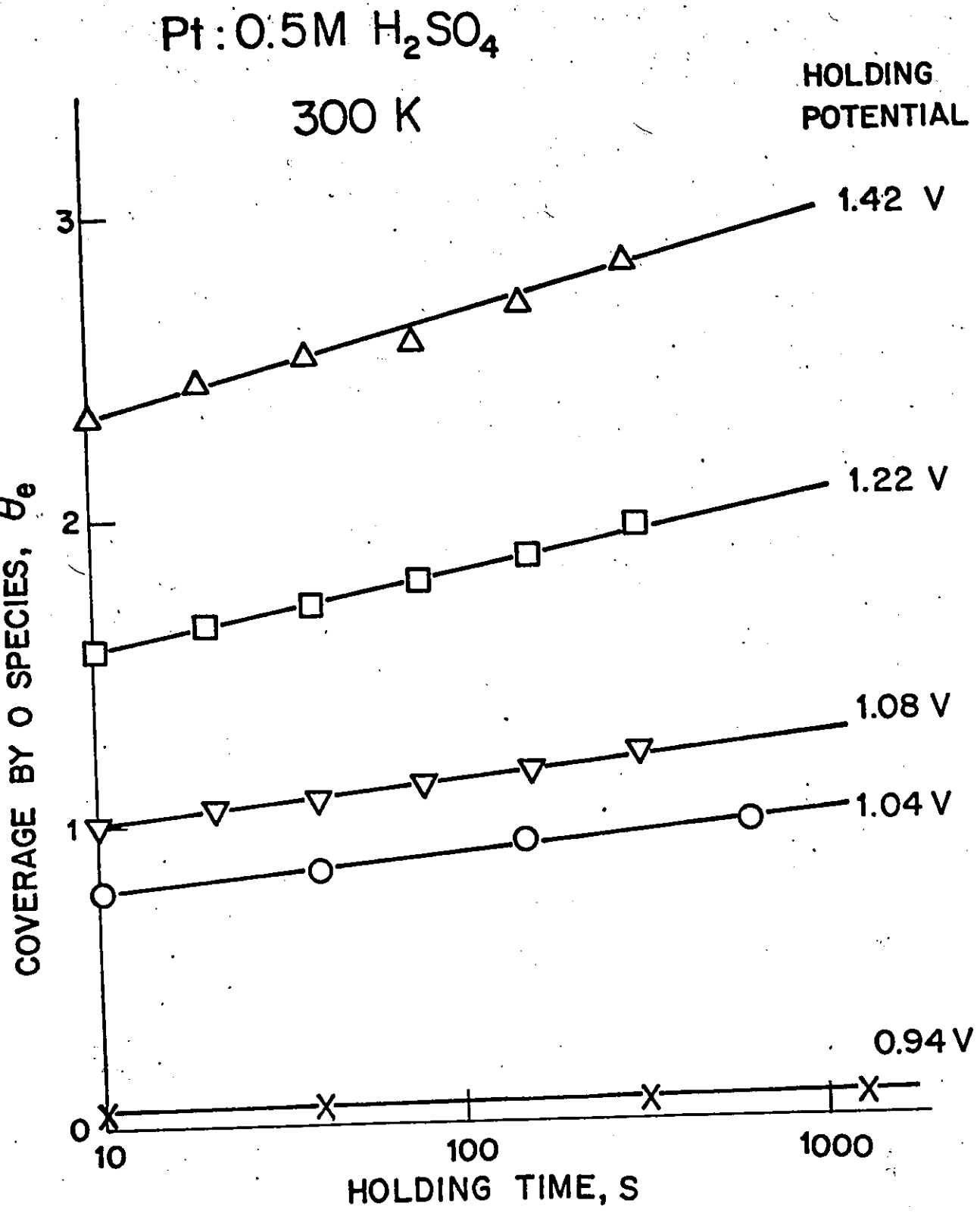

FIG 39 COVERAGE OF O SPECIES ON Pt AS A FUNCTION OF HOLDING TIME AT VARIOUS ANODIC POTENTIALS

coverage, temperature and solution composition. However, the bonding states resulting from the secondary processes were more successfully investigated by rapid reduction sweeps (Fig. 40 and reference 229). The oxidation-reduction cycle is reversible at coverages below about θ_e = 0.27 in 5 M H_2SO_4 or $HClO_4$ at 5 V s^{-1}[229]. At coverages below ca. 0.15 the oxidation is essentially reversible even at sweep rates as low as 0.05 V s^{-1} (Figs. 10 and 11), i.e. the secondary processes are either relatively slow or reversible under these conditions. As higher coverages of O species are reduced, a strongly-bound state (O_{C2}) is observed in the reduction sweep, but finally the predominant oxide (reduced in the composite $O_{C2,3}$ peak) has an intermediate bond energy. The coverage in the most strongly bound state (O_{C2}) apparently reaches a limiting value, after which the state of intermediate energy (O_{C3}) increases in coverage to dominate the familiar $O_{C2,3}$ composite peak to such an extent that it appears to be a single peak.

6.1.4 Effects of specifically adsorbed anions and of pH

It is well known that the energy required to displace strongly specifically adsorbed anions (e.g. Cl^-) from Pt increases the potential needed to electrodeposit O species[99,241]. Previous workers have therefore usually studied the oxidation of Pt in H_2SO_4 or $HClO_4$ solutions, and most have assumed that SO_4^{2-}, HSO_4^- and ClO_4^- ions would not affect the electrodeposition of O species. Effects of these ions were studied in the experiments recorded below.

Figure 41 shows that when the concentration of H_2SO_4 is reduced, the discharge of O species begins at lower potentials. Similar,

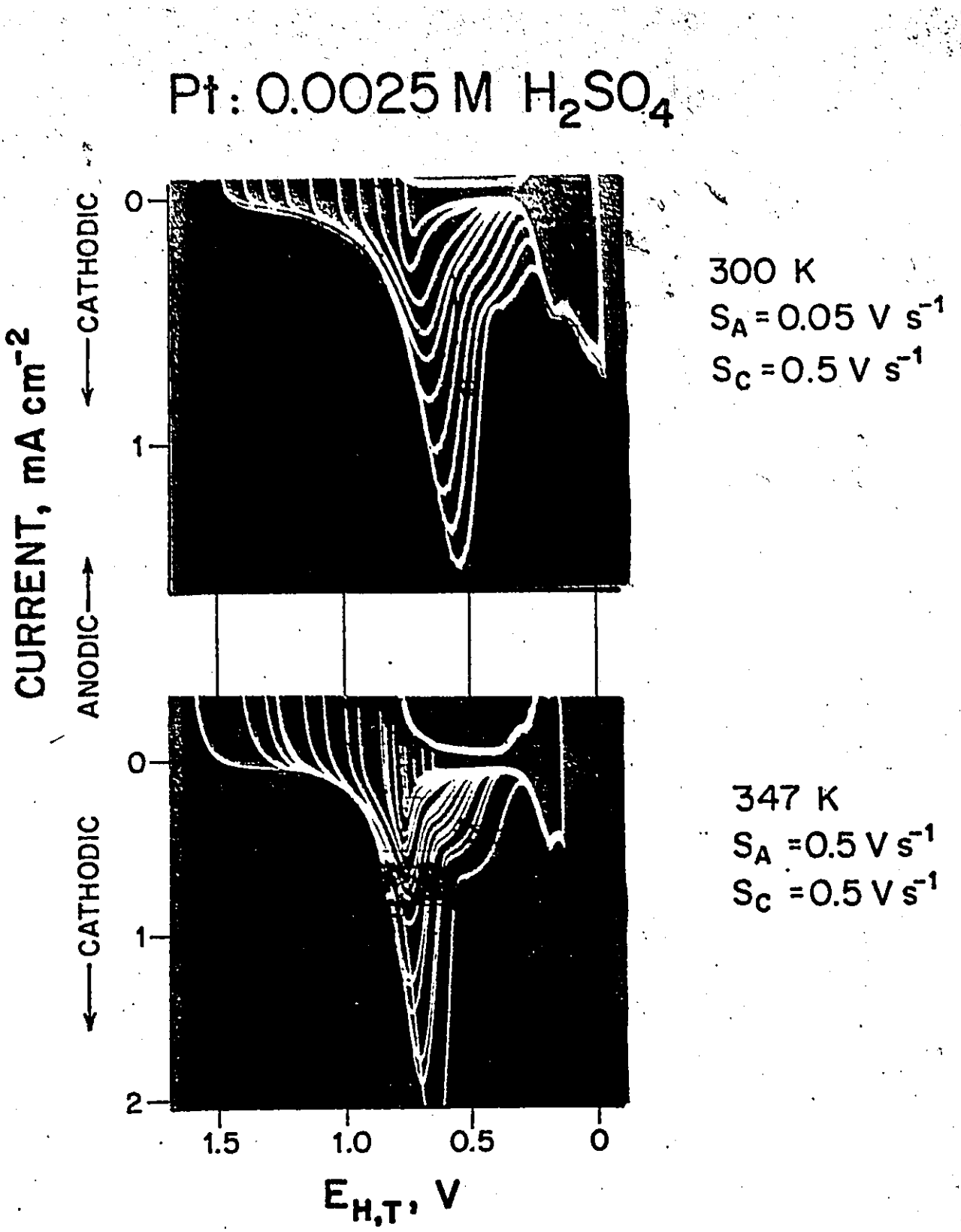

FIG 40 RESOLUTION OF MULTIPLE STATES OF OXIDATION OF A Pt ELECTRODE IN RAPID REDUCTION SWEEPS FROM A SERIES OF ANODIC END-POTENTIALS IN 0.0025 M H_2SO_4

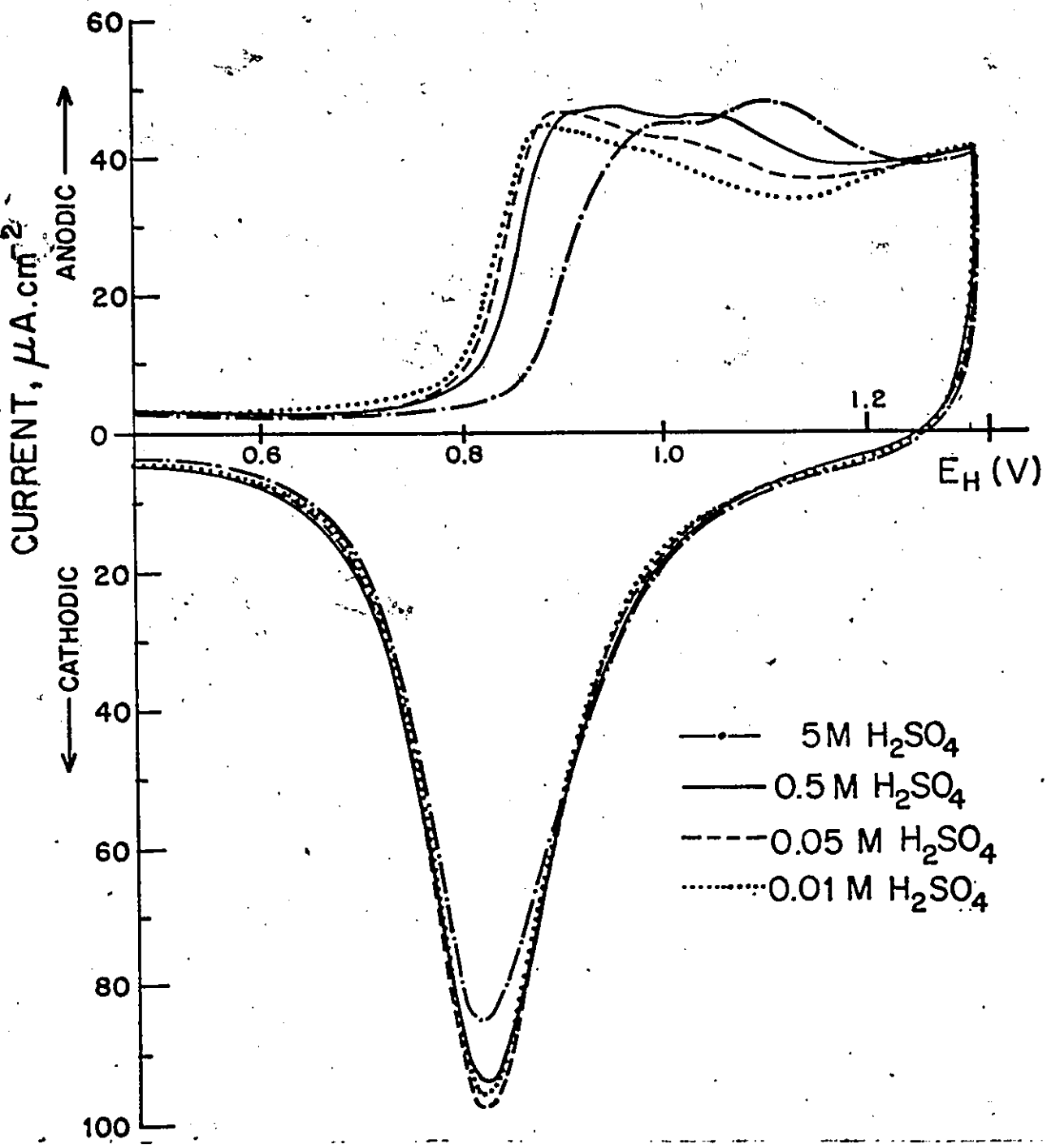

FIG 41 EFFECTS OF CONCENTRATION OF H_2SO_4 ON THE POTENTIODYNAMIC CURRENT-POTENTIAL PROFILE AT Pt ($s = 0.05\ V\ s^{-1}$)

though smaller, effects are observed in $HClO_4$ solutions. However, by the time the electrode potential reaches about 1.3 V (Fig. 41), the total charge passed is independent of the anion concentration. Thus, although the coverage of O species deposited in states $O_{A1,2}$ and O_{A3} is reduced by the presence of specifically adsorbed anions, there is an equivalent increase in the charge deposited in O_{A4-6}, since when such potentials are reached, the anions are presumably desorbed.

Increasing the reaction temperature both decreases the deposition peak potentials (Fig. 42), and redistributes the deposited species so as to increase the coverage in the more strongly bound states (Fig. 43, cf. Fig. 41). The difficulties inherent in experiments in nearly-boiling solutions give rise to slight variations in the reduction sweep profile. It appears, however, that even at 368K the specific adsorption of SO_4^{2-} and HSO_4^- are sufficient to cause considerable increases in the potential at which O species begin to discharge, which masks the redistribution effect.

The effects of solution pH were studied in a series of 0.5 M sulphate solutions (H_2SO_4, Na_2SO_4 and Na_2SO_4-NaOH) and representative current-potential profiles are compared in Fig. 44. As the pH is raised, the O_{A1} peak becomes distinctly resolved at potentials less positive than those of the O_{A2} peak. Although the potential range of the O_{A1} peak is that at which many types of solution impurity are oxidized, if present, the O_{A1} reaction was confirmed to be a surface process by showing that the oxidation and reduction currents in this region are independent of solution stirring and that a <u>linear</u> relationship exists between the O_{A1} peak current and the sweep rate. The O_{A1} peak is also

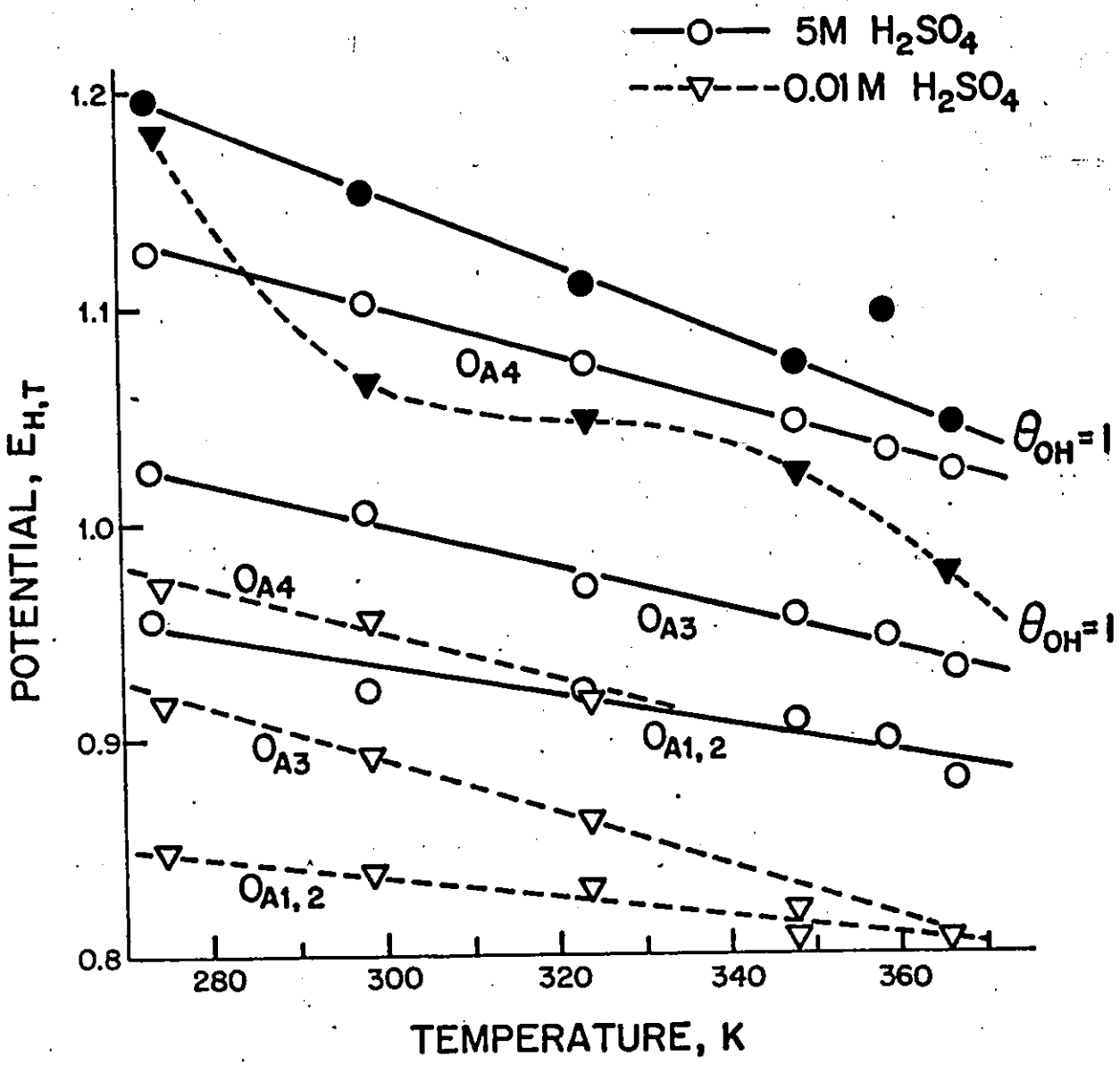

FIG 42 EFFECTS OF SOLUTION TEMPERATURE ON OXIDATION PEAK POTENTIALS AT Pt ($s=0.05\ V\ s^{-1}$)

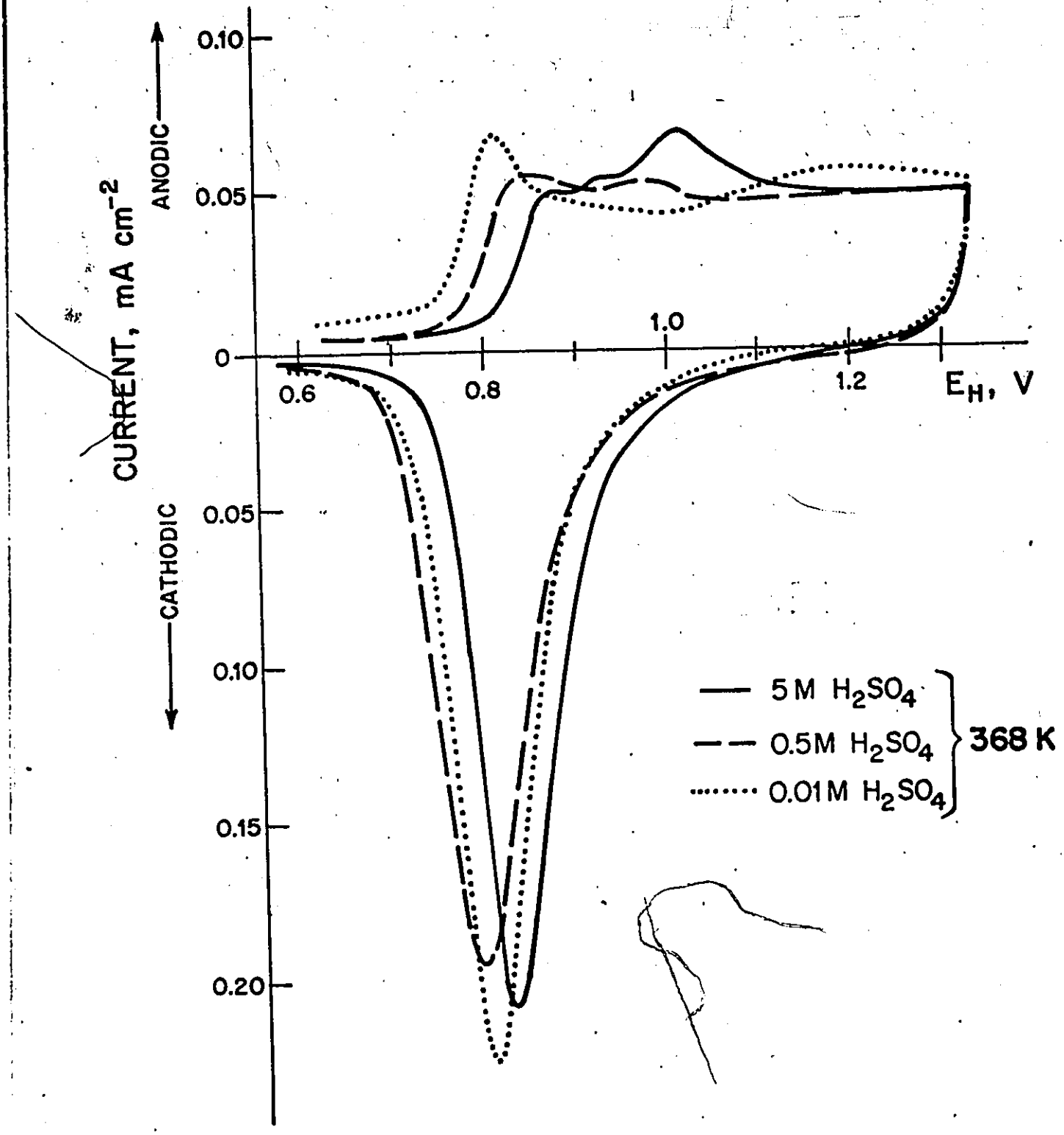

FIG 43 EFFECTS OF CONCENTRATION OF H_2SO_4 ON THE POTENTIODYNAMIC CURRENT-POTENTIAL PROFILE AT Pt AT 368 K ($s = 0.05\ V\ s^{-1}$)

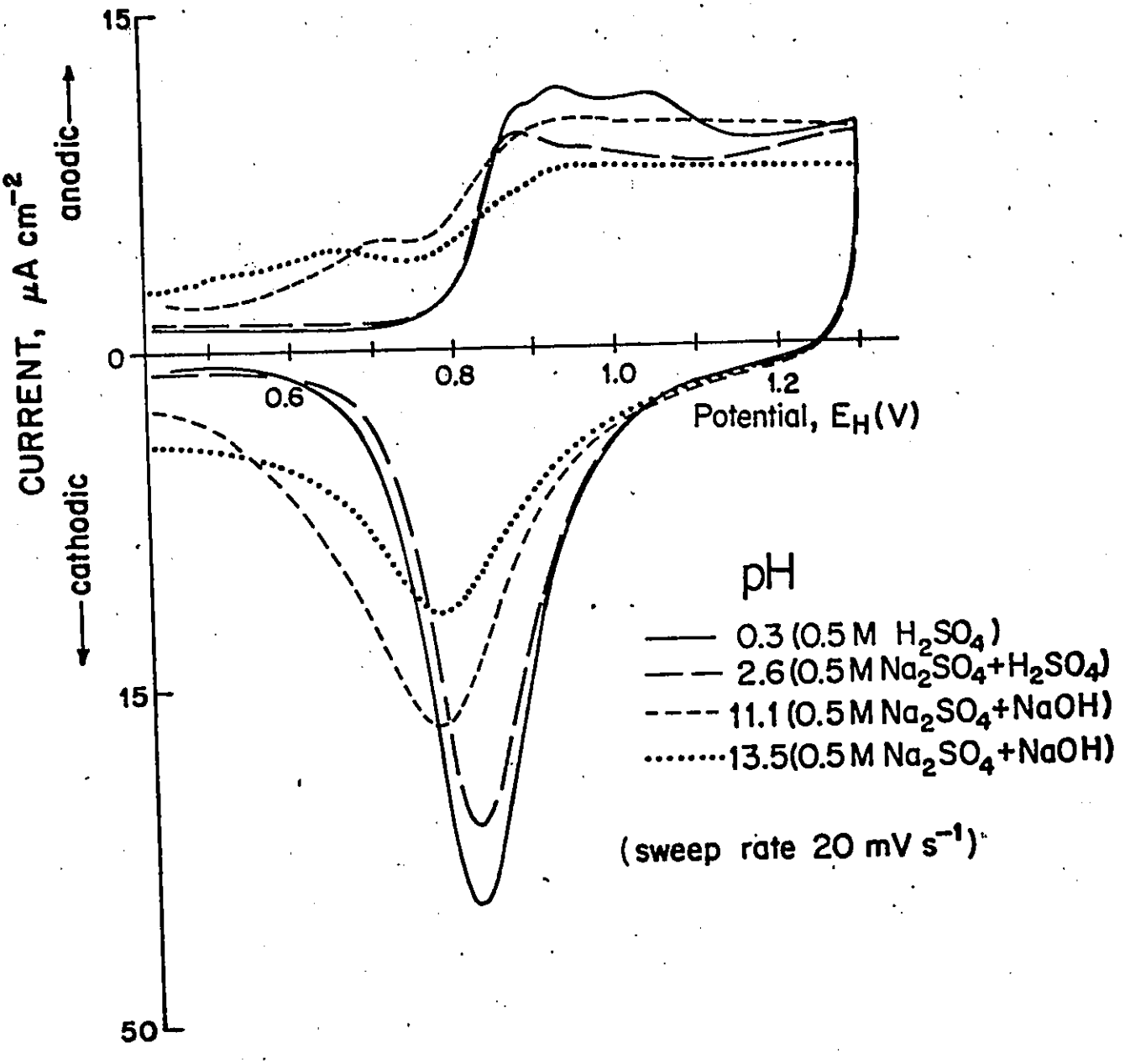

FIG. 44 EFFECTS OF SOLUTION pH ON THE POTENTIODYNAMIC CURRENT-POTENTIAL PROFILE AT Pt IN 0.5 M SULPHATE SOLUTIONS

resolved in acid solutions at fast sweep rates (see the data in Fig. 34). Although the appearance of the O_{A1} peak in alkaline solutions reduces the potential at which an oxidation charge equivalent to one electron per surface atom has been passed, when the coverage exceeds the equivalent of ca. two electrons per surface atom, the total charge passed is essentially independent of the solution pH (scatter ±12%).

Figure 45 shows that the potentials of the oxidation peaks in acid solution generally vary with the pH in the same way as that of the Pt/H_2 electrode, i.e. as predicted by the Nernst equation. However, as the $HSO_4^- \overset{K_a}{\rightleftharpoons} SO_4^{2-} + H^+$ equilibrium shifts to the left at low pH (pK_a = 1.92), the increasing coverage of specifically adsorbed ions increases the potentials for deposition in the various states, as described above in connection with Fig. 41. Although the O_{A2}, O_{A3} and O_{A4} peaks are much less well resolved in alkaline solutions (Fig. 44), probably because of the difficulty of preparing NaOH to the same level of purity as that of the other salts and acids, it appears from Fig. 46 that their potentials are consistent with those of the $O_{A1,2}$, O_{A3} and O_{A4} peaks in acid solution. The O_{A1} peak, however, shifts to lower potentials as the pH is raised, and therefore becomes resolved separately from the O_{A2} peak.

6.1.5 Reconstruction of the Pt surface

Although the crystallography of the surfaces of the three single-crystal Pt electrodes obtained from Dr. Will had not recently been investigated, their potentiodynamic sweep profiles were at first

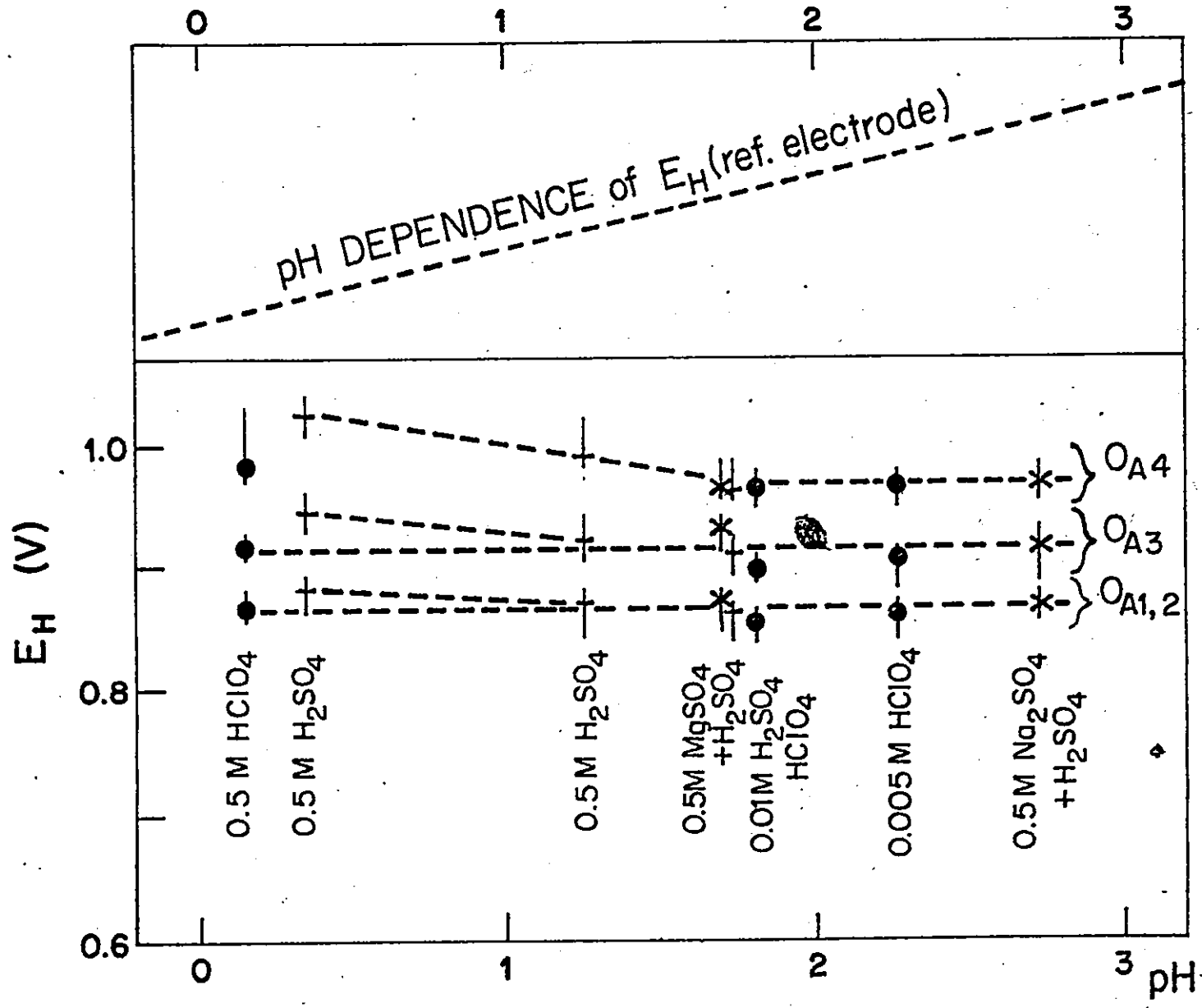

FIG 45 THE pH DEPENDENCE OF OXIDATION PEAK POTENTIALS IN ACID SOLUTIONS ($s = 0.05\ V\ s^{-1}$)

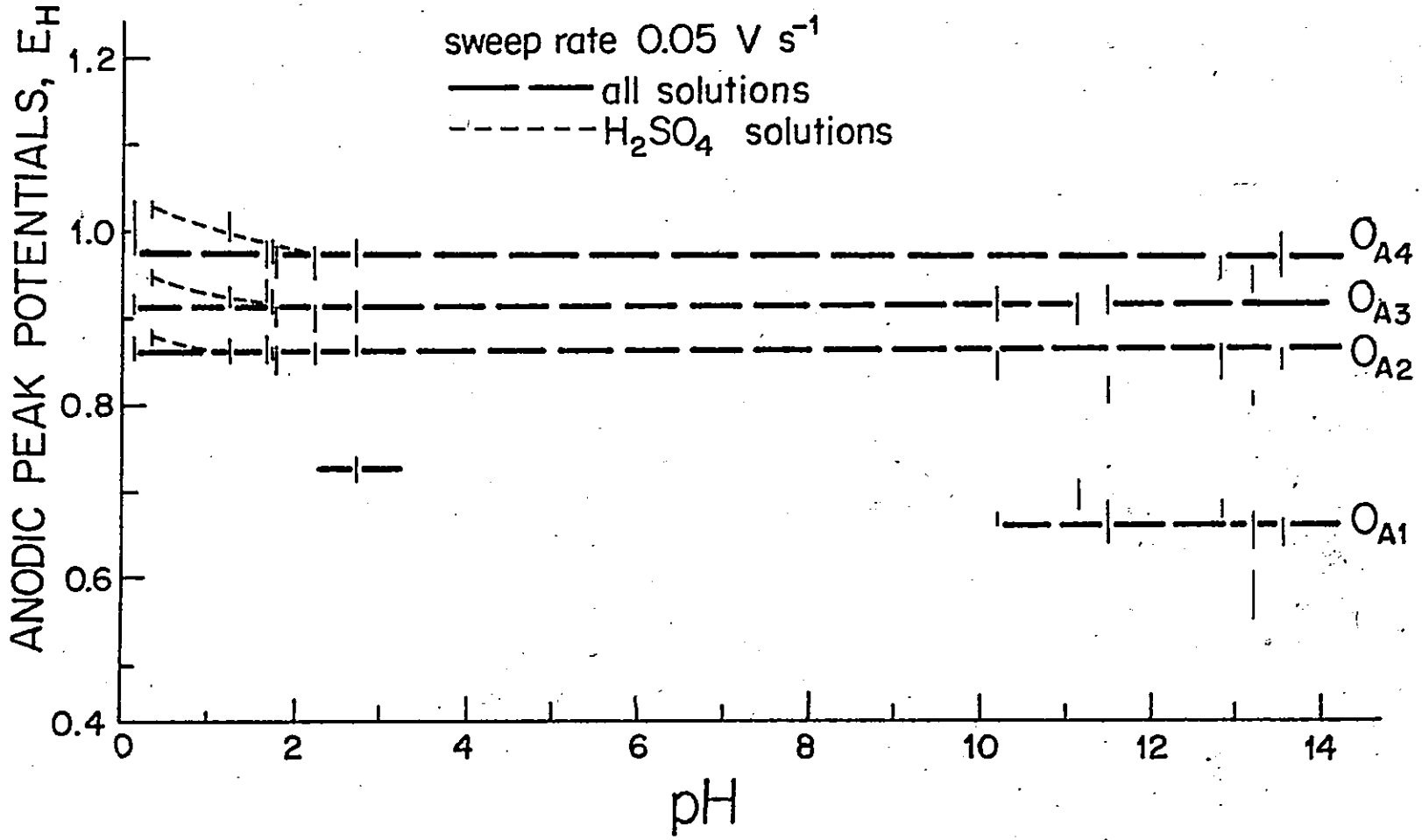

FIG 46 THE pH DEPENDENCE OF OXIDATION PEAK POTENTIALS (s = 0.05 V s^{-1})

quite distinctive (Fig. 33). However, during the course of a long series of experiments involving tens of thousands of potential cycles to 1.3 - 1.4 V on each crystal, the current-potential curves became less distinguishable from one another, and progressively more like that of polycrystalline Pt. Subsequent reflection electron diffraction analysis by Dr. P. B. Sewell (National Research Council, Ottawa) confirmed that all the surfaces had become microscopically polycrystalline. In fact, over 60% of the surface of each electrode was occupied by (110) crystal faces.

In another series of experiments, a polycrystalline Pt wire electrode was subjected to extremely rapid potential cycling (sweep rates of up to 1 kV s^{-1}) to anodic potentials ranging from 1.1 to 1.5 V. After several hundred thousand cycles, when the sweep rate was readjusted to 0.05 V s^{-1}, the current-potential profile had changed to a slight extent. Fig. 47 shows that it now resembled that of a Pt (100) single-crystal in every respect. The surface of the electrode was no longer shiny but a middle-grey colour resembling that of lightly platinized Pt. The changes in the current-potential profile were maintained throughout a further 10 h of potential cycling at 0.05 V s^{-1}.

To check that the changes in oxidation behaviour were due to restructuring of the Pt surface rather than, e.g., the adsorption of impurities, the wire was then dipped into hot aqua-regia for 120 s, thoroughly washed, and then replaced in the solution. The current-potential profile obtained, however, was then characteristic of a Pt (111) surface rather than of the original polycrystalline Pt wire (Fig. 48), and remained so as the potential cycling was continued for several hours.

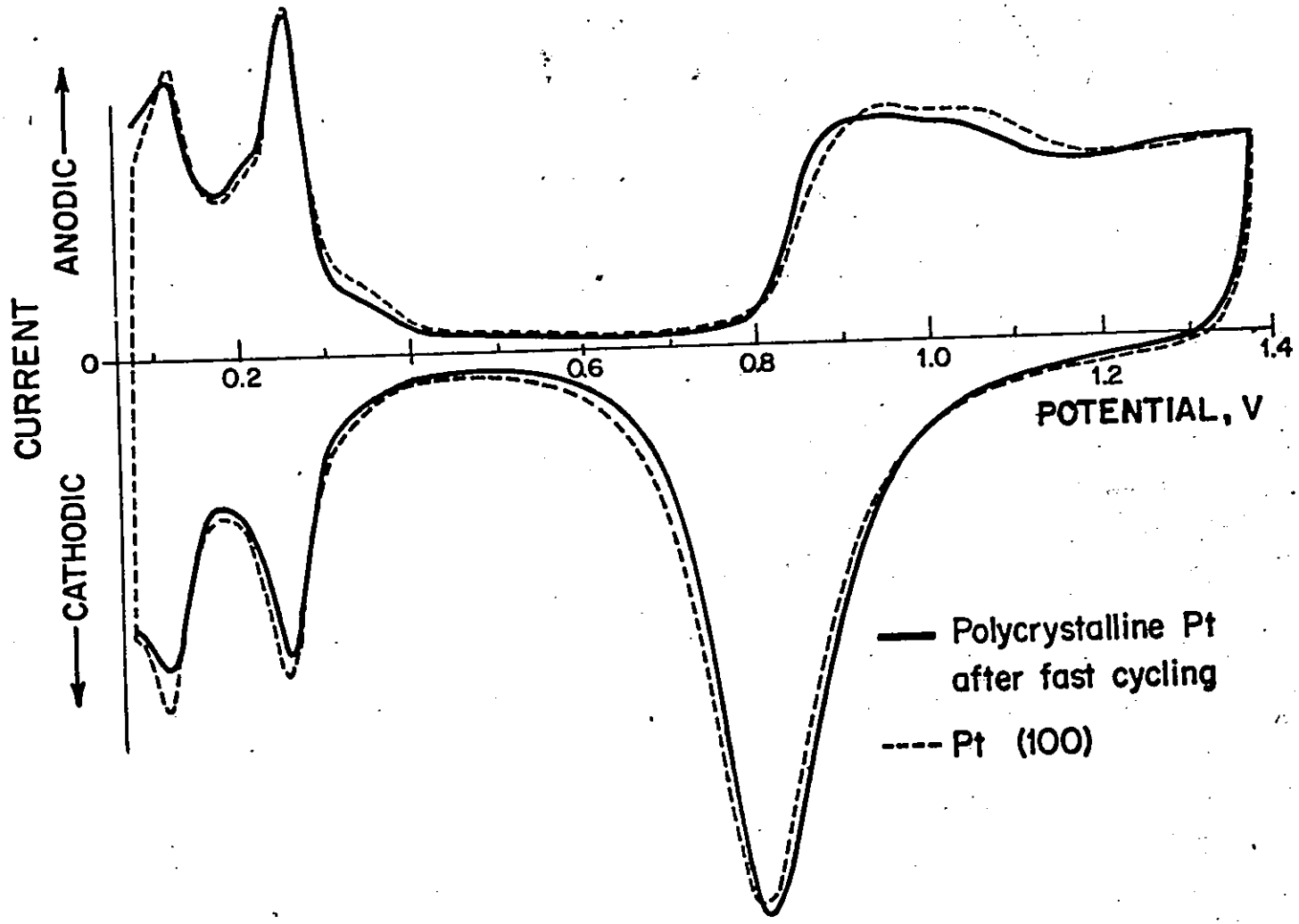

FIG 47 COMPARISON OF POTENTIODYNAMIC CURRENT-POTENTIAL PROFILE AT Pt ELECTRODE PREVIOUSLY USED FOR EXPERIMENTS INVOLVING VERY FAST SWEEP RATES WITH THAT AT A SINGLE-CRYSTAL Pt (100) SURFACE ($s = 0.05\ V\ s^{-1}$)

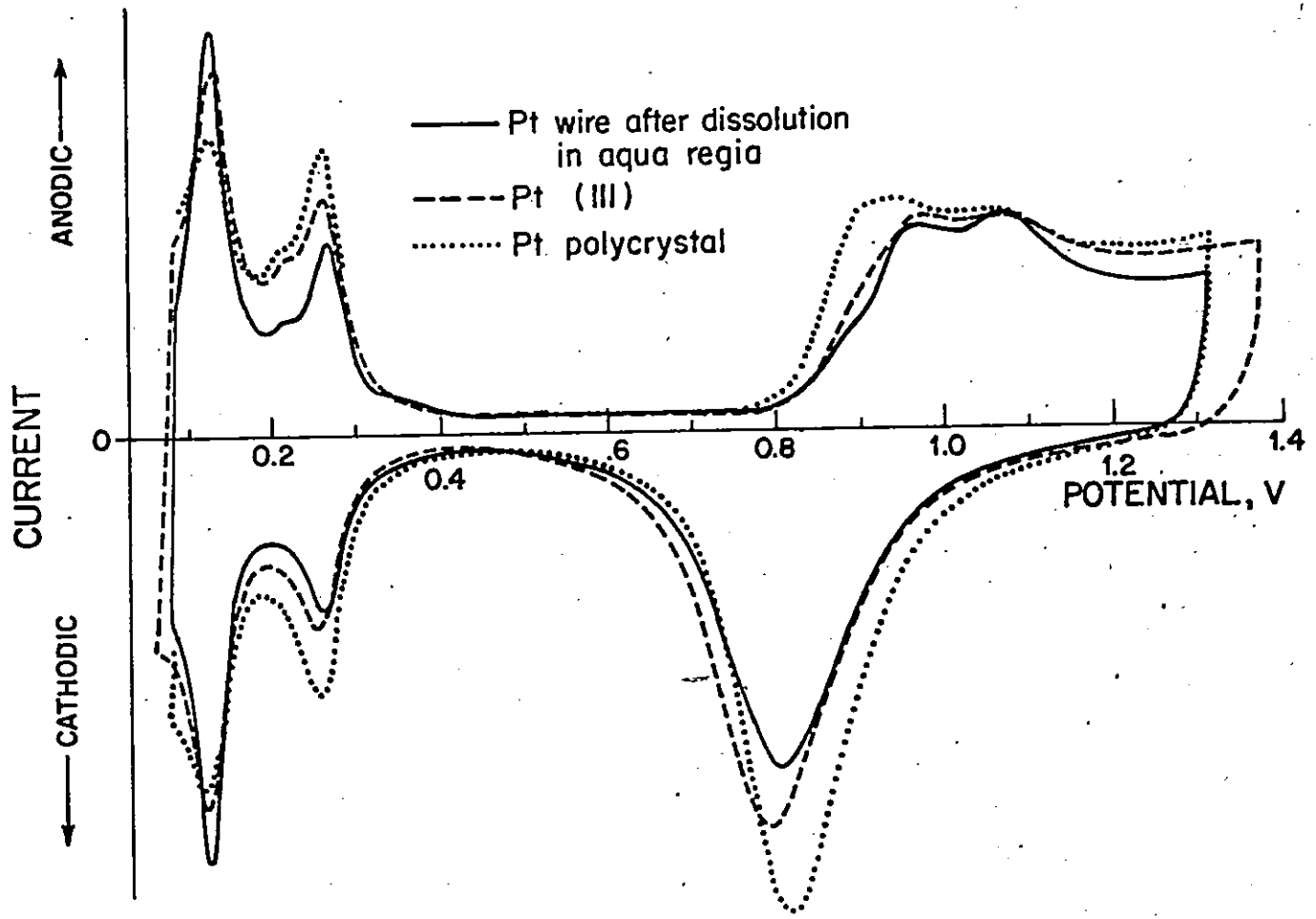

FIG 48 COMPARISON OF POTENTIODYNAMIC CURRENT-POTENTIAL PROFILE AT A Pt ELECTRODE PARTIALLY DISSOLVED IN AQUA REGIA WITH THOSE AT A Pt (111) SINGLE-CRYSTAL SURFACE AND ON A Pt POLYCRYSTAL ($s = 0.05\ V\ s^{-1}$)

6.2 Preliminary discussion

6.2.1 Origin of multiple bonding energies in anodic deposition of O species

Since the first three anodic peaks (e.g. $O_{A1,2}$, O_{A3} and O_{A4} in acid solutions) all arise at coverages much less than a monolayer ($\theta_e = 1$), they cannot be related to a sequence of oxidation states of Pt in a completed oxide film since this would require that some atoms in the Pt surface would remain unoxidized while otherwise identical atoms were undergoing further oxidation to higher oxidation states. In addition, only <u>two</u> oxidation states of Pt occur in bulk compounds, and have been detected in stable Pt surface oxides by ESCA[279].

The current peaks resolved in the anodic oxidation of Pt represent only small variations in a relatively constant oxidation current profile (Fig. 1). Since the same current-potential profile is observed at both smooth and platinized Pt electrodes[229], and the same four oxidation peaks are resolved at single-crystal surfaces (Fig. 33), the relative constancy of the oxidation current cannot be attributed to the occurrence of one or two peaks at slightly different potentials on each of a large number of crystal planes exposed in the surface of a polycrystalline electrode. Instead, it must be related to the overlapping of the currents from the four peaks which <u>are</u> resolved.

It is possible that not all the oxidation peaks represent a simple discharge process. One of them may represent an electrochemical dehydrogenation reaction leading to a bridging O atom on two Pt sites[229], i.e.

$$\text{Pt-OH} + \text{Pt} \rightarrow \begin{matrix}\text{Pt}\\ \diagdown\\ \diagup\\ \text{Pt}\end{matrix}\!\!>\text{O} + \text{H}^+ + \text{e}$$

Although such a mechanism may well occur during the oxidation of Pt, it would only account for a second anodic peak, whereas at least four are observed.

If it is concluded that several of the peaks represent the deposition of the same species at Pt, they must correspond to bonding in several types of environment, each having a characteristic peak potential (or range of deposition potentials). Since the same states of deposited species appear at single crystals (Fig. 33), they must be attributed to extrinsic rather than intrinsic heterogeneity. That is, the component of the deposition potential required to overcome the interaction between the species being discharged and the previously-discharged species is effectively "quantized" into one of three values according to the OH coverage on Pt, and another corresponding to the electrodeposition of O atoms. The earlier theory that surface sites on Pt have intrinsically different "activities"[227,228], is disproved by the result that the same distinct bonding states appear at single-crystal surfaces (Fig. 33 and cf. references 248,249) as they do in the case of H deposition (Section 5.1.2).

The extrinsic heterogeneity giving rise to the different bonding states is thought to arise primarily from the repulsion of like charges on adjacent dipoles formed by discharged O species bound to Pt atoms in the electrode surface. The electronegativity difference between O atoms or OH groups and Pt atoms will cause their bond to be polar, as noted by Bowden in 1929[182]. Frumkin[236], and, more recently, Petrii and Kotlov[99] have confirmed that Pt-O dipoles contribute to the potential at the electrode surface. The ionic charge in the double-

layer decreases with increasing potential[236], showing that the negative charge on deposited O species is sufficient to expel anions from the double-layer.

To calculate the magnitude of the dipole-dipole repulsions between O species discharged at adjacent metal atoms, we take the electronegativity of Pt as 1.91, of O as 3.5[591] and of OH as 2.16[592]. Pauling's formula[591] may then be used to calculate the fraction (f) of an electronic charge located at each end of the dipole:

$$f = 1 - \exp\{-1/4(\chi_{Pt} - \chi_o)\}$$

The result obtained is 0.328e for Pt-O and 0.061e for Pt-OH. Coulomb's law may then be used to calculate the pairwise interactions involved in bringing a dipole to the central site between four nearest neighbour dipoles on a Pt (100) surface. The interaction energies thus calculated are 1.33 V for Pt-O species and 0.035 V for Pt-OH. Although this type of calculation has been extended to include interactions with other species, further from the one being discharged, it involves the simplifying assumption that the dielectric constant in the double-layer at the Pt surface will be unity. It suffices, however, to show that the different energies of the $O_{A1,2}$, O_{A3} and O_{A4} states which cover a range of 0.15-0.27 V may indeed be accounted for by this type of interaction between Pt-O dipoles.

The existence of dipole-dipole repulsions between discharged species will tend to restrict deposition to those sites which form a symmetrical array, maximizing their separation at the coverage involved and hence minimizing the repulsion. As the coverage increases so as to

fill one array, further deposition will begin to form another, in which the deposited species are all closer together and the dipole-dipole repulsions are correspondingly greater.

The most closely packed array possible is that in which the deposited species are in 1:1 correspondence with Pt atoms in the electrode surface. In the next most closely packed, deposited species will not approach more closely than "diagonally-nearest" neighbour positions in the metal surface, in the next they will not approach more closely than next-nearest neighbour positions, and so on. These separations define not only the interaction energy involved in discharge into a particular array site, but also the maximum coverage in that state. Table 2 shows the maximal coverages in the three types of array described above, and the coverage predicted at the current peaks assuming both that the deposition is reversible (peaks symmetrical about maximum) and that the range of potentials of each peak does not overlap the peak potential of the next. The maximum coverage in each array is also expressed as a formula representing the maximum OH:Pt ratio at the electrode surface. Since the assumption that the peaks do not overlap is clearly a simplification (see e.g. Fig. 1), the agreement between the predicted values of coverage at the peaks and the experimental values (derived from Fig. 29) listed in Table 2 is thought to be satisfactory.* The fact that the coverages on poly-

*It should be emphasized that this model of the occurrence of discrete interaction energies through array formation is highly simplified. In reality, deposition will probably occur in complex arrays containing not only the Pt-OH dipoles discussed above, but also place-exchanged OH-Pt species (Section 6.2.2). However, insufficient data is at present available to allow the calculation of the interaction energies to be expected in such a duplex array.

TABLE 2

PREDICTIONS OF COVERAGES AT OXIDATION PEAKS BASED ON ARRAY MODELS

(111)						(100)						Polycrystalline Pt	
Theoretical				Experimental		Theoretical				Experimental		Experimental	
Distance of closest approach	Lattice occupancy formula	Maximum coverage	Coverage to peak	Peak	Coverage to peak	Distance of closest approach	Lattice occupancy formula	Maximum coverage	Coverage to peak	Peak	Coverage to peak	Peak	Coverage to peak
Diagonally nearest neighbours	Pt_3OH	0.33	0.166	$O_{A1,2}$	0.11	Next nearest neighbours	Pt_4OH	0.25	0.125	$O_{A1,2}$	0.10	$O_{A1,2}$	0.12-0.16
Half nearest neighbours	$Pt_3(OH)_2$	0.66	0.498	O_{A3}	0.39	Diagonally nearest neighbours	Pt_2OH	0.5	0.375	O_{A3}	0.31	O_{A3}	0.37-0.40
All nearest neighbours	PtOH	1.00	0.83	O_{A4}	0.83	All nearest neighbours	PtOH	1.0	0.750	O_{A4}	0.78	O_{A4}	0.78

crystalline Pt electrodes are much more like those on (111) than an (100) single crystals is of interest with regard to the restructuring of Pt electrodes during potential cycling, and will be discussed in Section 6.2.4.

Tilak, Angerstein-Kozlowska and Conway[221] have verified that the current-potential profile of peaks $O_{A1,2}$, O_{A3} and O_{A4} in acid solutions may be derived empirically as the sum of three Langmuir or Temkin isotherms, corresponding to the filling of three successive sub-monolayer arrays. The best simulation was obtained with coverages of θ_e = 0.25, 0.25 and 0.5 for the three component peaks, i.e., those appropriate to the model of arrays on Pt (100) (Table 2). The first two component peaks correspond to Langmuir isotherms, but the third has a g-factor of 1.2. In terms of the array model, this would suggest that the species deposited in the first and second arrays are sufficiently far apart for their interaction energy not to vary significantly with the coverage, whereas the filling of the final array would increase the number of (relatively close) "diagonally-nearest" neighbours from zero to four as the array is filled, making the required deposition energy increase with coverage. This type of simulation does not recognize that the electrodeposition potential may be changed as previously-deposited species undergo the secondary processes. Such effects will be discussed in Section 6.2.2, below.

The filling of successive arrays provides a more specific explanation of the occurrence of multiple sub-monolayer states of bonding, than the general concepts of progressive changes in the electronic properties of a metal surface resulting from surface bond

formation, introduced in Section 2.3.3. The fact that the crystallography of the Pt surface affects the electrodeposition of O species much less than that of H, strengthens the view that the anodic oxidation potentials are influenced to a considerable extent by interactions between the deposited O species themselves, whereas the H deposition potentials reflect almost entirely the intrinsic strength of the Pt-H bond. The array model can, of course, only be countenanced in a chemisorption system in which it is probable that the electronegativity difference between the metal atoms and the deposited species is such as to make the bond between them substantially polar, since the arrays only arise because of the repulsive forces between the deposited species. A more detailed discussion of the causes of multiple peaks will be reserved for Chapter 11.

6.2.2 The secondary processes

Since the three predominant current peaks observed in the deposition of the first monolayer (θ_e = 1) of O species are not detected in the reduction sweep, no matter how high is the overall sweep rate (even 750 V s^{-1}), it is clear that the secondary processes causing hysteresis are an integral part of the oxidation mechanism. The secondary processes following the discharge of O species into the metastable states observed in the anodic sweep have two main effects: (i) the bonding of the O species becomes stronger, and (ii) time-dependent continuing oxidation can occur at a given constant potential.

At coverages below θ_e = ca. 0.15, the secondary processes are either relatively slow or reversible, since the oxidation-reduction

cycle is then reversible in both acid (Fig. 10) and alkaline (Fig. 11) solutions, even at sweep rates as low as 0.05 V s^{-1}. At higher coverages however, hysteresis, which is thought to be caused by surface rearrangement processes leading to more stable surface compounds[229], begins to arise. The strong (and polar) bonding forces between Pt atoms and O species, indicated by the considerable underpotential of the sub-monolayer deposition, would be expected to produce more stable surface structures if the O species exchanged places with atoms in the Pt surface so as to form an "ionic lattice". Such place-exchange would change the dipole-dipole interactions between adjacently deposited species from repulsion to attraction. In addition, the reversal of the dipole moment at the place-exchange site would provide an attractive interaction towards O species subsequently deposited at adjacent bare sites. Thus, the underpotential for the deposition of further O species will be increased near the place-exchange site, so that if place-exchange (non-electrochemical process) occurs at constant potential, this will give rise to continued electrodeposition at constant potential. A physical rearrangement of this type would presumably be field-assisted (cf. references 179,218 and 593) and therefore proceed logarithmically with time at constant potential (Fig. 39). Since the mechanism of the discharge process is thus the same whatever the extent of place-exchange (only the underpotentials are changed), an interrupted anodic sweep subsequently returns to the same current-potential curve as without the hold, although the currents passed as the sweep is resumed are reduced by amounts corresponding to the oxidation charge passed during the hold[230]. Presumably the dipole-dipole repulsion between O species

discharged into the metastable anodic states will tend to cause place-exchange at all coverages, although the nature of the resulting rearrangement may be expected to change as the coverage reaches a monolayer. The fact that the dipole-dipole repulsion energy may be reduced by place-exchange as well as by separation of the deposited species into arrays makes a realistic model of the occurrence of distinct electrodeposition energies associated with array formation more complicated than that described in the previous section. However, there will still be a discrete sequence of possible deposition energies, since the number of energetically different deposition sites available at any given potential will be very small.

The increase in the coverage of the strongly bound $O_{A1,2}$ states with increasing temperature at low H_2SO_4 concentrations (Fig. 43, cf. Fig. 41) is attributed to an increase in the rate of place-exchange with temperature, so that at some regions of the surface place-exchange has already allowed the surface to be oxidized to the extent that the O_{A3} reaction may begin, while the potential is still within the range of the $O_{A1,2}$ peak. Similar effects are found in the oxidation of Au (Fig. 58), and are analogous to the effects of diminishing the sweep rate which makes the increased rate of place-exchange detectable at Au surfaces, even at room temperature (Section 7,1.3).

Rapid reduction sweeps (Fig. 40 and reference 229) suggest that two types of rearranged surface structures are produced by place-exchange, in addition to the reversibly-reducible species deposited at low coverage. The more strongly bound of these (O_{C2}), apparently reaches a limiting coverage, but the more weakly bound continues to

increase in coverage, and forms the familiar O_{C3} peak. This peak may be associated with the reduction of species formed by the electrochemical dehydrogenation reaction discussed in Section 6.2.1. The similarity of the oxide reduction potentials on the principal index faces of Pt (Fig. 33) suggests that the bonding energies of the rearranged structures are largely independent of the crystallography of the substrate. In addition, when the reaction temperature is raised to 366K, and the oxide film is therefore given more opportunity to become equilibrated, the half-width of the O_{C3} peak falls to about 75 mV (at 0.05 V s^{-1}) suggesting the existence of attractive forces between the deposited species (Section 1.2). It seems therefore, that the rearranged structures behave more like two-dimensional surface phases and less like independently-bonded chemisorbed species. Since the states of the oxide film resolved in the reduction sweep are all more clearly resolved on Au than on Pt electrodes, further discussion of this matter will be given in greater detail in Section 7.2.3.

6.2.3 Effects of anions and pH

The experiments showed that even the most weakly adsorbed anions require a measurable energy for their displacement by electrodeposited O species. The coverage of specifically adsorbed anions was increased in three ways: (i) by increasing their concentration in the solution, (ii) by reducing the pH, and (iii) by allowing them more time to adsorb.

Both HSO_4^- and ClO_4^- ions increase the potential of the submonolayer oxidation states when their concentration exceeds about 0.01 M

(Fig. 41), but the effects are much smaller with ClO_4^-. This is consistent with radiotracer data showing that HSO_4^- is more strongly specifically adsorbed than ClO_4^- at Pt[237-239], and therefore more difficult to displace.

Since the O_{A1} peak (0.5 - 0.8 V) is resolved at high pH in solutions of NaOH + 0.5 M Na_2SO_4 (Fig. 44) as well as in Na_2CO_3 (Fig. 11), and NaOH, but is not resolved at low pH in $HClO_4$ solutions, the absence of surface oxidation at these potentials at low pH must relate to the strength of the specific adsorption bonding. The potential of zero charge of Pt moves to more positive potentials (when referred to a Pt/H_2 electrode in the same solution) as the pH increases[586]. At higher pH the reduced electronegativity of the Pt surface at the potential of peak O_{A1} will thus weaken the specific adsorption of the anions (of the added salt or acid) and allow the discharge of O species to begin at lower potentials. The reduced coverage of specifically adsorbed anions at high pH is confirmed by the fact that the double-layer capacitance is always greater in alkaline solutions (Fig. 38, cf. Fig. 37). A similar conclusion on the effect of pH on the oxidation of Pt was reached earlier by Khazova, Vasiliev and Bagotskii[312] from data on the oxidation rates of organic compounds at Pt.

Specifically adsorbed HSO_4^- and SO_4^{2-} ions are apparently displaced by O species discharged into states O_{A2} to O_{A6}, but not by the more strongly bound species in state O_{A1}, possibly because the latter O species are discharged between the adsorbed anions. It should be noted that specifically adsorbed anions (HSO_4^-, SO_4^{2-} and ClO_4^-) affect the electrodeposition of O species in a rather different way to that of

H (Section 5.1.6). Firstly, the current-potential profile is much less affected. Secondly, only the deposition of O species is affected, whereas specifically adsorbed ions affect both the cathodic and anodic sweeps in H deposition rather similarly. Thirdly, their primary effect is to control the potential at which deposition of O species begins (i.e. to "push" the anodic peaks to higher potentials), whereas in H deposition only a redistribution of the H atoms among previously available bonding states is observed (i.e. the current peaks are "pushed" up and down). As with the electrodeposition of H, effects of SO_4^{2-}, HSO_4^-, and ClO_4^- ions on the electrodeposition of O species are much less than those of halide ions.

The fact that the extension of the cathodic range of a sweep to include the H_{C4} and H_{C5} peaks increases both the potential at which Pt begins to oxidize and the currents in the low-coverage peaks (Fig. 9) is not at present understood. Extending the cathodic range to potentials more negative than the p.z.c. of Pt would be expected to reduce the coverage of specifically adsorbed anions (blocking the oxidation process), whereas the effects on the current-potential curve are similar to those of <u>increasing</u> the concentration of HSO_4^- ions in the solution (Fig. 41). The effects are however less than in the case of Fig. 41 possibly because only the coverage of anions is being affected whereas increasing the concentration of H_2SO_4 also increases the strength of the specific adsorption bond by lowering the pH. It appears that whenever the conditions are such as to increase the coverage of HSO_4^- ions, the anodic double-layer capacitance is reduced and the anodic double-layer becomes "flatter" and "longer". This suggests that the constancy

of the double-layer currents at Pt may be related in some way to the bonding of specifically adsorbed anions.

When the specific adsorption of anions prevents the electrodeposition of O species at lower potentials, there is always a corresponding increase in the oxidation currents at higher potentials (Figs. 41, 43 and 44). Thus, despite the redistribution of the O species among the bonding states, the total deposition charge in potentiodynamic sweeps to beyond 1.25 V is <u>not</u> affected by the solution composition (Figs. 41 and 43).

6.2.4 Dissolution-redeposition and surface reconstruction

The experiments involving very rapid potential cycling clearly produced a predominance of Pt (100) crystallites in the electrode surface (Fig. 47), and the current-potential profiles of other well-used electrodes (e.g. Fig. 32) also began to show features characteristic of Pt (100) and (110) surfaces (particularly in the electrodeposition and oxidation of H). The restructuring of Pt (100) and (111) single-crystal surfaces into polycrystals with a predominance of (110) orientations after much slower potential cycling (e.g. 0.1 V s^{-1}) was confirmed by Dr. Sewell's reflection electron diffraction studies (Section 6.1.5). The formation of (100) and (110) surfaces may be favoured under conditions of dissolution and redeposition either because their low surface atomic densities allow easy removal and redeposition of Pt as oxides are formed and reduced, or because the (100) and (110) surfaces have a lower surface energy. Unfortunately, the surface energy of Pt has apparently not been measured on single-crystal surfaces.

The chemical dissolution of a Pt surface, on the other hand, produces a predominance of (111) orientations (Fig. 48). This is not unexpected, since atoms in the close-packed planes of a polycrystal will be more strongly bound than those in any other plane, and consequently their slower dissolution will lead to an increase in the proportion of the surface showing (111) orientations.

The existence of dissolution-redeposition processes is also shown by recent work in this laboratory[594] in which polycrystalline Pt surfaces, roughened by potential sweep programmes involving high potentials[156,308,309], became smoother (i.e. their area, measured by Q_H, was reduced) when cycled with an upper potential limit of between 1.1 and 1.4 V, but not when left on open-circuit in a similar solution.

Quantitative studies in other laboratories have shown that measurable amounts of Pt are dissolved[270,308,314,595] when the anodic end-potential of a potentiodynamic sweep exceeds about 1.1 V[299,300], and that when the end-potential exceeds about 1.4 V, the electrode becomes auto-platinized on a very fine scale[135,184]. This led Biegler to suggest that the "clean" current-potential profile at Pt (e.g. Fig. 1) can only be achieved by "activating" the electrode by a series of sweeps to high anodic potentials[308]. However, the quantities of Pt involved in the dissolution-redeposition reactions are much too small to reconstruct the electrode surfaces under the conditions of the experiments reported in Sections 6.1.2 to 6.1.5. Using Rand and Woods' data[300] for potentiodynamic dissolution rates in 0.5 M H_2SO_4, only 40% of an electrode surface could be redeposited in 10 cycles to 1.46 V (assuming that all the dissolved Pt was redeposited and that no

redeposited atom was dissolved). With the anodic limit of 1.32 V used in most of the studies described here only about 20% of the surface could be reconstructed in 10 cycles. However, in the purest solutions prepared as described in this thesis a "clean" current-potential profile has been achieved during the second cycle with a new Pt electrode[582]. There is thus no doubt that the "activation" effects reported by other workers are in fact related to the oxidative removal of impurities from the electrode, or the pre-electrolysis of the solution, rather than to any structural changes in the electrode surface.

CHAPTER 7

ELECTRODEPOSITION OF O SPECIES ON Au

7.1 Results

7.1.1 General features of the current-potential profile

The general features of the current-potential profile for the electrodeposition of O species on Au are shown in Figs. 49 and 50. The considerable hysteresis in the oxidation-reduction cycle makes the resolution of surface bonding states particularly sensitive to the experimental conditions involved. As with the oxidation of Pt, a series of current peaks (designated O_{A1}, O_{A2}, O_{A3}, etc.) is observed in the anodic sweep (Fig. 49) as O species are electrodeposited in distinct states.

The distinct states detected in the reduction of oxidized Pt electrodes at high sweep rates and very low temperatures, are resolved at Au under much less extreme conditions (e.g. 0.05 V s^{-1} and 274 K, as in Fig. 50), which makes them much more amenable to quantitative study. The predominant cathodic current peaks are designated O_{C1}, O_{C2} and $O_{C3,4}$ in order of the increasing oxide coverage which leads to their formation. As may be seen from Fig. 50, they occur in the order O_{C1}, $O_{C3,4}$, O_{C2} as the potential is decreased in the cathodic sweep. When the preceding anodic sweep has deposited a high coverage of O species, potential-independent currents, designated O_{C5}, appear at still more cathodic potentials (Fig. 49).

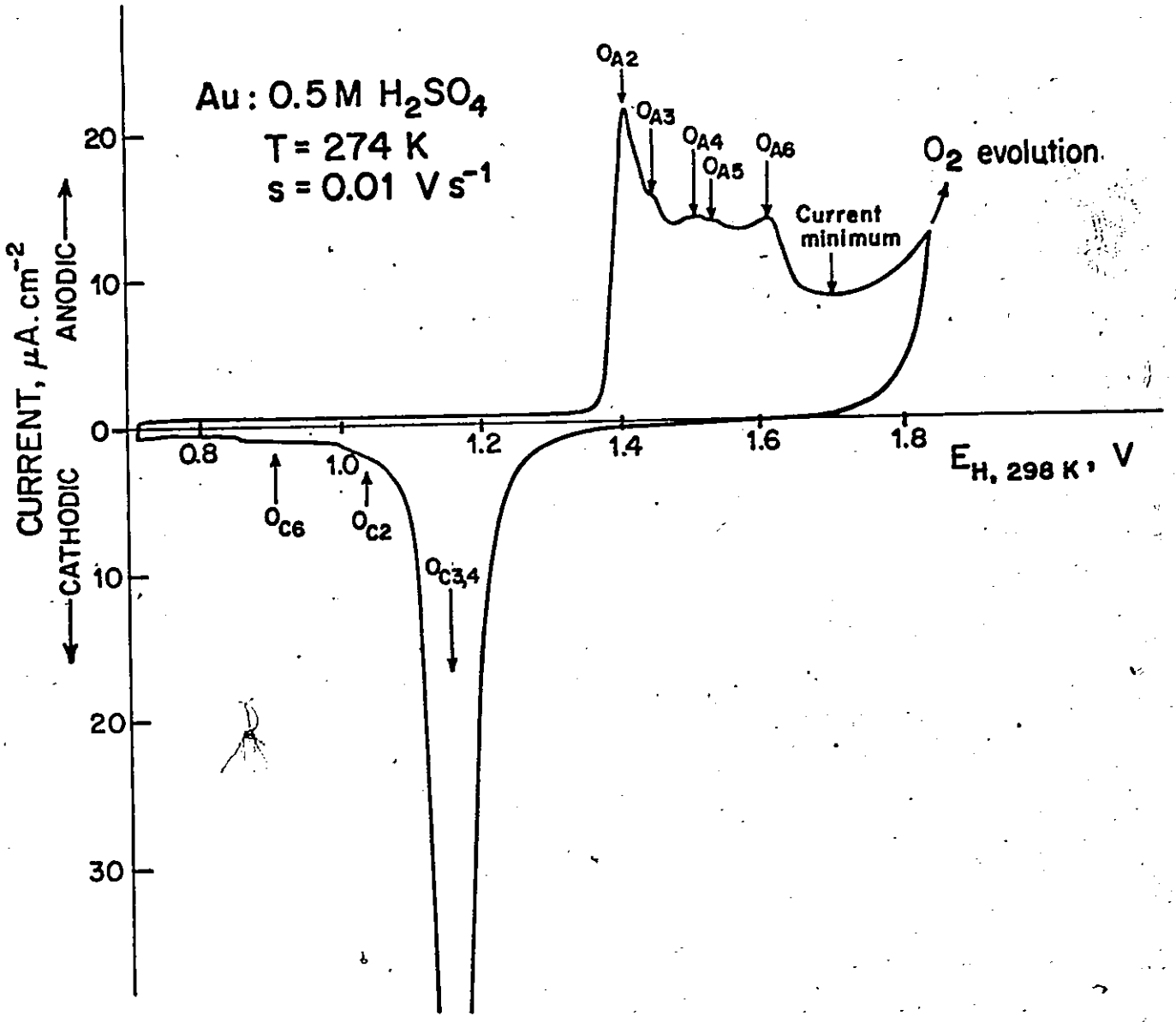

FIG 49 POTENTIODYNAMIC CURRENT-POTENTIAL PROFILE AT Au IN 0.5 M H_2SO_4 AT 274 K SHOWING GOOD RESOLUTION OF ANODIC STATES (s = 0.01 V s^{-1})

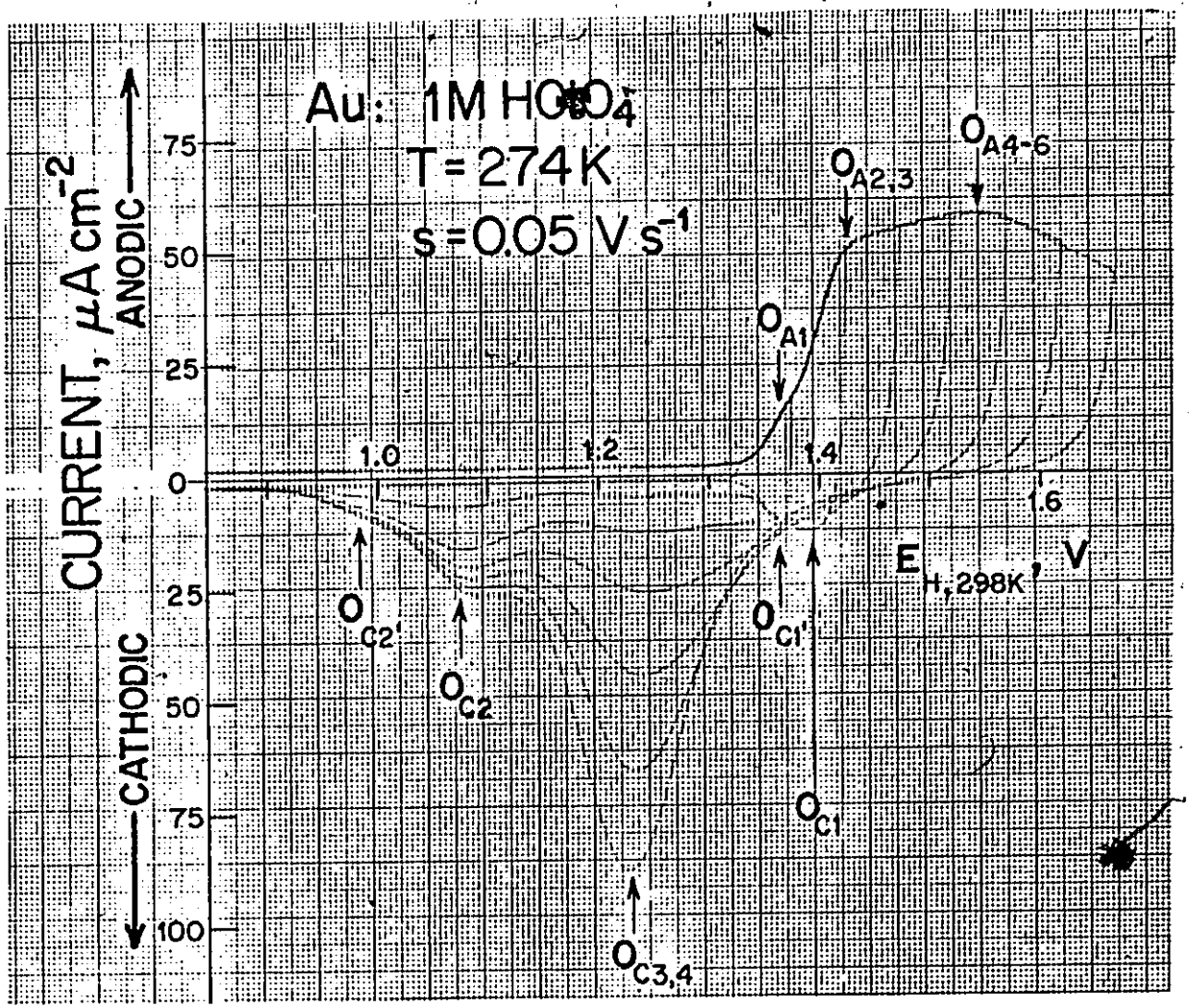

FIG 50 POTENTIODYNAMIC CURRENT-POTENTIAL PROFILE AT Au IN 1 M $HClO_4$ AT 274 K SHOWING GOOD RESOLUTION OF STATES IN CATHODIC SWEEP ($s = 0.05\ V\ s^{-1}$)

7.1.2 Calculation of the coverage by O species

Interpretation of the behaviour of electrochemically deposited O species at Au is made difficult because no monolayer chemisorption of H occurs on which to base calculations of the coverage of O species, as at Pt. However, the areas of Au electrodes can be derived according to a method developed by Michri, Pschenichnikov and Burshtein[585]. These authors measured the areas of Au electrodes by B.E.T.[596] (low temperature adsorption of Ar and Kr), and found that the oxidation charge passed on the same electrodes at potentials below that of the well-defined current minimum immediately preceding the evolution of O_2 in 0.5 H_2SO_4 (Fig. 49) was 400 μC per real cm^2, over a wide range of temperatures and sweep rates. The constancy of this measure of charge was checked in the present work over the range of sweep rates (0.01 to 100 V s^{-1}) and of temperatures (274-365K) to be employed, and the standard deviation was found to be less than 5% of the mean in all cases. An example of the results obtained is given in Table 3 where

TABLE 3

Roughness of an Au Electrode Calculated from Oxidation Charge to the Current Minimum

Sweep Rate	Temperature			
	273.9 K	296.2 K	324.0 K	364.5 K
0.01 V s^{-1}	1.42	1.29	1.47	1.45
0.1 V s^{-1}	1.32	1.34	1.31	1.43

estimates of the roughness factor (real area/geometric area) of one of the Au electrodes used are recorded. A considerable proportion of the observed scatter probably arises from the difficulty of accurately estimating the potential of the current minimum which is often rather shallow and broad.

Not all the electrodes used, however, were measured individually in this way. The areas of other electrodes were found by multiplying the area of an electrode calibrated by the above method by the ratio of the oxidation charge passed up to a convenient anodic potential (e.g. to 1.55 V) on the electrode of unknown area to that on the electrode of known area determined in an identical solution at the same sweep rate and temperature.

The average surface atomic density of polycrystalline Au electrodes was calculated by scaling down the accepted value[597] for polycrystalline Pt electrodes (about 1.4×10^{15} atoms cm^{-2}, corresponding to a "one-electron monolayer" charge of 220 $\mu C\ cm^{-2}$) by the ratio of the square of the metallic radius of the Pt atom to that of Au. This of course involves the assumption that the distribution of crystal faces on polycrystalline Au electrodes is identical to that on Pt electrodes. The value of surface atomic density thus derived for Au is 1.2×10^{15} atoms cm^{-2} and the charge for the one-electron monolayer 200 $\mu C\ cm^{-2}$. Coverages were then calculated, as in the oxidation of Pt, in terms of the number of electrons passed per atom in the Au electrode surface, thus:

$$\theta_e = \frac{q_{oxidation}}{200A}$$

where A is the real area of the electrode in cm^2. Electrode areas calculated by this method agree very well (within about 1%) with those calculated[594] by comparing the double-layer charging currents at Au electrodes with those on Pt electrodes, the areas of which were known from the H deposition charge.

7.1.3 Hysteresis in the current-potential profile

In order to add further comparative evidence for the oxidation mechanism developed for Pt (see Chapter 6), the current-profile at Au was studied over a wide range of potentials, sweep rates and temperatures, as described below. Increasing the sweep rate and decreasing the temperature have similar effects on the current-potential profile for Au. Thus, a similar current-potential profile to that observed at 274 K at 0.05 V s^{-1} (Fig. 50) may be obtained even at 365 K, by increasing the sweep rate to 100 V s^{-1} (Fig. 51). If, however, the temperature is increased without any alteration in the sweep rate (Fig. 52 cf. Fig. 50), the anodic peaks move to less positive potentials and the cathodic peaks generally move to more positive potentials (Fig. 53). These effects are obviously characteristic of slow processes with an appreciable activation energy. Temperature changes in H_2SO_4 solutions produce effects additional to those in $HClO_4$ solutions, which result from changes in the equilibrium coverage of specifically adsorbed HSO_4^- ions. Despite the shifts of the anodic peak potentials with increasing temperature (Fig. 53), it is found that the charge passed in each of the various stages of surface oxidation signified by the anodic peaks is almost independent of temperature (Fig. 54) as if

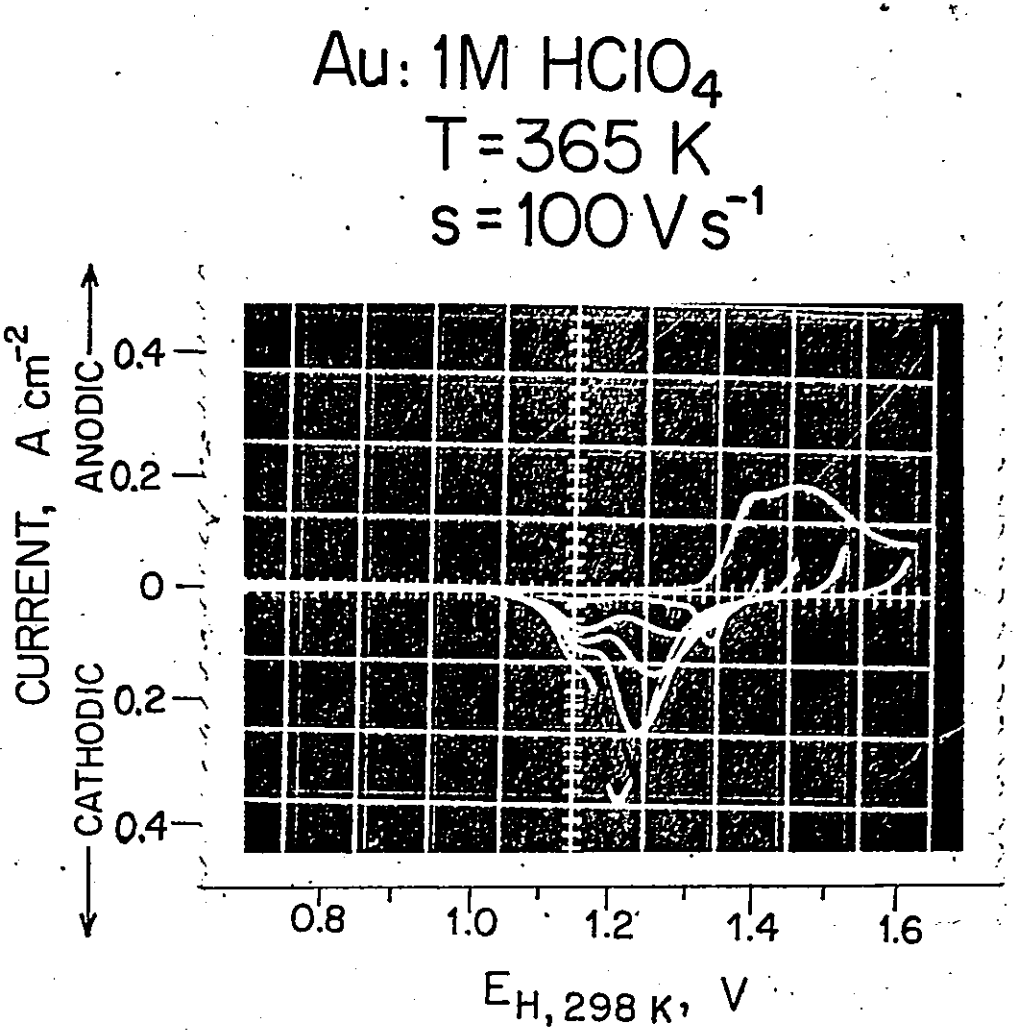

FIG 51 POTENTIODYNAMIC CURRENT-POTENTIAL PROFILE AT Au IN 1 M $HClO_4$ AT 365K (s = 100 V s^{-1})

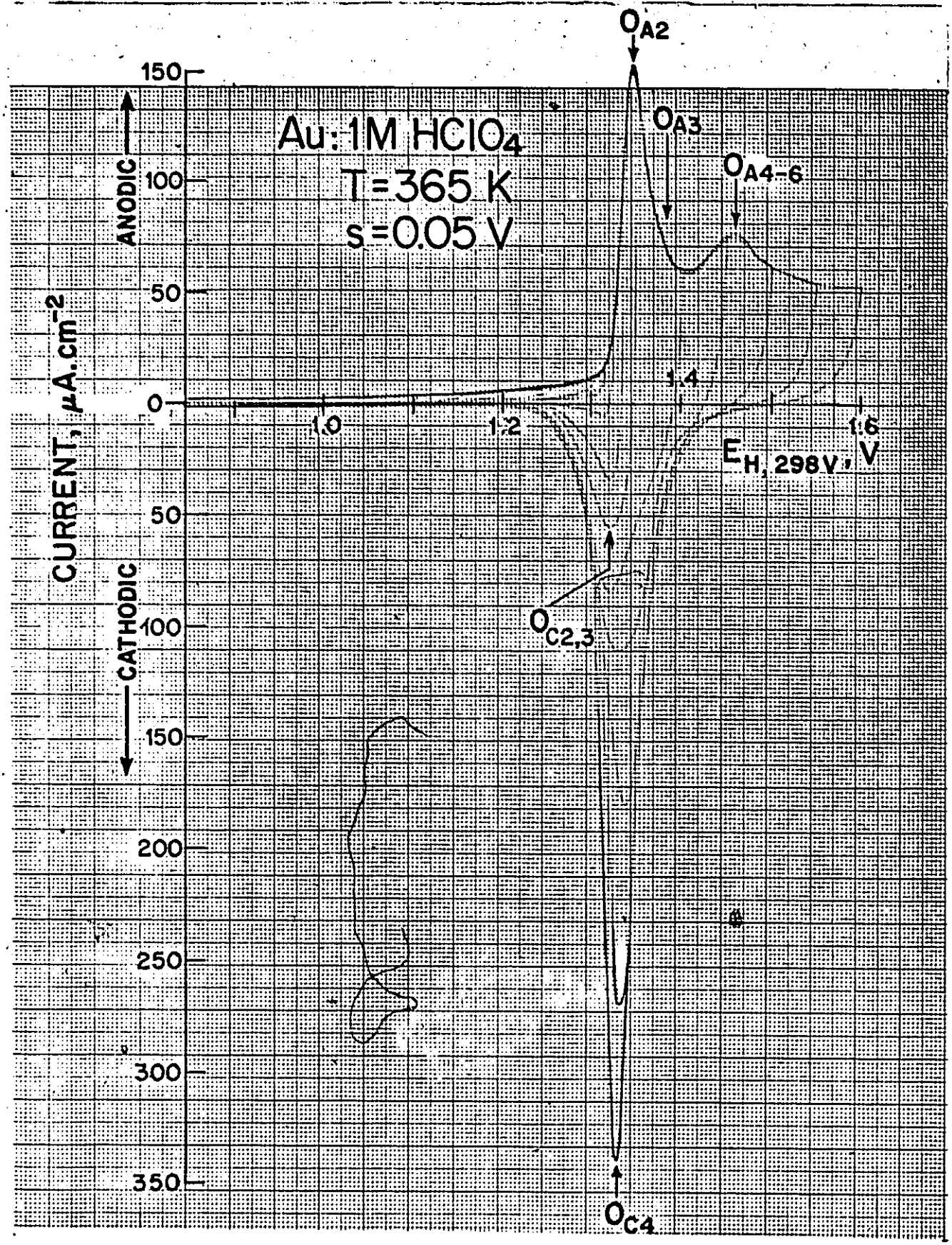

FIG 52 POTENTIODYNAMIC CURRENT-POTENTIAL PROFILE AT Au IN 1 M $HClO_4$ AT 365 K ($s = 0.05\ V\ s^{-1}$)

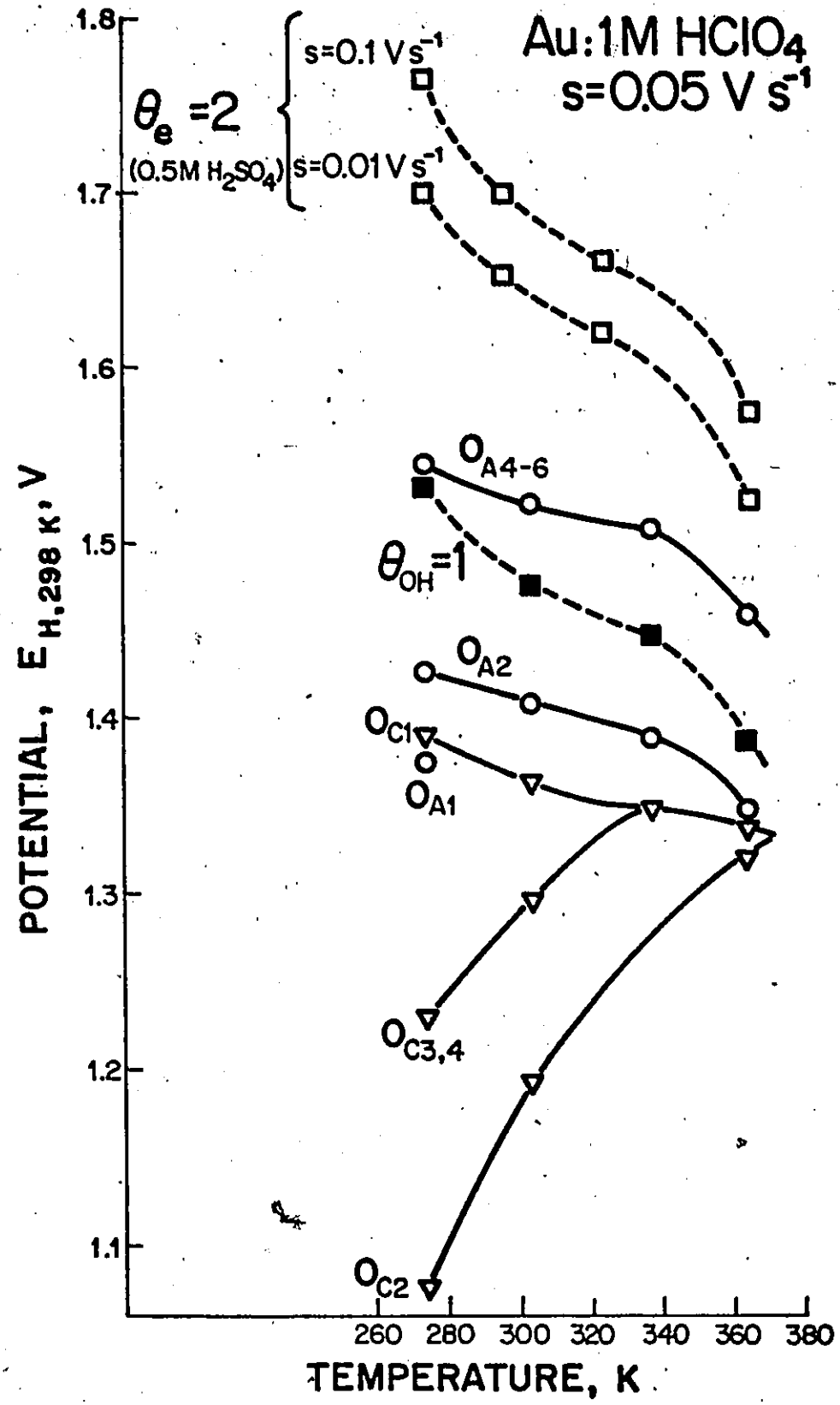

FIG 53 TEMPERATURE DEPENDENCE OF PREDOMINANT CURRENT PEAKS IN THE POTENTIODYNAMIC OXIDATION / REDUCTION OF Au SURFACES

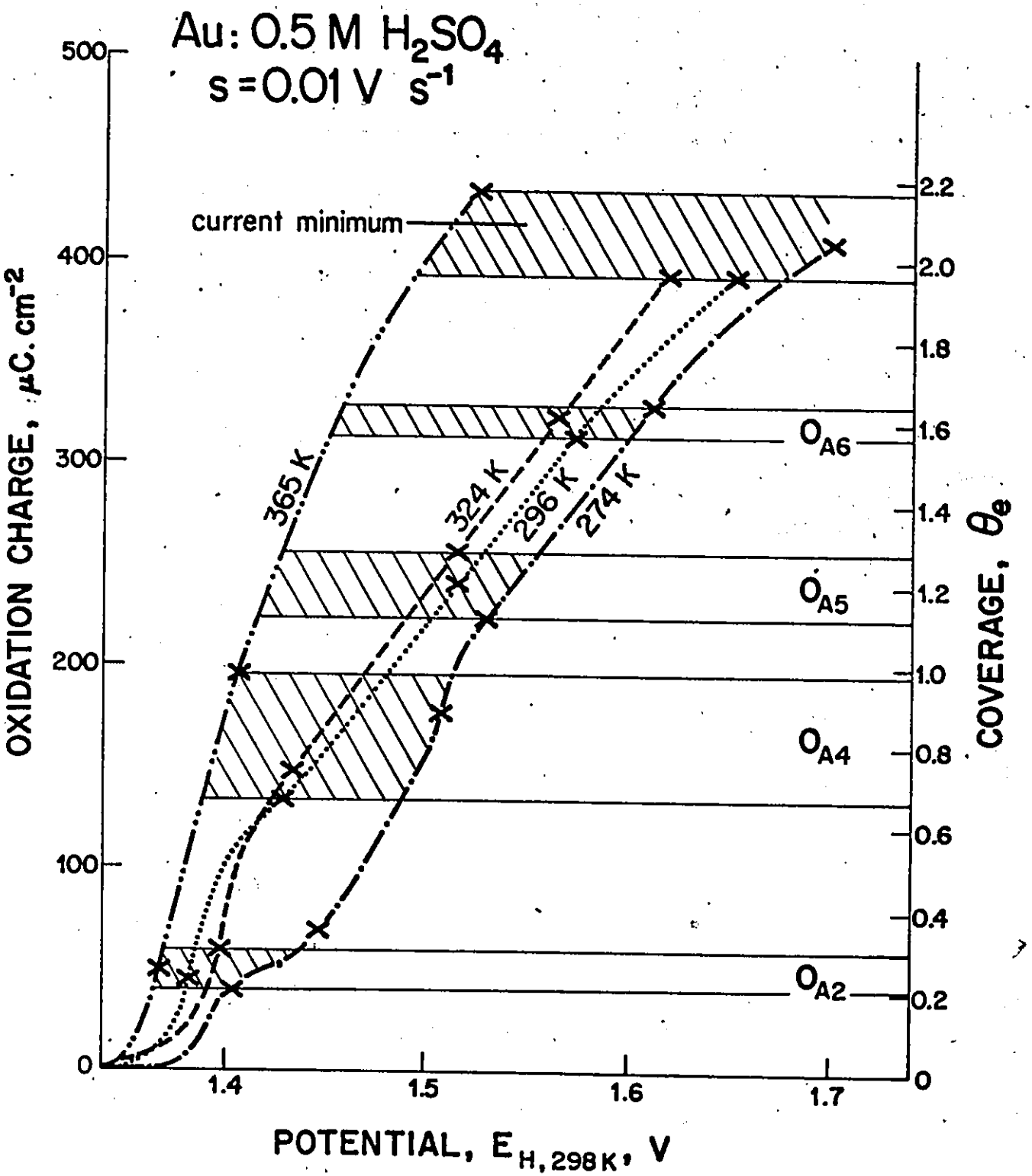

FIG 54 COVERAGE AT VARIOUS CURRENT PEAKS IN THE ANODIC OXIDATION OF Au SURFACES AT 0.01 V s^{-1} AT DIFFERENT TEMPERATURES

each state of surface bonding has a characteristic limiting coverage. [For clarity, all the data points except the integrated charge at the current peaks have been omitted from Fig. 54]. This presumably is the basis for the satisfactory use of the current minimum at various temperatures and sweep rates in the method of electrode area measurement developed by Michri et al.[585].

Figure 55 shows that the potentials of the better-resolved peaks vary linearly with the log of the sweep rate over five orders of magnitude. At higher sweep rates, the current minimum preceding O_2 evolution in the anodic sweep, and therefore the evolution of O_2 itself, occurs at more positive potentials, although always at the same coverage (θ_e = 2). The anodic peak potentials increase by about 0.022 V per decade of increase in the sweep rate and the potential of the $O_{C3,4}$ peak decreases by about 0.04 V per decade. At sweep rates of above about 10 V s^{-1}, however, the potential of the $O_{C3,4}$ peak shifts by about 0.1 V per decade and that of O_{C2} by only about half this amount. These experimental sweep rate dependencies do not correspond to any simple electron-transfer-controlled rate-limiting step. They may possibly imply that the kinetics of the electron transfer reaction is modified by the presence of the partial film of polar O species at the electrode interface[598]. The resolution of individual states of the deposited species is gradually lost in the anodic sweep at rates above about 0.1 V s^{-1}, particularly in H_2SO_4 solutions where the anodic profile merges into a single broad peak. The i_p/s^* ratio for the dominant anodic peak (O_{A2}) is almost constant at about 1.5 mF cm^{-2} throughout the range of sweep rates studied, possibly increasing slightly at rates below 0.01 V s^{-1} (Fig.56).

*i_p = peak current; s = sweep rate.

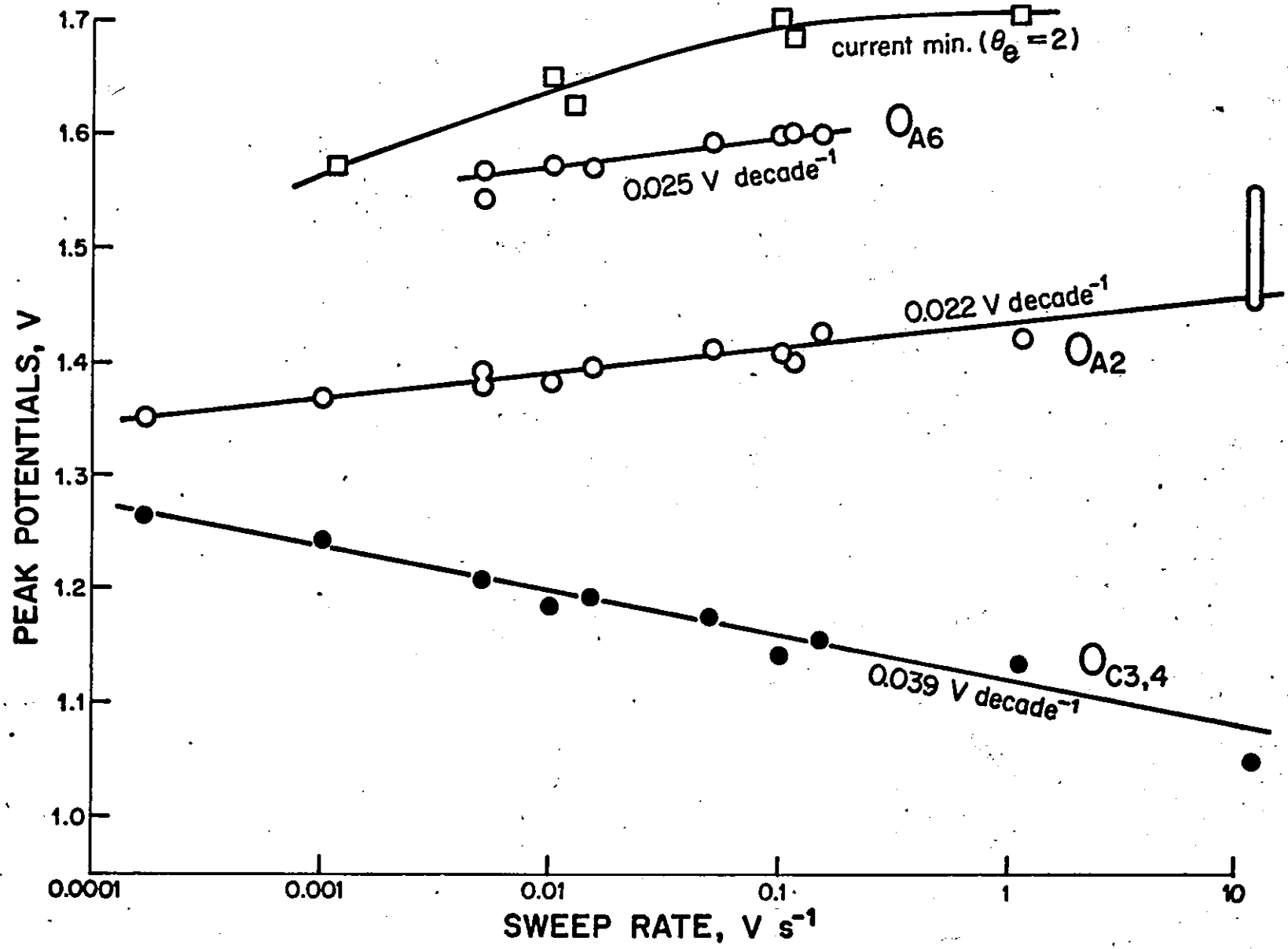

FIG 55 SWEEP RATE DEPENDENCE OF POTENTIALS OF PREDOMINANT CURRENT PEAKS IN THE POTENTIODYNAMIC OXIDATION / REDUCTION OF Au SURFACES

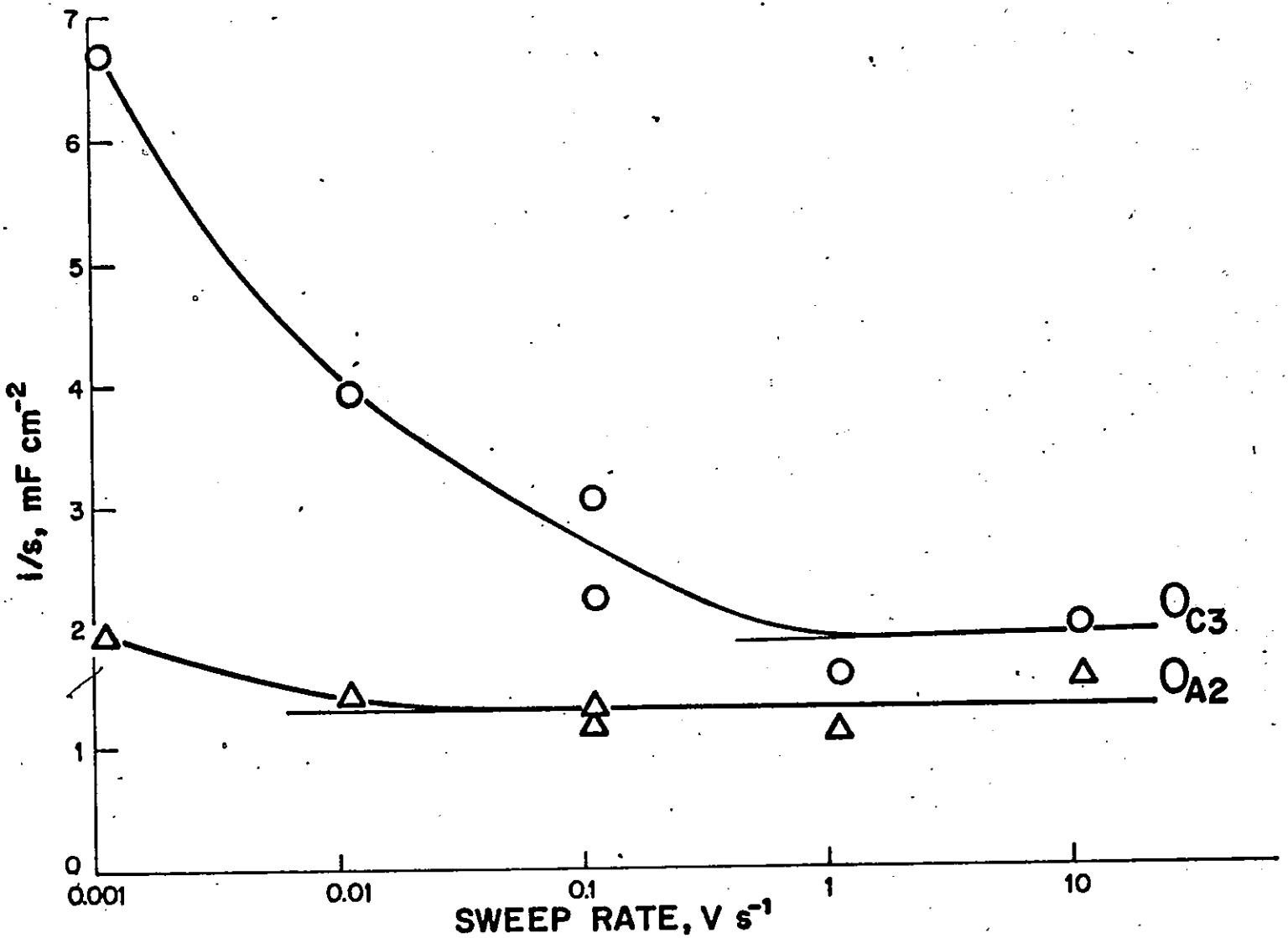

FIG 56 SWEEP RATE DEPENDENCE OF PSEUDOCAPACITANCE (i_p / s) OF PREDOMINANT CURRENT PEAKS IN THE POTENTIODYNAMIC OXIDATION / REDUCTION OF Au SURFACES

For peak O_{C3} on the other hand, the ratio i_p/s was only constant (at about 2 mF cm^{-2}) at above 1 V s^{-1}. At slower sweep rates (Fig.56), it increased to about 7 mF cm^{-2} at 0.001 V s^{-1}. This anomalous behaviour at low sweep rates is explained by the fact that place-exchange (see Section 6.2.2) is continuously altering the coverage in the various bonding states. As with the oxidation of Pt the maximum coverage of O species which may be reduced reversibly (i.e. in peak O_{C1}) increases with decreasing temperature and increasing sweep rate. The maximum coverage of reversibly deposited species observed was $\theta_e = 0.27$ (at 10 V s^{-1} in 0.5 M H_2SO_4 at 300 K), an identical value to that measured on Pt at 100 V s^{-1} in 5M H_2SO_4 at 243 K[229]. Peaks O_{C2} and $O_{C3,4}$ move to more negative potentials as the sweep rate is increased or the temperature decreased, since they are currents for kinetically irreversible processes, (cf. Figs. 51 and 52, and see Fig. 53).

This separation of the peak potentials allows an accurate measurement of the charge passed in reduction from each state of the deposited species, as shown typically in Fig. 57. The initially-deposited O species are mainly reduced reversibly (in peak O_{C1}), but as the total coverage increases, O_{C2} and then O_{C3} are seen as the predominant stable states of the O species bonded at Au. Further increases in coverage lead to the development of the O_{C4} peak, the potential of which becomes less positive as the coverage increases. The O_{C4} peak first appears at potentials below that of O_{C3} at temperatures of 337 K and below in 1M $HClO_4$ (Figs. 50,58). However, at 365 K (Fig. 52), O_{C4} first appears at a higher potential than O_{C3}, although it still shifts to lower potentials as higher coverages of oxide are reduced.

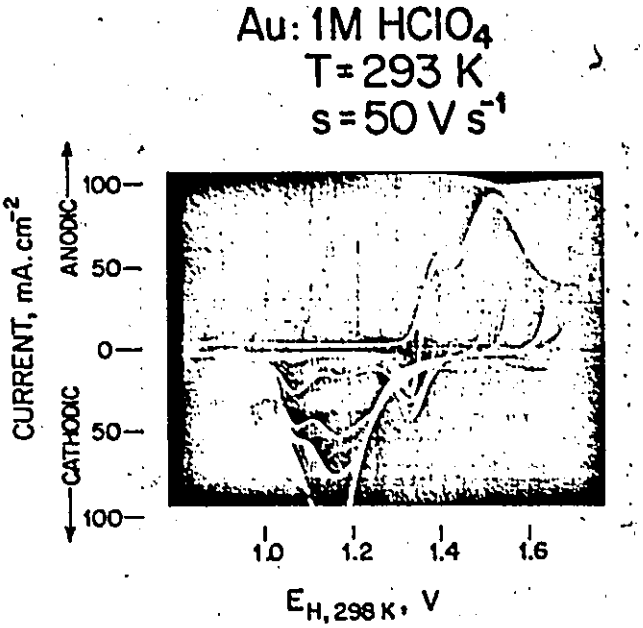

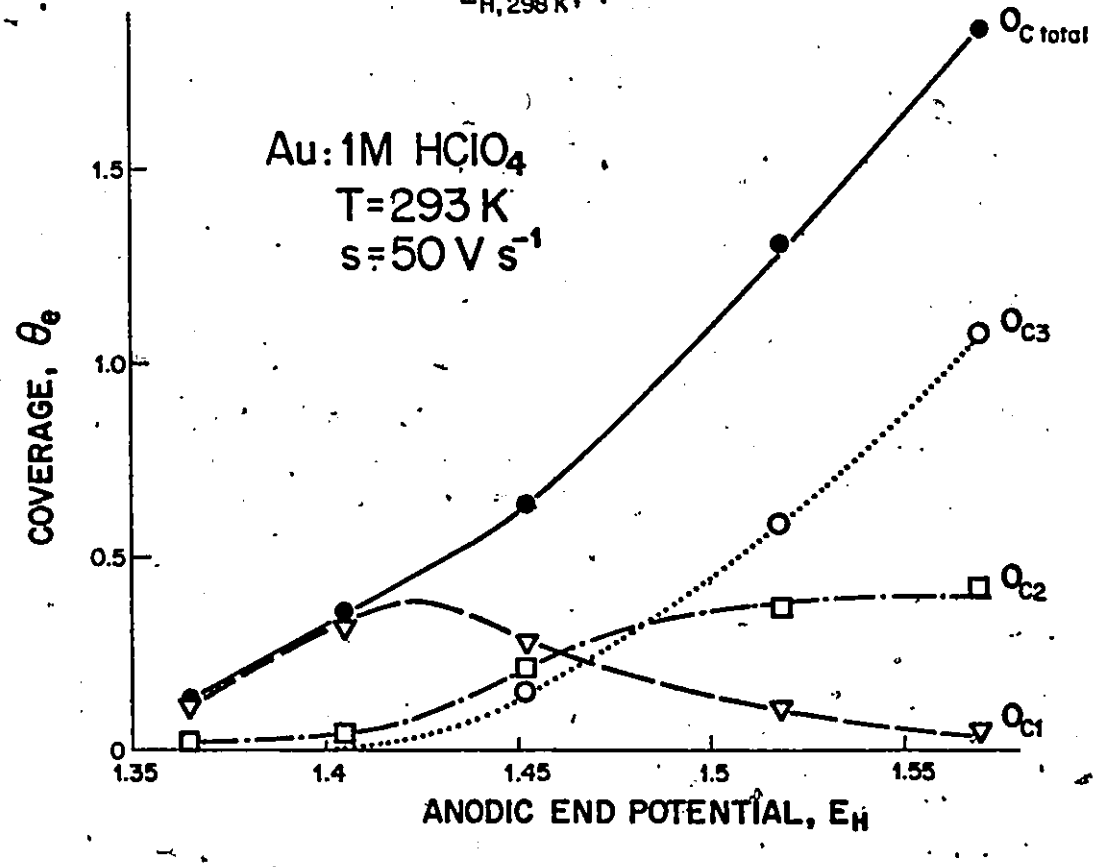

FIG 57 (Top) POTENTIODYNAMIC CURRENT-POTENTIAL PROFILES AT Au IN 1 M $HClO_4$ INVOLVING A SERIES OF ANODIC END-POTENTIALS ($s = 50\ V\ s^{-1}$) (Bottom) ESTIMATES OF COVERAGES CORRESPONDING TO THE COMPONENT CATHODIC PEAKS

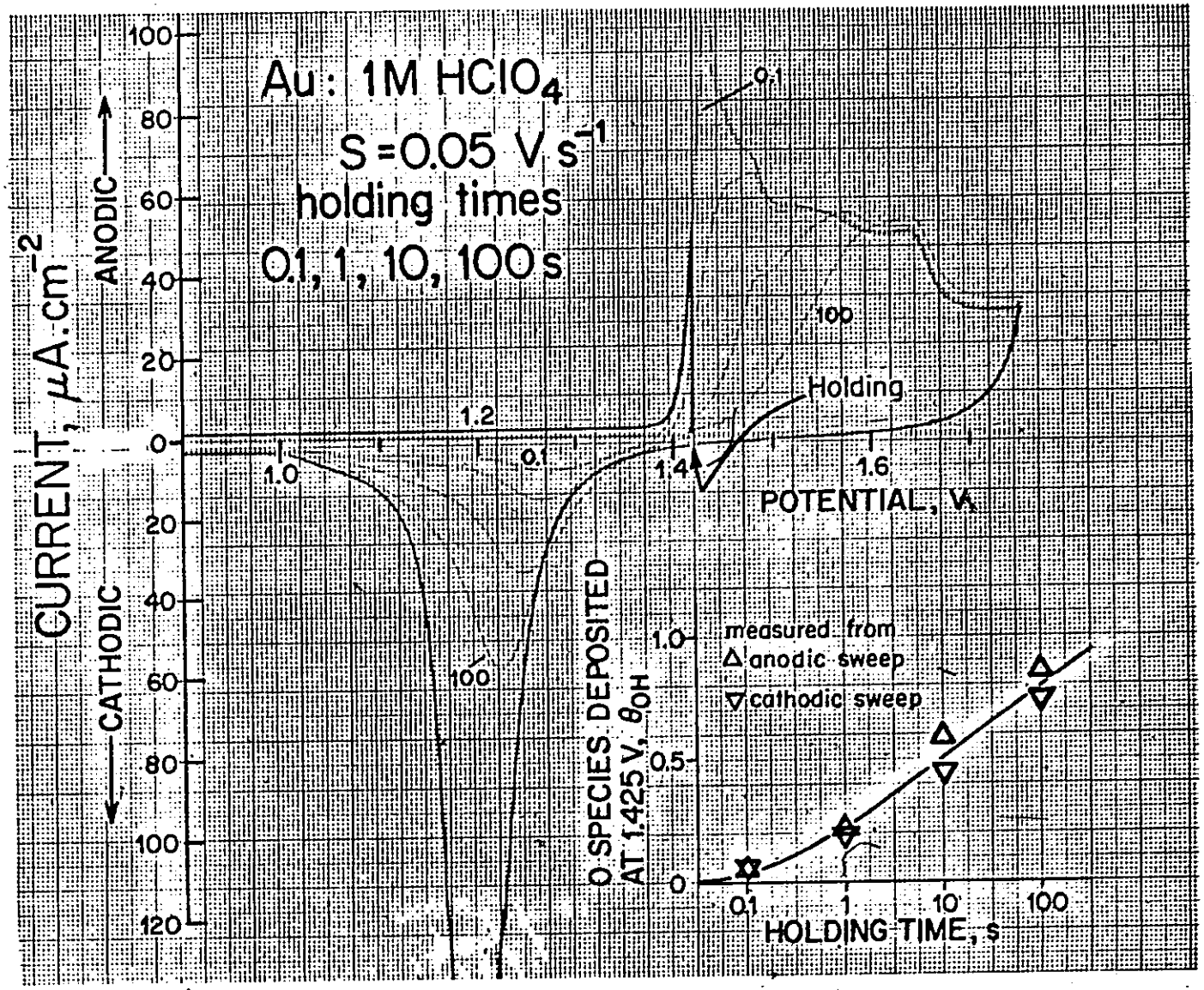

FIG 58 EFFECTS OF INTERRUPTING THE POTENTIAL SWEEP FOR 1, 10, AND 100 s AT 1.425 V ON THE SUBSEQUENT ANODIC OR CATHODIC SWEEP. INSET SHOWS THE AMOUNT OF OXIDE FORMED AS A FUNCTION OF LOG (INTERRUPTION TIME)

The charges corresponding to the various current peaks in the reduction sweep in Fig. 57 are consistent with the suggestion of Goldstein, Zalkind and Veselovskii[342] that the species reduced in peak O_{C1} at low coverages are reduced in O_{C2} at higher coverages, having undergone a transformation from one state of bonding to another in the meantime. The kinetics of transformations between the various states of the deposited species which are resolved in rapid cathodic sweeps cannot, unfortunately, be studied at constant coverage, since interrupting the sweep at a potential within the region of anodic oxidation (i.e., at a potential above about 1.4 V) discharges additional O species during the potential hold. This is illustrated in Fig. 58, which shows the potentiostatic deposition of O species after a sweep to 1.425 V, both directly by the increased charge passed in subsequent reduction sweeps, and indirectly by the smaller charge passed during resumed anodic sweeps. The charge passed during the potential hold (measured by either method) increases with the logarithm of the holding time, as found by previous authors[335,341,344]. This type of behaviour is in marked contrast to that of the UPD* of Pb on Au where the deposition current falls immediately to zero if the potential sweep is interrupted, indicating that no slow processes are continuing.

If the place-exchange processes are allowed to further equilibrate the state of the surface by either a reduction in the sweep rate (e.g. to 0.001 V s^{-1} at room temperature) or by an increase in temperature (e.g. to 365 K as in Fig. 52), only one current peak (a composite of O_{C2}, O_{C3} and O_{C4}) is clearly resolved in the cathodic current-potential profile. This is mainly O_{C2} at the lowest coverages

*Although the electrodeposition of O species at Au does not occur at potentials below 1.23V, the oxidation of Au is still effectively UPD, since the potential for significant rates of O_2 evolution was 1.55-1.65 V.

but O_{C3} (at almost exactly the same potential), and then O_{C4}, at higher coverages (Fig. 52). Since the potentials of the anodic and cathodic peaks approach one another under such conditions (Fig. 53 and Fig. 55), the initial deposition of O species gains an appearance of reversibility, although the O_{A1} and O_{C1} states are not in fact resolved (Fig. 52).

It has been pointed out Section 1.2 that the half-width of a potentiodynamic current peak can be related to the extent of interactions between the deposited particles. If a one-electron discharge process is involved, half-widths greater than about 0.09 V indicate repulsive interactions, and smaller values show attractive forces. The half-width becomes infinitely narrow as the attractive interaction parameter reaches a value of $g \approx -4$[24] (Fig. 2).

The half-width of the composite reduction peak in the cathodic sweep at an oxidized Au electrode begins to fall as the peak moves to less-positive potentials under the influence of the O_{C4} peak. In addition, the reduction current falls rapidly on the cathodic side of the $O_{C3,4}$ peak at high temperatures, espetially at low sweep rates, showing that a more stable surface compound is being formed under such conditions*. With a sweep rate of 0.05 V s^{-1}, the half-width of the composite $O_{C3,4}$ peak decreases from ca. 0.120 V at 274 K to ca. 0.040 V at 365 K. Reducing the sweep rate to 0.01 V s^{-1} decreases the half-width of $O_{C3,4}$ still further, to 0.020 V at 0.01 V s^{-1} and 365 K. Similar decreases in half-width were observed in the reduction of oxidized Pt surfaces with increasing temperature (Section 6.2.2).

*In the limiting case of the dissolution of a bulk surface compound which shows no UPD behaviour, the cathodic current will first rise rapidly as if to form a narrow peak (Tafel behaviour), but as the dissolution is completed the current will fall almost instantaneously to zero.

H is not chemisorbed on Au. Extending the cathodic limit of the sweep to potentials more negative than that of the reversible H/H_2 electrode merely produces an exponential increase in the cathodic current corresponding to the Faradaic evolution of H_2.

7.1.4 Effects of the presence of HSO_4^-, SO_4^{2-} and NO_3^- ions

During the course of experiments involving the electrodeposition of metals on Au, it was noted that the potential required to initiate the discharge of O species was always higher in the presence of sulphate* and NO_3^- ions than in $HClO_4$ solutions. Experiments in aq. $HClO_4$ starting from low concentrations showed that even the ClO_4^- ion has a small effect on the potential required to initiate the oxidation of Au. Sulphate ions, however, caused already a measurable change in the current-potential profile in 0.1M $HClO_4$ at a concentration of only 10^{-7} M, and the potential of the O_{A2} peak shifted a total of 0.045 V positively as the sulphate ion concentration was increased to 10^{-3} M (Fig. 59). This addition of sulphate ions also reduced the coverage in state O_{C2} (Fig. 59). In other experiments, the sulphate ion coverage was varied by re-oxidizing electrodes which had only been partially reduced, by reversing the cathodic sweep "within" the peak O_{C3} (Fig. 60). This altered the time during which sulphate ions could adsorb on the bare surface and, when this time was minimized, re-oxidation began at much lower potentials, more characteristic of sweeps in the absence of sulphate ions.

*The expression "sulphate ions" is used here to include both HSO_4^- and SO_4^{2-} ions and thus improve the readability of the text, since the nature of the specifically adsorbed ion species is not known.

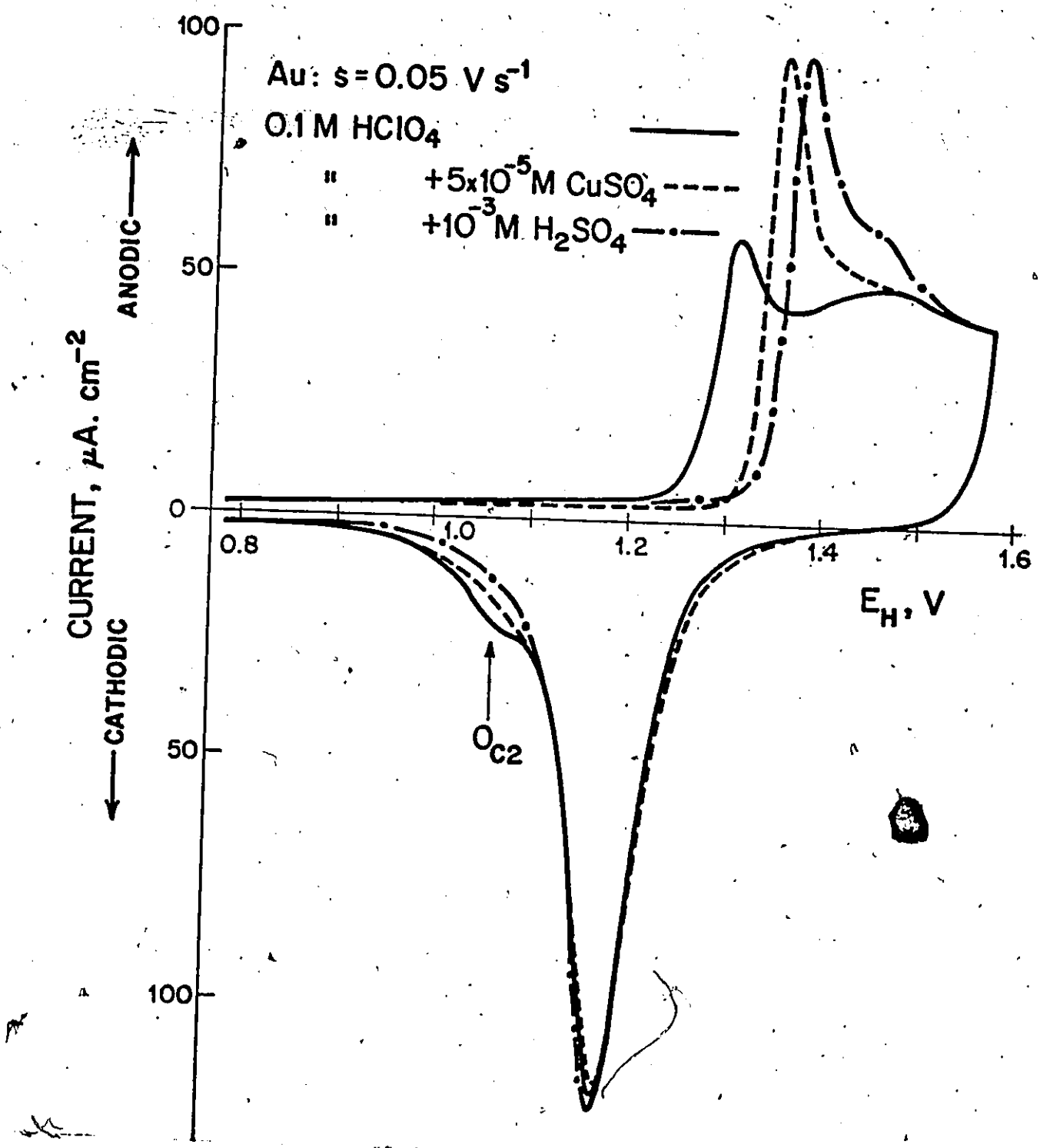

FIG 59 EFFECTS OF ADDITIONS OF $CuSO_4$ AND H_2SO_4 ON THE POTENTIODYNAMIC CURRENT-POTENTIAL PROFILE AT Au IN 0.1 M $HClO_4$

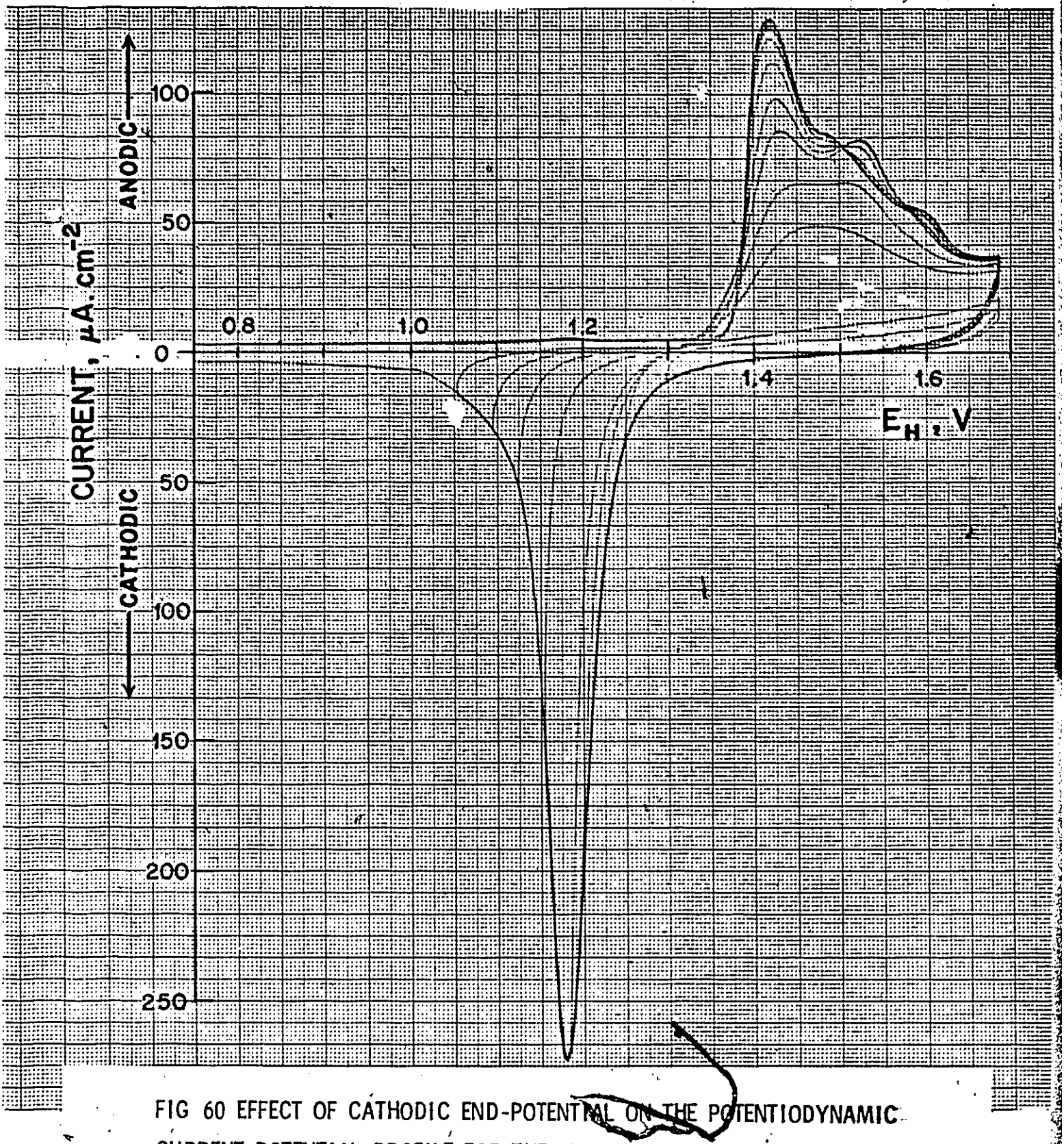

FIG 60 EFFECT OF CATHODIC END-POTENTIAL ON THE POTENTIODYNAMIC CURRENT-POTENTIAL PROFILE FOR THE ANODIC OXIDATION OF Au IN 0.5 M H_2SO_4 ($s = 0.05\ V\ s^{-1}$)

The energy (potential) required to displace specifically adsorbed sulphate ions from the positively charged Au surface increases the potential required to discharge O species to a value well positive to the original O_{A2} peak (Fig. 59). Once the sulphate ions are displaced, however there exists an overpotential for deposition in as many states as were previously blocked by the sulphate ions so that the anodic current increases rapidly. As a result, the initial oxidation peak ($O_{A2,3}$) has a higher aspect ratio than would be the case in $HClO_4$ solutions. The fact that O species are still deposited in the O_{A1} state in sulphate solutions, although oxidation does not then commence until potentials above that of the O_{A2} state in $HClO_4$, was confirmed by fast reduction sweeps. These showed that the reversible reduction peak O_{C1} arises in 0.5 M H_2SO_4 (Fig. 61) at the same potential, and with about the same maximum coverage (θ_e = 0.3) as measured in 1M $HClO_4$ (Fig. 57). It is of course to be expected that anions will affect the electrodeposition of O species much more than they will the reduction of anodically formed oxide films. The change in the profile of the O_{C1} peak in Fig. 61, from  to  with increasing coverage arises not because of increasing irreversibility in the reduction process, but because the amount of O species deposited is intially controlled by the desorption of anions, rather than by the normal potential-dependent surface reaction.

Somewhat better resolution of the oxidation states in the anodic sweep was achieved in H_2SO_4 solutions than in $HClO_4$, perhaps because the H_2SO_4 was available in slightly purer form. The optimum resolution, shown in Fig. 49, was obtained in 0.5 M H_2SO_4 with a sweep

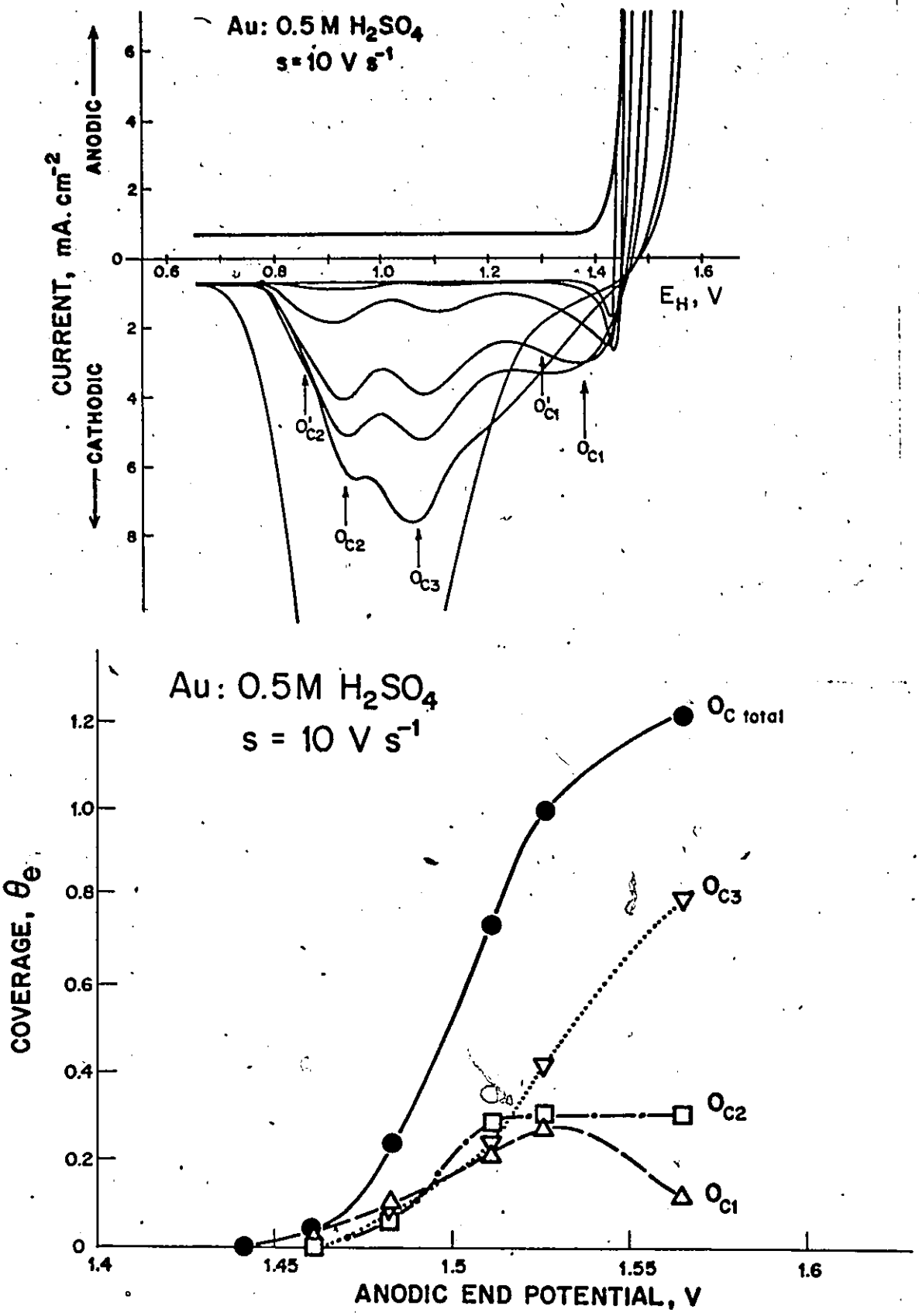

FIG 61 (Top) POTENTIODYNAMIC CURRENT-POTENTIAL PROFILES AT Au IN 0.5 M H_2SO_4 INVOLVING A SERIES OF ANODIC END-POTENTIALS (s = 10 V s^{-1}) (Bottom) ESTIMATES OF COVERAGES CORRESPONDING TO THE COMPONENT CATHODIC PEAKS

rate of 0.01 V s^{-1}. At lower sweep rates, the anodic profile gradually degenerates into only two peaks, one apparently arising from O_{A1-3} and the other from O_{A4-6}. At higher sweep rates (e.g. 5 V s^{-1}), the anodic peaks merge more together, forming a single broad peak in H_2SO_4, although in $HClO_4$ the O_{A2} peak remains distinguishable (Figs. 51 and 57(a)) with a potential below that of a broad composite oxidation peak (O_{A4-6}).

The addition of NO_3^- ions to 1M $HClO_4$ solutions produced the same changes in the anodic profile as sulphate ions (i.e. oxidation was displaced to more positive potentials, making the O_{A2} peak taller) although quantitatively less (Fig. 62). It may therefore be concluded that the specific adsorption of NO_3^- on Au is weaker than that of sulphate ions.

The above effects of specifically adsorbed anions disappear as the coverage of O species exceeds about $\theta_e = 1$ (i.e. at potentials above about 1.475 V in Fig. 59). This is shown, for instance, by the fact that the potential required to deposit a coverage of O-species corresponding to $\theta_e = 2$ is the same within ±0.015 V in 0.5 M H_2SO_4 and in 1M $HClO_4$ + 2 x 10^{-3} M NO_3^- over the entire temperature range (274-365 K).

7.2 Preliminary discussion

7.2.1 Origin of multiple anodic states

In general, at least four peaks are resolved in the anodic deposition of O species on Au. These states of O species on the surface are in addition to the reversibly reduced state O_1, shown to exist at low coverages (Figs.49,50,52,57 and 61). Such a number is too large

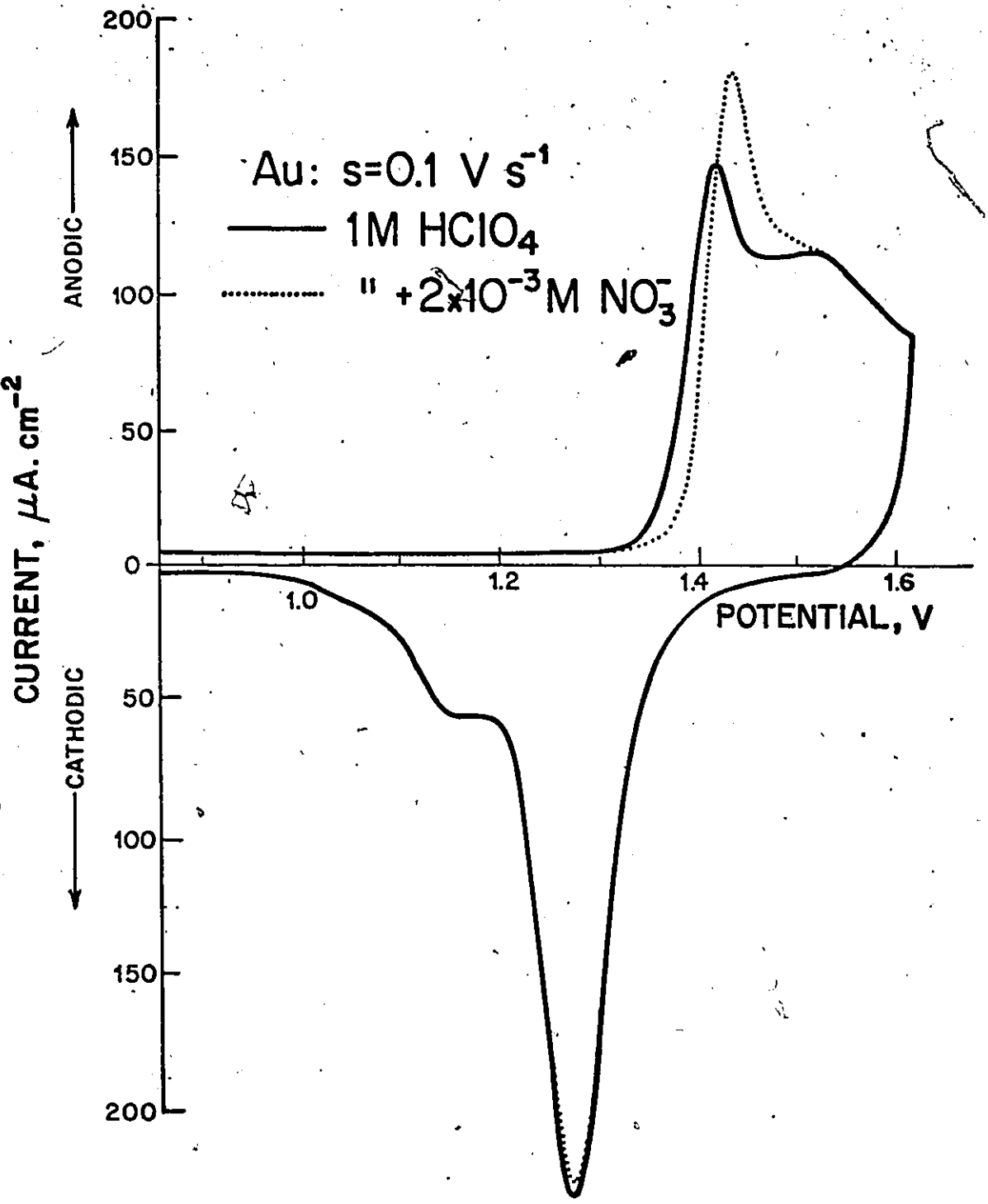

FIG 62 EFFECTS OF ADDITIONS OF $Pb(NO_3)_2$ ON THE POTENTIODYNAMIC CURRENT-POTENTIAL PROFILE AT Au IN 1 M $HClO_4$

to be explained by a sequence of increasing oxidation states of Au itself, commonly proposed in earlier work[175,318,327,330,353] as a basis for interpretation of data in which fewer states were resolved. In any case, all six anodic peaks resolved in this work appear at coverages of less than $\theta_e = 2$, and there is no reason to suggest that certain regions of the surface will be oxidized to higher states while others remain unoxidized. Whatever the nature of the multiple states observed in the anodic oxidation, more than one chemisorption "state" must correspond to a single oxidation state of Au.

A more reasonable explanation for the occurrence of multiple states of the electrodeposited species is that proposed for the origin of multiple states in the oxidation of Pt. As will be shown below, it may equally well be applied to the present results. Thus, the anodic peaks are interpreted as being associated with the formation of various (energetically different) arrays of discharged O species on (or in, see next section) the Au surface. The mutual repulsion between dipoles consisting of O species and Au atoms will maximize their separation. This array model is consistent with the fact that other workers have found slightly different current-potential profiles on different single-crystal faces of Au[353,354], since the coverage and energy of each successive array would vary with the symmetry and coordination of the bonding sites involved.

The potential required to deposit an OH group from H_2O will depend not only on the mutual separation of the chemisorbed species in the array being formed at the given coverage, but also on which of the previously-deposited species are now in sub-surface sites through place-

exchange, and which may have been further oxidized by deprotonation, as will be discussed in the next section. Thus, the anodic peaks must be related not only to the formation of repulsive arrays, but also to the energies of specific vacant sites within these arrays as modified by their local coordination by previously-deposited species.

At high temperatures and at low sweep rates, the anodic current-potential profile shows essentially only two peaks (e.g. Fig. 52), which are probably O_{A1-3} and O_{A4-6}. This profile may arise because place-exchange is so favoured under these conditions that surface arrays of dipolar O species on Au never develop and the two anodic current peaks correspond only to the deposition of two types of O species, possibly OH groups at lower potentials and O atoms at higher potentials (see Section 7.2.3).

7.2.2 Place-exchange

The hysteresis in the cyclic oxidation and reduction of Au surfaces, and the logarithmic decay of the anodic currents when an anodic sweep is interrupted[335,341,344], suggest that the post-electrochemical processes occurring during the anodic oxidation of Au are similar to those proposed in the mechanism developed for the oxidation of Pt in Section 6.2.2. Thus, some of the electrodeposited O species will exchange places with the Au atoms to which they are bound so as to form more stable "ionically bound" surface phases. Place-exchange will be assisted by (a) repulsive forces between the surface dipoles of O species bonded to the substrate and (b) the double-layer field at the electrode-solution interface. The repulsive forces will not

generally be large enough to facilitate place-exchange in the presence of the water dielectric at the interface unless the surface dipoles are closer than second-nearest neighbour atoms in the substrate surface. The field effect, however, will increase as more positive potentials are reached, and will be the main factor when place-exchange begins at very low coverages (e.g. $\theta_e < 0.1$) as at Au. The place-exchange process will be activation-controlled, so its rate at a given potential will increase with temperature, as is of course found experimentally. The rate of place-exchange at a given potential and temperature will depend on the zero-field free-energy change for the process, and the latter will depend on the lattice energy of the metal. A major difference between Au and Pt with respect to place-exchange is that Au has a much smaller lattice energy than Pt*. We would therefore expect the interactions between surface dipoles and especially the effect of the interfacial field, to give rise to place-exchange at lower coverages on Au than on Pt, and this is experimentally well-established[337]. Place-exchange introduces the possibility, and hysteresis requires, that the O species in subsurface states will be reduced directly, without undergoing a reverse place-exchange so as to return to the surface location where they were discharged.

Figure 58 shows that the coverage of O species increases with the time of holding at 1.425 V from $\theta_e < 0.1$ at the time the sweep was interrupted to $\theta_e > 0.8$. This result may be explained in the following

*This is shown, for example, by the fact that the boiling point of Au, 2670 K, is much lower than that of Pt, 4570 K.

three ways: (i) Each Au atom arriving in the surface as a result of place-exchange immediately offers a site for the discharge of another OH species and place-exchange can occur several times at each such site during the potentiostatic oxidation, (ii) Au-OH species formed by previous electrodeposition are oxidized to Au-O or Au_2O_3 by an electrochemical deprotonation[229], or (iii) the place-exchange occurring at constant potential changes the energetics of the surface so that deposition can occur at unoxidized atoms where discharge would otherwise have required a higher potential. These mechanisms will now be evaluated in turn below.

Mechanism (i) may be excluded for three reasons: (a) if place-exchange could occur several times at some sites while other sites remained bare, the charge passed in the anodic peaks should be a function of the sweep rate and temperature (i.e. of the time and energy available for place-exchange), which is not the case (Fig. 54). (b) Au atoms which have moved outside the original plane of the electrode surface as a result of place-exchange will be somewhat isolated from the bulk metal by the presence of the non-metallic O species beneath them. They will thus be less "metallic" and therefore presumably less efficient as electron acceptors in the discharge process than bare atoms elsewhere in the electrode surface where no reaction has taken place. (c) The existence of discontinuities in both ellipsometry[357] and reflectivity[358] data obtained at Au surfaces oxidized to a coverage of $\theta_e = 1$ suggests that the nature of the deposit changes at this coverage. No abrupt change would be expected in mechanism (i). It should also be mentioned that the discontinuities in the optical

data support the view that, at coverages below $\theta_e = 1$, the deposited species is OH rather than O.

Mechanism (ii) may be rejected because of the magnitude of the coverage increase during potentiostatic oxidation. The initial coverage of $\theta_e < 0.1$ could only be increased to about 0.2 or 0.3 respectively, if previously deposited Au-OH species were further oxidized during the potential hold to form Au-O or Au_2O_3 locally, whereas values exceeding $\theta_e = 0.8$ were observed experimentally.

Mechanism (iii) could arise for two reasons. Place-exchange would clearly alter the electronic properties of the surface by changing the distribution of charge on the positive ion lattice, and this could conceivably cause a local alteration in the energy of the hybrid bonding orbitals. However, a much simpler explanation is available in terms of dipole-dipole interactions. It will be energetically unfavourable to deposit another OH group near one previously deposited, because of the repulsion of like charges. (This is the cause of the formation of arrays, as discussed above). However, if the previously deposited species has undergone place-exchange, the attraction of unlike charges will increase the bond energy for deposition nearby, compared with that for a bare surface at the same potential. This would give rise to anodic peaks with a narrow half-width, as observed in the potentiodynamic oxidation of Au, particularly at high temperatures and slow sweep rates. We may therefore conclude that the rate of potentiostatic oxidation will be controlled by the rate of production of locally favourable sites for further deposition arising from place-exchange, which is itself caused by the dipole-dipole repulsion between adjacent "unrearranged"

Au-OH species at low coverages, and possibly by a Cabrera-Mott[216] type of "high-field" mechanism at high coverages[218,593].

7.2.3 Significance of the states resolved in the cathodic reduction of O species

The tendency to form dipolar surface arrays and the tendency towards place-exchange will compete at all coverages. The nature of the oxidation processes occurring at various coverages will now be reviewed as a basis for a discussion of the significance of the various peaks in the cathodic sweep profile, which is more clearly resolved at Au than at Pt.

At coverages below about $\theta_e = 0.1$, the discharged O species are sufficiently far apart (at least 3-4 atomic diameters of Au) that the dipole-dipole repulsions are relatively weak, and do not contribute to the rate of place-exchange, which is therefore low at low coverages, low temperatures and fast sweep rates. Thus the initial deposits are reduced reversibly in fast cathodic sweeps (Figs. 57(a), 61(a)), as are the initially-formed surface oxide species at Pt[229].

As the coverage exceeds about $\theta_e = 0.15$ (average separation ca. 2-3 atomic diameters of Au) with increasing potential in the anodic sweep, the quantity of O species reduced reversibly in the "unrearranged" state O_{C1} begins to fall even at high sweep rates and low temperatures. This arises for three reasons: (a) the increasingly positive end-potential (at a given sweep rate) allows more time for place-exchange during the sweep; (b) the increasing interfacial field facilitates the place-exchange; and (c) the reduced separation of the chemisorbed

species corresponding to the increased coverage also increases the rate of place-exchange. The OH groups which are now in sub-surface sites as a result of place-exchange, are bound up to 7 kcal mol^{-1} more strongly than those still on the surface, since the potential of the O_{C2} peak which is associated with their reduction is up to 0.3 V less positive than that of the O_{C1} peak. It is one of the most interesting features of the oxidation of Au that these species continue to be reduced from the O_{C2} bonding state even when the total coverage exceeds $\theta_e = 2$ and O_2 has been evolved at the surface. These species, which are deposited at the potentials of the O_{A2} peak (Figs. 58,60), possibly in the unresolved O_{A1} state, are thus thought to undergo a field-assisted transformation to a much more strongly bound state (O_{C2}) from which they cannot be reduced until almost all the subsequently deposited species have been reduced. The charge corresponding to O_{C2} appears to depend to some extent on the nature of the anions adsorbed at the electrode surface (Fig. 59).

At higher coverages, or with slower sweep rates (i.e. for longer times of equilibration of the oxide layer), O species are reduced in increasing numbers from the O_{C3} state, which has an intermediate bonding energy, about 4 kcal mol^{-1} stronger than that of O_{C1} at 274 K (Fig. 50). The fact that O_{C2} is still resolved at high coverages and low sweep rates (e.g. Fig. 49) shows that the species reduced in O_{C3} do not arise from those reduced in O_{C2} at shorter times or lower coverages. In addition, the production of the O_{C3} state through the disproportionation reaction

$$2\ Au\text{-}OH \rightarrow AuO + Au + H_2O$$

as proposed by Ferro et al.[599] is excluded since this would provide sites for reversible deposition at all coverages, whereas the coverage in the reversible reduction peak (O_{C1}) decreases (producing an equal coverage of species reduced in O_{C2}[342]) as the peak O_{C3} begins to appear (Figs. 57(b),60(b)).

The appearance of the O_{C3} peak in the cathodic sweep seems to correspond to the start of deposition in state O_{A4} during the anodic sweep. At higher coverages (i.e. with deposition in state O_{A6} during the anodic sweep), the O_{C4} peak appears in the cathodic sweep. Unlike the cathodic peaks involved in the reduction of oxide at lower coverages, whose potentials are independent of coverage, the O_{C4} peak potential moves to less-positive potentials as the coverage increases, showing that the bonding energy of the deposit increases over this range of coverages. This is confirmed by the fact that the half-widths of composite $O_{C3,4}$ peaks decrease with increasing coverage (Figs. 50,52), increasing temperature (Figs. 50,52), and increasing time of potentiostatic holding (Fig. 58 and reference 337), as higher coverages are reduced from the O_{C4} state. The two-dimensional "oxide" thus behaves more like a three-dimensional bulk compound (which would be reduced in an infinitely narrow peak) as it equilibrates, and as the coverage approaches $\theta_e = 2$. The species bound in state O_{C4} cannot arise from those reduced from state O_{C3} at lower coverages, since at high temperatures the O_{C4} state is less-strongly bound than O_{C3} (Fig. 52). The increase in bonding energy of the O_{C4} state with increasing coverage thus probably relates to the increased coherence of the two-dimensional "oxide" lattice as its last vacant sites are filled. If, as was

suggested on p.192, peaks O_{A4-6} correspond to a 2-electron discharge process depositing atomic O on the surface, then the reduction peaks O_{C3} and O_{C4} will relate to the reduction of atomic O rather than that of hydroxyl groups. Both these peaks, but perhaps especially O_{C3}, may be expected to be augmented by reduction currents from O atoms which were deposited as hydroxyl groups in peaks $O_{A2,3}$, but which have since become deprotonated.

In addition to the four predominant states of the deposited species described above (O_{C1}, O_{C2}, O_{C3}, O_{C4}), three other types of reduction process were observed. All of them have also been observed in the reduction of oxidized Pt electrodes. In the first case, a shoulder $O_{C1'}$ appears on the cathodic side of peak O_{C1} as peak O_{C2} begins to develop (Figs. 50,57,61), representing species which are bound about 1 kcal more strongly than those reduced reversibly in O_{C1}. It may be that place-exchange modifies the energetics of the surface for some distance from the place-exchange site so that discharged species which have not undergone place-exchange become more strongly bound if they are near a place-exchange site (they would then be reduced in peak $O_{C1'}$) than otherwise (reduced in O_{C1}).

Secondly, a small peak $O_{C2'}$ has been detected as a shoulder on the cathodic side of O_{C2}. It may possibly be a transformation product of species reduced in $O_{C1'}$ at lower coverages.

The O_{C5} region (Figs. 49,50,58) probably has a different signfficance, since the currents in it are almost independent of potential and coverage, i.e., are essentially only time-dependent. If place-exchange were able to occur more than once at some sites at the

high coverages involved, then the O species which had effectively diffused into the bulk electrode would have to diffuse back to the surface again before they could be reduced. In the terminology proposed by Schuldiner[200-202], these species are "dermasorbed". The existence of such a mechanism is to some extent corroborated by Fig. 54, which shows that the oxide charge passed at the current minimum between peak O_{A6} and O_2 evolution does increase at the highest temperature studied, suggesting that although the amount of O species on and in the surface remains constant, increased bulk diffusion rates at the high temperature allow more O species to penetrate the bulk Au lattice. Under these conditions, the microscopic processes of place-exchange begin to give way to field-assisted diffusion[218,593] as a mechanism for oxide film growth.

It is surely significant that the total number of cathodic peaks resolved (O_{C1}, $O_{C1'}$, O_{C3}, O_{C4}, O_{C2}, $O_{C2'}$) is the same as the total number of anodic peaks (O_{A1}, O_{A2}, O_{A3}, O_{A4}, O_{A5}, O_{A6}). The additional cathodic peak is due to "alloying". It is to be hoped that future workers may clarify the relationships between individual anodic and cathodic peaks.

7.2.3.1 Summary of reaction scheme for the surface oxidation and reduction processes

On the basis of these data, the following reaction scheme may be tentatively proposed. Peaks O_{A1} and perhaps O_{A2} represent the deposition of OH groups at coverages low enough for no nearest-neighbour Au sites to be occupied. (i.e. $\theta_e < 0.25$ on Au(100), or $\theta_e < 0.33$ on

Au(111)). The combination of dipole-dipole repulsion and field-assisted place-exchange transfers alternate ones of these species into strongly-bound sub-surface states. The reduction peak subsequently involved will show a corresponding change from O_{C1} to O_{C2}. The place-exchange reaction will bring Au atoms to sites above the original surface, and adjacent atoms will offer increasingly strongly-bonding sites as the coverage of place-exchanged OH-Au species increases, as evidenced by the narrowness of the oxidation peaks O_{A3}, O_{A4}, O_{A5}. The potentials of deposition in states O_{A4-6} are sufficiently high for the deposit to be in the form of atomic O. Peak O_{C3} will probably represent the reduction of O atoms, both those deposited in O_{A4} and those produced by the deprotonation of hydroxyl groups deposited in states O_{A2-3}. At higher coverages, place-exchange will cause the oxide to begin to behave more like a two-dimensional phase, as shown by the movement of the O_{C4} peak to less-positive potentials. The existence of repulsive forces leading to place-exchange of O atoms deposited in state O_{A6} is shown by the low aspect ratio of the O_{A6} peak.

7.2.4 The coverage at which O_2 evolution begins

The saddle point in the current-potential profile preceding O_2 evolution at Au occurs at a coverage of exactly $\theta_e = 2$, over a wide range of temperatures and sweep rates (Section 7.1.2). Because of the nature of a symmetrical saddle point the O_2 evolution currents may be expected to be about half the current at that point, i.e. the evolution of O_2 will in fact begin at a somewhat lower coverage. The contribution of O_2 evolution to the total anodic charge cannot be accurately estimated

as the existence of hysteresis and the consequent oxidation during the cathodic sweep prevent accurate calculation of the charge corresponding to reduced oxide.

Although O_2 evolution is thermodynamically possible over the full range of potentials at which O species are deposited if the activity of O_2 at the electrode surface is unity, the overvoltage of this process evidently drops as a critical coverage is reached. Since this coverage is unaffected by the sweep rate or temperature, it may be concluded that the deposit on which O_2 begins to evolve is uniform in thickness, rather than locally nucleated and thickened.

There would be no reason for such a discontinuity in the properties of the film if oxidation were to occur by the deposition of two successive monolayers of Au-OH (Fig. 63(a)), particularly if place-exchange continued to occur at coverages around $\theta_e = 2$. Fig. 63(d) shows that a coverage of $\theta_e = 1.5$ may be reached when place-exchange has only occurred at every alternate site. The provision of further sites for OH deposition on a $\theta_e = 1.5$ film would, however, be expected to require considerably more lattice distortion energy than before, since the "ionic oxide" lattice resulting from place-exchange would be locally complete and would tend to resist the passage of similarly charged ions past one another. It would therefore be expected that the deposition potential would increase abruptly at a coverage of $\theta_e = 1.5$, which is not found experimentally (Fig. 54).

The model developed in the previous section would lead to a structure shown schematically in Fig. 63(c) as O_2 begins to evolve. The measured coverage would then be $\theta_e = 1.75$ on Au(100).

(a) $\theta_e = 2$; $2\,AuOH$

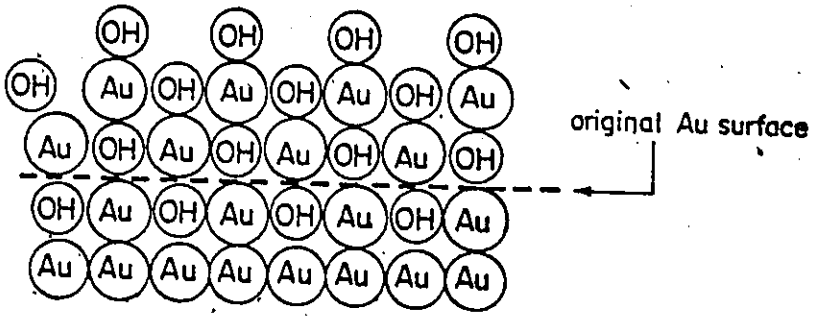

(b) $\theta_e = .2$; AuO

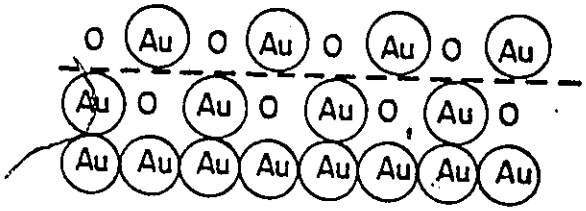

(c) $\theta_e = 1.75$; $(AuO)_3 . AuOH$

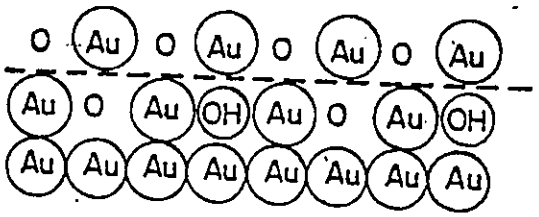

(d) $\theta_e = 1.5$; $Au_2(OH)_3$

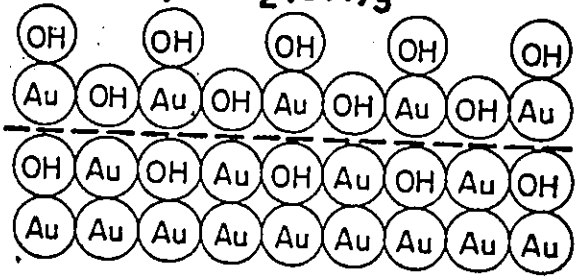

FIG 63 SCHEMATIC REPRESENTATION OF VARIOUS SURFACE "OXIDES" AT Au ILLUSTRATING POSSIBLE OXIDATION MECHANISMS

The coverage is lower than $\theta_e = 2$(Fig.63(b)) because the reversibly deposited species, reduced in O_{C1} at low coverages, which transforms to state O_{C2} remains in that state even though the rest of the surface may have been strongly oxidized (since the O_{C2} charge and potential appear invariant with coverage). Were the O_2 peak to represent the reduction of the same species as would be deposited later, i.e., O atoms at higher potentials, there is no reason that it should appear at a different potential in the cathodic sweep. The model developed in the last Section implies (i) that O_2 evolution occurs at a lower overvoltage than the electrodeposition of O species at Au "atoms" arriving in the surface by place-exchange (i.e., these Au atoms are "demetallized"), and (ii) that Au-OH species are not deprotonated after place-exchange. Although stable Au(II) compounds do not occur in the bulk state, the Au atoms in the surface as a result of place-exchange would presumably provide sites for the deposition of O atoms at higher potentials while O_2 is being evolved. This would lead to the formation of a monolayer of an Au_2O_3-type surface phase, since any sub-surface OH-Au species would presumably be deprotonated at sufficiently high potentials. It has previously been mentioned that it is the consensus of earlier work that the passivating film on Au electrodes is indeed Au_2O_3[312-3,325,329-31,334].

Whatever the details of the reaction pathway, however, it appears that the onset of O_2 evolution at coverages slightly below $\theta_e = 2$ is related to the unavailability of "metallic" Au atoms in the electrode surface. O atoms discharged on this largely ionic surface tend to recombine rapidly and evolve O_2. The thickening of the oxide occurs slowly as a parallel reaction by the normal field-assisted diffusion process for oxide film growth.

7.2.5 Influence of specifically adsorbed anions

Specifically adsorbed anions affect oxidation processes at Au electrodes in the same way as at Pt. Nitrate and particularly sulphate ions increase the energy required to initiate the deposition of O species (Figs. 59,60,62). This has the effect of making the low-coverage, reversibly deposited state O_1 difficult to resolve[337], except at fast sweep rates. Since independent quantitative data on the specific adsorption of these ions at Au is not available, explanations for their effects must remain speculative.

The increase in energy required for the discharge of O species caused by the anions shows that the latter are present at appreciable coverage and are only slowly displaced from Au surfaces as a result of oxidation. The anion effects decrease both with decreasing sweep rate and increasing temperature, under which conditions the displacement of the anions from the surface by H_2O molecules would be favoured. Although specifically adsorbed anions increase the energy required to initiate surface oxidation at Au, they do not appear to affect the distribution of the O species among the bonding states resolved in the anodic sweep (Section 7.1.4). This presumably shows that the discharge reaction cannot occur until the specifically adsorbed anions are displaced from the discharge site. The reduced coverage of the species corresponding to the O_{C2} state in the presence of specifically adsorbed anions is not at present understood. Perhaps the specifically adsorbed anions affect the maximum coverage of OH groups which may be deposited (and place-exchanged) before the electrode potential is sufficiently high for O atoms to be generated.

CHAPTER 8

ELECTRODEPOSITION OF Cu ON Pt

8.1 Results

8.1.1 Calculation of Cu coverages

The real surface area (A/cm^2) of Pt electrodes was measured by the charge required to deposit a monolayer of H atoms (Q_H, μC), i.e.

$$A = \frac{Q_H}{220}$$

The coverage of Cu was then calculated on the assumption that the electrodeposition or electrodissolution of Cu will require the passage of two electrons per Cu atom deposited, i.e.

$$\theta_{Cu} = \frac{q_{Cu}}{2x220A} \quad \text{or, more simply} \quad \theta_{Cu} = \frac{q_{Cu}}{2Q_H}$$

Cu "coverages" will be expressed in this way whether or not $\theta < 1$, without implying that all the Cu atoms are touching Pt atoms in a single layer at all coverages.

8.1.2 General features

UPD of Cu on Pt is reversible at elevated temperatures (Fig. 64(a)) and at very slow sweep rates (Fig. 65). The first four bonding states, in order of increasing coverage (Cu_{1-4}), have closely spaced bonding energies, but state Cu_5 represents a distinctly weaker bond. Under some conditions, a sixth bonding state (Cu_6) is resolved with an energy just greater than that in bulk Cu metal.

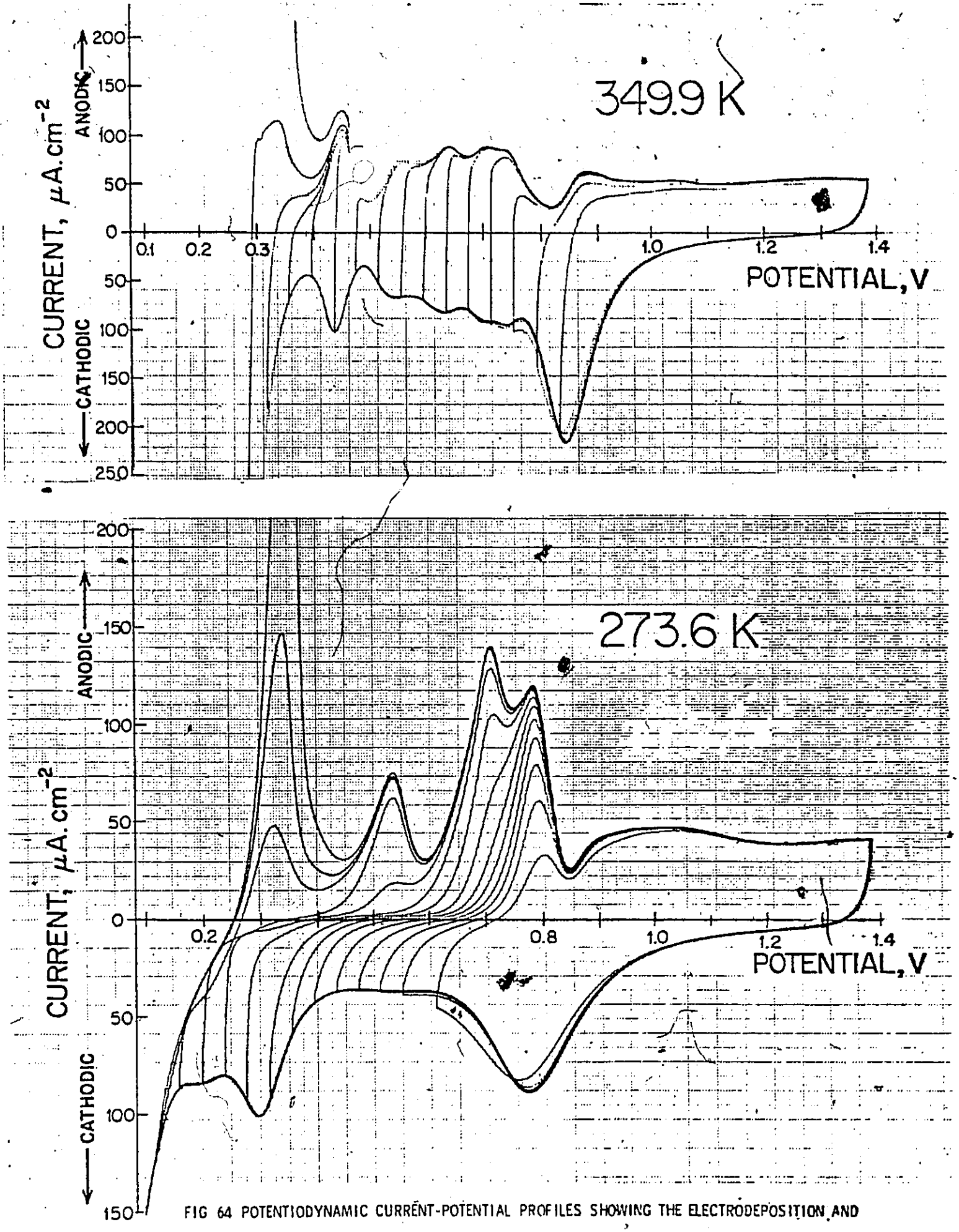

FIG 64 POTENTIODYNAMIC CURRENT-POTENTIAL PROFILES SHOWING THE ELECTRODEPOSITION AND OXIDATION OF Cu AT Pt AND INVOLVING A SERIES OF CATHODIC END-POTENTIALS. ELECTROLYTE 1 M $HClO_4$ + 0.01 M $CuSO_4$; REFERENCE ELECTRODE Pt/H_2 IN 1 M $HClO_4$; $s = 0.05\ V\ s^{-1}$.

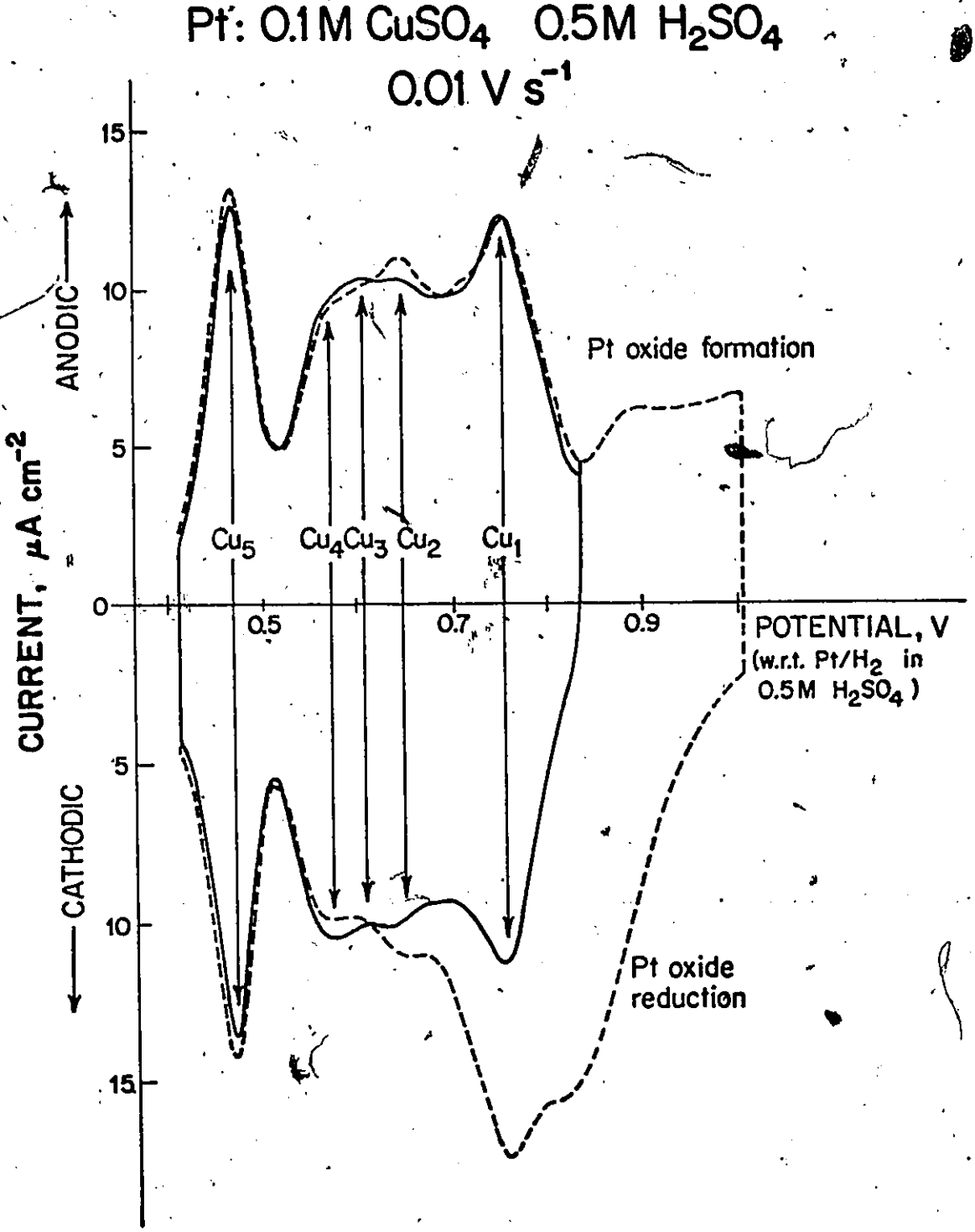

FIG 65 POTENTIODYNAMIC CURRENT-POTENTIAL PROFILES FOR THE REVERSIBLE UPD OF Cu AT Pt. DOTTED LINE SHOWS SWEEP TO A MORE POSITIVE END-POTENTIAL INVOLVING OXIDATION OF THE Pt SUBSTRATE ($s = 0.05\ V\ s^{-1}$)

The bonding energies in states Cu_{1-4} are so closely spaced (within a total range of 6.9 kcal) that it is difficult to estimate accurately the coverages associated with the individual states. In a series of measurements at room temperature, the following data were, however, obtained:

Bonding states	θ_{Cu}
$Cu_{A1} + Cu_{A2}$	0.54
$Cu_{A1} + Cu_{A2} + Cu_{A3}$	0.74
$Cu_{A1} + Cu_{A2} + Cu_{A3} + Cu_{A4}$	1.01
$Cu_{A1} + Cu_{A2} + Cu_{A3} + Cu_{A4} + Cu_{A5}$	1.33

The total Cu deposition charge passed before deposition of bulk Cu was equivalent to an apparent coverage of $\theta_{Cu} = 1.5$.

The combined charge in states Cu_{A1-4}, and the charge in state Cu_{A5} are shown over a wide range of temperature in Fig.66. In both cases, the amount of UPD is outstandingly constant. Slight differences between the coverages shown in Fig.66 and those tabulated above probably reflect errors in the estimation of the area of the Pt electrode via the H charge.

When the direction of a potential sweep depositing Cu at elevated temperature is reversed at a series of underpotentials (Fig.64(a)), the current simply changes sign, without any evidence of kinetic irreversibility (at 0.05 V s^{-1}) or of hysteresis. At slow sweep rates in concentrated $CuSO_4$ solution the UPD is also reversible at room temperature (Fig.65), like that of H on Pt. If, however, the anodic

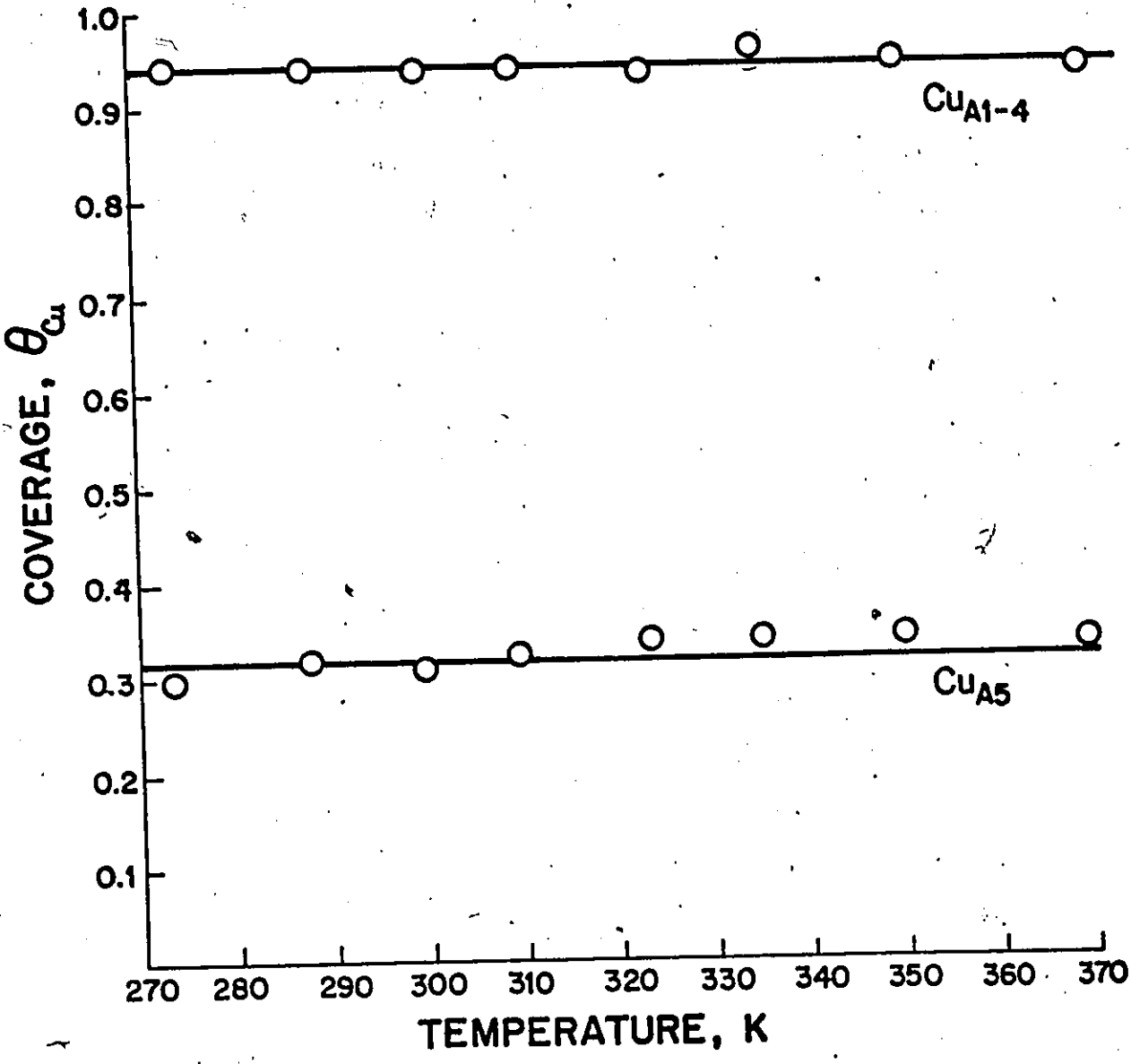

FIG 66 COVERAGES OF UNDERPOTENTIALLY DEPOSITED Cu CORRESPONDING TO THE TOTAL OF THE CURRENT PEAKS Cu_{A1-4} AND TO Cu_{A5} AS A FUNCTION OF TEMPERATURE IN 1 M $HClO_4$ + 0.01 M $CuSO_4$ SOLUTION ($s = 0.05\ V\ s^{-1}$)

end-potential is increased beyond the value required to dissolve the Cu, additional cathodic currents appear during Cu deposition arising from the reduction of O species discharged during the anodic sweep. This diminishes the resolution of the states of underpotentially deposited Cu at low coverages (Fig. 65).

8.1.3 Cathodic processes

Resolution of the individual states of Cu deposited in the cathodic sweep is also lost in dilute solutions of Cu^{2+}, at low temperatures and at high sweep rates. However, the anodic processes remain essentially reversible under these conditions, as shown for example, by the fact that the i_p/s values* for the anodic current peaks are constant for $s \leq 20$ V s^{-1}, while the cathodic peaks shift with sweep rate at above 0.2 V s^{-1}.

The irreversibility of Cu deposition at low temperatures is shown in Fig.64(b). Similar effects appear if the Cu concentration is reduced or the sweep rate increased. It must be emphasized that the rate-determining step under such conditions is not simply diffusion of Cu^{2+} ions from the bulk of the solution to the electrode, since the extent of diffusion control is $\neq$ 10%. Studies of the effect of solution stirring begun at various points in the potential cycle show that although the cathodic UPD currents are increased by stirring, the electrodissolution from underpotential states is not affected.

The development of the current-potential profile as the Cu^{2+} concentration of the solution is increased (Fig.67) suggests that the more

*i_p = peak current; s = sweep rate

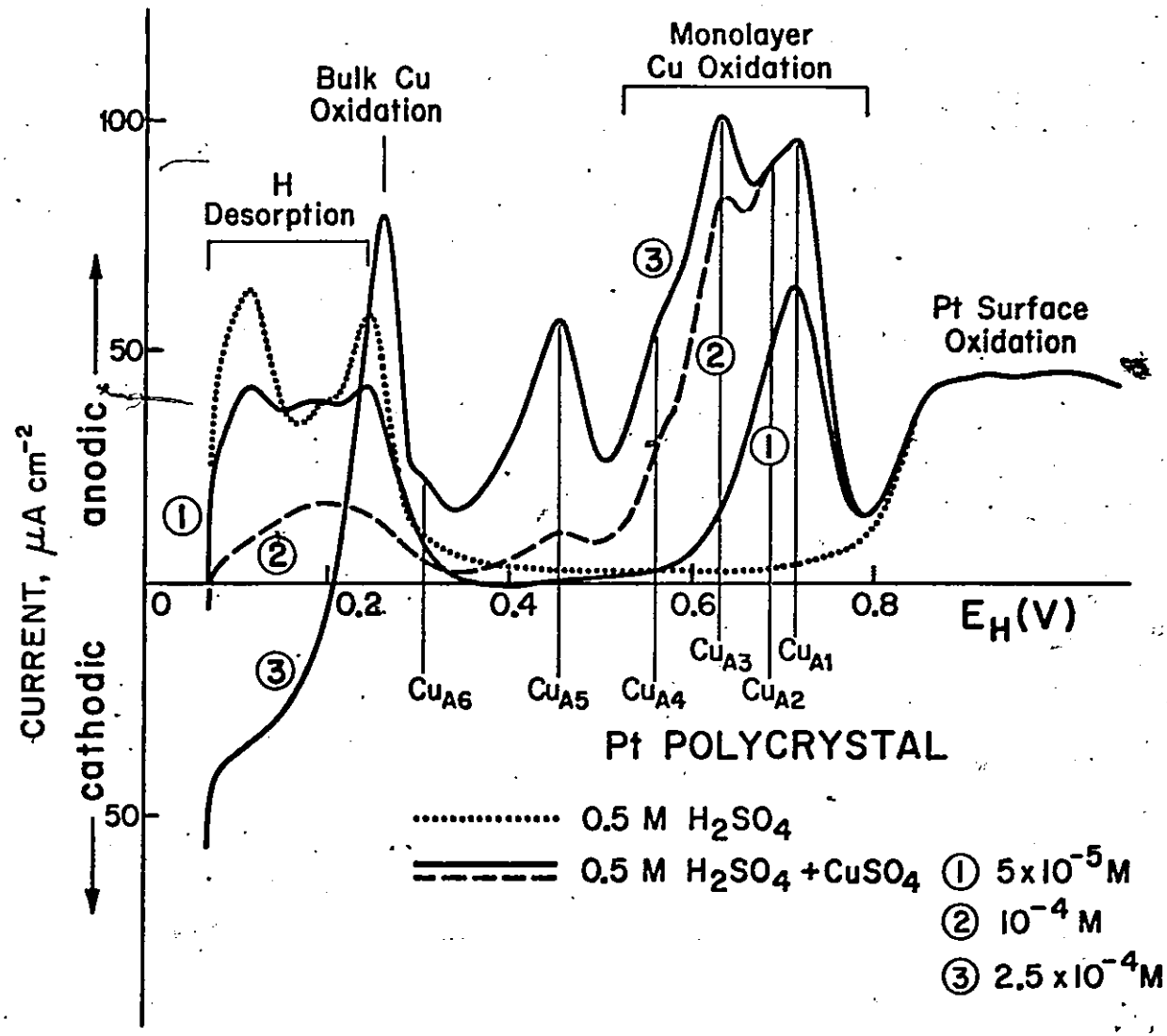

FIG 67 POTENTIODYNAMIC CURRENT-POTENTIAL PROFILES FOR THE OXIDATION OF Cu UNDERPOTENTIALLY DEPOSITED AT Pt FROM SOLUTIONS OF DIFFERENT Cu CONCENTRATION (REFERENCE ELECTRODE Pt/H_2 IN 0.5 M H_2SO_4 ; $s = 0.05\ V\ s^{-1}$)

strongly bound states are completely occupied before deposition commences in the more weakly bound states. (Individual sites will obviously be filled in order of decreasing energy under all conditions). Experiments in which the amounts of Cu deposited potentiostatically (measured by fast anodic sweeps) increased with time to a value characteristic of the deposition potential confirmed that the bonding states have definite maximal coverages.

8.1.4 Deposition of bulk Cu

If the cathodic deposition sweep is continued to potentials less positive than 0.2 V, no further "structure" of current peaks is observed. The discharge current merely rises to a constant, diffusion-controlled value, which is maintained as bulk Cu deposits become visible on the Pt. Bubbles of H_2 are finally evolved at about -0.5 V. The corresponding anodic dissolution sweeps show that only the currents ionizing Cu from states more weakly bound than Cu_6 (i.e. those associated with the deposition of bulk Cu), increase with the amount of Cu deposited. Thus (reversible) deposition at potentials cathodic to those of the Cu_{C6} state is effectively on bulk Cu metal, while deposition at more positive potentials (UPD) produces states which have definite coverage limits, with bonding energies strengthened (relative to Cu on bulk Cu) by the presence of the Pt substrate.

8.1.5 Anodic processes

The kinetic limitations described above are not observed in the anodic processes. With a sweep rate of 0.05 V s^{-1} in 10^{-2} M

$Cu(ClO_4)_2$ + 1 M $HClO_4$, the electrodissolution peak potentials are independent of temperature at above 323 K (Fig.68). At the temperature is lowered from 323 K, however, the Cu-Pt bond energies increase, peak Cu_{A5} develops a lower aspect ratio, peak Cu_{A3} becomes more pronounced, and the separate resolution of peaks Cu_{A2}, Cu_{A3} and Cu_{A4} is gradually lost (Figs.64(b),67). A similar loss of resolution of the anodic peaks is observed as the sweep rate is increased. At sweep rates below 0.1 V s^{-1} in 0.1 M $CuSO_4$ + 0.5 M H_2SO_4, the peak potentials corresponding to states Cu_{A1} to Cu_{A5} are constant (Fig.69). At faster sweep rates, however, states Cu_{A2}, Cu_{A3} and Cu_{A4} are not separately resolved, and appear as a single peak in both the anodic and cathodic sweep. [In these experiments the anodic and cathodic sweep rates were equal, and the end-potentials were adjusted to the limits of the underpotential reactions of Cu at the sweep rate concerned]. Since the individual current peaks overlap considerably and only the apparent peaks of their sum are recorded, it is not possible to distinguish whether the change in the anodic profile with sweep rate relates to changes in the reversible peak potentials of the underpotential bonding states, or to a redistribution of the Cu among states of constant energy.

8.1.6 Effects of specifically adsorbed anions

The UPD of Cu on Pt is altered to some extent by the nature of the anions present, particularly by those which are strongly specifically adsorbed. The current-potential profiles in $Cu(ClO_4)_2$ - $HClO_4$ and $CuSO_4$ - H_2SO_4 solutions are essentially similar. When small

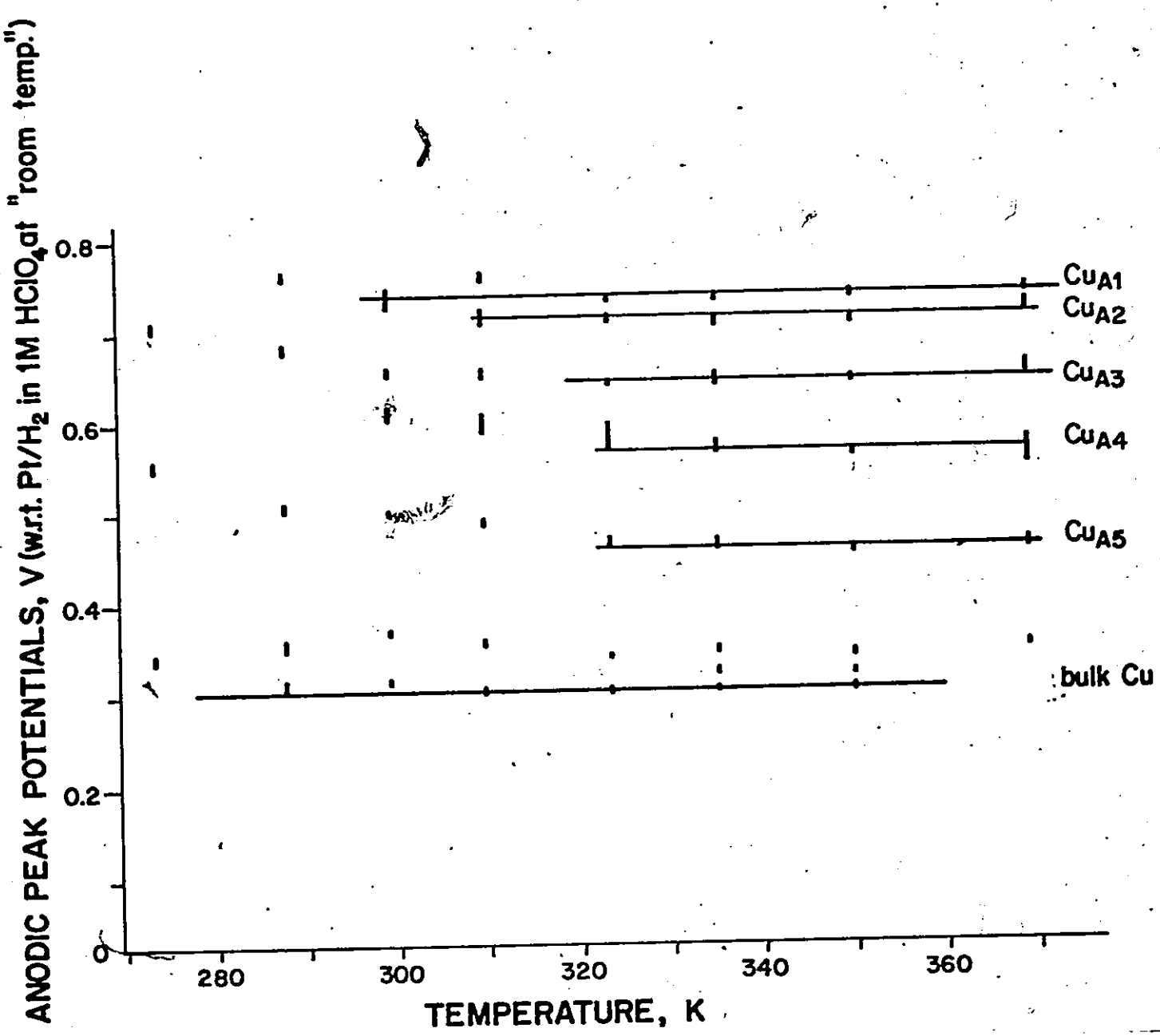

FIG 68 POTENTIALS OF THE CURRENT PEAKS IN THE OXIDATION OF Cu UNDERPOTENTIALLY DEPOSITED AT Pt FROM 1 M $HClO_4$ + 0.01 M $CuSO_4$ SOLUTIONS AT DIFFERENT TEMPERATURES ($s = 0.05\ V\ s^{-1}$)

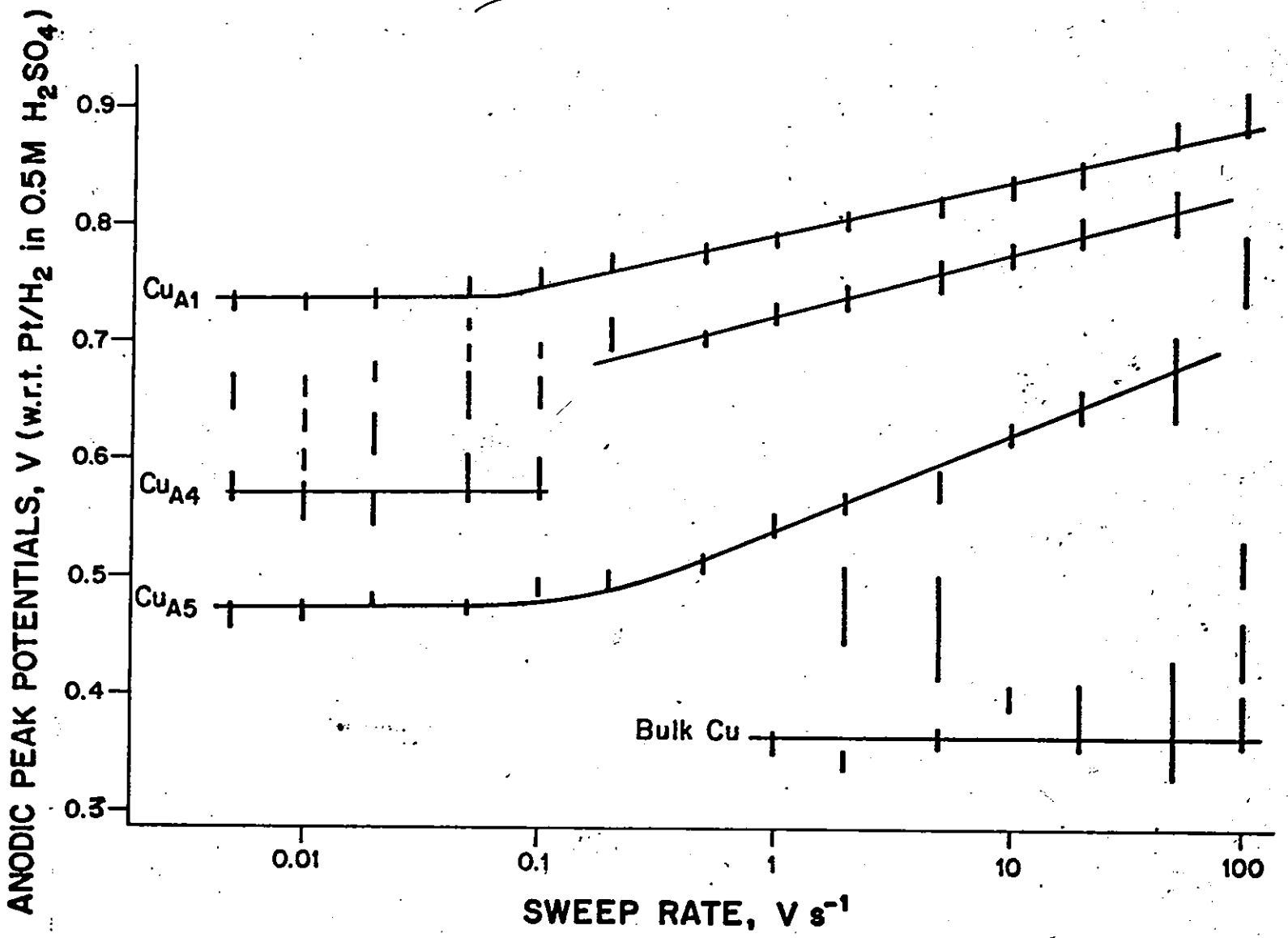

FIG 69 POTENTIALS OF THE PREDOMINANT ANODIC PEAKS IN THE OXIDATION OF Cu AT Pt AS A FUNCTION OF THE SWEEP RATE IN 0.5 M H_2SO_4 +0.1 M $CuSO_4$ SOLUTION

amounts of NaCl are added, however, a considerable redistribution of the Cu among the bonding states is observed (Fig. 70). The Cl^- also inhibits the discharge of O species, which improves the resolution of the low-coverage Cu peaks, and an apparent fifth desorption peak is observed in the anodic dissolution of the Cu monolayer (Fig. 70).

8.1.7 Relation between deposition of Cu and states of co-deposited H

Figure 71 shows that the charge associated with the electrodissolution of Cu from Pt as Cu^{2+} is exactly twice the corresponding charge for H deposition. The Cu was deposited potentiostatically, and the measurements made from a subsequent cathodic-anodic sweep at 20 V s^{-1}. The linearity of this plot and its expected slope give indirect confirmation that the Cu is deposited in a fully-discharged state. In sweeps at 20 V s^{-1}, considerable amounts of Cu are dissolved from state Cu_{A5} (e.g. $\theta_{Cu_{A5}} = 0.15$) while the coverage in states Cu_{A1-4} is still well below a monolayer (e.g. $\theta_{Cu_{A1-4}} \leq 0.8$).

It is important to note that the maximum (total) coverage in states Cu_{A1-4} in a slow sweep corresponds to a 1:1 epitaxial monolayer of Cu on Pt atoms; under fast-sweep conditions the monolayer charge includes that passed in the Cu_{A5} peak as well as that in the Cu_{A1-4} peaks, the latter being then relatively smaller than under slow-sweep conditions.

As Cu is electrodeposited on Pt in increasing quantities, the coverage in the different H adsorption states is affected in different ways (Fig. 72). Low coverages of Cu increase the coverage

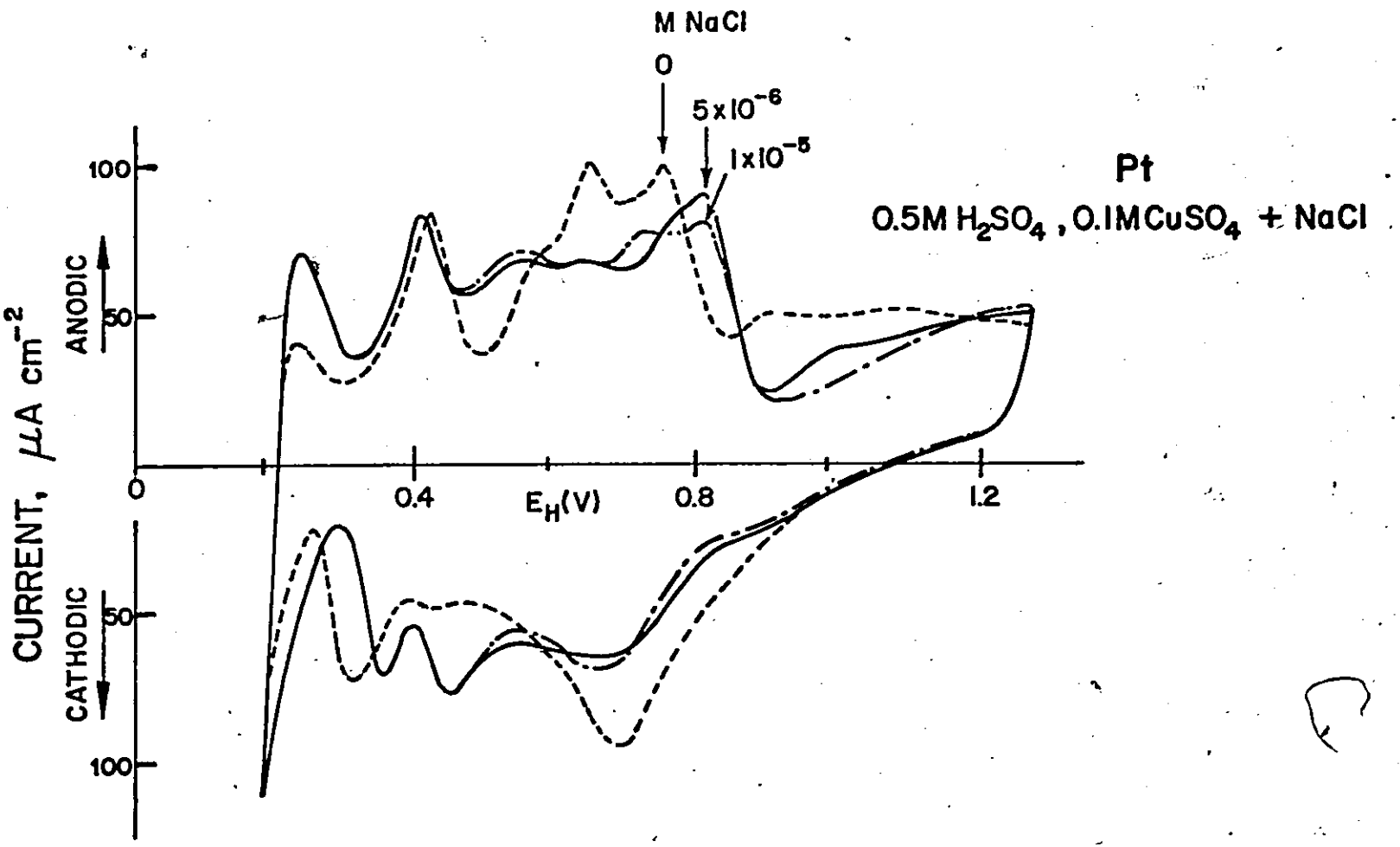

FIG 70 THE EFFECT OF Cl^- IONS ON THE POTENTIODYNAMIC CURRENT-POTENTIAL PROFILE FOR THE UPD OF Cu AT Pt (REFERENCE ELECTRODE, Pt / H_2 IN 0.5 M H_2SO_4 ; $s = 0.05\ V\ s^{-1}$)

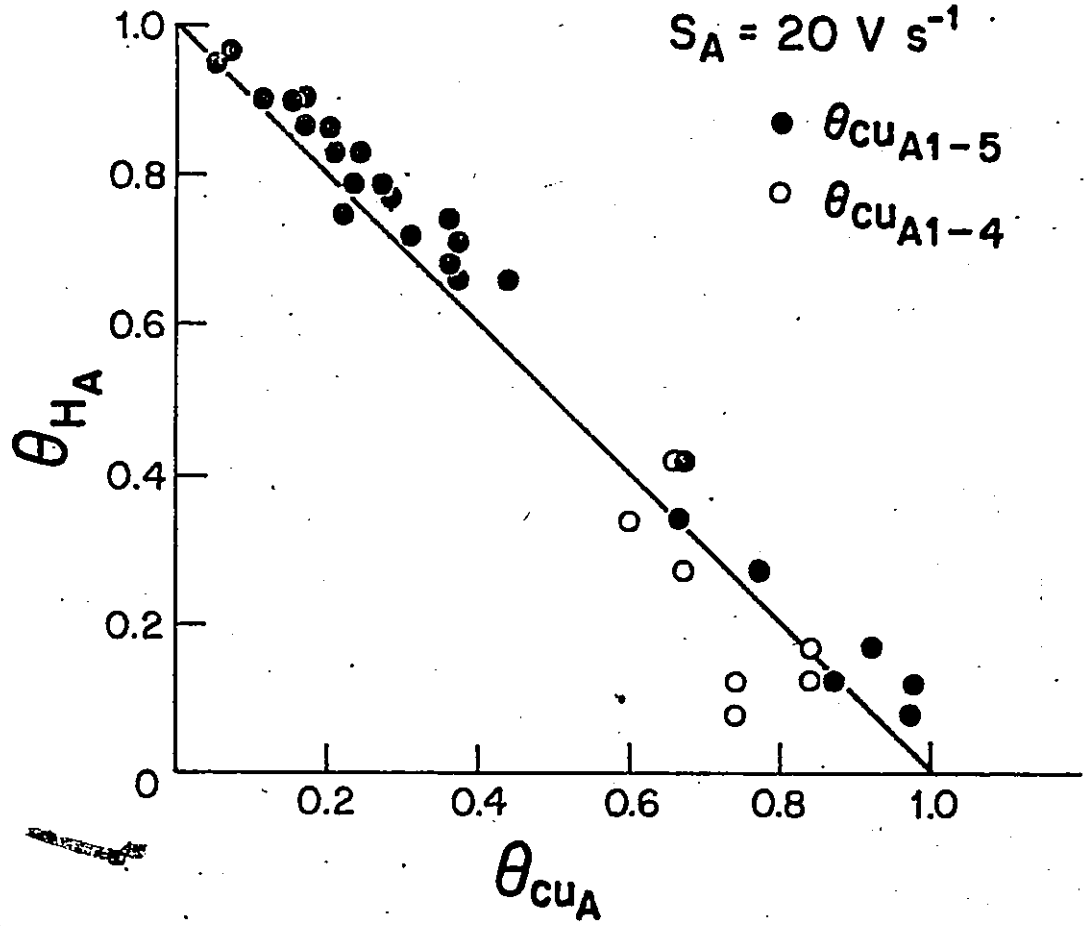

FIG 71 COVERAGE OF UNDERPOTENTIALLY DEPOSITED H AS A FUNCTION OF THE COVERAGE OF Cu PREVIOUSLY UNDERPOTENTIALLY DEPOSITED AT Pt FROM A 0.5 M H_2SO_4 SOLUTION

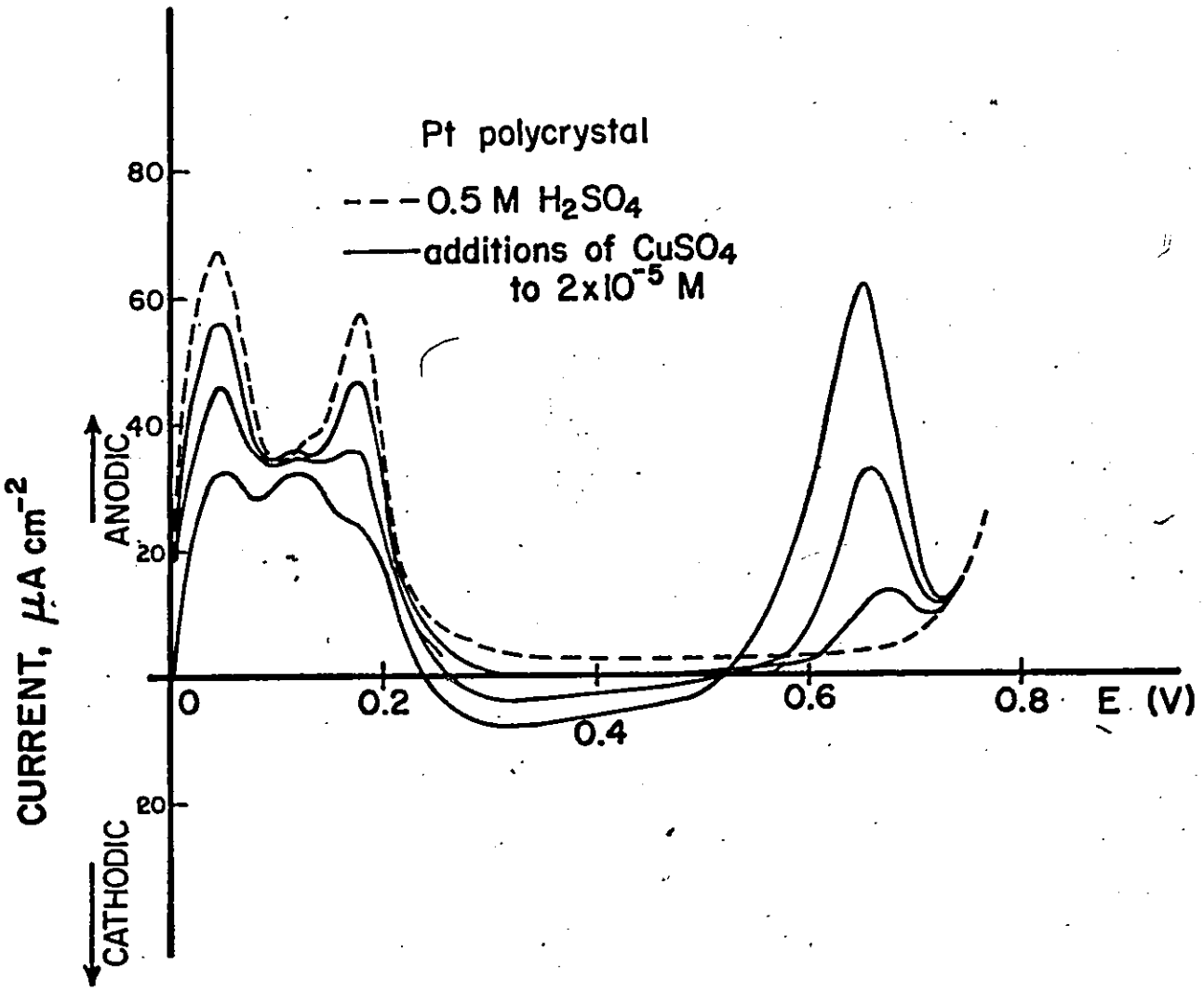

FIG 72 SELECTIVE BLOCKING OF BONDING STATES FOR UNDERPOTENTIALLY DEPOSITED H AT Pt BY UNDERPOTENTIALLY DEPOSITED Cu OXIDIZED FROM A SINGLE STATE (REFERENCE ELECTRODE Pt/H_2 IN 0.5 M H_2SO_4 ; $s = 0.05\ V\ s^{-1}$)

in state H_3 but decrease those in states H_2 and $H_{4,5}$. Resolution of the H states is lost at higher Cu coverages, although it appears that the major portion of the H is still bound in state H_3. [The constancy of the O-species reduction charge under these conditions shows that the changes in the H profile were not due to the co-adsorption of impurities during the potentiostatic Cu deposition].

8.2 Preliminary discussion

8.2.1 The component processes

In previous studies of the UPD of Cu on Pt,[372-374,379,381] only three bonding states (Cu_1, Cu_3 and Cu_5) were discussed. The present work shows that Cu may be underpotentially deposited in at least six bonding states having distinctly different energies. When an electrodeposited Cu monolayer is dissolved anodically at a slow sweep rate (e.g. 0.05 V s^{-1}), only states Cu_{A1-4} are revealed. However, if the dissolution is conducted in a fast sweep, significant amounts of Cu are dissolved in peak Cu_{A5} (Fig.71) before the more strongly bound Cu in the "monolayer" states Cu_{A1-4} is dissolved. Thus the charge corresponding to the Cu_{A1-4} states under these conditions is less than at lower sweep rates. This suggests that at any one time, all the electrodeposited Cu atoms are bound in the same state, and that at slow sweep rates they will all have sufficient time to rearrange themselves on the surface into the successive bonding states Cu_{A1-4} (with corresponding dissolution or discharge currents to bring the coverage to the new equilibrium values) as the potential is changed. The non-equilibrium distribution of the Cu

among the bonding states observed at fast sweep rates could then be explained in terms of the inability of the Cu atoms to move between the states as fast as the potential was being changed.

8.2.2 Relation of the cathodic current-potential profile to kinetics of discharge of Cu^{2+} ions

It was noted in Section 1.5.1.8 that the discharge of Cu^{2+} ions occurs in two successive one-electron-transfer steps. The exchange current of the Cu^{+}/Cu equilibrium is always at least 1000 times greater than that of the Cu^{2+}/Cu^{+} equilibrium[405], so the rate-limiting step in the discharge process will be $Cu^{2+} + e \rightarrow Cu^{+}$. This reaction will occur across the double-layer, at a rate determined by the electrode potential, the concentration of Cu^{2+} in the bulk solution, and the rate at which Cu^{2+} can diffuse to the reaction site.

The difference in the exchange currents places a restraint on the rate of discharge of Cu^{2+} ions, but not on the rate of the reverse reaction, since the Cu^{+} ions produced in the first (fast) step are likely to remain there long enough to lose a second electron before diffusing away into the solution. The different kinetic limitations of the cathodic and anodic processes at bulk Cu were first described by Bockris and co-workers[399-401]. They are reflected in the present work by the difference of the sweep-rate dependence of the current peak potentials. This was about 0.12 V per decade of sweep rate for the deposition of sub-monolayer quantities, but only about 0.05 V per decade for the corresponding anodic processes (Fig. 69).

Cu begins to electrodeposit on Pt at potentials of about

0.8 V, and Pourbaix's data[397] show that the equilibrium Cu^+/Cu^{2+} ratio at 0.8 V is about 10^{-10}. Although the experiments described here give no indication of the state of equilibrium of the various ionic processes under the dynamic conditions involved, it seems very plausible that the diminution in Cu discharge currents at low Cu^{2+} concentrations, at low temperatures and at fast sweep rates is primarily due to the limited rate of production of Cu^+ ions in the $Cu^{2+} + e \rightarrow Cu^+$ redox reaction.

As Cu deposition proceeds, the Cu^+ originally present in the double-layer will be discharged, so that further deposition must involve the slow $Cu^{2+} \rightarrow Cu^+$ reaction, and this will give the appearance of hysteresis (Fig.64(b)). Under such conditions (e.g. Figs.64(b),73) the net cathodic current is frequently independent of potential in a range between the oxide reduction peak and the first resolved Cu deposition peak. This has been described as a limiting-current region[374] but such terminology is misleading, since although the net cathodic current is constant as Cu deposition begins, the component of the current arising from Pt oxide reduction falls at less positive potentials, so the cathodic currents due to Cu deposition are in fact increasing smoothly in this range towards the first resolved Cu deposition peak (at about 0.3 V in Fig. 64(b)).

The rate control under such conditions will be complex. At higher potentials, the production of Cu^+ ions will be slow and both potential- and time-dependent. At less positive potentials, however, the production of Cu^+ will increase rapidly with decreasing potential and it will

also become increasingly possible to deposit Cu directly from Cu^{2+} ions. The equilibria concerned are[608]:

$$Cu^{2+} + e \rightleftharpoons Cu^{+} \qquad E^\circ = 0.153 + 0.059 \log \frac{[Cu^{2+}]}{[Cu^{+}]}$$

$$Cu^{+} + e \rightleftharpoons Cu \qquad E^\circ = 0.520 + 0.059 \log [Cu^{+}]$$

$$Cu^{2+} + 2e \rightleftharpoons Cu \qquad E^\circ = 0.337 + 0.030 \log [Cu^{2+}]$$

Although the resolution of individual cathodic deposition states is largely lost under these conditions, the existence of a peak corresponding to deposition in states Cu_{C1-4} and a smaller peak corresponding to Cu_{C5} (Figs.64(b),73) shows that the Cu atoms are still being deposited in states having definite coverage limitations.

At higher temperatures, the rate of production of Cu^{+} ions increases, so the deposition is reversible at all coverages (Fig.64(a)). The deposition may also be made reversible at room temperature if the availability of Cu^{+} at the electrode is increased by increasing the Cu^{2+} concentration and decreasing the sweep rate (Fig.65). Finally, the slow production of Cu^{+} from Cu^{2+} accounts for the continued UPD currents observed when cathodic sweeps are interrupted for controlled periods of time under conditions where the anodic but not the cathodic processes are reversible.

As the temperature is raised, the charge corresponding to the dissolution of bulk Cu becomes less than that involved in its deposition. This may arise either because the chemical stripping of bulk Cu ($Cu + Cu^{2+} + 2Cu^{+}$)[408,409] has a considerable temperature

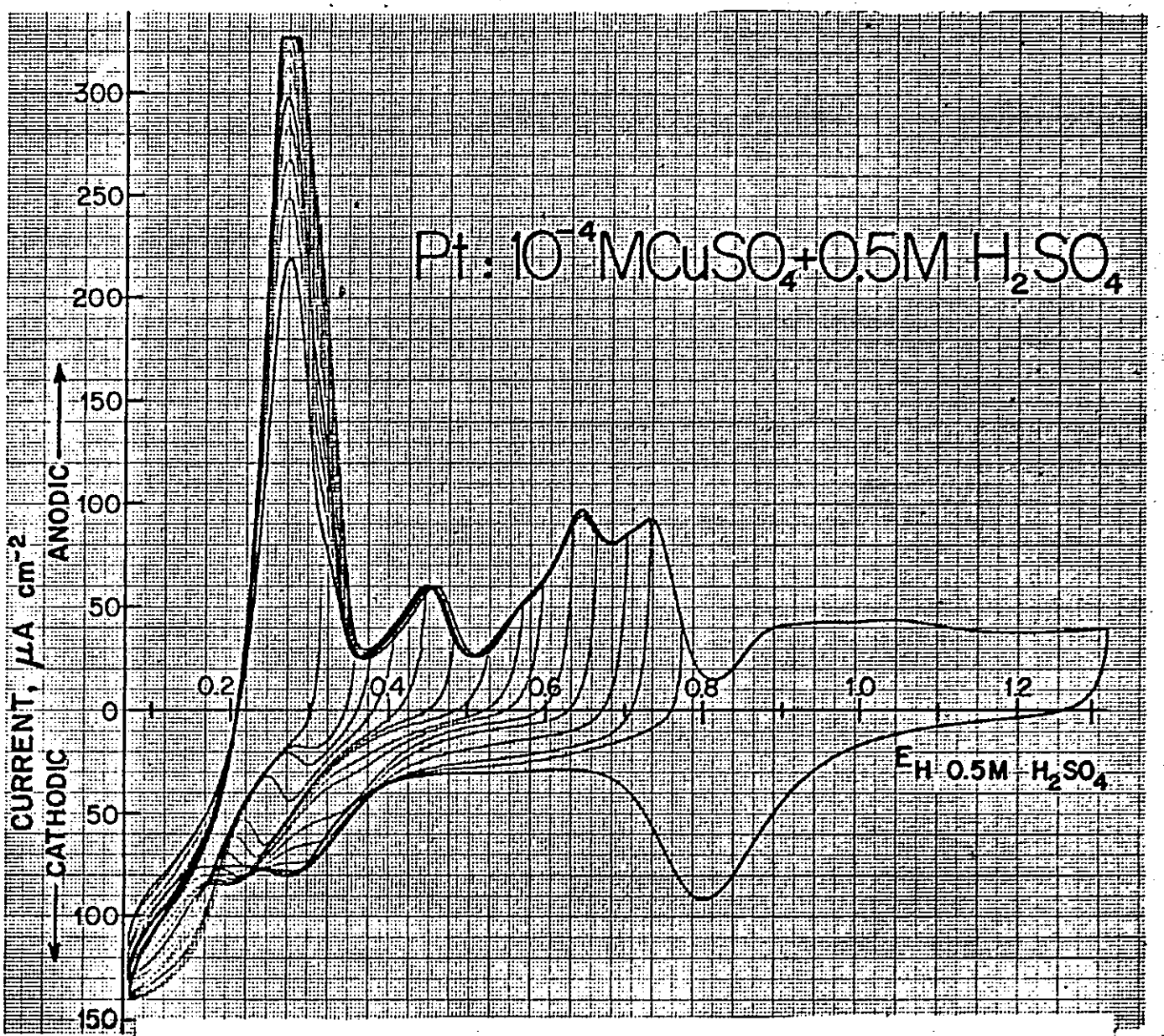

FIG 73 POTENTIODYNAMIC UPD OF Cu AT Pt INVOLVING A SERIES OF CATHODIC END-POTENTIALS IN 10^{-4} M $CuSO_4$ + 0.5 M H_2SO_4 (REFERENCE ELECTRODE Pt / H_2 IN 0.5 M H_2SO_4 ; $s = 0.05\ V\ s^{-1}$)

coefficient, or because some of the Cu^+ ions formed in the first stage of the anodic dissolution are able to diffuse away from the electrode before losing their second electron (slow process).

8.2.3 Deposition at "coverages" exceeding $\theta = 1$

The energy of the states corresponding to monolayer coverage (Cu_{1-4}) is quite distinct from that of the Cu_5 bonding state, which is itself distinct from the bulk Cu-Cu bond (Figs. 64,65,73). The accuracy with which the total charge in the Cu_{1-4} peaks corresponds to a monolayer coverage (Fig.66) strongly suggests that at coverages below $\theta_{Cu} = 1$ all the Cu atoms will occupy identically coordinated sites on the electrode surface, i.e. in 1:1 epitaxy with Pt atoms. At higher coverages, however, the Cu atoms can no longer all occupy identical sites. Subsequently deposited atoms may either bond in interstitial positions between Cu atoms already on the surface, or else displace these atoms from their epitaxial positions so as to approach the Pt surface more closely.

In the latter mechanism the maximum coverage of Cu in a single plane parallel to the surface is that of a close-packed monolayer of Cu atoms (having no unique epitaxial relationship to Pt atoms). Since Cu atoms are substantially smaller than Pt atoms, a close-packed monolayer of them would have a "coverage" of $\theta_{Cu} = 1.49$ in a (100) lattice plane and $\theta_{Cu} = 1.29$ in a (111) lattice plane. Experimentally, bulk Cu deposition is observed at about $\theta_{Cu} = 1.5$. At coverages above $\theta_{Cu} = 1$, each discharged Cu atom will touch at least three previously deposited Cu

atoms, pushing them aside from their 1:1 epitaxial bonding positions. With further deposition, the number of Cu atoms touching one another would increase rapidly until they formed a complete close-packed layer, and the development of metallic properties in the electrodeposit (deposition of "bulk" Cu) could be associated with the completion of this close-packed layer. It is clear from Figs. 64(a) and 65 that when hysteresis is absent, the Cu_5 state is completely filled before metallic properties are developed. The fact that in fast (20 V s^{-1}) sweeps the Cu_{A5} state appears while the coverage in states Cu_{A1-4} is still only about $\theta_{Cu} = 0.5$, although at slow (0.05 V s^{-1}) sweep rates the states are filled one by one in order of decreasing energy (Fig.64(a)), strongly suggests that the rearrangement between epitaxial and close-packed chemisorbed states may be a relatively slow process.

In the alternative mechanism, originally proposed by Breiter[379], Cu atoms discharged at coverages below $\theta_{Cu} = 1$ remain at the same sites, and subsequently discharged Cu atoms will lie between and slightly above them. Breiter suggested that local nucleii of deposited Cu would thicken until they reached a critical size at which they would develop metallic properties. It is evident, however, that states Cu_5 and Cu_6 cannot be associated with local second and third layers of Cu atoms, since by its nature UPD must be uniform on an electrode surface (atoms deposited at random or in regular arrays across the whole surface), and the coverage in state Cu_5 is much less than a monolayer (Fig. 66). In addition, the number of nucleii formed, and hence the deposition charge required to build nucleii of a critical

size on the original monolayer, would be expected to be temperature-dependent, which is experimentally not the case (Fig. 66).

In an experiment where Cu was discharged on to an electrode on which varying amounts of Cu were already present (Fig. 73), it is clear from the bunching together of the current-potential curves that there are three essentially different types of bonding states: Cu_{1-4}, Cu_5, and (Cu_6 and Cu_{bulk}). State Cu_5 could, according to Breiter,[379] represent the formation of patches of a second layer of Cu atoms, some of which (statistically) become large enough to have metallic properties, but the physical reality of state Cu_6 (which Breiter did not observe) is not clear. There is apparently no direct experimental data available on the persistence of epitaxy in Cu-deposition systems, although it is known that Cu deposits are of uniform thickness to at least $\theta_{Cu} = 1$ on C[375], and to about $\theta_{Cu} \approx 2$ on Ag[394].

8.2.4 Alloying

Breiter[389] concluded that since the amount of Cu that could be dissolved from Cu films on Pt electrodes was independent of the (galvanostatic) anodic current between 20 mA and 2 A, deposited Cu did not diffuse into the Pt. However, since his electrode had an area of about 16,000 cm^2 ($q_{H_A} = 3.6C$), the current densities involved were only about half those for the anodic monolayer peaks involved in the present potentiodynamic studies with a sweep rate of 0.05 V s^{-1}. Thus, the possibility of alloying which is reversible at the sweep rates studied here cannot be excluded.

8.2.5 Effect of competing adsorbates on the bonding of Cu

Changing the supporting electrolyte solution from H_2SO_4 to $HClO_4$, and adding NaCl, confirmed the result of Degeiso and Rogers[368] that the effect of anions on the UPD of Cu increases in the order $ClO_4^- < SO_4^{2-} < Cl^-$. The main effect of anions is an apparent redistribution of deposited Cu atoms among the bonding energy states available. The total coverage over all the various states is, however, not changed. The appearance of a fifth current peak within the profile (Cu_{A1-4}) for desorption of the final monolayer of Cu (Fig.70) may possibly be an artefact due to the addition of currents from closely-spaced, overlapping peaks, or alternatively the distribution of Cu among the bonding states in the absence of Cl^- may obscure the presence of the fifth monolayer state under normal conditions. The present results do not allow a distinction to be made between these two possibilities. Cl^- ions also increase the potential range corresponding to the electrodissolution of the Cu monolayer. This might arise from changes in the bond energies of the various states, or from increased repulsive interaction or reduced attractive interaction between electrodeposited Cu atoms, or both.

8.2.6 Effects of electrodeposited Cu atoms on the bonding of H

Although small numbers of Cu atoms (e.g. $\theta_{Cu} = 0.2$) are deposited in a single bonding state at all sweep rates, they prevent the adsorption of H atoms in at least two or three states (Figs.67,72). Two explanations of this result are possible. In the first, all the electrodeposited H atoms would at any given time be in identical states (i.e. at identical sites), and would normally all transform to subsequent

states (sites) - with electrodissolution or deposition as required to achieve the equilibrium coverage - as the potential was changed. However, the relatively larger Cu atoms, located according to their own coverage (which will be essentially constant in the potential range of H deposition) will prohibit the access of H atoms to some sites where they would otherwise be stably bonded at certain coverages. The only other explanation is that the multiple chemisorption states do not correspond to any specific bonding coordination or location, but instead arise from more complex quantum mechanical interactions between deposits and the substrate involving delocalized bonding states, in such a way that the bonding of one species perturbs the bonding states subsequently available to other species.

CHAPTER 9

THE ELECTRODEPOSITION OF Cu ON Au

9.1 Results

9.1.1 Determination of Cu coverage

The real area of Au electrodes was calculated according to the method of Michri, Pschenichnikov and Burshtein[585], as discussed in Section 7.1.2. Cu coverages were then calculated on the assumption[412,413] that Cu is deposited in a fully discharged state, i.e. two electrons are passed per Cu^{2+} ion discharged. The Cu coverage is then expressed as

$$\theta_{Cu} = \frac{q_{Cu}}{2x200xA}$$

where q_{Cu} μC is the integrated deposition or dissolution charge, the real electrode area is A cm^2, and the passage of one electron per surface atom on polycrystalline Au involves a charge of 200 μC cm^{-2} (see page 182).

9.1.2 General features of the potentiodynamic current-potential profile

A typical current-potential profile at Au in $Cu(ClO_4)_2$ - $HClO_4$ solution is shown in Fig.74. The Cu coverage reaches about $\theta_{Cu} = 0.75$ when Faradaic (coverage-independent) electrodeposition begins. What was thought by previous workers[410-412] to be a single

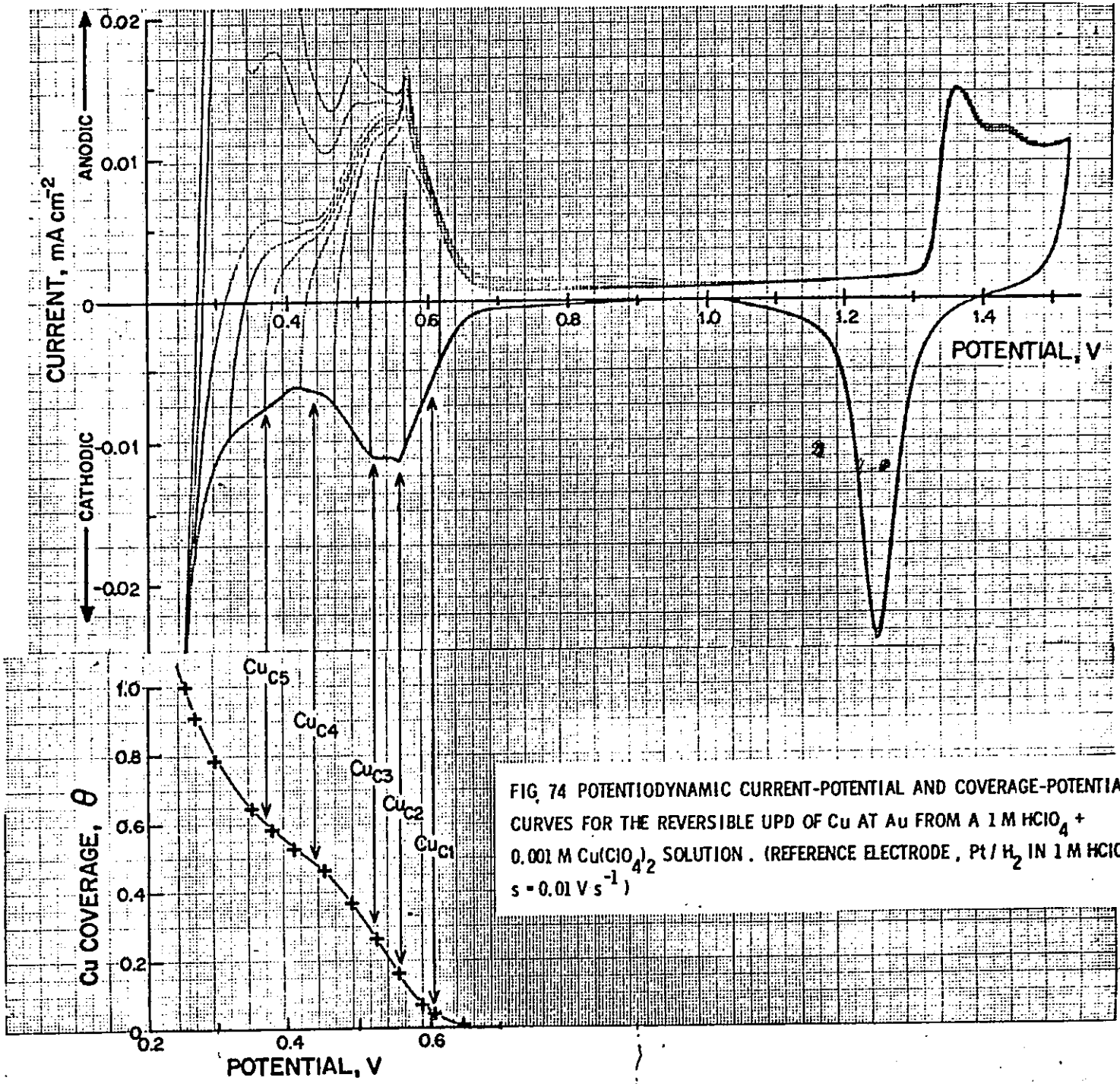

FIG. 74 POTENTIODYNAMIC CURRENT-POTENTIAL AND COVERAGE-POTENTIAL CURVES FOR THE REVERSIBLE UPD OF Cu AT Au FROM A 1 M $HClO_4$ + 0.001 M $Cu(ClO_4)_2$ SOLUTION. (REFERENCE ELECTRODE, Pt/H_2 IN 1 M $HClO_4$; $s = 0.01\ V\ s^{-1}$)

UPD peak in the potential range 0.65 to 0.40 V* is evidently (Fig.74) at least four component current peaks, with a combined coverage of about $\theta_{Cu} = 0.5$.

The UPD is only reversible (anodic and cathodic currents exactly equal) in state Cu_{C1}. As the coverage exceeds about $\theta_{Cu} = 0.1$, the bonding state represented by the sharp "spike" peak Cu_{C2} begins to appear. Since the current peaks of the state Cu_2 normally protrude very little beyond the surrounding current envelope, it is difficult to estimate its coverage with any accuracy. It is almost certainly less than 0.1, and the half-width of the peak is less than 0.04 V, possibly much less.

The interruption of very slow (0.001 V s^{-1}) potential sweeps shows that the Cu_2 peaks represent a normal deposition process rather than an abrupt transformation. Holding the potential 0.013 V cathodic to the Cu_{A2} peak for 30s reduces the peak current by about 7% whereas holding -.025V cathodic for 10 and 100s reduces it by only about 4% and 6% respectively. Such results show that the Cu_2 process is not time-dependent, but only potential-dependent.

If the deposition sweep is continued to potentials cathodic to the current minimum following peak Cu_{C4}, one further deposition state (Cu_{C5}) is observed before Tafel-type electrodeposition begins. The electrodissolution profile then shows a peak corresponding to the removal of bulk Cu as well as the Cu_{A5} peak, (Fig.75). Additional

*Potentials were measured to a Pt/H_2 electrode in a cell compartment to which the Cu salt had not been added. This reference electrode was maintained at room temperature in all the experiments.

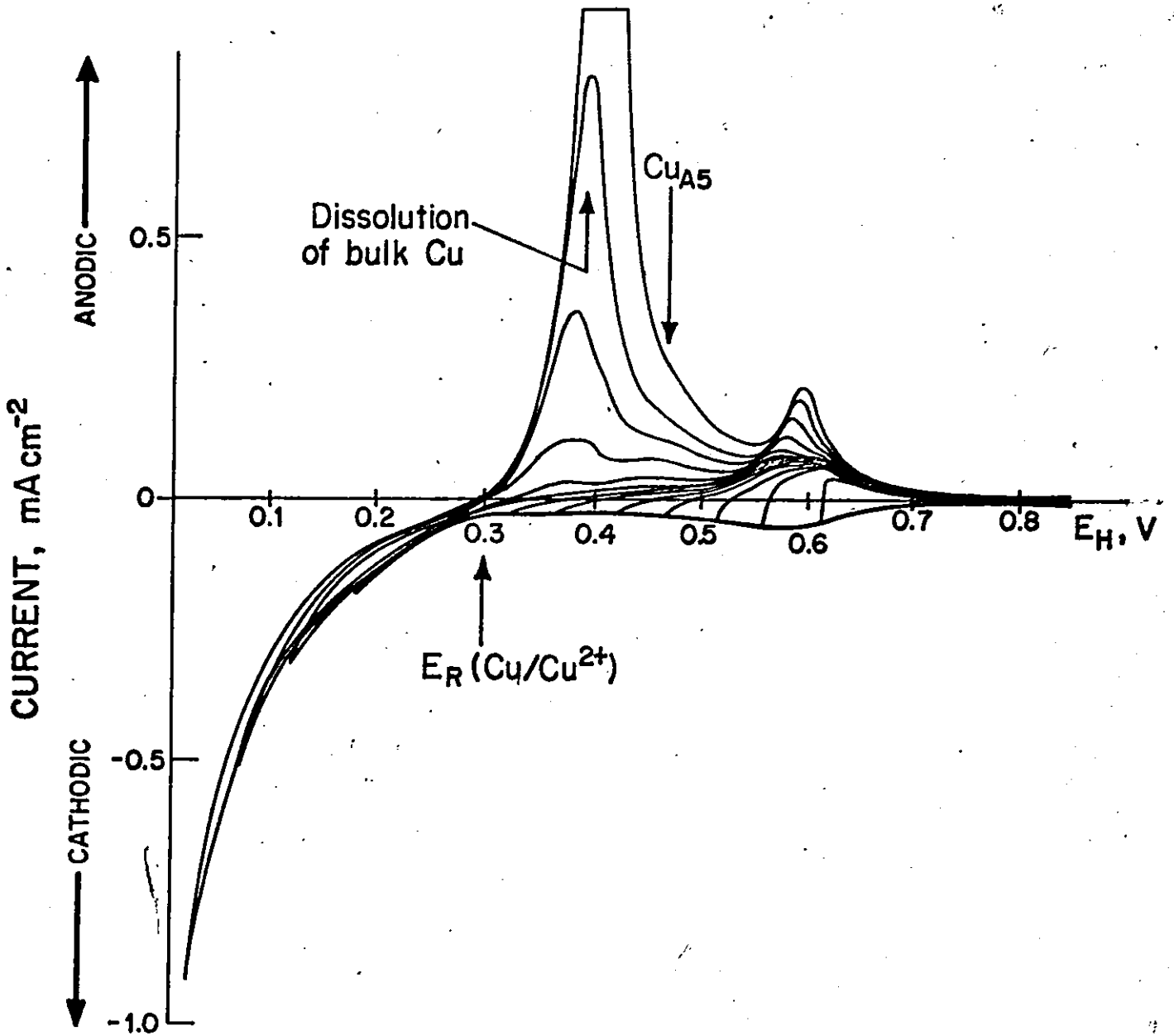

FIG 75 POTENTIODYNAMIC CURRENT-POTENTIAL PROFILES AT Au IN 1 M $HClO_4$ + 0.001 M $Cu(ClO_4)_2$ SHOWING BOTH UPD AND OPD OF Cu (REFERENCE ELECTRODE Pt / H_2 IN 1 M $HClO_4$; s = 0.05 V s^{-1})

anodic currents also appear over the range of potentials of the Cu_{Al-4} peaks. Since these additional currents are reduced by solution stirring, they are to be attributed to the oxidation of Cu^{+} ions produced in the chemical stripping of bulk Cu[408,409].

9.1.3 The slow step in the discharge reaction

An apparent hysteresis appears in the cyclic current-potential profile as the sweep rate is increased or the temperature lowered. At above about 320K, the UPD is reversible at sweep rates below about 0.05 V s^{-1}. At 277K, on the other hand, there is substantial hysteresis at 0.005 V s^{-1}, although very little at 0.001 V s^{-1}.

The characteristics of the hysteresis are shown in Fig. 76 by potentiodynamic sweeps taken to successively more negative end-potentials. At low temperatures and moderate sweep rates all the anodic peak potentials lie within a range of about 0.05 V, and the total half-width of the anodic peaks is only about 0.08 V. The potentials of the resolved anodic peaks are plotted vs temperature in Fig.77(a) and corresponding estimates of the charge in the composite Cu_{Al-4} and Cu_{Cl-4} peaks are shown in Fig.77(b).

Figure 78 shows that the UPD of Cu takes place at more positive potentials as the temperature is raised. The maximum coverage shown is that to the current minimum between the peaks Cu_{C4} and Cu_{C5}, which is independent of the reaction temperature (total variation about ±6% between 274 and 363K). Thus, although the UPD currents clearly increase with temperature, the total coverage in states Cu_{Cl-4} is constant. The effect is analogous to the constancy of the charge

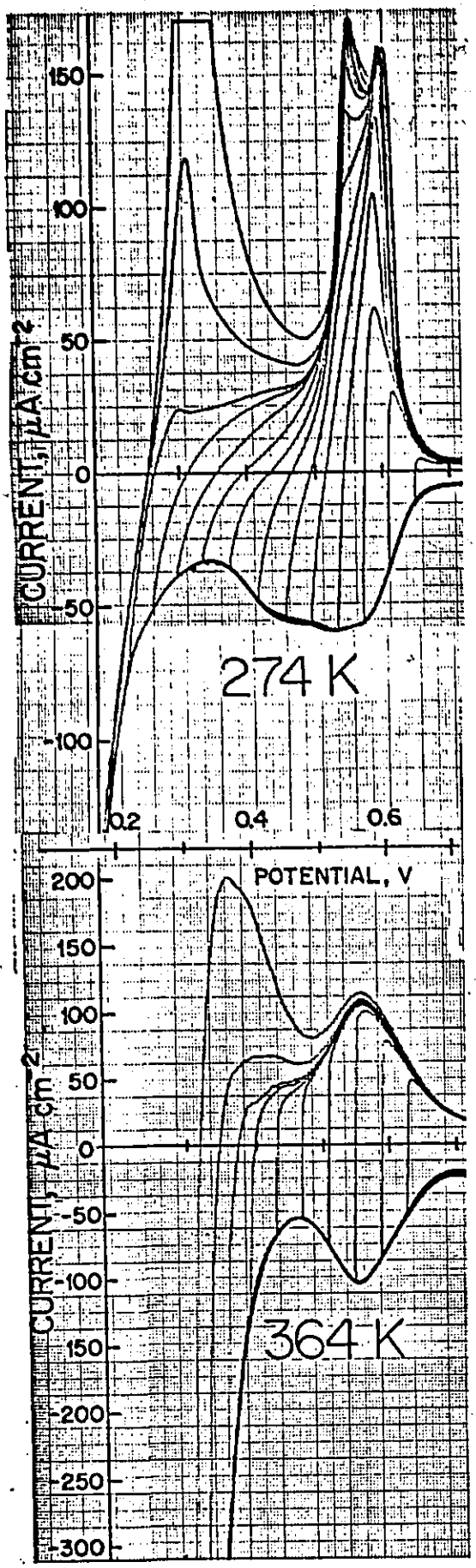

FIG 76 POTENTIODYNAMIC CURRENT-POTENTIAL PROFILES AT Au IN 1 M $HClO_4$ + 0.01 M $CuSO_4$ INVOLVING A SERIES OF CATHODIC END-POTENTIALS AT (a) 274 K (b) 364 K ($s = 0.05\ V\ s^{-1}$)

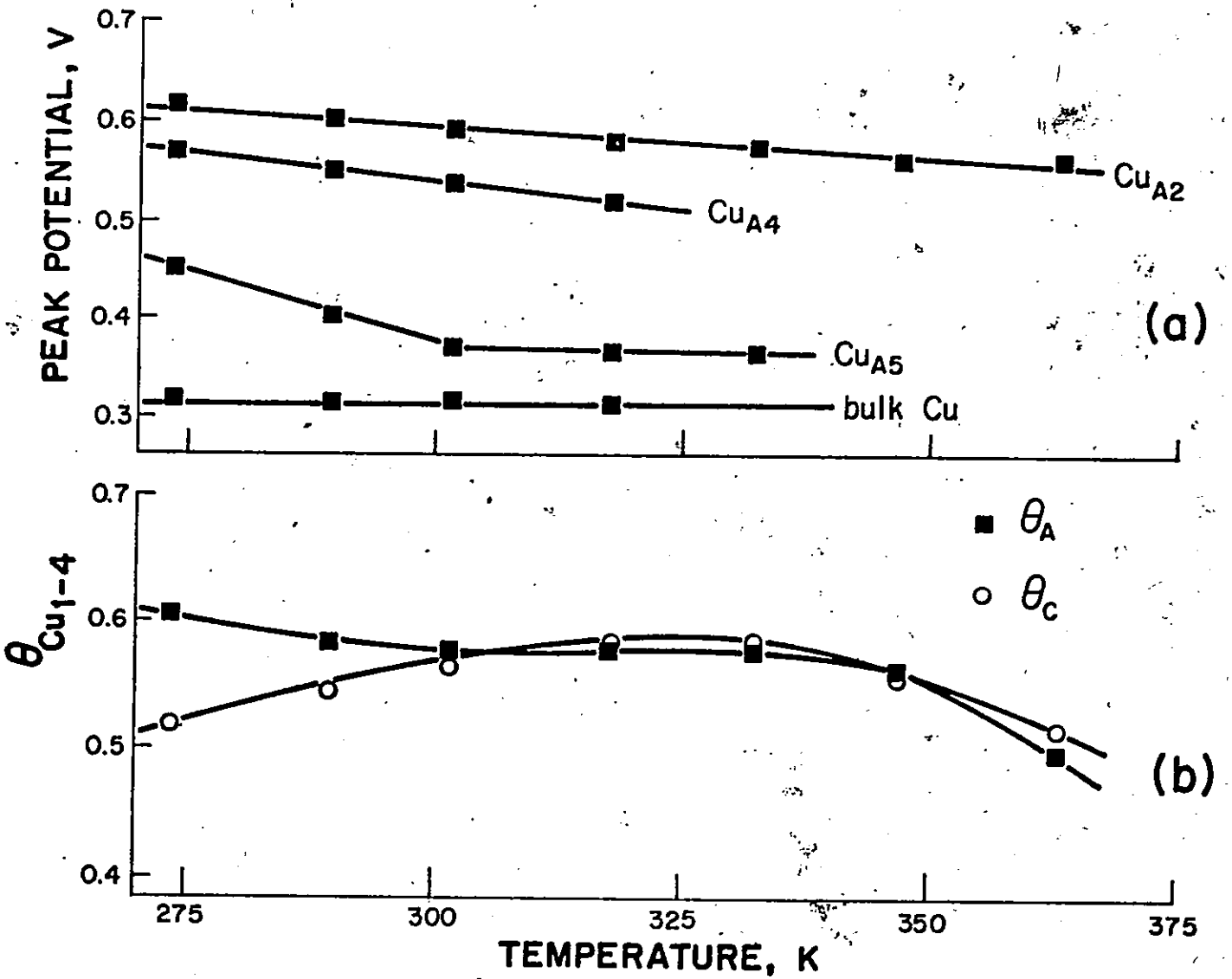

FIG .77 TEMPERATURE DEPENDENCE OF (a) PEAK POTENTIALS IN THE OXIDATION OF Cu UNDERPOTENTIALLY DEPOSITED ON Au (b) TOTAL COVERAGE OF Cu CORRESPONDING TO THE PEAKS Cu_{1-4} SOLUTION 1 M $HClO_4$ + 0.01 M $CuSO_4$ · REFERENCE ELECTRODE Pt/H_2 IN 1 M $HClO_4$ $s = 0.05\ V\ s^{-1}$)

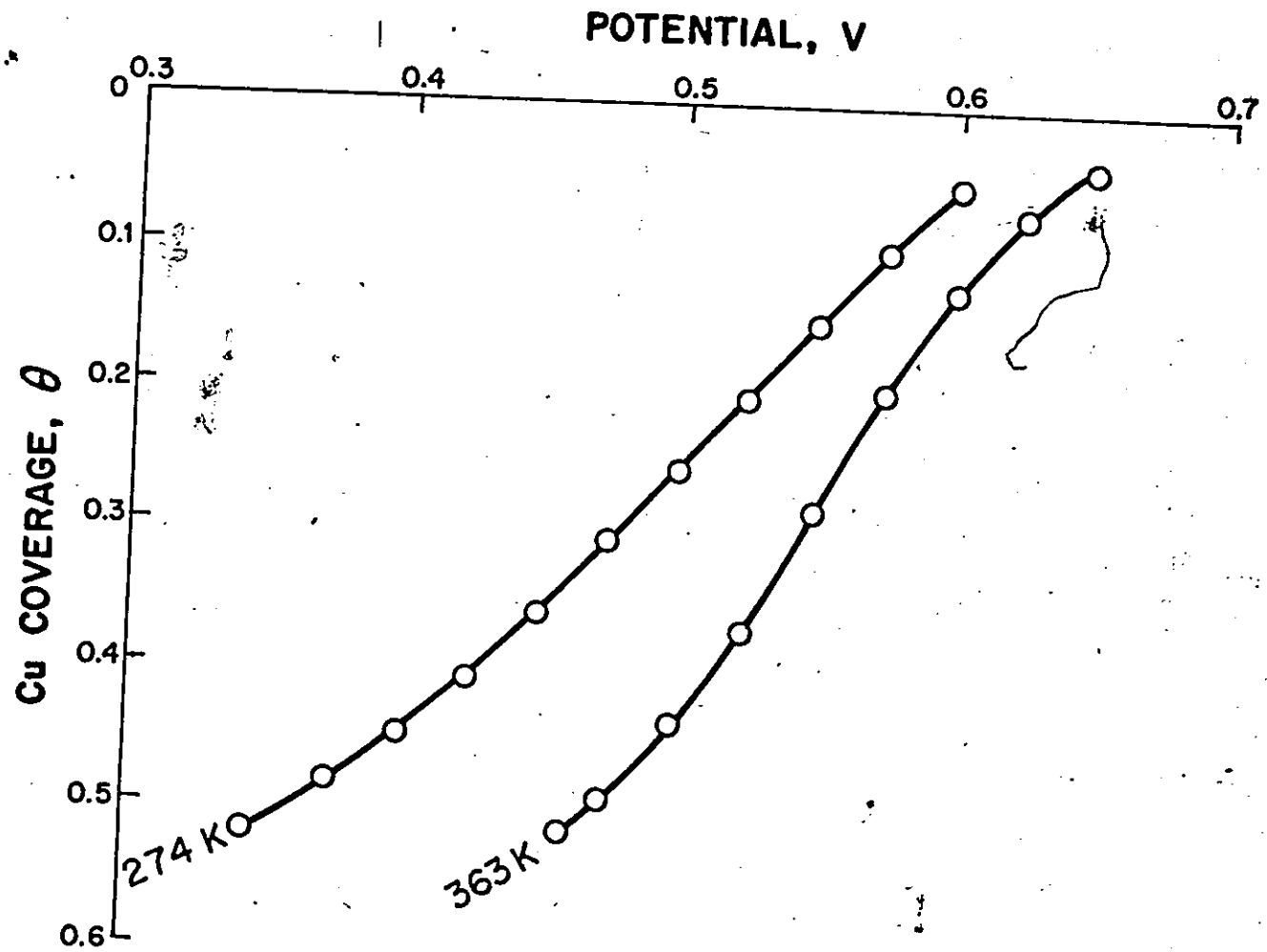

FIG 78 COVERAGES OF Cu DEPOSITED AT Au FROM A 1 M $HClO_4$ + 0.01 M $CuSO_4$ SOLUTION AS A FUNCTION OF THE DEPOSITION POTENTIAL AT 274 AND 363 K ($s = 0.05\ V\ s^{-1}$)

in the deposition of O-species on Au at potentials up to the current minimum before O_2 evolution, noted by Michri, Pschenichnikov and Burshtein[585]. At high temperatures, the Cu_{Cl-4} states merge to form a single peak, and the UPD occurs over a narrower range of potentials (Fig. 76(a)). Thus the reversible potentials of the Cu_{Cl-4} states move together as the temperature is raised. [If, instead, the individual peaks had all become narrower at higher temperatures, their resolution would have improved].

At higher sweep rates (i.e. $>0.05 V s^{-1}$), bulk Cu electrodeposition begins at less positive potentials (with a Tafel current-potential curve), although the potential of zero current during the electrodissolution of bulk Cu remains within about 0.04 V of the reversible Cu^{2+}/Cu potential (calculated assuming that all the Cu in the solution is present as Cu^{2+}). This allows state Cu_{C5} to be resolved, which was previously reported by Schmidt, Beutler and Lorenz[413] as a "second UPD peak". At high sweep rates and low Cu concentrations, the UPD currents become fairly constant over the potential range 0.45-0.30 V (Fig. 75). "Coverages" in excess of a monolayer may be deposited by these "constant" currents before a Tafel-type current increase is observed. The corresponding electrodissolution profiles show currents which fall very rapidly at potentials beyond peak Cu_{A1}, typical of a coverage-independent bulk dissolution process. This type of behaviour is also visible in the results of Takamura et al.[412] (their Fig. 6).

The "constant" deposition currents contain a diffusion-controlled component, but are only about 20% of the maximum discharge current observed at lower potentials in the deposition of bulk Cu.

They are therefore ascribed to a current limitation in the slow redox reaction $Cu^{2+} + e \rightarrow Cu^{+}$ which precedes the final electrodeposition stage, as discussed in the previous chapter.

When the deposition rate is limited by the rate of the Cu^{2+}/Cu^{+} redox reaction, Cu deposition continues during an interruption of the cathodic sweep so as to raise the Cu coverage to its equilibrium value at the holding potential. After the potential hold, the deposition currents are initially lower than those observed in an uninterrupted sweep, but they reach the same values at more negative potentials. The effect is similar to that observed in the interruption of the anodic electrodeposition of O species on Pt or Au (Figs. 32,58). Logarithmically different holding times have to be employed in the UPD region to study the potentiostatic deposition of Cu which would normally occur (potentiodynamically) at lower potentials. The effects of holding are not affected by solution stirring.

Evidence for a slow place-exchange process is presented in Fig.79. Constant residual anodic currents persist at potentials above those of the Cu_{Al} state in anodic sweeps following the deposition of bulk Cu. The corresponding anodic charge increases with the amount of Cu previously deposited. Since solution stirring does not affect these currents, it may be concluded that they represent the electrodissolution of Cu atoms which have diffused back to the metal/solution interface after having dissolved in the Au surface. After considerable alloying had taken place on an Au electrode, no potential programme could be devised to restore the original current-potential profile,

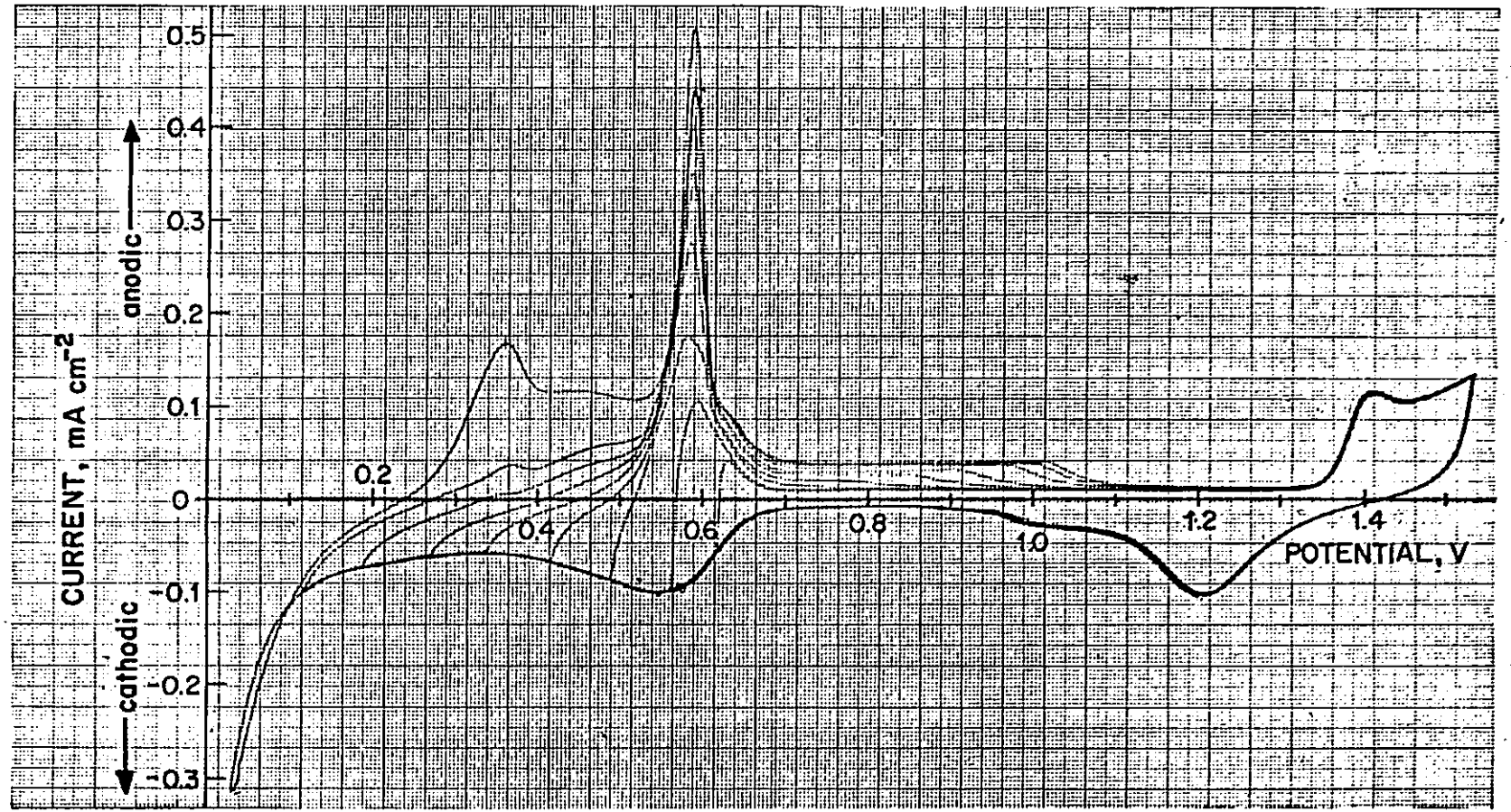

FIG 79 POTENTIODYNAMIC CURRENT-POTENTIAL PROFILES AT Au IN 1 M $HClO_4$ + 0.01 M $Cu(ClO_4)_2$ SHOWING EVIDENCE OF SURFACE ALLOYING ($s=0.05\ V\ s^{-1}$)

and the detailed structure of the UPD peaks was no longer resolved. This suggests that some "surface conditioning" process, associated with the disruption of the Au lattice, may occur. A model of this type has been developed by Smialowski et al. for the diffusion of H into the surface of Ni electrodes[609-611].

9.1.4 Effects of specifically adsorbed anions

The distribution of underpotentially deposited Cu among the current peaks is slightly altered when the deposition is carried out in the presence of SO_4^{2-} rather than of ClO_4^- ions, although the total coverage in states Cu_{Cl-4} is unaltered. Fig.80 shows that the current-potential profile varies little with the $CuSO_4$ concentration in the range 0.001-0.1 M, at a sweep rate of 0.05 V s^{-1}, when all the curves are plotted from the reversible Cu/Cu^{2+} potential. The spike peak Cu_{C2} is only visible in the cathodic sweep at higher Cu concentrations, i.e. when the slow process in Cu deposition does not limit the discharge rate.

9.2 Preliminary discussion

9.2.1 The mechanism of electrodeposition

The analysis of the mechanism of electrodeposition of Cu on Au is complicated by two factors. Firstly, kinetic limitations in the discharge rate of Cu^{2+} make the cathodic processes irreversible except at high temperatures, high Cu concentrations, and very slow sweep rates. Secondly, if the cathodic sweep is continued so that bulk Cu deposition occurs, diffusion-controlled anodic currents arise

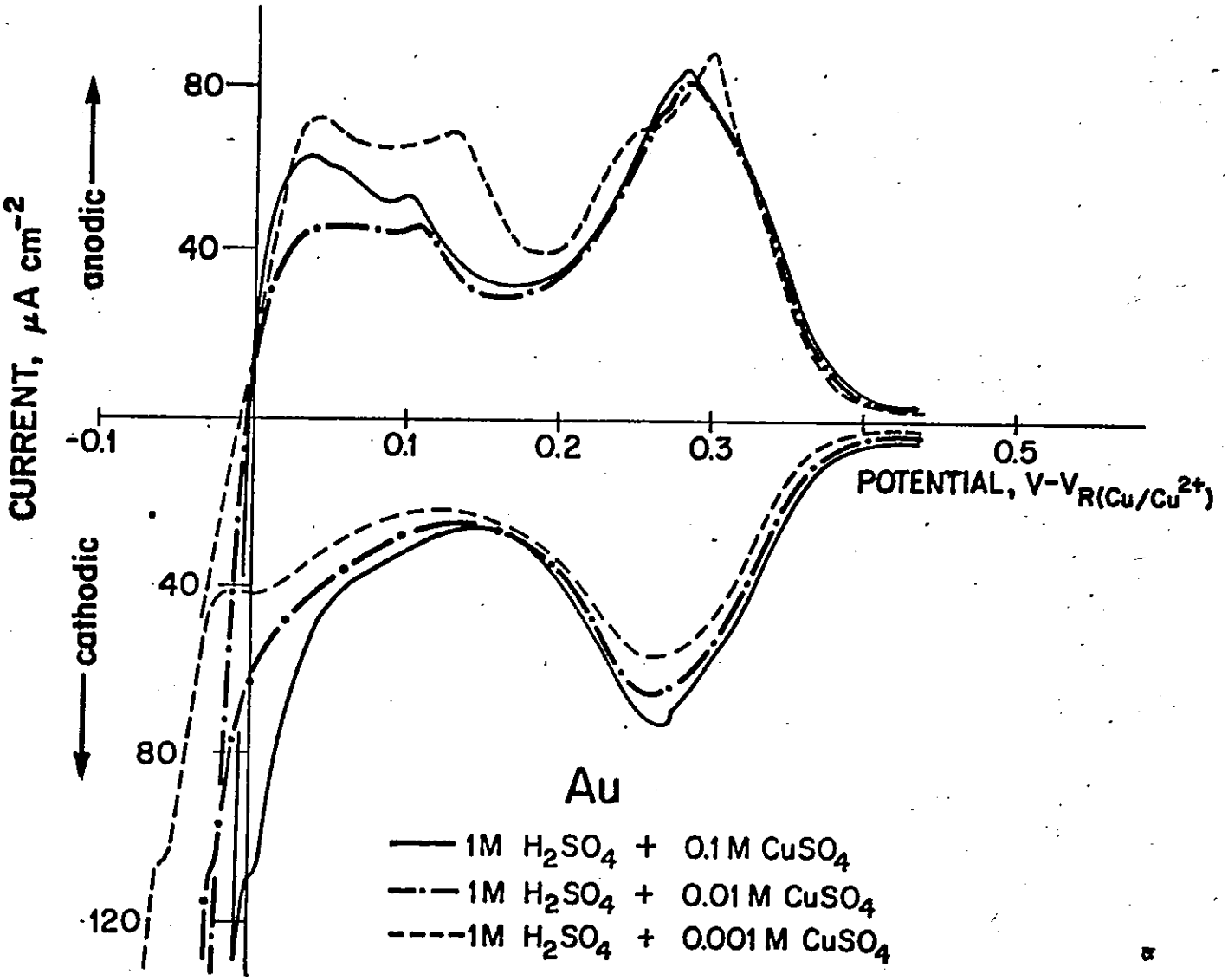

FIG 80 EFFECTS OF $CuSO_4$ CONCENTRATION ON THE POTENTIODYNAMIC CURRENT-POTENTIAL PROFILE AT Au IN 1 M H_2SO_4 + $CuSO_4$ SOLUTIONS ($s = 0.05\ V\ s^{-1}$)

from the oxidation of Cu^+ at the same potentials as those for electrodissolution from the UPD bonding states.

However, the reversible deposition observed at slow sweep rates and high temperatures shows that the UPD of Cu on Au can occur in at least <u>five</u> distinct bonding energy states. Bulk electrodeposition of Cu begins when the UPD coverage is only about $\theta_{Cu} = 0.5 - 0.7$, i.e. well before the electrodeposited Cu atoms would be close enough to touch one another. [Cu atoms will not be <u>preferentially</u> deposited touching previously-deposited atoms, or multiple bonding states would not be observed]. At coverages above $\theta_{Cu} = 0.5$-0.7, the potential is sufficiently cathodic for Cu to bond directly to previously-deposited Cu atoms, and the deposition current increases exponentially as bulk Cu deposits are formed. There seems no reason to suggest that the underpotentially deposited Cu atoms will rearrange themselves on the Au surface into local close-packed arrays before bulk Cu deposits are formed. As soon as elements of a Cu lattice are established, however, the formation of bulk Cu deposits will presumably occur preferentially on close-packed planes of the Cu lattice, so as to reduce the surface energy[612].

9.2.2 Hysteresis and alloying

The use of high sweep rates shows that the UPD of Cu is reversible at coverages below about $\theta_{Cu} = 0.15$. Figure 81 shows that at higher coverages the Cu atoms are only dissolved from more strongly bound states than those in which they were deposited. This hysteresis cannot be explained simply in terms of the slow reaction in Cu deposition, since the deposition current <u>decreases</u> as the electrode potential falls

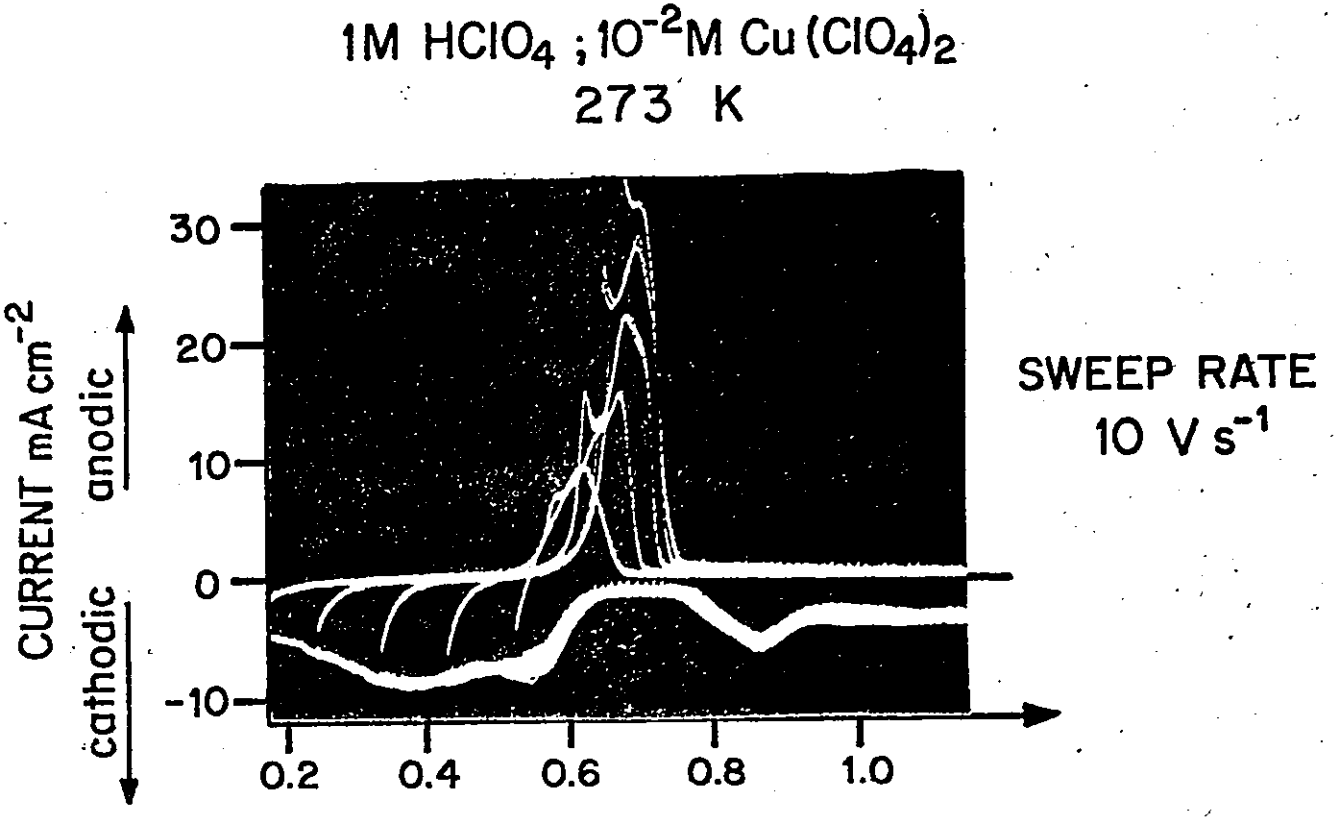

FIG 81 HYSTERESIS IN THE CURRENT-POTENTIAL PROFILE FOR THE UPD OF Cu AT Au AT 10 V s^{-1} FROM A 1 M $HClO_4$ + 0.01 M $Cu(ClO_4)_2$ SOLUTION AT 273 K

(cf. Fig. 79). It is instead thought to arise from place-exchange between chemisorbed Cu atoms and the Au atoms to which they are initially bound, which brings the Cu atoms to (more strongly bound) sites of higher coordination when the deposition coverage exceeds a critical value. However, unlike the similar (Figs. 40,57) hysteresis processes occurring in the electrodeposition of O species on Au and Pt, the place-exchange (alloying) of Cu on Au is reversible at slow sweep rates and high temperatures, since the overall process is reversible under these conditions.

The essential difference between the structures formed by the place-exchange of O species on Pt or Au and of Cu on Au is that in the first case the considerable electronegativity difference between the two species will stabilize an ionic surface lattice having Au and O species in alternate sites, whereas, in the second case, the bonding of the Cu will be almost entirely metallic. It will thus be energetically possible for Cu atoms to diffuse into the bulk Au lattice rather than necessarily remain close to the surface. When the potential of the sweep is high enough to reionize Cu from the Au surface, those Cu atoms which are dissolved in the Au will return to the electrode surface at a rate governed by the bulk diffusion coefficient. The Cu atoms will be electrodissolved as soon as they reach the surface, since the electrode potential will be higher than the equilibrium Cu dissolution potential for that coverage. The rate of diffusion of Cu to the Au surface would be expected to be constant during the anodic sweep if the rate of the (non-electrochemical) place-exchange process were limiting during the cathodic sweep.

The arrival of Cu atoms at the Au surface at a constant rate would account for the constant residual anodic currents observed at potentials above those of the Cu_{Al} peak (Fig.79), which appear when bulk Cu is deposited on the electrode. Similar constant currents were observed by Tilak, Conway and Kozlowska[613] in the reduction of thick oxide layers on Ag, and the effect is present in the deposition of Pb on Au to a very small extent (Figs. 83,87,89).

If Cu atoms thus move to more stably bound sites and dissolve in the Au lattice, even at low coverages, the question must be asked: Why do the states of chemisorption of Cu reach such definite limiting coverages (Fig.77(b)) despite the fact that many of the initially discharged Cu atoms are supposedly no longer on the surface? After all, when O species are electrodeposited on Au, the charge in the low-coverage deposition states is very much dependent on the time allowed for place-exchange. The difference may arise from the nature of the chemisorption bond. Since the bond energies in Au oxidation are governed by the formation of arrays of Au-O dipoles, the replacement of surface O species by Au atoms will in a real sense offer identical sites for further discharge. In the case of Cu electrodeposition, however, the chemisorption bond energies are largely governed by delocalized (metallic) interactions, so the properties of the Au will be perturbed by the discharge in the same way whether the Cu atoms are on the Au surface or below. Thus, the states of deposited Cu may still reach limiting coverages governed by the wave-mechanical interactions (metallic bonding) even while some fraction of the electrodeposited atoms are alloyed in the Au electrode just below its surface.

The hysteresis could alternatively arise from the stabilization of a reconstructed Au surface due to the dissolution of Cu in the electrode surface. Stronger bonding of electrodeposited Cu to the reconstructed surface would then give rise to hysteresis. Although Fig.79 shows that the initially deposited Cu atoms apparently do not remain close to the Au surface, since they take several seconds to diffuse back to be dissolved in the anodic sweep, it is possible that the reconstructed surface is continuously stabilized by the presence (or flux) of Cu atoms amongst the Au atoms near the electrode surface.

CHAPTER 10

ELECTRODEPOSITION OF Pb ON Au

10.1 Results

10.1.1 Calculation of Pb coverages

Since the coverages of underpotentially deposited Pb measured in this study are lower than those measured by a number of other authors, the area of the Au electrode on which this work was carried out was checked in some detail. The geometric area of the Au foil and its connecting wire was 2.99 cm^2. The real surface area was measured, after the completion of all the experiments, by the method of Michri, Pschenichnikov and Burshtein[585]. The data obtained, using sweep rates of 0.1 and 0.01 V s^{-1} and a wide range of temperatures in 0.5 M H_2SO_4, are shown in Fig. 82. According to the average of these values, the electrode had a real area of 4.13 cm^2, i.e. the roughness factor was 1.38.

The charge passed in Au oxide formation at potentials up to 1.5 V did not increase by more than about 5% during the experiments with Pb, so it was assumed that the real electrode area had remained constant. The coverages of underpotentially deposited Pb were calculated on the assumption that the atoms were fully discharged when deposited, i.e.

$$\theta_{Pb} = \frac{P_{Pb}}{2 \times 200 \times 4.13} \quad *$$

*See page 182 for discussion of the surface atomic density of Au.

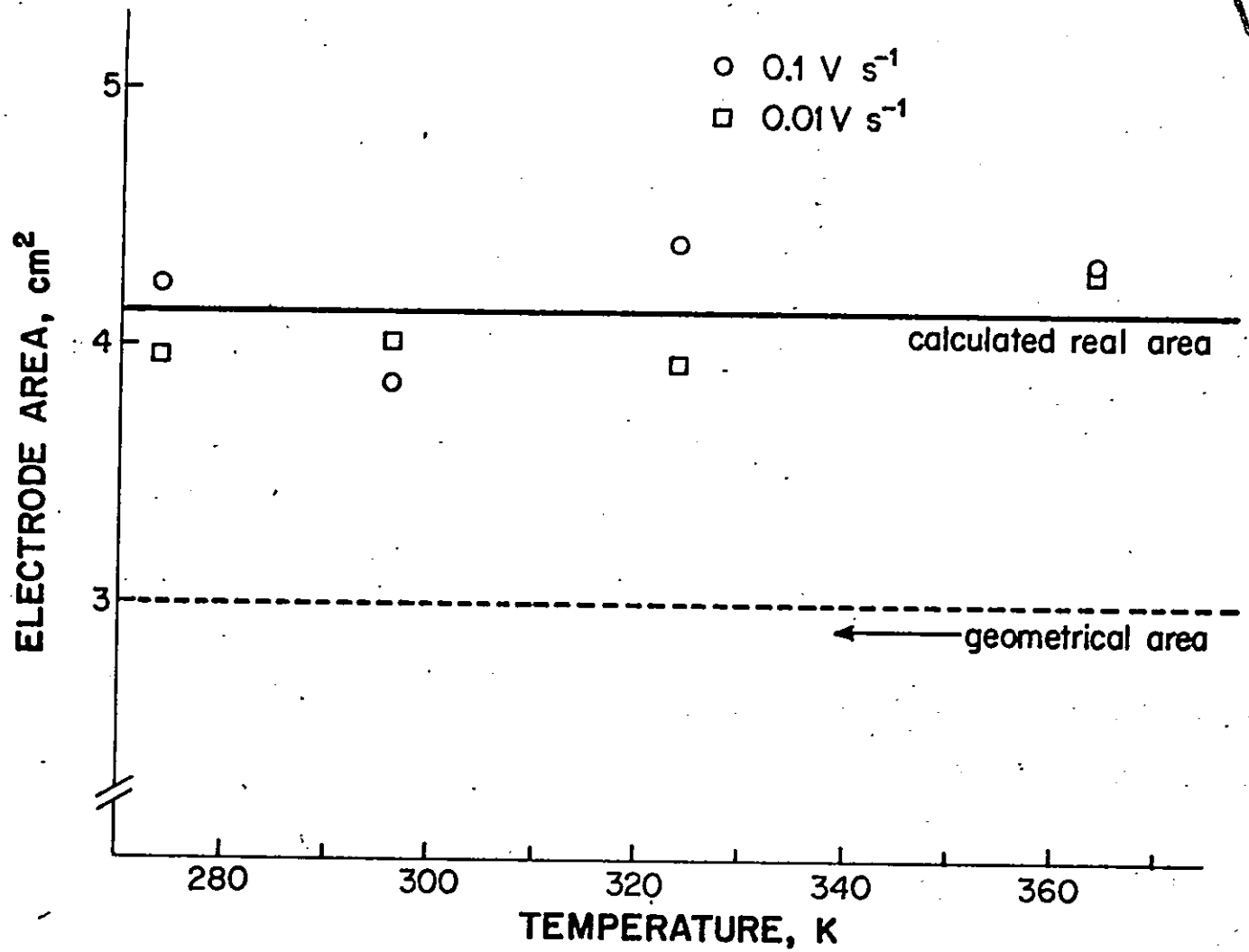

FIG 82 ESTIMATES OF THE AREA OF AN Au ELECTRODE MADE AT DIFFERENT TEMPERATURES AND SWEEP RATES ACCORDING TO THE METHOD OF MICHRI , PSHENICHNIKOV AND BURSHTEIN[585]

Attempts to measure the Pb coverage by taking the charge to the current minimum preceding O_2 evolution as 400 μC per real cm^2 in the 1 M $HClO_4$ - 10^{-3} M $Pb(NO_3)_2$ solution commonly used for electrodeposition (i.e. assuming that the measurement of the Au area proposed by Michri et al.[585] would apply regardless of the solution composition), were discarded. A lower apparent value of the electrode area is then obtained (averaging 3.38 cm^2 in the temperature range 274-364 K), possibly because the extent of Au oxidation is reduced by specifically adsorbed NO_3^- ions (see Section 7.1.4).

10.1.2 General observations

Figure 83 shows the current-potential and charge-potential curves for Au in 10^{-3} M $Pb(NO_3)_2$ + 1 M $HClO_4$ at 0.05 V s^{-1}. The potentials were measured with respect to a Pt/H_2 electrode in 1 M $HClO_4$. Estimates of the potentials of all seven UPD bonding states found in this study are shown, although not all are resolved under the conditions of Fig.83.

The Pb coverage at various distinguishable stages of the UPD is shown for four different temperatures in Fig.84. Neither the energies of the individual states nor their coverages are significantly affected by the temperature. The only visible change in the current-potential profile as the temperature is raised is that peaks Pb_1 and Pb_2 merge to form a single broad peak at above about 320 K. Since the reference electrode remained at room temperature, the constancy of the peak potentials shows that the temperature coefficients of the reversible potentials of deposition in all the states are similar

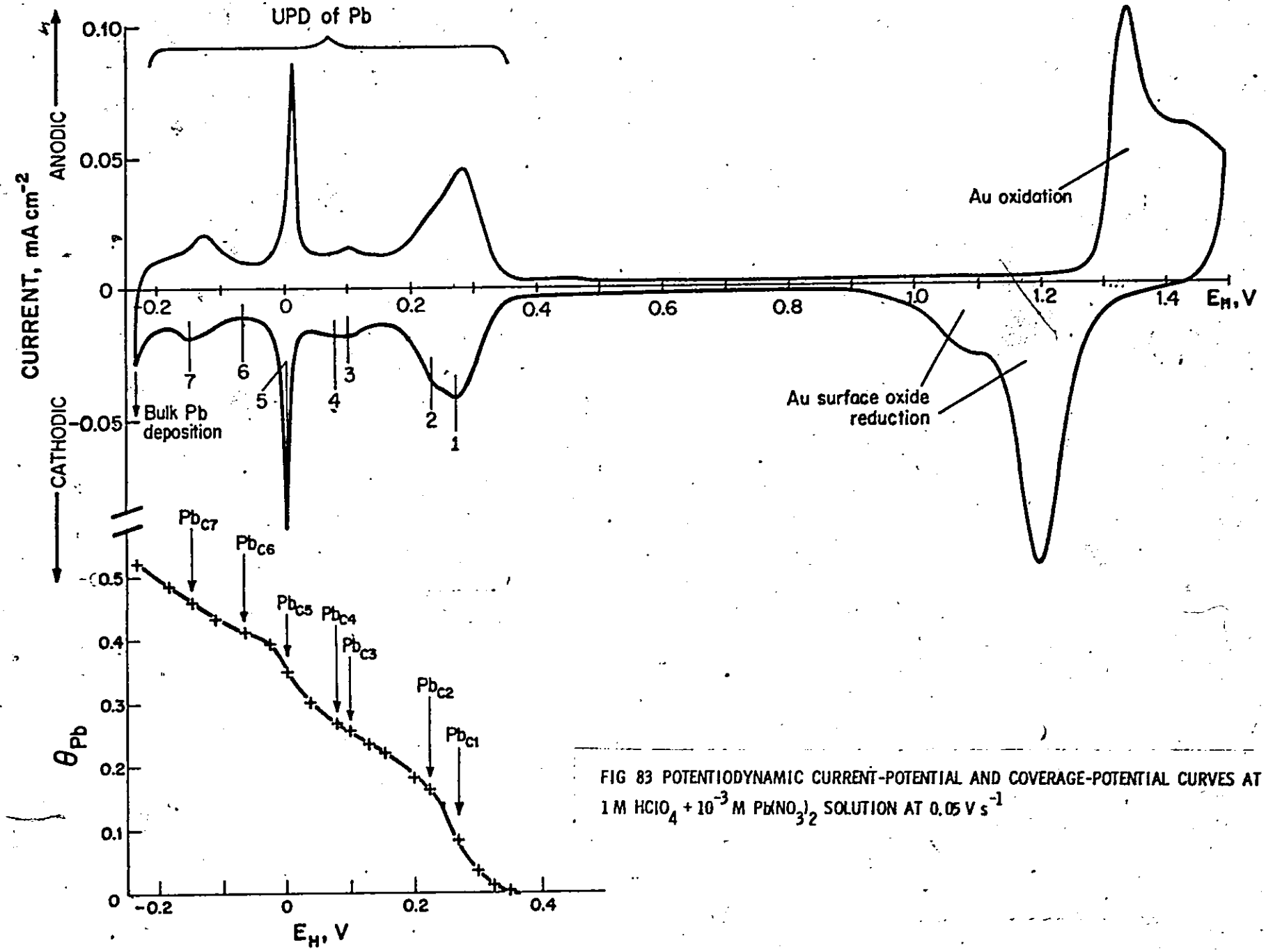

FIG 83 POTENTIODYNAMIC CURRENT-POTENTIAL AND COVERAGE-POTENTIAL CURVES AT Au IN 1 M $HClO_4$ + 10^{-3} M $Pb(NO_3)_2$ SOLUTION AT 0.05 V s^{-1}

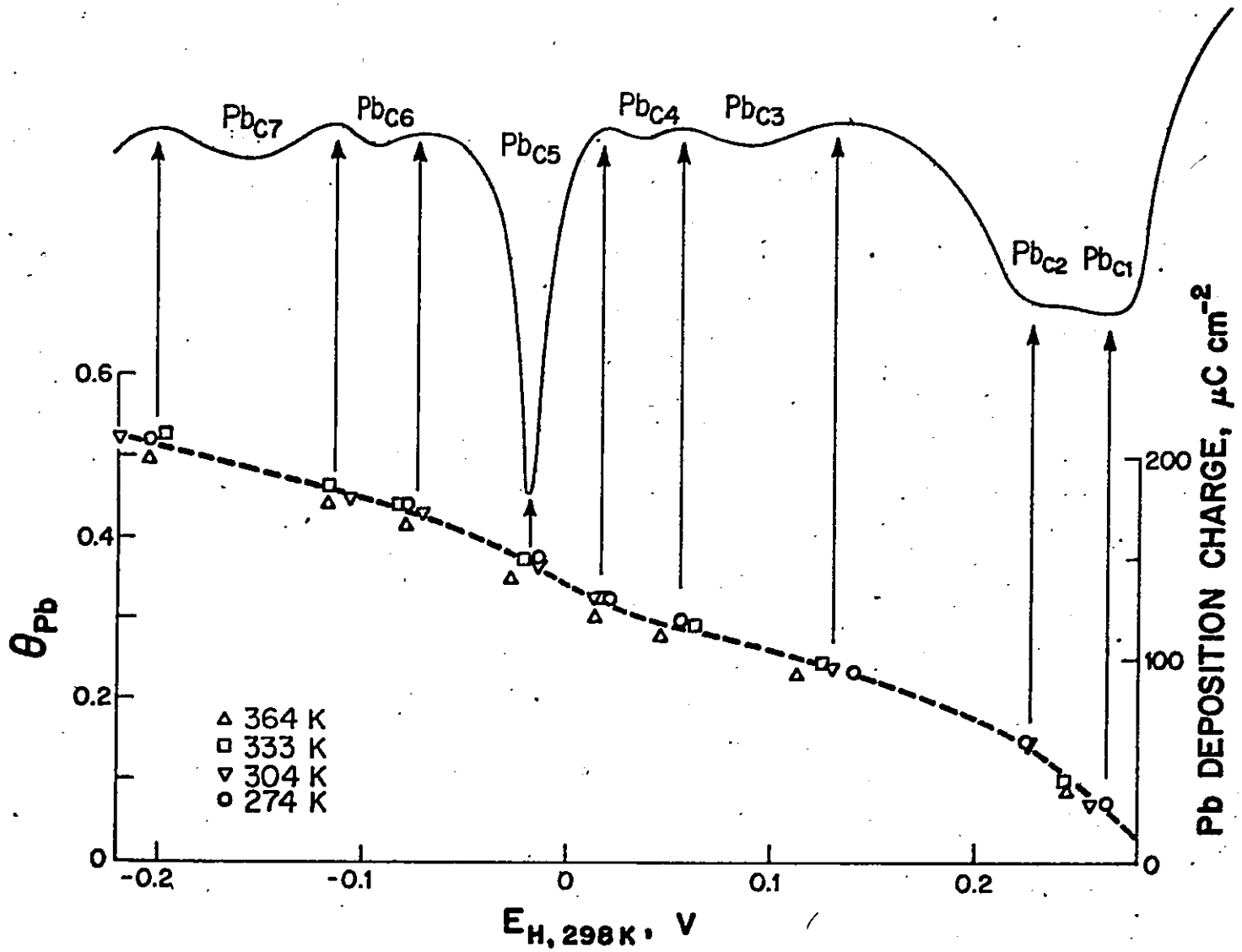

FIG 84 INTEGRATED DATA SHOWING COVERAGES OF Pb UNDERPOTENTIALLY DEPOSITED ON Au DURING CATHODIC SWEEPS AT 0.05 V s^{-1} AT 274, 304, 333, AND 364 K. (CURRENT-POTENTIAL CURVE IS ONLY SCHEMATIC)

and small, and suggests that the surface reactions involved may also be similar. In addition it shows the absence of temperature-dependent anion adsorption effects. The only anion adsorption effects observed in this study were the small and reproducible diffusional currents associated with the reduction of NO_3^- ions at potentials below about 0.1 V and sweep rates below about 0.02 V s^{-1}.

10.1.3 Reversibility

The electrodeposition of Pb on Au is an unusually reversible reaction compared to the other chemisorption systems studied in this work. The reversibility of the anodic dissolution processes is shown by the constancy of the anodic peak potentials at sweep rates up to at least 20 V s^{-1} (Fig.85). Peaks Pb_{A3} and Pb_{A4} are not resolved separately at the temperature of this experiment (300 K), and Pb_{A6} and Pb_{A7} have been omitted since they are not well resolved at fast sweep rates.

As the sweep rate is raised or the temperature lowered, the rate of Pb deposition becomes diffusion-controlled. Thus although a.c. modulation experiments (Fig.86) show that the electrochemical processes involved are reversible at sweep rates up to at least 10 V s^{-1}, an unmodulated sweep at 10 V s^{-1} (Fig.87) has an appearance of hysteresis, caused by a diffusion-limited supply of Pb^{2+} during the cathodic sweep. As the solution temperature is raised to 365 K, however, the increased rate of solution diffusion removes the restriction on the rate of the cathodic process (Fig.88) so that the unmodulated sweep is reversible

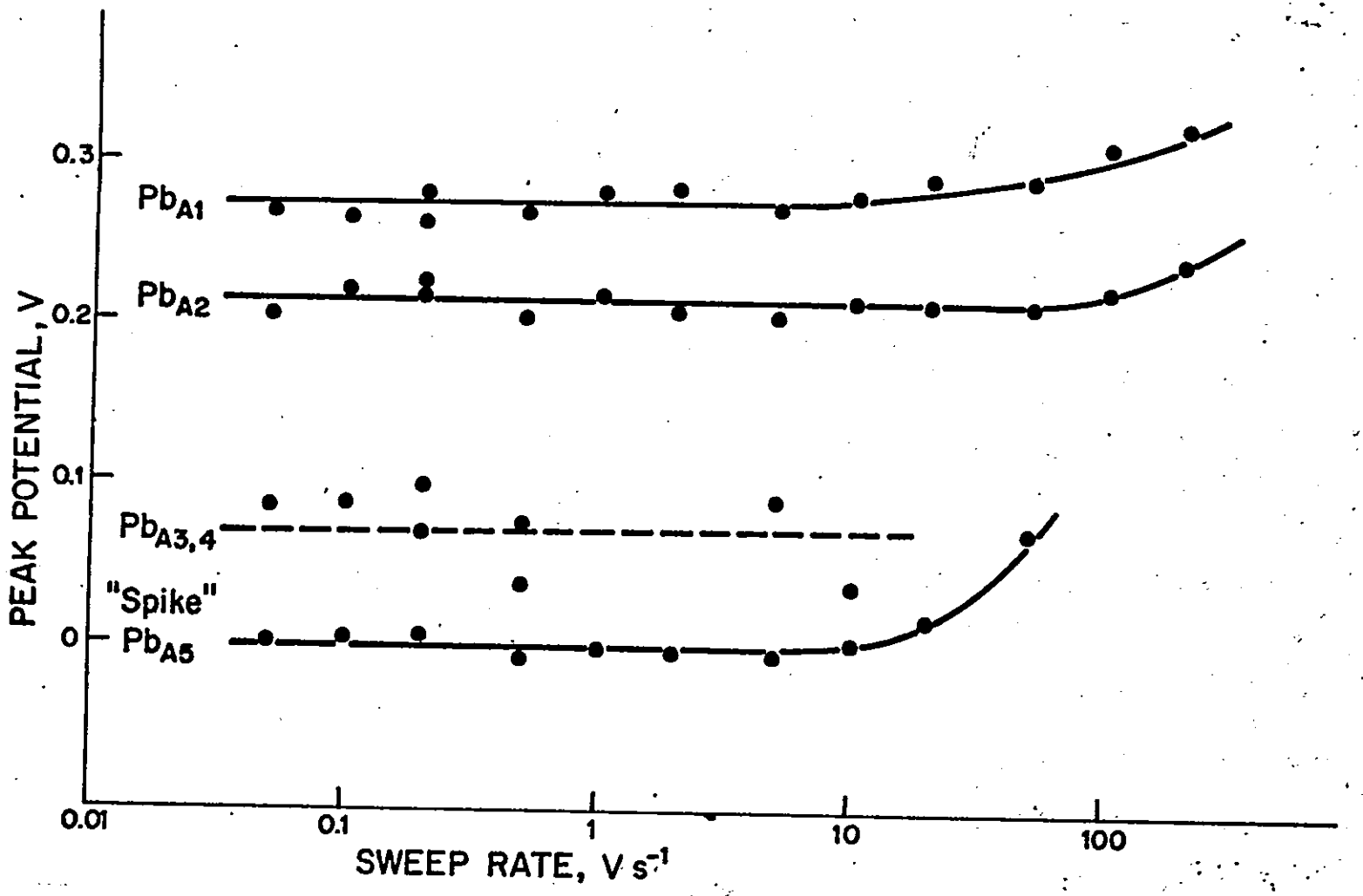

FIG 85 SWEEP RATE DEPENDENCE OF POTENTIALS OF PREDOMINANT CURRENT PEAKS IN THE POTENTIODYNAMIC OXIDATION OF Pb UNDERPOTENTIALLY DEPOSITED AT Au FROM 1 M $HClO_4$ + 10^{-3} M $Pb(NO_3)_2$ SOLUTION

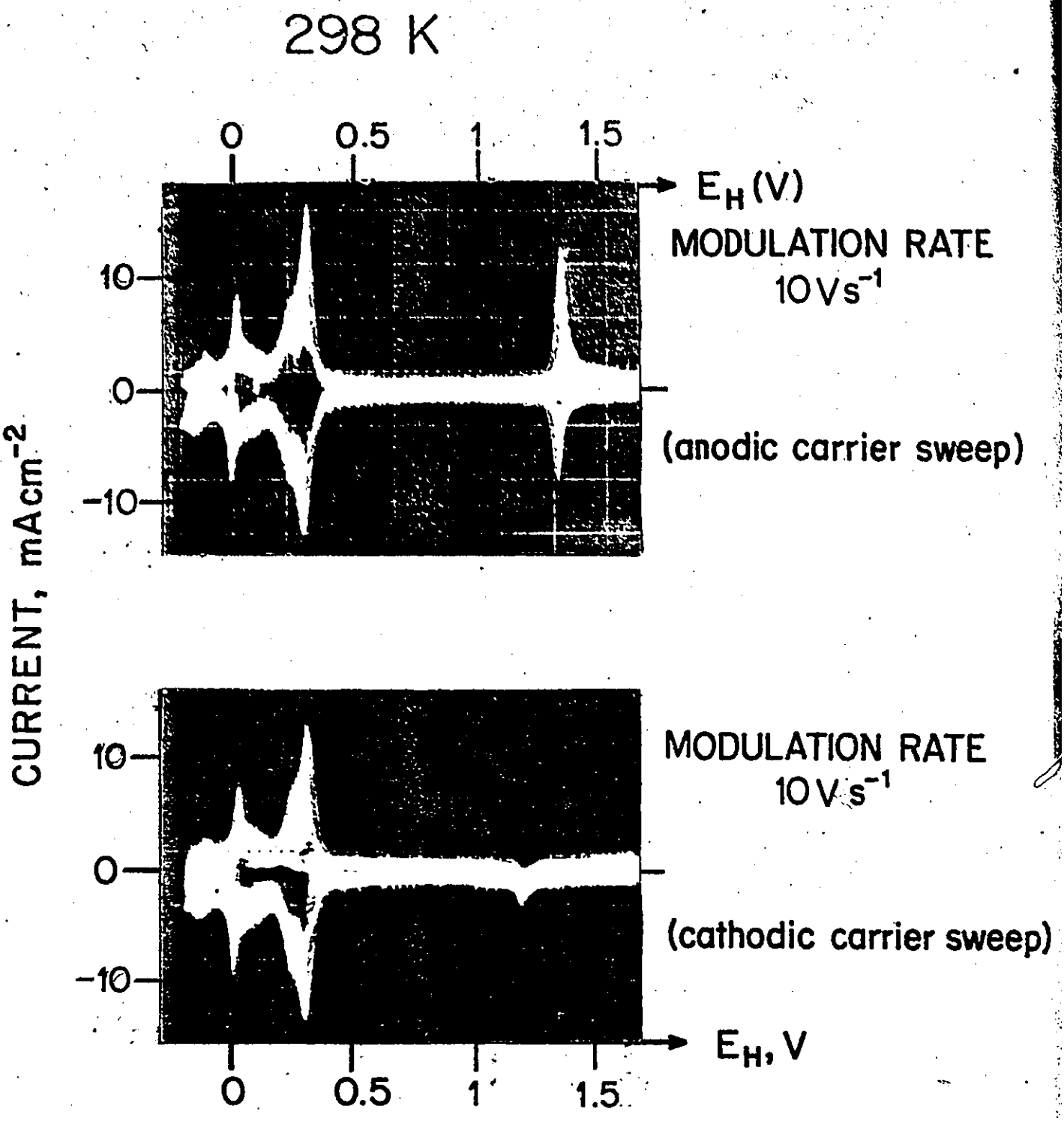

FIG 86 CURRENT-POTENTIAL PROFILES AT Au IN 1 M $HClO_4$ + 10^{-3} M $Pb(NO_3)_2$ SOLUTION OBTAINED WITH A TRIANGULAR MODULATION OF AMPLITUDE 0.025 V AND SWEEP RATE 10 V s^{-1} SUPERIMPOSED ON A CARRIER SWEEP OF 0.1 V s^{-1}

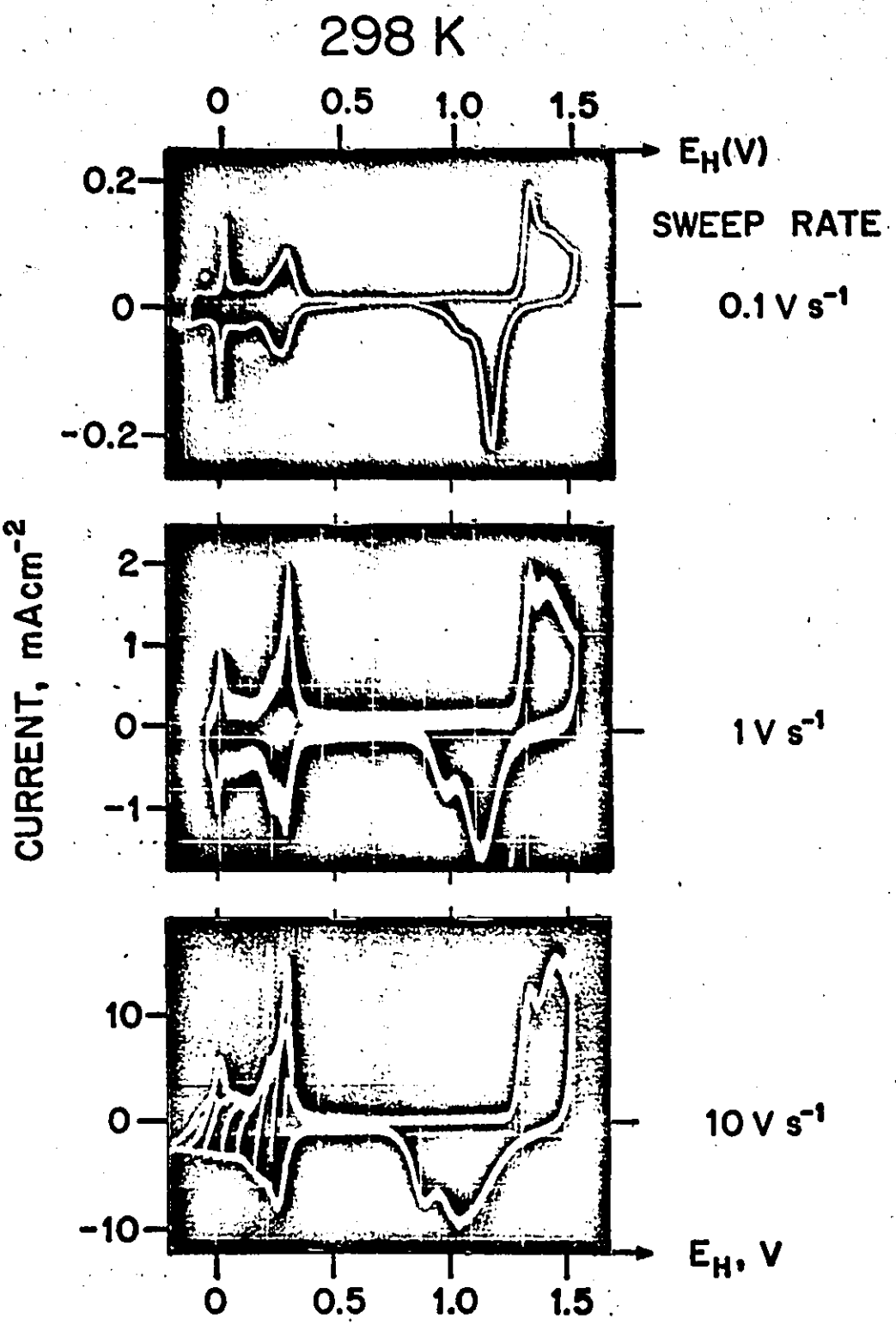

FIG 87 POTENTIODYNAMIC CURRENT-POTENTIAL PROFILES AT Au IN 1 M $HClO_4$ + 10^{-3} M $Pb(NO_3)_2$ SOLUTION AT 298 K USING SWEEP RATES OF 0.1, 1, AND 10 V s^{-1}. (A SERIES OF CATHODIC END-POTENTIALS WAS EMPLOYED IN THE DATA OBTAINED AT 10 V s^{-1})

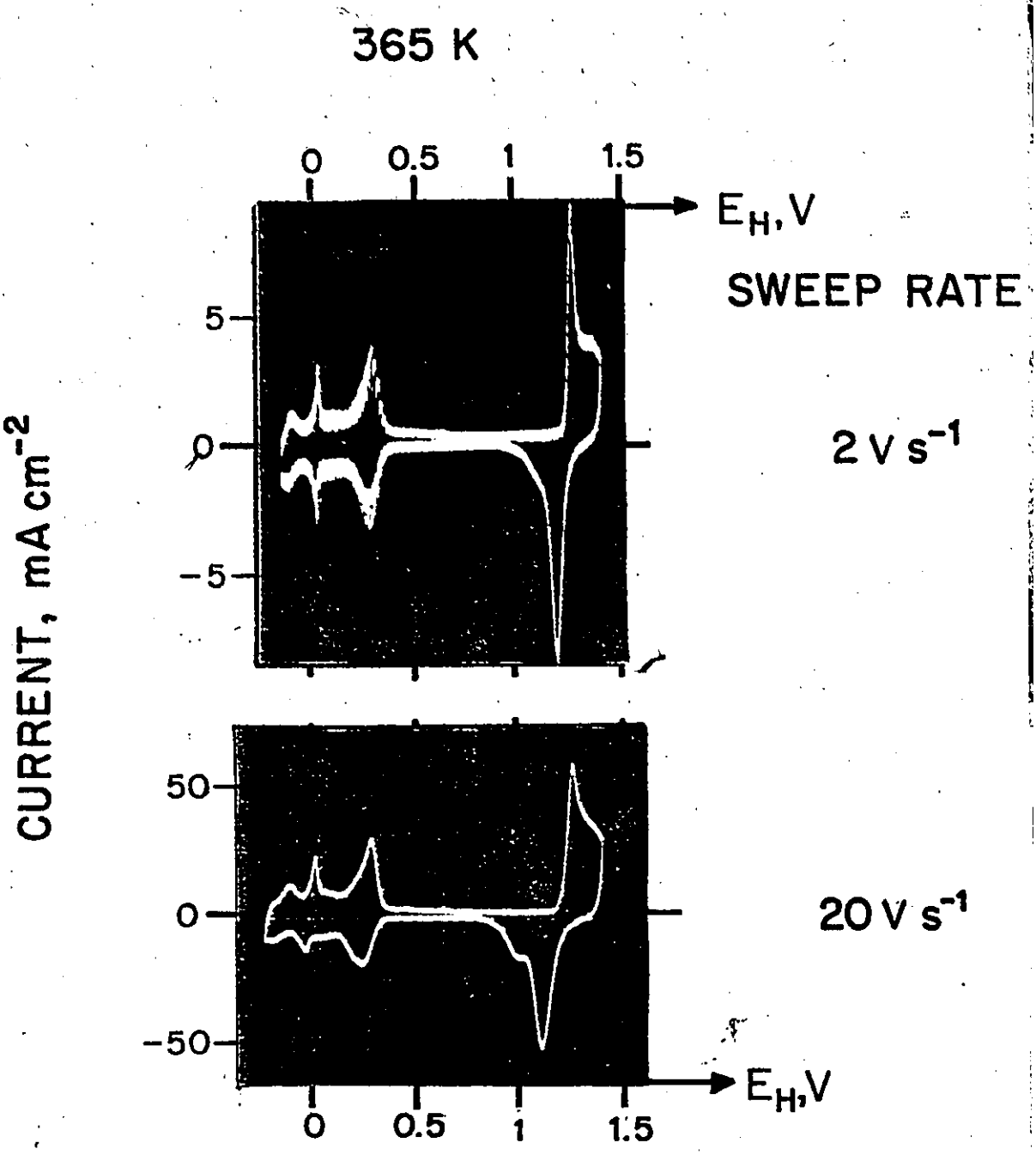

FIG 88 POTENTIODYNAMIC CURRENT-POTENTIAL PROFILES AT Au IN 1 M $HClO_4$ + 10^{-3} M $Pb(NO_3)_2$ SOLUTION AT 365 K USING SWEEP RATES OF 2 AND 20 V s^{-1}

even at 20 V s^{-1}. At 277 K, the cathodic process is partially diffusion-controlled even at 0.1 V s^{-1} (Fig. 89).

10.1.4 The bonding state Pb_5

The unusual "spike" peak Pb_5 was investigated in detail. Figure 90 shows the effect of holding the potential within the potential range of the spike and later re-establishing the sweep. The result is identical with that of holding the potential in any other part of the current-potential profile for UPD. Thus the Pb_5 peak is not an abrupt current impulse spread over a small range of potentials by kinetic factors. Its behaviour is qualitatively similar to that of all the other electrodeposition and dissolution peaks.

The current-potential profile of peak Pb_{A5} is shown on a greatly-expanded potential scale in Fig. 91. Residual currents from NO_3^- oxidation have been subtracted from the data obtained at 0.002 and 0.0002 V s^{-1}. The unusual characteristic of the peak Pb_5 in relation to those normally encountered in UPD systems is its high aspect ratio. At a sweep rate of 0.0002 V s^{-1}, the half-width of the peak is only 8 mV (Fig. 91). Theoretical work in this laboratory[24] has shown that very narrow electrodeposition peaks arise if the free energy of the electrodeposition process falls as the coverage increases*, as if there were an attractive interaction between deposited atoms. This is treated mathematically by introducing an interaction parameter (g) with a negative value into an isotherm of the form:

* cf. the Langmuir isotherm where the free energy of adsorption is independent of coverage.

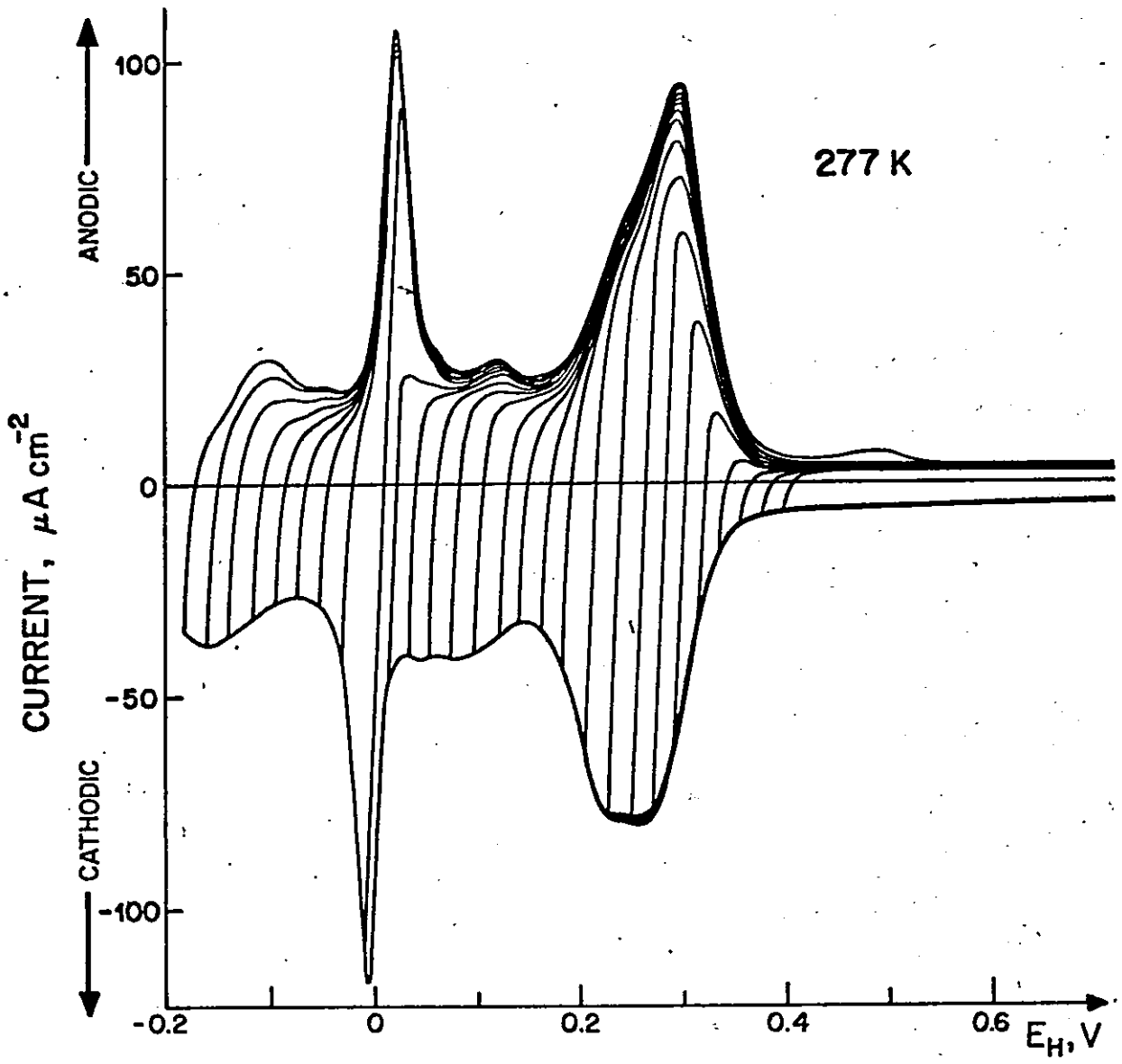

FIG 89 POTENTIODYNAMIC CURRENT-POTENTIAL PROFILES AT Au IN 1 M $HClO_4$ + 10^{-3} M $Pb(NO_3)_2$ SOLUTION AT 277 K INVOLVING A SERIES OF CATHODIC END POTENTIALS ($s = 0.1\ V\ s^{-1}$)

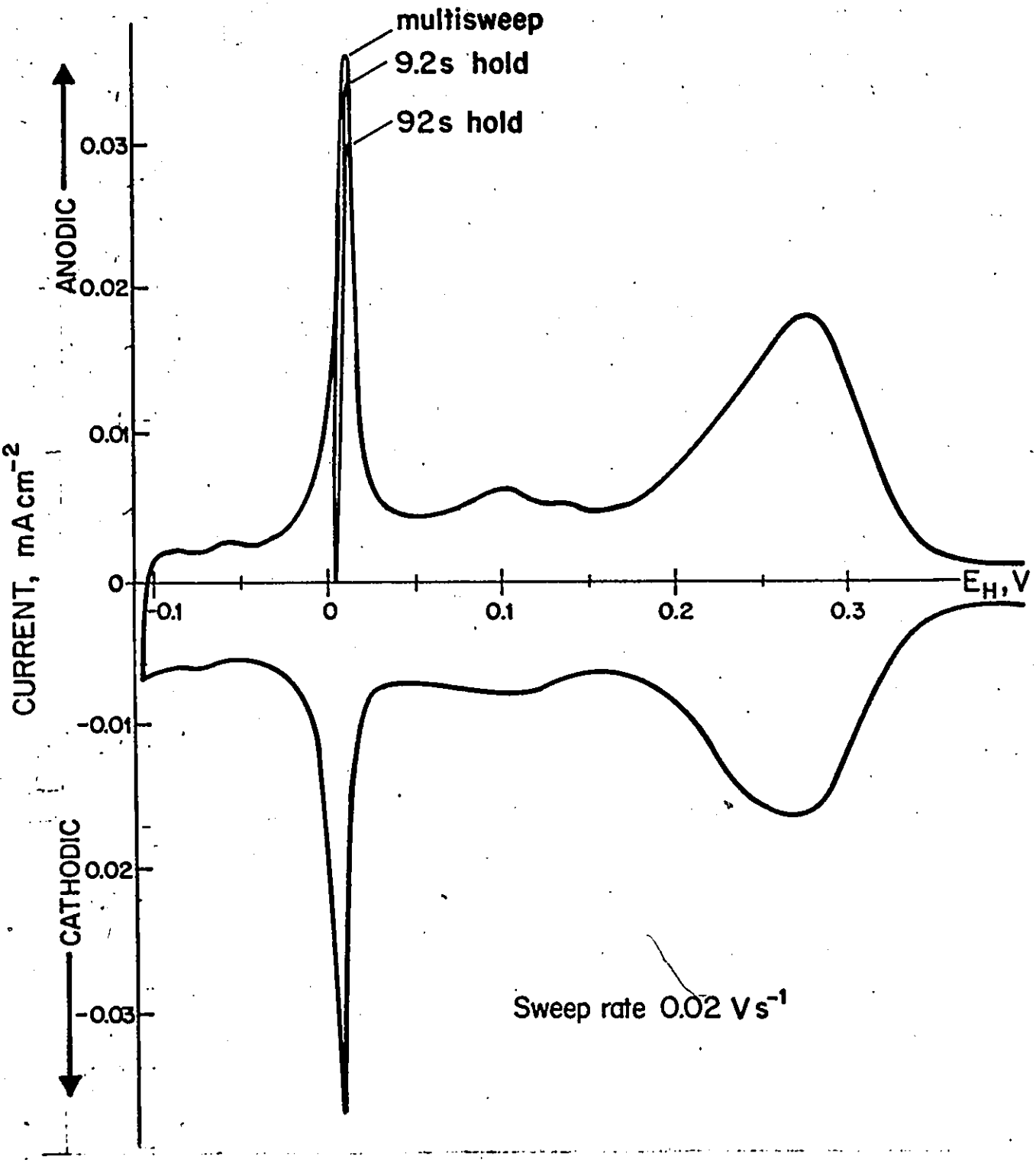

FIG 90 CURRENT-POTENTIAL PROFILE FOR THE UPD OF Pb AT Au, SHOWING THE EFFECTS OF INTERRUPTING THE ANODIC SWEEP WITHIN THE POTENTIAL RANGE OF THE Pb_{A5} SPIKE PEAK. SOLUTION 1 M $HClO_4$ + 10^{-3} M $Pb(NO_3)_2$, SWEEP RATE 0.02 V s^{-1}

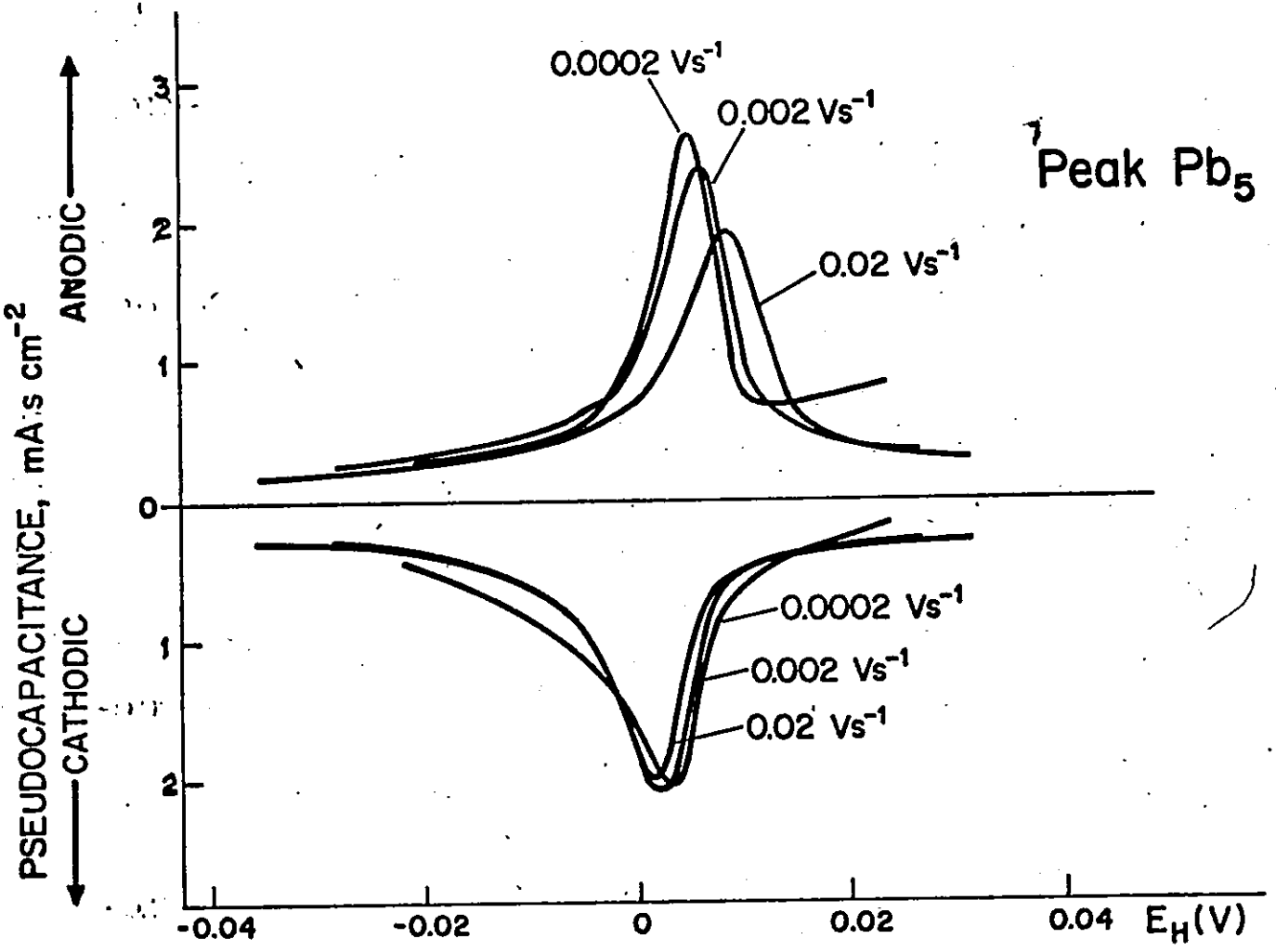

FIG 91 PSEUDOCAPACITANCE (I_p / s) ASSOCIATED WITH THE UPD OF Pb ON Au IN THE POTENTIAL RANGE OF THE Pb_5 PEAK MEASURED AT SLOW SWEEP RATES IN 1 M $HClO_4$ + 10^{-3} M $Pb(NO_3)_2$ SOLUTION

$$\left(\frac{\theta}{1-\theta}\right) \exp(g\theta) = K\, C_{Pb}{}^{2+} \exp\left(\frac{VF}{RT}\right) \quad 16$$

By comparison with theoretical current-potential profiles generated from this equation[16,24], the value of g required to produce a peak of the shape of Pb_{A5} was estimated as between -3 and -4. With an interaction parameter of this magnitude, the transition region between reversible and irreversible behaviour stretches over at least 3.5 decades of sweep rate, compared to 2.5 decades with no interaction. The change in the current-potential profile of the peak with sweep rate (Fig. 91) is consistent with the change in the theoretically calculated behaviour for a surface reaction in the range of sweep rates between fully reversible and fully irreversible behaviour[24].

10.2 Preliminary discussion

10.2.1 Reversibility and place-exchange

When the supply of reactant ions is not limited by a slow pre-electrochemical process (e.g. solution diffusion), electrodeposition reactions can be irreversible for two reasons: (a) the discharge of the hydrated ion itself may be kinetically slow, or (b) time-dependent surface processes (e.g. place-exchange, lattice rearrangement) may change the state of the deposit in the time interval before the electrode potential returns (in the sweep) to a value sufficiently positive to reionize the deposit, giving rise to hysteresis. The high degree of reversibility of the UPD of Pb on Au shows that neither of these features is significant in this system.

Other workers have reported, however, that bulk deposits of Pb dissolve slowly into Au if they remain on the surface for a long time, or if the temperature is high[421,422,427] (see Section 1.6.1.8). Under the conditions of the present experiments, time effects were negligibly small except in a few cases where slight alloying was indicated (after deposition of bulk Pb) by small constant currents continuing at potentials anodic to those for removal of deposits formed only at underpotentials (Figs. 83,87 and 89).

Surface rearrangement processes have already been discussed for systems where the adsorbate species are about the same size as the substrate atoms (e.g. O species on Pt), or slightly smaller (e.g. O species on Au, Cu on Pt, Cu on Au). Since Pb atoms are about 25% larger in diameter than Au atoms, the slowness of alloying in this system may relate not so much to a relatively small driving force (i.e. insufficiently strong Pb-Au bonds, or weak interactions between chemisorbed Pb atoms) as to a high activation barrier in place-exchange. The electronegativity difference between Pb and Au is less than that between Cu and Au[614] so the increased reversibility of adsorption of Pb compared to that of Cu may also relate to the smaller dipole moments associated with the Pb-Au bond. The slowness of the rearrangement process is not a property of the Au lattice itself, since both OH (radius approximately 1.37 Å) and Cu (radius 1.28 Å) species show irreversible deposition, while Ag[615] (radius 1.44 Å) and Pb (radius 1.75 Å) are deposited reversibly. Thus the electrodeposition of Pb on Au does not exhibit hysteresis because the surface rearrangement processes leading to alloying are so slow that

discharged Pb atoms do not leave the state in which they were deposited during the time interval before the reionization potential is reached. The deposition of O species on Ir[20,616-618] is probably a similar case, although long-time variations in the extent of reversible oxidation have been observed with this metal.

10.2.2 Accurate measurement of Pb coverage

An accurate knowledge of the Pb coverage as a function of potential is essential to a valid discussion of the mechanism of its UPD, and in particular of the significance of the multiple states of the deposited atoms. The deposition charge may be easily measured in pure solutions, but the accuracy of the coverage measurement depends on the accuracy with which the surface area of the Au electrode is known, and no direct method of measuring the roughness of Au electrodes has been devised.

Table 4 shows that published estimates of the total UPD coverage (i.e. the coverage at which bulk Pb is nucleated) vary from 0.59 to 1.25. In the first four publications[358,419,421,422], no allowance was made for the roughness of the Au electrode, and the maximum coverage is only quoted in terms of the geometrical area of the electrode.

Vicente and Bruckenstein[425] estimated the real area of their Au disc electrode by the method of Brummer and Makrides[343,619] in which the coverage after 5 min oxidation at 1.45 V (measured by the reduction charge) is taken as exactly θ = 1 for a two-electron-

TABLE 4. ESTIMATES OF TOTAL UPD CHARGE OF Pb ON Au

Authors	Date	Total UPD Charge
Mills and Willis[419]	(1953)	500 μC per geometric cm^2
Schmidt and Gygax[421]	(1967)	420–465 μC per geometric cm^2
Takamura, Takamura, Nippe and Yeager[358]	(1970)	400 μC per geometric cm^2
Schmidt and Wüthrich[422]	(1972)	374 μC per geometric cm^2 (1.94 μmol cm^{-2})
Vicente and Bruckenstein[425]	(1973)	206 μC per real cm^2
Adžić, Yeager and Cahan[423]	(1974)	300 μC per geometric cm^2 on polycrystalline Au 245–273 μC per geometric cm^2 on single-crystal Au
Takamura, Watanabe and Takamura[426]	(1974)	490 μC per geometric cm^2
This work		210 ± 15 μC per real cm^2

transfer process. They found that the maximum amount of Pb which could be deposited on Au without showing the bulk Pb removal peak had a dissolution charge of 350 μC per geometric cm^2 on an electrode with a roughness factor of 1.7, i.e. the maximum UPD charge was 206 μC per real cm^2, which compares well with the value of 210 μC per real cm^2 found in the present work.*

Adzic, Yeager and Cahan[423] measured the total UPD charge as about 300 μC per geometric cm^2 on polycrystalline vacuum-deposited Au films and 245-273 μC per geometric cm^2 on single-crystal surfaces (these latter figures are derived from the charges obtained to 0.0 V scaled up by the same ratio as found for the polycrystalline surfaces). Since these electrodes were prepared for reflectance studies, they were probably quite smooth. Taking an arbitrary value of 1.1 for their roughness would give the total UPD coverage as 273 μC per real cm^2 for polycrystalline Au and 223-248 μC per real cm^2 for the single-crystals. Earlier work in Yeager's laboratory[358] gave the UPD charge in a poorly-resolved $Pb_{Cl,2}$ peak as 400 μC cm^{-2}, but an associated measurement of the oxidation charge to 1.7 V as 1.25 mC cm^{-2} suggests that their electrode had a roughness factor of about 3. This would reduce Yeager's estimate of $q_{Pb_{Cl,2}}$ to about 130 μC, compared to the value of about 100 μC per geometric cm^2 found in the present work (Fig. 84).

*Vicente and Bruckenstein[425] concluded however that the maximum deposition charge in the UPD "monolayer" (assumed to be square-packed Pb atoms, non-epitaxial with the Au substrate), was 247 μC per real cm^2, on the basis of a discontinuity in plots of the Pb dissolution charge versus the time of diffusion-controlled deposition. Nevertheless when the deposition charge was of this magnitude, the bulk Pb dissolution peak was observed in the anodic sweep.

Takamura, Watanabe and Takamura[426] measured the charge in peaks Pb_{C1-5} as 490 μC per geometric cm^2. This value is surprisingly high, since their work involved reflectance studies which would normally require smooth electrodes. However a preliminary "triangular potential pulse" employed to clean the electrodes may also have roughened them.

Thus, although most previous authors have concluded that the Pb coverage exceeds a monolayer in the UPD region, a critical analysis of their data shows that their estimated coverages are in almost all cases too high.

Measuring the Au electrode area by the BET-related method of Michri, Pschenichnikov and Burshtein[585] involves an uncertainty measured by those authors as "within 10%", and in the present work as ±7% (Fig. 1). This error will be carried over to the coverage measurements so that the total UPD charge measured in the present work is 210 ± 15 μC cm^{-2}, i.e. bulk Pb deposition commences when $\theta_{Pb}=0.52\pm0.04$. The significance of this figure will now be examined.

10.2.3 Epitaxy in Pb deposition

The fact that the chemisorption energy of Pb electrodeposited on Au reaches the energy for electrodeposition on bulk Pb while the coverage is still only about 0.5 immediately raises the question of the physical nature of the transformation from UPD to bulk deposition. Vicente and Bruckenstein[425] tentatively proposed that bulk deposition might be preceded by the formation of a square-packed monolayer of Pb atoms having no 1:1 epitaxial relationship

with the Au substrate. However, this would require a coverage of $\theta_{Pb} = 0.65$, or 0.75 for a close-packed monolayer of Pb atoms. Vicente's results[425], as well as the present data, show that bulk Pb dissolution is already occurring at coverages of $\theta_{Pb} = 0.55$. This does not rule out a mechanism involving non-epitaxial deposition in a square-packed monolayer of Pb atoms, although there seems no obvious physical reason why bulk Pb deposition should commence when this monolayer is only 85% complete.

If directional and localized bonding forces locate each Pb atom at sites where the co-ordination by underlying Au atoms is identical, the maximum coverage in the first layer of Pb would be $\theta_{Pb} = 0.5$ on (100) faces of Au and $\theta_{Pb} = 0.33$ on (111) faces (Fig. 92). [Obviously the epitaxial monolayer coverage cannot reach $\theta_{Pb} = 1$, since this would involve a closer packing of Pb atoms than in Pb metal]. Pb atoms electrodeposited on Au (100) at coverages above 0.5 can no longer "touch" Au atoms in the electrode surface, but will lie in a layer further from the Au surface than the previously-deposited Pb atoms, and will all touch at least three or four previously deposited Pb atoms. It is therefore possible that the coverage at which bulk Pb deposition begins ($\theta_{Pb} = 0.52 \pm 0.04$) corresponds to the maximum coverage attainable by Pb atoms having a 1:1 relationship with the Au surface atoms of a polycrystalline Au substrate.

Evidence that noble metal electrodes exhibit predominantly (100) faces in potentiodynamic studies is found in computer simula-

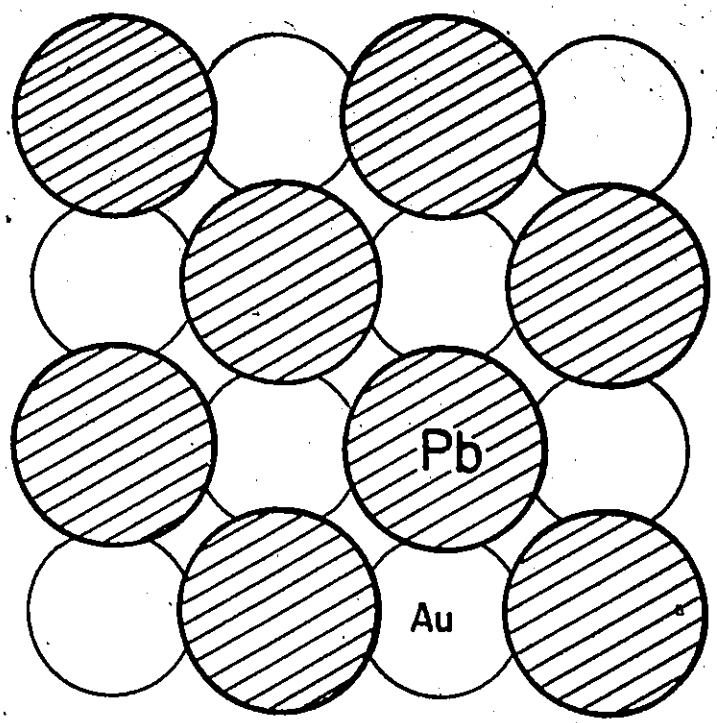

(100) Au

1Pb : 2 Au

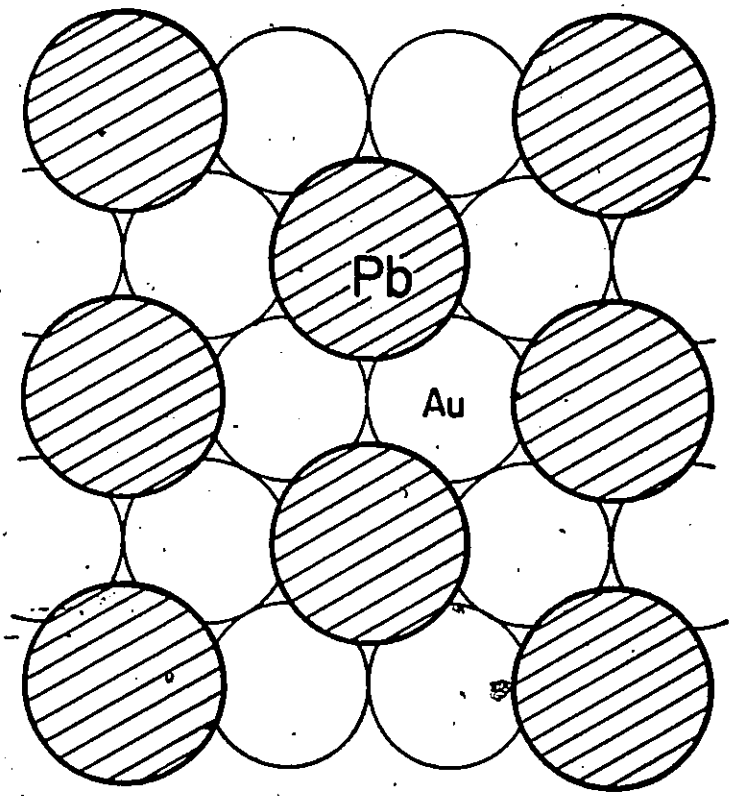

(111) Au

1Pb : 3 Au

FIG 92 SCHEMATIC DIAGRAMS OF Au(100) AND (111) SINGLE-CRYSTAL SURFACES COVERED BY THE MAXIMUM NUMBER OF Pb ATOMS WHICH CAN OCCUPY IDENTICAL Au SURFACE SITES

tions of the current-potential curve for the oxidation of Pt where the ratios of the charges in the component peaks correspond much more closely to those predicted for a (100) surface than those for a (111) surface[221]. In addition, the work of Adžić et al.[423] showed that the total underpotential coverage of Pb decreased with increasing closeness of packing of the Au surface atoms ((110) < (100) < (111)) as would be expected if the Pb deposition were epitaxial.

Takamura, Watanabe and Takamura[426] found that the reflectance of Au electrodes changes discontinuously with the deposition charge as Pb is deposited at underpotential*. The nature of the changes are sensitive to the wavelength of the light used[423], although one discontinuity was generally observed at a point in the current-potential curve between peaks Pb_{C2} and Pb_{C3}, i.e. at a (real) coverage (derived from the present results) of $\theta_{Pb} = 0.13$ (Fig. 3). Takamura et al.[426] related this discontinuity to a supposed limiting coverage of a 1:1 epitaxial monolayer of Pb on Au (100) (which would really occur at $\theta_{Pb} = 0.5$, as discussed above). They concluded that Pb deposited at potentials negative to peaks Pb_{C2} has the dielectric constant of bulk Pb, while lower-coverage surface species have an intermediate dielectric constant because the Pb atoms, although metallically bonded to the Au, are strongly influenced by the properties of the Au. However, a general feature of the present work is the reversibility of UPD in many systems at coverages below about $\theta_{Pb} = 0.1$ to 0.15, whereas deposition at higher coverages may be irreversible due to place-exchange[229] or reconstruction of the deposit/substrate interface, which would relieve repulsive forces between the deposited species at

*McIntyre has recently disputed the existence of any discontinuity in the optical properties of Au during the UPD of Pb[620].

higher coverages. Lateral interactions between Pb atoms could modify the electrical properties of the Pb layer, and thus account for the discontinuity observed by Takamura et al.[426]; however, it is unlikely that they are repulsive in the coverage range 0.15-0.5, as in the case of O species on Pt or Au.

The reflectivity discontinuity may alternatively result from the changes in the double-layer occurring near the p.z.c. of Au (0.24 V[621]). This type of interpretation has recently been proposed for reflectivity changes during the electrodeposition of H on Pt[622] at the potential where specifically adsorbed anions are desorbed.

A different point of view in the interpretation of reflectivity data in this system is offerred by the recent work of Kolb, Leutloff and Przasnyski[623]. Their analysis suggests that reflectivity changes during the deposition of Pb are primarily due to electronic changes in the Au surface itself, rather than showing the optical properties of Au and Pb averaged according to their surface occupancy. These authors concluded that interpretation of reflectivity changes in terms of the nature of the chemisorption bond is at present not generally possible.

If further Pb deposition continues in 1:1 epitaxy on top of the original epitaxial monolayer of Pb atoms, the resulting lattice will not be identical with a Pb metal crystal unless all the mismatch strain between the bulk Au lattice and the bulk Pb lattice may be accomodated in two layers of Pb atoms. Various estimates have been

made of the maximum misfit energy tolerable in epitaxial deposition[624]. The theory of Van der Merwe and Frank[625] shows that, in one dimension, misfit strains of over 9% can only be accomodated with a network of dislocations. The strain energy in the interface increases linearly with the dislocation density, but with the square of the lattice misfit. Unfortunately, a detailed analysis of all the possible epitaxial relationships between bulk Pb and bulk Au will be rather complex and, in any case, little reliable experimental data is available for deposition on single-crystal Au.

Of course, the two-dimensional Pb lattice formed epitaxially might coincidentally approximate to some plane section through a bulk Pb crystal. In this case, further electrodeposition would not thicken the Pb layer uniformly, but would develop close-packed planes of the Pb lattice so as to minimize the surface energy.

10.2.4 Significance of the chemisorption state Pb_5

Adžić, Yeager and Cahan[423] recently suggested that the Pb_5 peak is associated with the completion of electron transfer to previously adsorbed and <u>partially</u> discharged Pb ions. This is based on the electrosorption valence theory of Schultze[386] which was criticized in Section 1.5.1.3.

Figure 84 shows that the Pb coverage up to but not including the Pb_{C5} peak is about $\theta_{Pb} = 0.33$ and that the coverage in the bonding state Pb_{C5} is about $\theta_{Pb} = 0.1$. A simple calculation shows that the mechanism of Adžić et al.[423,626] would predict an average charge of about

+1.0 e on Pb ions adsorbed at potentials positive to peak Pb_5. The consequent electrostatic repulsion between partially ionized adsorbed species would be expected to produce peaks with a much lower aspect-ratio than is observed (e.g. Fig. 83). As already noted, there may be a broad peak underlying peaks Pb_3 - Pb_7, but the coverage in such a state at potentials positive to those of Pb_5 is probably much less than θ_{Pb} = 0.2 (Fig. 83). The present results show that the broad initial peak discussed by Adžić et al.[423], Vicente and Bruckenstein[425] and recently by Takamura, Watanabe and Takamura[426], is in fact the sum of Pb_1 and Pb_2 for which the interaction parameters (g) are probably close to zero, judging by the half-width of the estimated component peaks. It may therefore be concluded that Pb atoms are chemisorbed in a fully-discharged state.

The physical meaning of the <u>increase</u> in chemisorption bond strength with increasing coverage in state Pb_5 (shown by the narrow aspect ratio of the peak) is not at present understood. It might be argued that the fact that deposition in state Pb_5 is less reversible than that in states filled at lower coverage (Fig. 85) suggests that a surface rearrangement is associated with deposition in Pb_5. However, although deposition in state Pb_5 begins at the coverage limit of epitaxial deposition on Au (111) surfaces, the comparative evidence from studies of Pt electrodes suggests that the predominant surface orientation on polycrystalline Au electrodes is that of (100) planes, as mentioned on p. 239.

CHAPTER 11

GENERAL DISCUSSION

11.1 Common features of the electrodeposition systems studied

The previous chapters describe the initial stages of electrodeposition on a bare metal surface in six deposit/substrate systems. A consideration of the features common to the data from all the systems will now be used to build up a general picture of electrodeposition mechanisms. The common features are as follows:

(i) The first species to be discharged (A) bond more strongly* to the substrate (S)

$$A^{\pm} + S \pm e \xrightarrow{\Delta G^{\circ}_{UPD}} A\text{-}S$$

than those discharged later when the deposit begins to behave thermodynamically as bulk A and the bonding occurs as if between A and bulk A**.

$$A^{\pm} + (A_{solid})_n \pm e \xrightarrow{\Delta G^{\circ}_{OPD}} (A_{solid})_{n+1}$$

It follows that in UPD the coverage must always be uniform and not involve any local thickening. OPD, on the other hand, may occur by nucleation and growth. The deposited layer always behaves as bulk A by the time its thickness exceeds one or two atomic layers (see, e.g. references 4,627-631).

---

*The "bond strengths" referred to in this chapter are in fact measured as standard free energies, ΔG°, i.e., the electrode potentials at the current peaks which occur at approximately half coverage in the bonding states concerned.

**See Section 11.6.2 (page 269) for further discussion of this point.

(ii) UPD occurs in a series of bonding states characterized by distinct standard free energies. As the coverage increases, states of successively smaller bonding energy are filled.

(iii) Specifically adsorbed ions restrict UPD in states filled at low coverage. However none of the ions studied reduces the total electrodeposition charge passed at underpotentials.

(iv) The shape of the current-potential profile for UPD appears to depend more on the nature of the substrate than on that of the deposit (e.g. the curve for the UPD of Cu on Au is more like that of Pb on Au than that of Cu on Pt).

(v) The electrochemical act of discharging an $A^{\pm}$ ion at a metal surface is frequently followed by other non-electrochemical reactions, and these can lead to (a) the formation of two-dimensional surface compounds, (b) non-epitaxial deposition, or (c) alloying or intermetallic compound formation.

Detailed consideration will now be given to the origin and significance of the multiple states of bonding observed in UPD. The modification of these states in the presence of other surface species gives additional information about the nature of surface bonding, and a general distinction may be made between Faradaic electrodeposition and specific adsorption. Finally, the information about the nature of the surface reactions obtained as a function of coverage in the six systems studied will be used to construct a general scheme to classify the surface reactions occurring at all stages of Faradaic electrodeposition processes.

11.2 The origin and significance of multiple states of bonding in UPD

The energetically-distinguishable sub-monolayer free energies of deposition observed in the six UPD systems studied are also a general feature of the 77 metal electrodeposition systems for which data is available. [Data in which only one UPD bonding state was detected were generally obtained using unpurified solutions, and may therefore be discounted]. Many examples of multiple submonolayer bonding energies have also been reported in the adsorption of gases on metals (e.g. references 70,76,117,632,633). Five possible causes of the multiplicity of surface bonding states will now be examined:

(1) Intrinsic heterogeneity of substrate due to polycrystallinity

(2) Desorption of anions or other adsorbates

(3) Formation of a series of surface compounds similar to bulk compounds

(4) Repulsive electrostatic interactions between electrodeposited species

(5) Modification of the electronic properties of the substrate associated with UPD, possibly leading to reactive reconstruction of the substrate surface.

11.2.1 Intrinsic heterogeneity of substrate due to polycrystallinity

Any discussion of the origin of multiple states of bonding in UPD must first consider whether the states arise merely from intrinsic heterogeneity of the surface, viz., polycrystallinity with exposure of various principal lattice planes, or from induced heterogeneity arising from effects of previous deposition.

The theory that the multiple bond energies observed in the electrodeposition of H and metal atoms on polycrystalline Pt and Au substrates are related to successive deposition on different crystal faces exposed in the surface[110,381,423] is disproved by the present experiments with single-crystal Pt substrates (Section 5.1.2 and 6.1.2). The same states of bonding found on polycrystalline substrates also appear on carefully characterized homogeneous surfaces. Similar results have been obtained by Bagotskii et al.[248,249], and by Sotto in the oxidation of single-crystal Au[353]. Experiments showing the redistribution of electrodeposited H among bonding states at Pt also lend support to this conclusion. The populations but not the energies of the bonding states of H are changed by specifically adsorbed anions (Section 5.1.6), by changes in the solution pH (Section 5.1.4), and by previously deposited Cu atoms (Section 8.1.7). Since anions and Cu atoms cannot materially change the surface crystallography, the different distributions of bonding states cannot be associated with deposition on surfaces containing different distributions of crystal planes.

11.2.2 Desorption of anions or other adsorbates

The fact that the distribution of underpotentially deposited species among the surface bonding states apparently changes as strongly adsorbing species are added to the solution raises the possibility that the energies relate to the structure of the double-layer at the electrodeposition potentials concerned. Frumkin[82] was the first to propose such a mechanism. In view of the earlier surface potential studies of Mignolet[465], he suggested that the two predominant bonding states of H

(H_{C2} and $H_{C4,5}$) observed in deposition on Pt from acid solutions were associated with two orientations of the Pt-H surface dipoles. More recently Bagotskii[81] and Breiter[106] have suggested that the H_{A3} peak also arises from effects of specifically adsorbed anions. However, while the unusual properties of the H_{A3} peak do relate to some extent to the specific adsorption of anions (Section 5.2.1), the occurrence of multiple bonding states is a general feature of UPD from all types of solutions. In particular, as the concentration of specifically adsorbing ions is reduced, the current-potential profile for UPD becomes independent of the nature of the ions present (Fig. 12). There is no evidence from radiotracer studies of specific adsorption that the surface excess of ions changes discontinuously with changing potential, and changing the ionic concentrations in the solution does not create new bonding states for UPD. It may therefore be concluded that multiple bonding states do not arise from the effects of specifically adsorbed ions.

11.2.3 Formation of a series of surface compounds similar to bulk compounds

11.2.3.1 Oxides

A number of workers studying the oxidation of Pt[166,168,169] and Au[353] have suggested that the different states of bonding observed represent the formation of a series of oxides in which the metal takes up a series of increasing oxidation states. This theory may be ruled out for two reasons, (a) the number of peaks detected in potentiodynamic oxidation is greater than the sum of all chemically reasonable integer states of oxidation, even if surface compounds may have oxidation states

which are not stable in bulk materials; (b) the theory would require the unreasonable assumption that some areas of the surface could be highly oxidized while other areas were unoxidized, since the coverages corresponding to each of the six current peaks detected in potentiodynamic oxidation (e.g. Figs. 49 and 54) are all substantially below a monolayer.

11.2.3.2 Intermetallics

The fact that pairs of metals studied in UPD reactions often form a series of intermetallic compounds with one another in bulk alloys has raised the possibility[372,421,428] that the multiple states of bonding might relate to the formation of a series of surface intermetallics. This theory is, however, disproved by the reasoning applied above to oxides, i.e., the number of peaks is greater than the number of bulk intermetallics (Cu-Pt: 6 peaks, 4 intermetallics; Cu-Au: 5 peaks, 3 intermetallics; Pb-Au: 7 peaks, 2 intermetallics), and the coverage in each peak is substantially less than a monolayer.

11.2.4 Repulsive interactions between electrodeposited species

It has been suggested in Sections 6.2.1 and 7.2.1 that in systems where the electronegativity of the deposited species differs considerably from that of the substrate, dipole-dipole repulsions will tend to maximize the separation of the species from one another, so that deposition will occur in a series of symmetrical superlattice arrays. The component of the electrodeposition energy relating to the dipole-dipole repulsions will vary according to the geometry of the

array being filled, so that the isotherms associated with electrodeposition in successive increments of coverage (successive arrays) will have successively higher g factors[221]. This model gives a good account of the multiple states of bonding observed in the oxidation of Pt and Au (Sections 6.2.1 and 7.2.1), but cannot be applied to the UPD of metals, where the bonding is largely non-polar.

11.2.5 Modification of the electronic properties of the substrate associated with UPD

The theoretical work reviewed in Sections 2.3.2 and 2.3.3 shows that the wave functions calculated for electronic states at a metal surface depend critically on the potential function used to represent the surface. The interfacial fields associated with electrodeposition may be considered as the sum of the double-layer field controlled by the external circuitry and the localized short-range fields arising from the presence of foreign species. Presently available theoretical treatments of chemisorption unfortunately do not show whether the perturbation of the surface states caused by these fields will cause the bonding energy to take up a series of discrete values as the coverage (field) increases. Realistic calculations of bond energies are much too complex to be evaluated rigorously. The mechanisms considered below are thus largely hypothetical at this stage.

11.2.5.1 Localization of surface states for polar bonding

Grimley pointed out a number of years ago[528] that if the surface density of states function is such that the applied substrate/solution

potential-difference only localizes a fraction of an electron at each atom in the surface, the maximum coverage of a species which forms polar bonds can only be a fraction of a monolayer at the potential concerned, because localized surface states are required to form the image charge. If, in addition, surface density-of-states functions at individual surface sites pass through a series of maxima as changes in the electrode potential change the Fermi energy, as in the calculations of Penn for surface sites on W[634], it seems plausible that the successive localization of new surface states with increasing potential could account for the appearance of multiple (polar) bonding states. Such effects would arise in addition to those originating from direct interaction between the electrodeposited species as discussed in 11.2.4 above.

11.2.5.2 Ligand field effects: use of a series of hybrid bonding orbitals

Multiple bonding energies in the chemisorption of H[70,112,113] and O[253,254] on Pt from the gas phase have previously been ascribed to bonding at a succession of different surface sites at which different hybrid bonding orbitals are available. Theoretical bonding energies at different surface sites have been evaluated for a number of chemisorption systems[114-120,127,128,131]. Ligand field theory is used to find the location of possible bonding orbitals, which are generally hybrids of the dangling bonds produced by the splitting of the electronic levels of the metal atoms according to the geometry of the field of the positive ion lattice at the metal surface (Section 2.3.3.2). Present ligand field theories do not, however, predict that the most stable surface

bonding configuration will change discontinuously as the coverage increases, i.e., in such a way as would give rise to multiple states of bonding.

It is possible that ligand field effects would account for multiple states of bonding if (a) local fields arising from the presence of the electrodeposited species cause a secondary splitting of the bonding orbital levels or (b), gradual changes in the energies of the split levels with increasing interfacial field lead to the stabilization of one hybrid bonding orbital over another. Some justification for this last proposal is offered by Kelly's calculations[564] showing that the density of states curve differs at different sites on single-crystal surfaces. However, there is at present insufficient evidence to prove or disprove whether the multiple states of bonding arise from these ligand field effects.

Since the maximum amount of UPD corresponds to less than one monolayer in all the systems studied*, it seems reasonable to expect that if different bonding sites are stabilized in turn by ligand field effects, at any given time all the discharged atoms will be in sites of identical coordination, i.e., that species discharged earlier move (over distances small compared to the lattice spacing) to sites of different coordination similar to those at which discharge is occurring at the coverage concerned.

---

*For discussion of alternative mechanisms involving coverages in excess of an epitaxial monolayer in the Cu on Pt and Pb on Au systems see pp. 215, 243.

11.2.5.3 Formation of surface superlattice arrays because of indirect interactions between deposited species; reactive reconstruction of substrate surface

A number of authors have attempted to evaluate the effects of previously deposited species on the energy of subsequently available bonding sites in terms of the wave mechanics of the surface. Grimley[635,636] has shown that the amplitude of the surface wave functions oscillates with distance from a chemisorbed species. The indirect interaction experienced by another species which is later deposited nearby arises from the perturbation of the bulk states caused by the earlier bonding, and the model may therefore only be applied to deposition systems in which the bonding is partially delocalized*. The indirect interactions[635,636] persist over much greater distances than those over which direct attractions or repulsions between deposited species are significant.

Einstein and Schreiffer[637] found that in the case of a simple cubic tight-binding solid the indirect interactions were about an order of magnitude smaller than the bonding energy at zero coverage. The calculated nearest neighbour interactions were frequently repulsive while the next-nearest, third-nearest and fourth-nearest were attractive.

---

*Although Grimley[546] has suggested that the bonding of foreign atoms at a metal surface will usually be only partially delocalized, the real extent of delocalization in UPD bonds is poorly understood. For example Bowles and Cranshaw[638] concluded from Mössbauer spectroscopy of ^{119}Sn electrodeposited on Pt that the bonding was metallic even at submonolayer coverages. On the other hand, Kolb[639] concluded from differential reflectance spectroscopy that there was substantial polarity in the bonding of Tl atoms electrodeposited on Au. Even in the case of the substitutional solid solution of metal atoms in the lattice of another metal, there is no general agreement on whether the bonding will be delocalized or whether states will "screen" the foreign atom[492,506,507] (p. 91).

Einstein and Schreiffer suggested that such interactions could lead to the formation of the surface superlattice arrays of chemisorbed gas atoms: c(2x2), 2x2 and c(4x2) frequently observed in LEED studies of the chemisorption of gases on (100) surfaces.

These effects of indirect interactions show that the filling of successive surface superlattices during UPD may be a general feature of systems in which the bonding is predominantly metallic as well as those in which it is substantially polar (discussed in case (iv) above). It is at present impossible to calculate whether the modification of the bonding states arising from direct repulsive forces will be more important in determining the spectrum of bonding states than the indirect interactions via the electronic properties of the substrate. The resolution of two peaks (θ_{Cl} and $\theta_{Cl'}$) in the reversible reduction of low oxide coverages at Au might, for example, be interpreted as showing that the effects of indirect interactions may be observed at coverages below those at which repulsive forces alone would be sufficient to cause place-exchange in the surface.

Reactive Reconstruction

Since the bonds formed in UPD are of comparable strength to those between atoms in the substrate surface, it might be expected that the electrodeposition of foreign species could cause slight movements of substrate atoms near the deposition site in order to achieve the most stable bonding configuration. This rearrangement of the substrate surface, known as reactive reconstruction, will clearly depend on the distance of the deposition site from other previously deposited species.

Electron-optical studies of the deposition of H on Pt[123,134,137], O on Pt[137,253,258], O on Au[137], Na on Pt and Au[137], and S on Pt[596] show that the structure of the rearranged substrate surface changes discontinuously with coverage as the deposited species fill successive surface superlattices. The various ordered structures produced by reactive reconstruction have very similar surface free energies[258]. The surface reconstruction involved is a two-dimensional analogue of order-disorder transformations in bulk solids. It may be noted in passing that the fact that current-potential profiles on different crystal faces are relatively similar (Sections 5.1.2 and 6.1.2) is evidence in favour of reactive reconstruction rather than ligand field effects being the cause of the multiple states of bonding. The crystal fields associated with the different principal index planes of the substrates would be quite different from each other, regardless of the coverage of the deposit, whereas the reconstructed surfaces may well be similar.

Comrie and Weinberg have very recently correlated multiple bonding energies in the chemisorption of CO from the gas phase on Ir(111) surfaces with the establishment of new surface structures[633]. This confirms the theory that multiple states may be caused by the successive development of surface superlattice arrays arising from direct or indirect interactions between the deposited species.

11.2.6 Summary

The foregoing discussion proves that the stabilization of new bonding states during UPD is not related to any pre-existing properties of the substrate, but arises directly from the process of deposition,

i.e., from direct or indirect interactions between the deposited species. Although the multiple states may possibly relate to bonding at randomly distributed sites involving a succession of different coordinations by substrate atoms, it seems more likely that UPD will fill a succession of surface superlattice arrays, and that the appearance of each state will signify deposition within a particular array.

11.3 Significance of the similarity of current-potential profiles for UPD of different atoms at a single substrate

Comparisons of the current-potential profiles obtained at Pt and Au in this work in the presence of various dischargeable ions show that the form of the profile depends much more on the nature of the substrate than on the deposit. For example, the profile for Cu deposition at Au is quite different from that at Pt, but rather similar to that of Pb at Au (Fig. 93). A comparison with data from the potentiodynamic profiles for UPD of other elements at Au shows that a composite low-coverage peak of the same general shape as Pb_{1-2} or Cu_{1-4} on Au exists also in the UPD of Tl[411,640], Sb[641], Bi[641] and Sn[642] at Au. Data for the UPD of Ag[411,615] and Cd[643] at Au, although less well resolved, are not dissimilar.

In the same way, the current-potential profile for the UPD of Cu at Pt shows similarities to that for the UPD of H at Pt, if conditions are chosen so that the coverage of specifically adsorbed ions is minimized (viz., UPD of Cu at very slow sweep rates, Fig. 65 and UPD of H in dilute acid, Figs. 12, 21(b). Comparative data for the UPD of other elements which could deposit in an atomic state at Pt are hard to find

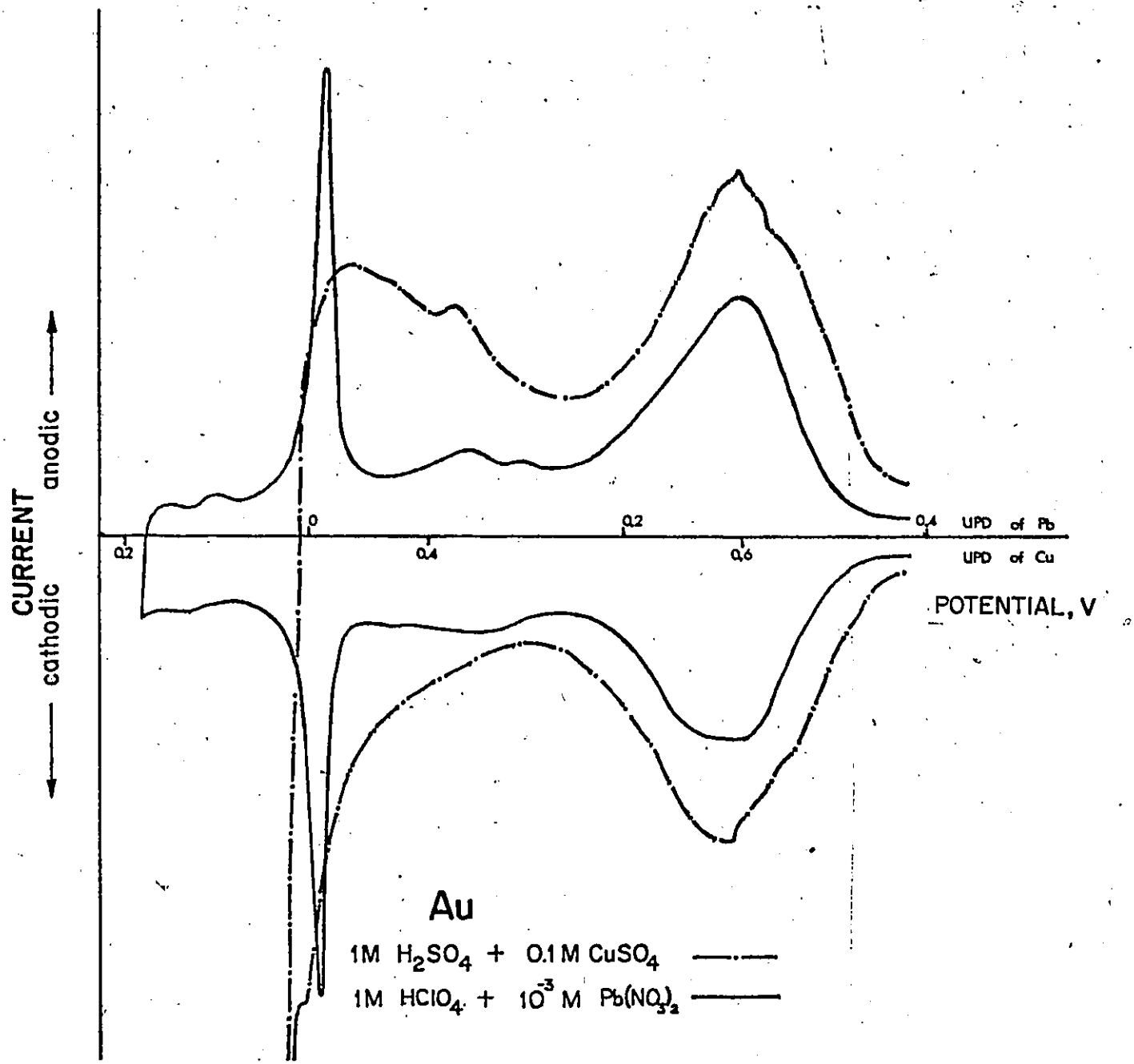

FIG 93 COMPARISON OF CURRENT-POTENTIAL PROFILES FOR THE UPD OF Cu AND Pb AT Au. THE CURVES HAVE BEEN SHIFTED RELATIVE TO ONE ANOTHER ON THE POTENTIAL AXIS. THE POTENTIALS SHOWN ARE AS MEASURED WITH REFERENCE ELECTRODES IN 1 M H_2SO_4 AND 1 M $HClO_4$, RESPECTIVELY

because so few have a range of underpotentials between those for H and O species at Pt.

There is also some evidence from the work of Schmidt and co-workers that current-potential profiles for the UPD of Bi[644], Pb[644], and Tl[644,645] at Ag are similar, and not unlike those at Au.

If these similarities are more than coincidental we may reason as follows. Since the passage of charge as a function of underpotential depends more on the nature of the substrate than the deposit, it may be concluded that the occurrence of surface bonding states at particular energies depends primarily on properties of the substrate. Lowering the substrate/solution potential difference in a cathodic sweep reduces the Fermi energy of the substrate metal, and if UPD does not alter the density-of-surface-states function of the substrate, the surface states associated with the interfacial field will be fully determined by the electrode potential. The surface states are involved directly in the bonding, so it is to be expected that the coverage in the various surface bonding states as well as the energies of the states will be determined primarily by the interfacial field* rather than by the chemical nature of the deposit.

This theory is consistent with an analysis of Kolb et al.[623] who recently showed that reflectance changes occurring during the UPD of Pb at Au were primarily caused by changes in electronic properties of the surface of the Au electrode itself (changes in its complex

*The localization of surface states will be governed not only by the applied surface field, but also by the microscopic local fields arising from polar bonds and place-exchange.

dielectric constant) rather than by superimposed effects related to the properties of the electrodeposited layer.

The changes in the electronic properties of a substrate resulting from UPD may alternatively be described in terms of reactive reconstruction (Section 11.3.5.2), and Somorjai[258] has emphasized that reactive reconstruction effects depend largely on properties of the substrate metal. LEED studies show that reconstructed surfaces bear a greater similarity to the substrate structure than to the bulk structure of the deposited species.

It is important to note that similarity of current-potential profiles for different UPD systems on a given metal is not associated with similarities in the total charge passed in UPD. As discussed in Section 11.2.3, the coverage at which UPD gives way to OPD is thought to relate to combined properties of the pair of reactants involved.

11.4 Modification of UPD states by specific adsorption and by UPD of other species

Even if the origin of multiple bonding states were to be established, there would remain the equally interesting question of how underpotentially deposited species bound in various states react differently to the presence of other species at the substrate surface, as for example in the sensitivity of the H_{A3} state to adsorbed anions (Section 5.1.3) or the properties of Pt oxide states in relation to electro-organic oxidation processes[646]. The present experiments have shown that the presence of other species at a substrate surface on which is occurring affects the UPD bonding in one of two ways, according to

whether the other species are specifically adsorbed ions or electrodeposited atoms.

The UPD systems in which the effects of specifically adsorbed ions were studied are listed in Table 5. Specifically adsorbed ions restrict the availability of surface sites for UPD. As anions desorb, however, an overpotential will arise for UPD in bonding states normally filled at lower potentials. The decreased deposition currents at high underpotentials and increased currents at low underpotentials give the impression that the specifically adsorbed ions change the coverage associated with each bonding state. Since the anions are all desorbed by the time the reversible potential for bulk deposition is reached, the total UPD charge is unaffected, and the final bonding of the underpotentially deposited layer is the same as if the ions had never been present.

TABLE 5

SPECIFICALLY ADSORBED IONS STUDIED IN UPD SYSTEMS

Specifically adsorbed ion	Underpotentially deposited species	Substrate	Section where effects discussed
HSO_4^-	H	Pt	5.1.6,5.2.1
HSO_4^-	O	Pt	6.1.4,6.2.3
HSO_4^-	O	Au	7.1.4,7.2.5
NO_3^-	O	Au	7.1.4,7.2.5
ClO_4^-	O	Pt	6.1.4,6.2.3
Cl^-	Cu	Pt	8.1.6,8.2.5

In certain cases, species previously deposited at underpotential can modify the bonding states available for the subsequent UPD of another species. The critical parameter appears to be relative size of the previously deposited atoms and the substrate atoms. If the previously deposited atoms are larger than those of the substrate, the distribution of energies in the subsequent UPD of H is unaffected, but the maximum UPD charge is reduced[390] in proportion to their coverage and relative cross-sectional area[647]. If the previously deposited atoms are smaller, e.g., Cu on Pt (Section 8.2.6), they change the distribution of energies but do not affect the total UPD charge. It is not possible to say whether this redistribution of energies relates to interactions between the two types of deposited particles of the types discussed in Sections 11.4.4 and 11.4.5 or to the physical unavailability of certain hybrid surface orbitals due to the presence of previously deposited metal atoms.

The UPD bonding states are also modified when cyclic UPD leads to irreversible alloying in the deposition of Cu on Au (Section 9.1.3) and of Hg on Au, probably because the concentration of deposited atoms within the substrate lattice becomes sufficient to modify the bulk properties of the substrate and consequently the properties of the surface.

11.5 The distinction between Faradaic electrodeposition and specific adsorption

11.5.1 The electrical character of chemisorbed species at electrodes

There is considerable confusion in the literature concerning the terminology to be applied to the adsorption of ions in relation to the electrodeposition of atoms or radical intermediates at electrode

surfaces. For example, a recent paper by Lorenz et al.[416] refers to the UPD of metallic monolayers as the "adsorption of ions" while a paper by Vijh[648] describes the specific adsorption of ions as "surface compound formation".

The qualitative difference between specific adsorption of ions and UPD is indicated from the fact that the (pseudo) capacitance associated with UPD is often 5-10 times greater than that of the double-layer. The reflectance behaviour of a layer of underpotentially deposited Cl atoms can also be quite different from that of the double-layer at Hg containing specifically adsorbed Cl^- ions at potentials on the positive side of the p.z.c. but below that for calomel formation.[655]

The general criterion for specific adsorption of an anion at an electrode is whether the surface excess, Γ_-, falls to zero at the p.z.c. in the absence of specific adsorption of a cation. Specifically adsorbed ions are held to the surface by strong electrostatic interactions with their image charges and by electron donor/acceptor interactions, and lie in the inner Helmholtz plane. Faradaic electrodeposition, on the other hand, is defined in terms of the formal equality of the charge on an ion with the number of electrons supplied in discharging it at the substrate surface. Faradaic electrodeposition is normally a continuous process. It is only non-continuous in UPD because the deposition sites are blocked by the deposited atoms themselves.

Gerischer et al.[466,467] recently showed that the strength of bonding (U_{AS}) of underpotentially deposited metals (A) on various substrates (S) is related to the difference of electronegativity between A and S

(Section 2.2.3), as are the bond energies of M-on metals[649]. The electronegativity difference also determines the partial charge on the Faradaically deposited metal atom, as is the case in the electrodeposition of H at various metals.

Examination of the form of resolved i-V profiles provides a sensitive experimental method for establishing whether appreciable residual charge is held by electrodeposited ad-atoms. For example, it is usually possible to analyse the form of the pseudocapacitance peaks in terms of their half-widths and establish if any appreciable positive or negative values of the interaction parameter g is involved (Section 1.2). With the peaks generated in H and metal deposition, g is usually near to zero or even slightly negative, thus indicating that no significant net charge resides on the deposited atoms. Only in the case of OH and O species on Pt is a small positive (repulsive) g factor required[221] to account for the overlapping peaks in the anodic sweep profile indicating a significant polarity in the OH-Pt or O-Pt bond.

Recently, the nature of Faradaically deposited species has been extensively discussed with regard to the extent of charge transfer involved in the deposition process. Conway and Bockris[650,651] examined this question in their microscopic theory of metal deposition processes in relation to the state of charge of metal atoms in bulk metals. More recently Vetter and Schultze published a series of papers[220,382,383] concerned with the degree of charge transfer, γ, arising in surface electrochemical processes. Schultze[386] called γ the "electrosorption valence" (see Section 1.5.1.3) while Frumkin, Damaskin and Petrii[384]

identified this factor with the thermodynamic coefficient $\frac{1}{F}\left(\frac{\partial q_m}{\partial \Gamma}\right)_{E,T}$ familiar in electrocapillary thermodynamics (they called this factor the "formal coefficient of charge transfer"). More particularly, Vetter and Schultze's papers drew attention to the apparent inadequacy of the conventional distinction between specific adsorption and Faradaic electrodeposition, because the species involved in both these processes can cause similar charge distributions at the substrate/deposit interface.

There is no doubt that Faraday's laws are exactly obeyed in OPD processes. However, as Conway and Bockris pointed out some years ago[650,651], this is not inconsistent with the deposited atoms having a partially ionic character at the surface (i.e. polar bonding). With eventual incorporation of the deposited atom in the bulk crystalline electrodeposit, the total average charge passed from the external circuit is ze for each z-valent cation deposited.

The partial charge on a deposited metal atom is exactly balanced by an equal and opposite charge in the metal surface, which originates from the deposit/substrate electronegativity difference and is associated with the formation of surface states under the influence of the interfacial field, as discussed in Chapter 2. Redistribution of charge in the A-S bond does not require the passage of charge in the external circuit except where a change in the polarity of the bond with increasing θ_M causes a change of double-layer capacity. This effect will, however, be small in the deposition of metal atoms since the double-layer capacity will probably not change by more than 10-20% on account of partially polar M-S bonds.

When M atoms are underpotentially deposited on a substrate S differing from M, it is difficult to see how the process can be qualitatively different from the OPD of M on the surface of bulk M. By analogy, a formal charge of z electrons must still be supplied to deposit an M atom from an M^{z+} ion. As was reviewed in Chapter 1, there is in fact quantitative experimental proof that the coefficient of charge transfer is exactly unity in the UPD of H and Cu at Pt and of Pb at Au. Whether the resulting A species, chemisorbed on the metal substrate S, has partial ionic character due to polarity in the chemisorption bond is a different question connected with the chemistry of A and S, and in no way diminishes the formal applicability of Faraday's laws for the microscopic process of electrodeposition.

11.5.2 Relation between chemisorption of ions and atoms, and ligand-metal interaction

A useful basis for considering the relationship between surface compound formation resulting from UPD and specific adsorption of anions seems to be offered by comparing the situation at a metal surface with that in ligand complexation of acceptor metal ions, usually of the transition metals. The analogue of specific adsorption is the complexation of transition metal cations by ions such as I^-, CN^- or Cl^- which occurs without changing their formal oxidation state, e.g.

$$Fe^{3+} + 6\ CN^- \rightarrow Fe(CN)_6^{3-}$$

or

$$Hg^{2+} + 4\ I^- \rightarrow HgI_4^{2-}$$

Nuclear quadrupole resonance studies have shown[652,653] that in other cases, e.g., $GeCl_6^{2-}$, $SnCl_6^{2-}$, there is an appreciable electron shift (about 0.5 e) from the Cl^- ions to the central metal atom (cf. the apparently discharged state of I at Pt[654]). The analogy between specific adsorption and ligand complexation is supported by the similarity of the order of ligand strengths for various ions and the order of specific adsorption bond strengths at Hg, i.e., $F^- < Cl^- < NO_3^- < Br^- < I^- < CN^- < CNS^- \leq SH^-$. In this connection, the chemisorption of Cl^- at Hg is particularly interesting, since there is a transition as the surface charge increases, from specific adsorption without formal charge transfer to stronger bonding with charge transfer, and electroreflectance studies suggest[655] that this change in state occurs quite abruptly.

The analogue of UPD or OPD is the case where complexation also involves oxidation or reduction of the metal atom, e.g.

$$Co(II).6\ H_2O^{2+} + 1/2\ I_2 \rightarrow Co(III)\ 5\ H_2O.I^{2+} + H_2O$$

or

$$Fe(CO)_5 + 2\ NO \rightarrow Fe(II)(CO)_2(NO^+)_2 + 3\ CO$$

It is thus possible to make a useful qualitative distinction between Faradaic electrodeposition and specific adsorption in the same way as between complexation processes involving formal change of valence, and those which merely involve a redistribution of charge between the interacting donor/acceptor species.

11.5.3 Summary of characteristics of different types of surface bonding

In the light of the above discussion, four types of adsorption

at electrode surfaces may be usefully distinguished, as follows:

I. Physical (electrostatic) adsorption

(a) Adsorbed ion retains its full charge.

(b) Surface excess falls to zero at the p.z.c.

(c) Attraction is weak (probably <100 cal mol^{-1}) and purely electrostatic, between the charge on the ion and that in the surface states which forms the classical image charge.

II. Specific adsorption

(a) The surface excess differs from zero at the p.z.c.

(b) Adsorption can be strong (several kcal mol^{-1}).

(c) Ion behaves as a ligand to metal atoms in the surface, but no net Faradaic charge is transferred in the external circuit. The metal-to-specifically-adsorbed-ion bond may be only partially ionic owing to internal redistribution of electrons.

(d) The adsorption bond is probably not localized at the adsorption site*.

III. UPD

(a) The electrodeposition charge passed in the external circuit equals that originally carried by the ions in solution which were deposited.

(b) A surface compound is formed, involving bonds, which are polar if electronegativity differences between the deposit and substrate cause a separation of charge.

---

*If the polar bonding were localized, one would expect the adsorbed ions to form mutually-repelling arrays and thus to show multiple states of adsorption as in the oxidation of Pt and Au (Sections 6.2.1 and 7.2.1). In fact measurements of the double-layer capacitance associated with specific adsorption show no evidence of multiple adsorption energies.

(c) Bonds formed are probably localized at the deposition site*, and are never fully metallic (cf. IV below).

IV. OPD

(a) Continuous electrodeposition currents may be passed at negligibly small overpotentials.

(b) The electrodeposition charge passed in the external circuit equals that originally carried by the ions in solution which were deposited.

(c) The bonding is always fully metallic (in the sense of being indistinguishable from that at the surface of a bulk metal).

The formal distinction between UPD and specific adsorption discussed above involves parameters which are not easily measurable. In practice, however, some empirical experimental characteristics may be used to identify the main features of the surface interaction, as follows:

(i) Specifically adsorbed ions can be displaced by UPD atoms or can be removed by washing. This is not the case with Faradaically deposited atoms, which can be removed only by passage of current.

(ii) The polarity of surface bonds may be estimated from the energy of interaction between the surface species, as represented by the g factor (eqn. (1)). In particular, the half-widths of current peaks obtained in potentiodynamic experiments give a direct measure of the lateral interactions involved, as discussed in Section 1.2 and above.

*The evidence for place-exchange in surface oxidation (Sections 6.2.2 and 7.2.2) suggests that the surface states forming the image charge will be localized at the deposition site, forming a local dipole. The interaction between adjacent dipoles is relieved by place-exchange which is evidenced by the well-known hysteresis in oxidation.

11.6 Classification of the processes involved in Faradaic electrodeposition

In this section it will be shown that a general classification scheme (Table 6) may be developed to include all types of Faradaic electrodeposition processes. The criteria involved in the various branching points of Table 6 will be discussed in turn.

In some systems, e.g. the electrodeposition of H at Au, significant coverage by deposited H only arises when the potential is "over" the reversible potential for bulk A* deposition while the coverage of A is still too small to measure (i.e., <2%). Branch (a) of Table 6 represents the condition of OPD occurring without prior UPD. This may well be a hypothetical condition, however, since it is probable that OPD is always nucleated on some coverage, however small, of underpotentially deposited species.

11.6.1 Epitaxy in UPD

When UPD begins on a bare metal surface, there is no reason to doubt that the electrodeposited species will all occupy identical sites at the substrate surface, i.e., that the UPD will be epitaxial. In cases where the deposited species is smaller than the atoms of the substrate surface (e.g., for H on Pt), epitaxial UPD would normally be expected to continue until the coverage reaches a monolayer in terms of bonding to the substrate surface atoms. If the deposited species are larger, however (e.g. for Pb on Au), the maximum coverage which can

*In this section, as in Section 11.1, A will refer to the deposited atoms and S to the substrate.

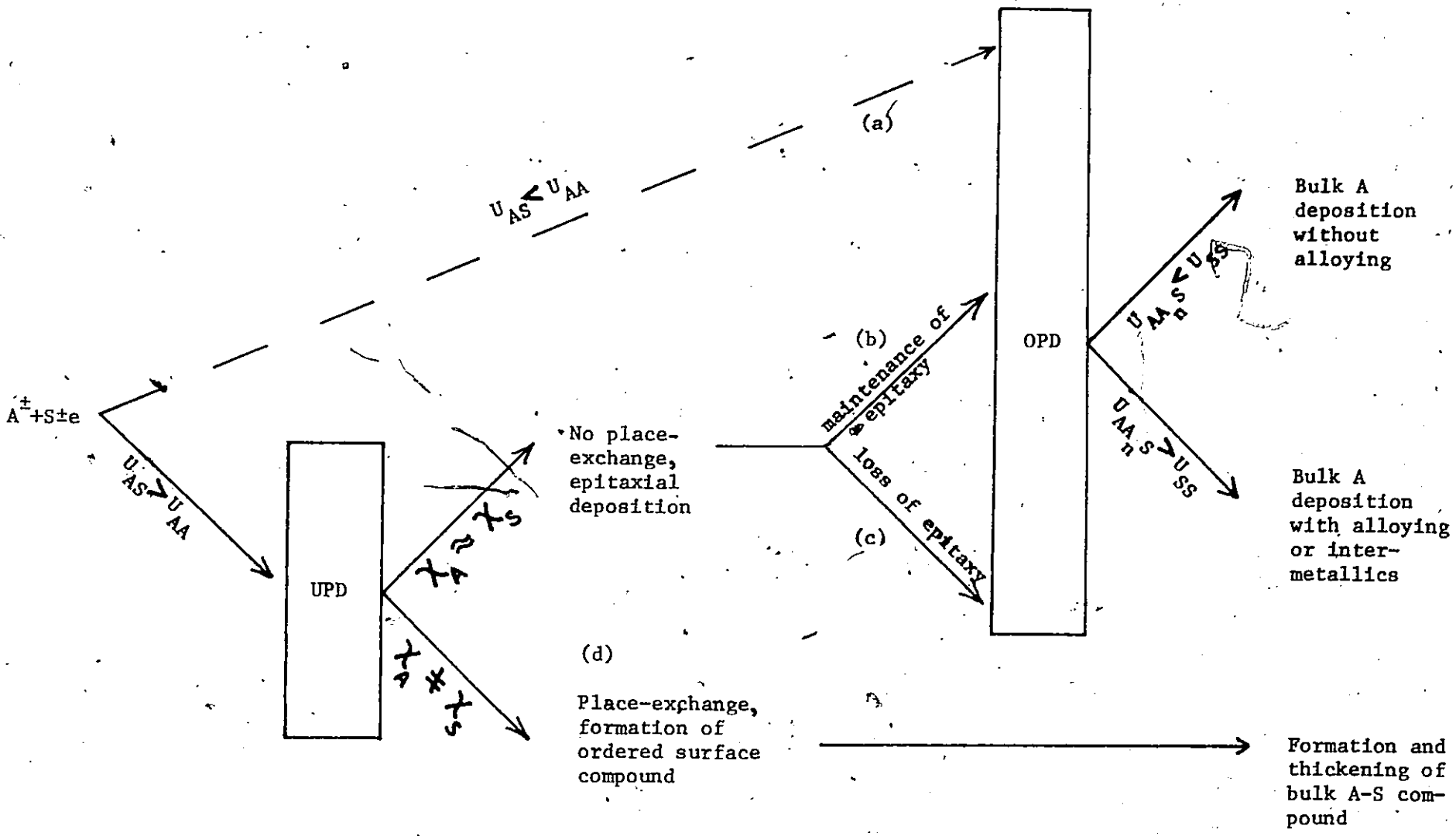

U = Substrate/deposit bond energy

χ = electronegativity

TABLE 6. CLASSIFICATION SCHEME FOR FARADAIC ELECTRODEPOSITION PROCESSES

be deposited epitaxially will be considerably less than a monolayer in terms of bonding to all substrate surface atoms available (Section 10.2.3).

The most reversible electrodeposition reactions studied are those in which the coverage was below the maximum epitaxial limit and place-exchange was absent, i.e., H on Pt, Pb on Au (branch (b) in Table 6). All the other systems involve features which complicate the assessment of reversibility, viz. the slow redox step in Cu deposition (Section 8.2.2) and irreversible place-exchange in the oxidation of Pt and Au (Sections 6.2.1 and 7.2.2).

In the UPD of Cu on Pt, the coverage definitely exceeds that of an epitaxial monolayer before OPD begins. As discussed in Section 8.2.3, this probably involves a progressive loss of epitaxy as the monolayer coverage is passed, and the formation of an non-epitaxial almost planar layer of Cu atoms essentially similar to that in a close-packed plane in bulk Cu, with no unique geometrical relationship between Cu atoms and Pt atoms. The alternative explanation, that Cu atoms deposited at coverages above $\theta_{Cu} = 1$ lie above the undisturbed epitaxially-deposited Cu layer cannot, however, be ruled out (Section 8.2.3).

11.6.2 Significance of the coverage at which OPD begins

The energy required for UPD might be expected to increase significantly as the coverage exceeds the maximum which can be deposited epitaxially in a single layer. The distortion of the previously-deposited layer involved in subsequent non-epitaxial deposition would be expected to cause an abrupt increase in the electrodeposition energy.

Another abrupt increase would be expected in cases where UPD continues by deposition of a second layer on a previously deposited epitaxial or rearranged monolayer. The experimental results, however, show a considerable variation in the maximum UPD coverage according to the nature of the deposit. In some systems, e.g., Cu on Pt, Pb on Au, H on Pt, the onset of OPD is associated with one of the energy discontinuities mentioned above, i.e., the limit of epitaxial coverage or the deposition of a second layer. In others, however, (e.g. Cu on Au, H on Pt at elevated temperatures) OPD begins before the limit of epitaxial coverage in a single layer is reached. Since the coverage at which OPD begins appears to be a cooperative property of the pair of reactants involved, no fundamental significance should be attributed to the maximum coverages measured in UPD. Even the 1:1 maximum coverage of H underpotentially deposited on Pt, for so long used as a measure of the areas of Pt electrodes, appears to be merely a fortunate consequence of the temperature range in which most experiments are conducted, as discussed in Section 5.1.5.

From a general thermodynamic point of view, the coverage at which OPD begins will depend on the standard free energy ΔG° of the process

$$A\text{-}A + 2S \rightleftharpoons^{\Delta G^\circ_{OPD}} 2A\text{-}S$$

(cf. p.244). The free energy of this process is given by

$$\Delta G = \Delta G^\circ + RT \ln \frac{\theta_A}{1-\theta_A} - RT \ln a_{A\text{-}A}^{1/2}$$

and $\Delta G = 0$ when underpotentially deposited A is in thermodynamic equilibrium with bulk A (as A-A in the present example). Strictly, deposition

in multiple states will be represented by multiple equations of this type. Hence, in the absence of kinetic effects, the more negative $\Delta G°$, the larger will be the θ_A at which OPD arises.

11.6.3 Processes following UPD

There is strong evidence that in many systems the underpotentially deposited species do not remain at the surface sites where they were discharged. Electrodeposited A species will tend to mix with surface S atoms in cases where the mixing reaction is exothermic. However, even if the heat of mixing is zero, considerations of entropy will tend to make A species dissolve in the surface. The tendency to mix will be opposed (a) by the coherence of the metal lattice (e.g. an electrodeposited metal will dissolve much more easily in an Hg substrate than in one of a solid metal), and (b) by attractive forces between the electrodeposited species or the local surface compounds they form.

11.6.3.1 Place-exchange - the tendency to form ionically bonded surface phases

In systems where the electronegativity of the deposit (χ_A) differs considerably from that of the substrate χ_S the UPD will follow branch (ii) in Table 6. As was discussed in Sections 6.2.1 and 7.2.2, the bonding of electrodeposited O species on Pt and Au has a polar character. The dipole-dipole repulsions between adjacently-deposited species not only create a tendency for electrodeposition to occur at sites spaced out in geometric arrays, but also tend to assist the exchange of A with substrate surface atoms S:

$$A\text{-}S \rightarrow S\text{-}A$$

The tendency for place-exchange to occur will increase with increases in (a) the interfacial field, (b) the dipole-dipole interaction energy, (c) the stabilization energy associated with the formation of the rearranged A-S surface compound. Place-exchange will be opposed kinetically by the coherence of the substrate. The coverage at which place-exchange becomes measurable will depend on the interplay between these four factors.

The coherence of the new surface phases formed by place-exchange is shown by the fact that their standard free energies of reduction are more negative than those of the electrodeposited species which have not undergone place-exchange, and which are still distinguishable experimentally. The hysteresis observed in the oxidation of noble metals (cf. the typical current-potential profiles at Pt, Fig. 1, and Au, Fig. 49) shows that the place-exchange is normally irreversible, i.e.

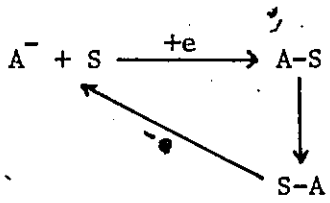

However, if at sufficiently high temperatures kT becomes comparable to the stabilization energy of the rearranged phase, place-exchange will become much more reversible, and the hysteresis will begin to disappear:

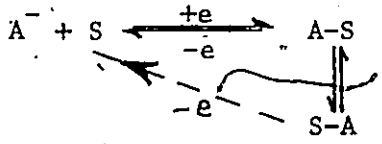

This type of behaviour was observed in the high temperature, cyclic oxidation/reduction of Au (Section 7.1.3, Fig. 52).

No further distinct bonding energies are observed when the coverage exceeds the equivalent of a monolayer of place-exchanged O atoms, and O_2 evolution begins. The continuing electrodeposition under these conditions is not strictly OPD, however, since the substrate is no longer a metal. It may better be regarded in terms of a normal field-assisted film-thickening process (Sections 1.4.1.8 and 1.4.2.8) and the parallel reaction of O_2 evolution, both of which follow the electrodeposition step.

11.6.3.2 Alloying

The dissolution (alloying) of electrodeposited atoms in a substrate surface is normally observed only after OPD. However, it will be discussed briefly at this stage because it was observed in the initial stages of OPD of Cu on Au (Section 9.2.2) and of Pb on Au (Section 10.2.1). The extent of interdiffusion between atoms of the metallic, overpotentially deposited layer, and those of the substrate metal will depend on the enthalpy and entropy of mixing, and will thus be related to the size difference between A and S atoms, and to the coherence of the substrate lattice. When there is a considerable difference between the electronegativities of A and S, ordered intermetallic compounds will be expected to form rather than random substitutional solid solutions (Section 2.3.1.2). Intermetallic compound formation has been observed in the OPD of Pb on Au by Schmidt and co-workers[421,422,428], as discussed in Section 1.6.1.8, in the OPD of Hg on Pt[656] and Au[657], and of Zn on Pt[658].

11.7 The usefulness of electrochemical data in the understanding of surface bonding

Perhaps the most striking conclusion of the present work is that the techniques of modern electrochemistry allow a far more detailed resolution of the energetics of surface bonding than has been achieved in studies of adsorption from the gas phase. Presently available theoretical analyses of surface bonding have been developed with regard to the poorly resolved gas phase adsorption data and do not even provide qualitative explanations of the well resolved multiple states of bonding observed in UPD. It appears unlikely that even semi-quantitative theoretical models of the systems studied will be developed within the next decade since, in addition to all the difficulties of calculating surface bonding states discussed in Chapter 2, the electrical properties of the metal-solution interface are poorly understood on an atomic scale even at single-crystal surfaces. For the present, the main value of electrochemical studies such as the present one is that they provide accurate and relatively well resolved data on the multiple states of bonding involved in chemisorption, how these states depend on the substrate, and how they are modified by the co-adsorption of ions from the solution.

It is to be hoped that accurate thermodynamic and kinetic data obtained electrochemically will in the future be collated with surface structural data obtained in high resolution electron optical equipment[659] (e.g. the positions of individual adatoms[661-663]). Such quantitative data could then be used to test more refined theories.

REFERENCES

1. P. Delahay, "New instrumental methods in electrochemistry", Interscience, N.Y., (1954).
2. W. Nicholson and S. Carlisle, Nicholson's J. (J. Nat. Phil.) 4, 179 (1800).
3. M. Faraday, Phil. Trans., 123, 23 (1833); 124, 77 (1834).
4. A. Oberbeck, Wied. Ann., 31, 337 (1887).
5. F.P. Bowden and E.K. Rideal, Proc. Roy. Soc., A120, 59, 80 (1928).
6. A. Hickling, Trans. Faraday Soc., 38, 27 (1942).
7. A.L. Hodgkin, A.F. Huxley and B. Katz, J. Physiology, 116, 424 (1952).
8. H. Gerischer and K.E. Staubach, Z. Elektrochem., 61, 789 (1957).
9. G.T. Crōft, J. Electrochem. Soc., 106, 278 (1959).
10. M.W. Breiter and F.G. Will, Z. Elektrochem., 61, 1177 (1957).
11. A. Sevčik, Coll. Czech. Chem. Commun., 13, 349 (1948).
12. F.G. Will and C.A. Knorr, Z. Elektrochem., 64, 258 (1960).
13. P. Dolin and B.V. Ershler, Acta Physicochim. U.R.S.S., 13, 747 (1940).
14. P.J. Ligane, Anal. Chem., 39, 485 (1965).
15. R.S. Nicholson, Anal. Chem., 37, 1351,(1965).
16. B.E. Conway and E. Gileadi, Trans. Faraday Soc., 58, 2493 (1962).
17. B.E. Conway, E. Gileadi and M. Dzieciuch, Electrochim. Acta, 8, 143 (1963).
18. R.S. Nicholson and I. Shain, Anal. Chem., 37, 190 (1965).
19. J.M. Hale and R. Greef, Electrochim. Acta, 12, 1409 (1967).

20. P. Stonehart, H.A. Kozlowska and B.E. Conway, Proc. Roy. Soc., A310, 541 (1969).

21. A.J. Appleby, J. Electrochem. Soc., 120, 1205 (1973).

22. A.M. Alquié-Redon, A. Aldaz and C. Lamy, J. Electroanal. Chem., 52, 11 (1974).

23. E. Laviron, J. Electroanal. Chem., 52, 355, 395 (1974).

24. J. Klinger, H. Angerstein-Kozlowska and B.E. Conway, unpublished work (1974).

25. J.N. Pring, Z. Elektrochem, 19, 255 (1913).

26. F.P. Bowden and E.K. Rideal, Proc. Roy. Soc., A120, 59, 80 (1928).

27. M. Knobel, J. Amer. Chem. Soc., 46, 2613 (1924).

28. J.G. Aston, J. Amer. Chem. Soc., 67, 2042 (1963).

29. F.P. Bowden, Nature, 122, 647 (1928).

30. F.P. Bowden, Proc. Roy. Soc., A125, 446 (1929).

31. J.D. Pearson and J.A.V. Butler, Trans. Faraday Soc., 34, 1163 (1938).

32. M.R. Tarasevich, K.A. Radyushkina and R.K. Burshtein, Elektrokhimiya, 3, 455 (1967).

33. S. Gilman, in "Electroanalytical Chemistry", ed. A.J. Bard, 2, 111 (1967), pub. Arnold.

34. T. Biegler, D.A.J. Rand and R. Woods, J. Electroanal. Chem., 29, 269 (1971).

35. R.V. Marvet and O.A. Petrii, Elektrokhimiya, 1, 1225 (1965).

36. I.N. Golyanitskaya, A.A. Sutyagina and G.D. Vovchenko, Russ. J. Phys. Chem., 47, 382 (1973).

37. S. Schuldiner and T.B. Warner, J. Electrochem. Soc., 112, 212 (1965).

38. W. Böld and M.W. Breiter, Z. Elektrochem., 64, 897 (1960).

39. B.I. Podlovchenko and E.A. Kolyadko, Electrokhimiya, 8, 1140 (1972).

40. R. Woods, J. Electroanal. Chem., 49, 217 (1974).

41. J. Honz and L. Nemeč, Coll. Czech. Chem. Commun., 34, 2030 (1969).

42. M.W. Breiter, H. Kammermaier and C.A. Knorr, Z. Elektrochem., 60, 37 (1956).

43. M.W. Breiter in Trans. Symp. on Electrode Processes, ed. E. Yeager, Philadelphia (1959), Wiley, N.Y. (1961).

44. I.M. Kolthoff and N. Tanaka, Anal. Chem., 26, 632 (1954).

45. J. Giner, Z. Elektrochem., 63, 386 (1959).

46. M.W. Breiter, Ann. N.Y. Acad. Sci., 101, 709 (1963).

47. H. Dietz and H. Gohr, Electrochim. Acta, 8, 343 (1963).

48. Z. Kublik, J. Electroanal. Chem., 5, 450 (1963).

49. H. Shimizu, Electrochim. Acta, 13, 27 (1968).

50. S. Trasatti and L. Formaro, J. Electroanal. Chem., 17, 343 (1968).

51. D.E. Icenhower, H.B. Urbach and J.H. Harrison, J. Electrochem. Soc., 117, 1500 (1970).

52. A. Capon and R. Parsons, J. Electroanal. Chem., 39, 275 (1972).

53. S. Iseki, K. Ohasi and S. Nagura, Electrochim. Acta, 17, 2249 (1972).

54. A.A. Sutyagina, I.N. Golyanitskaya, and G.D. Vovchenko, Elektrokhimiya, 8, 908 (1972).

55. S. Schuldiner, M. Rosen and D.R. Flinn, Electrochim. Acta, 18, 19 (1973) and J. Electrochem. Soc., 119, 412 (1972).

56. A.H.W. Aten, P. Bruin and W. DeLange, Rec. Trav. Chim., 46, 417 (1927).

57. M. Volmer and H. Wick, Z. Phys. Chem., A172, 429 (1935).

58. M.W. Breiter, J. Electroanal. Chem., 8, 230 (1964).

59. J.O'M. Bockris, ed., "The electrochemistry of cleaner environments", Plenum, N.Y. (1972).

60. L. Mond, W. Ramsay and J. Shields, Proc. Roy. Soc., 58, 242 (1895).

61. A. Eucken and B. Weblus, Z. Elektrochem, 55, 114 (1951).

62. E. Wicke and B. Weblus, Z. Elektrochem., 56, 169 (1952).

63. A.N. Frumkin and A. Slygin, Acta Physicochimica URSS, 5, 819 (1936).

64. T.C. Franklin and S.L. Cooke, J. Electrochem. Soc., 107, 556 (1960).

65. M.W. Breiter and B. Kennel, Z. Elektrochem., 64, 1180 (1960).

66. R.O. Lenza, W.E. Triaca and A.J. Arvia, J. Electroanal. Chem., 57, 113 (1974).

67. J.C.P. Mignolet, J. Chim. Phys., 54, 19 (1957).

68. W.J.M. Rootsaert, L.L. van Reijen and W.M.H. Sachtler, J. Catal. 1, 416 (1962).

69. R. Lewis and R. Gomer, Surface Sci., 17, 333 (1969).

70. S. Tsuchiya, Y. Amenomiya and R.J. Cvetanovich, J. Catal., 19, 245 (1970).

71. Y. Kubokawa, S. Takashima and O. Toyama, J. Phys. Chem., 68, 1244 (1964).

72. P.R. Norton and P.J. Richards, Surface Sci., 44, 129 (1974).

73. S. Trasatti, J. Chem. Soc., Faraday Trans. I., 68, 229 (1972).

74. T. Loučka and J. Weber, J. Electroanal. Chem., 26, App. 1, (1970).

75. W. Visscher and M. Blijlevens, J. Electroanal. Chem., 47, 363 (1973).

76. L. Schmidt, Cat. Rev.-Sci. Eng., 9, 115, (1974).

77. M.W. Breiter, Electrochim. Acta, 7, 25 (1962).

78. A.N. Frumkin, Z. Phys., 35, 792 (1926).

79. M.W. Breiter, J. Electroanal. Chem., 8, 449 (1964).

80. M. Bonnemay, G. Bronoël and G. Peslerbe, C.R. Acad. Sci. (Paris), 272C, 724 (1971).

81. V.S. Bagotskii, Y.B. Vassiliev and I.I. Pyshnograeva, Electrochim. Acta, 16, 2141 (1971).

82. A.N. Frumkin, N.A. Balashova and V.E. Kazarinov, J. Electrochem. Soc., 113, 1011 (1966).

83. A.N. Frumkin, O.A. Petrii and R. Marvet, J. Electroanal. Chem., 12, 504 (1966).

84. A,N. Frumkin, O.A. Petrii, A. Kossaya, V. Entina and V. Topolev, J. Electroanal. Chem., 16, 175 (1968).

85. A.N. Frumkin, O.A. Petrii and B. Damaskin, J. Electroanal. Chem., 27, 81 (1970).

86. N.A. Balashova and V.E. Kazarinov, Elektrokhimiya, 1, 512 (1965).

87. B.V. Ershler, Acta Physicochim., URSS, 7, 327 (1937).

88. M.W. Breiter, Electrochim. Acta, 8, 925 (1963).

89. V.S. Bagotskii, Y.B. Vassiliev, J. Weber and J.N. Pirtskhalava, J. Electroanal. Chem., 27, 31 (1970).

90. B.I. Podlovchenko, V.F. Stenin and A.N. Frumkin, Elektrokhimiya, 8, 129 (1972).

91. N.A. Balashova and V.E. Kazarinov in "Electroanalytical Chemistry", ed. A.J. Bard, 3, (1969), Dekker, N.Y.

92. R. Notoya, O.A. Petrii, S.Y. Vasina and A.N. Frumkin, Electrokhimiya, 8, 904 (1972).

93. N.A. Balashova, in Katal. Reakts. Zhidk. Faze.Tr. Veses. Konf. 2nd, Alma, Kaz. SSR (1966), published 1967.

94. Z.N. Malysheva, O.A. Petrii, and V.E. Kazarinov, Electrokhimiya, 9, 384 (1973).

95. A. Matsuda and R. Notoya, J. Res. Inst. Catal. Hokkaido Univ. 18, 59 (1970).

96. V.E. Kazarinov, O.A. Petrii and Z.N. Malysheva, Elektrokhimiya, 8, 924 (1972).

97. D.V. Sokolskii and M.N. Anchevskaya, Elektrokhimiya, 9, 723 (1973).

98. A.N. Gilmanov, S.I. Berezina, G.S. Vozdvizhenskii and V.D. Lapshin, Elektrokhimiya, 7, 1336 (1971).

99. O.A. Petrii and Y.G. Kotlov, Elektrokhimiya, 6, 404 (1970).

100. W. Vielstich, Z. Instrumentkende, 71, 29 (1963).

101. V.N. Alexeev, G.N. Zhutaeva, L.L. Knots, B.I. Lentsner, M.R. Tarasevich and N.A. Shumilova, Elektrokhimiya, 1, 373 (1965).

102. N.A. Shumilova, G.V. Zhutaeva, M.R. Tarasevich and R.K. Burshtein, Zh. Fiz. Khim., 39, 1012 (1965).

103. I.A. Harrison and Z.A. Khan, J. Electroanal. Chem., 26, 1 (1970).

104. V.S. Bagotskii and Y.B. Vassiliev, Electrochim. Acta, 11, 1439 (1966).

105. P. Stonehart and G. Kohlmayr, Electrochim. Acta, 17, 369 (1972).

106. M.W. Breiter, "Electrochemical processes in fuel cells", Springer-Verlag, Berlin and N.Y. (1969).

107. T.C. Franklin, M. Naito, T. Itoh and D.H. McLelland, J. Electroanal. Chem., 27, 303 (1970).

108. G. Bronoël and J.C. Pesant, C.R. Acad. Sci. (Paris), 278C, 993 (1974).

109. H. Urtizberea, A.J. Calandra and A.J. Arvia, J. Electroanal. Chem., 55, 145 (1974).

110. F.G. Will, J. Electrochem. Soc., 112, 451 (1965).

111. T. Biegler, Aust. J. Chem., 26, 2571, 2587 (1973).

112. W.A. Pliskin and R.R. Eischens, Z. Phys. Chem., NF24, 11 (1960).

113. M. Primet, J.M. Basset, M.V. Mathieu and M. Prettre, J. Catal. 28, 368 (1973).

114. G.C. Bond, Disc. Faraday Soc., 41, 200 (1966); Platinum Metals Rev., 10, 87 (1966).

115. D. Shopov, A. Andreev and D. Petkov, J. Catal. 13, 123 (1969).

116. G.C. Bond, Surface Sci., 18, 11 (1969).

117. W.H. Weinberg and R.P. Merrill, Surface Sci., 33, 493 (1972).

118. D.J.M. Fassaert, H. Verbeek and A. van der Avoird, Surface Sci., 29, 501 (1972), A. van der Avoird, Surface Sci., 18, 159 (1969).

119. B.I. Podlovchenko and R.P. Petukhova, Electrokhimiya, 8, 899 (1972).

120. A.Y. Gokhstein, Elektrokhimiya, 7, 594 (1971).

121. P.R. Norton and P.J. Richards, Surface Sci., 41, 293 (1974).

122. A.E. Morgan and G.A. Somorjai, Surface Sci., 12, 405 (1968).

123. B. Lang, R.W. Joyner and G.A. Somorjai, Surface Sci., 30, 454 (1972).

124. J.A. Panitz, J. Vac. Sci. Technol., 11, 206 (1974).

125. W.R. Graham and G. Erlich, Surface Sci., 45, 530 (1974).

126. P. Stonehart, Electrochim. Acta, 15, 1853 (1970).

127. T. Toya, J. Res. Inst. Catal., Hokkaido U., 8, 209 (1960).

128. J. Horiuti and T. Toya in "Solid State Surface Science" ed. M. Green, 1, Dekker, N.Y., (1969).

129. A. Slygin and A.N. Frumkin, Acta Physicochimica URSS, 3, 791 (1935).

130. A. Slygin, A.N. Frumkin and V. Medwedowsky, Acta Physicochimica URSS, 4, 911 (1936).

131. I.I. Zakharov , V.V. Pozumentshkov and V.D. Sutula, Kinetika i Kataliz., 14, 694 (1973).

132. A. Bewick and M. Tuxford, Symp. Faraday Soc., 4, 114 (1970); J. Electroanal. Chem., 47, 255 (1973).

133. T. Biegler, J. Electrochem. Soc., 114, 1261 (1967).

134. N. Furuya and S. Motoo, Denki Kagaku, 41, 231 (1973).

135. D. Untereker and S. Bruckenstein, J. Electrochem. Soc., 121, 360 (1974).

136. Y.D. Gamburg, R.P. Petukhova, B.I. Podlovchenko and Y.M. Polukarov, Elektrokhimiya, 10, 751 (1974).

137. E. Bauer in Int. Conf. on "La structure et les propiétés des surfaces des solides", Paris (1969), published 1970.

138. F.G. Will and C.A. Knorr, Z. Elektrochem., 64, 270 (1960).

139. A.Y. Gokhstein, Elektrokhimiya, 9, 285 (1973).

140. M.W. Breiter, Trans. Faraday Soc., 61, 749 (1965).

141. K.A. Radyushkina, R.K. Burshtein, M.R. Tarasevich and V.V. Kuprina, Elektrokhimiya, 6, 234 (1970).

142. R. Woods, Electrochim. Acta, 16, 655 (1971).

143. M. Rosen and S. Schuldiner, Electrochim. Acta, 18, 687 (1973).

144. G. Gruneburg, Electrochim. Acta, 10, 339 (1965).

145. M. Tahlinger and W. Volmer, Z. Phys. Chem., A150, 401 (1930).

146. J.A.V. Butler and G. Armstrong, Proc. Roy. Soc., A137, 604 (1932).

147. L. Jacobs and H.K. Whalley, Proc. Roy. Soc., A135, 192 (1932); A140, 489 (1933).

148. G. Armstrong, E.R. Himsworth and J.A.V. Butler, Proc. Roy. Soc., A143, 89 (1933).

149. J.A.V. Butler and G. Armstrong, J. Chem. Soc., (1934), 743.

150. J.A.V. Butler and G. Drerer, Trans. Faraday Soc., 32, 427 (1936).

151. B.V. Ershler, Doklady Akad. Nauk. S.S.S.R., 37, 226, 230 (1942).

152. B.V. Ershler, Acta Physicochim. U.R.S.S., 19, 139 (1944).

153. K.I. Rozental, P. Dolin and B.V. Ershler, Acta Physicochim U.R.S.S., 21, 213 (1946).

154. B.V. Ershler, Disc. Faraday Soc., 1, 269 (1947).

155. V. Nesterova and A.N. Frumkin, Zh. Fiz. Khim., 26, 1178 (1952).

156. A.D. Obrucheva, Zh. Fiz. Khim., 26, 1448 (1952).

157. K.J. Vetter and D. Berndt, Z. Elektrochem., 62, 378 (1958).

158. W. Böld and M.W. Breiter, Electrochim. Acta, 5, 145 (1961).

159. M.W. Breiter and J.L. Weininger, J. Electrochem. Soc., 109, 1135 (1962).

160. S.W. Feldberg, C.G. Enke and C.E. Bricker, J. Electrochem. Soc., 110, 826 (1963).

161. M.R. Tarasevich and K.A. Radyushkina, Elektrokhimiya, 6, 812 (1970).

162. L.D. Burke and T.O. O'Meara, Electrochim. Acta, 17, 2385 (1972).

163. F.J. Smale, Z. Phys. Chem., 14 577 (1894).

164. R. Ruer, Z. Phys. Chem., 44, 81 (1903); Z. Elektrochem., 9, 235 (1903); 11, 10 (1905); 11, 661 (1905).

165. M.C. Marie, Compt. Rend., 145, 117 (1907).

166. R. Lorentz, Z. Elektrochem., 14, 781 (1908); 15, 661 (1909).

167. G. Grübe, Z. Elektrochem., 16, 621 (1910).

168. R. Lorentz and E. Lauber, Z. Elektrochem., 15, 157, 206 (1910).

169. R. Lorentz and P.E. Spielmann, Z. Elektrochem., 15, 293, 349 (1910).

170. G. Masing and G. Laue, Z. Phys. Chem., A178, 1 (1937).

171. S. Altmann and R.H. Busch, Trans. Faraday Soc., 41, 333 (1945).

172. S.E.S. El Wakkad and S.H. Emara, J. Chem. Soc., (1952), 461.

173. B. Baker and W. MacNevin, J. Amer. Chem. Soc., 75, 1476 (1953).

174. F.C. Anson and J.T. Lingane, J. Amer. Chem. Soc., 79, 4901 (1957).

175. J.K. Lee, R.N. Adams and C.E. Bricker, Anal. Chim. Acta, 17, 321 (1957).

176. H.A. Laitinen and C.G. Enke, J. Electrochem. Soc., 107, 773 (1960).

177. J.S. Mayell and S.H. Langer, J. Electrochem. Soc., 111, 438 (1964).

178. S. Shibata, Bull. Chem. Soc. Japan, 37, 410 (1964).

179. W. Visscher and M.A.V. Devanathan, J. Electroanal. Chem., 8, 127 (1964).

180. L. Wöhler and F. Martin, Z. Elektrochem., 15, 769 (1909); Ber. der Deutch. Chem. Gesellschaft, 42, 3958, 4100 (1909).

181. A. Hickling, Trans. Faraday Soc., 41, 333 (1945).

182. F.P. Bowden, Proc. Roy. Soc., A125, 446 (1929).

183. K. Nagel and H. Dietz, Electrochim. Acta, 4, 1 (1961).

184. S. Shibata, Electrochim. Acta, 17, 395 (1972).

185. J.W. Ross and I. Shain, Anal. Chem., 28, 548 (1956).

186. D. Gilroy and B.E. Conway, Can. J. Chem., 46, 875 (1968).

187. K.G. Weil, J. Electrochem. Soc., 110, 640 (1963).

188. V.I. Lukyanycheva, V.I. Tikhomirova and V.S. Bagotskii, Electrokhimiya, 1, 262 (1955).

189. V.I. Tikhomirova, A.I. Oshe, V.S. Bagotskii and V.I. Lukyanycheva, Doklady Akad. Nauk. S.S.S.R., 159, 644 (1964).

190. A.K.N. Reddy, M.A. Genshaw and J.O'M. Bockris, J. Chem. Phys., 48, 671 (1968).

191. R. Greef, J. Chem. Phys., 51, 3148 (1969).

192. M.W. Breiter, Electrochim. Acta, 7, 601 (1962).

193. H. Wroblova, B. Piersma and J.O'M. Bockris, J. Electroanal. Chem., 6, 401 (1963).

194. C.M. Quinn and M.W. Roberts, Trans. Faraday Soc., 60, 899 (1964).

195. F.P. Bowden and L. Young, Research (London), 3, 235 (1950).

196. M.R. Tarasevich, V.A. Bogdanovskaya and V.S. Vilinskaya, Elektrokhimiya, 8, 89 (1972).

197. T.I. Zalkind and B.V. Ershler, Zh. Fiz. Khim., 25, 565 (1951).

198. A.V. Yuzhanina, V.I. Lukyanycheva, V.S. Bagotskii and N.A. Shumilova, Elektrokhimiya, 10, 630 (1974).

199. J. Horkans, B.D. Cahan and E. Yeager, Surface Sci., 46, 1 (1974).

200. S. Schuldiner and R.M. Roe, J. Electrochem. Soc., 110, 332, 1142 (1963).

201. T.B, Warner and S. Schuldiner, J. Electrochem. Soc., 111, 992 (1964).

202. S. Schuldiner and T.B. Warner, J. Electrochem. Soc., 112, 212 (1965).

203. T.V. Kalish and R.K. Burshtein, Doklady Akad. Nauk. S.S.S.R., 81, 1093 (1951); 88, 863 (1953).

204. A.J. Calandra, N.R. de Tacconi and A.J. Arvia, J. Electroanal. Chem., 49, 145 (1974).

205. R.O. Lenza, W.E. Triaca and A.J. Arvia, J. Electroanal. Chem., 57, 113 (1974).

206. R.V. Marvet and O.A. Petrii, Elektrokhimiya, 1, 1225 (1965).

207. T.P. Hoar, Proc. Roy. Soc., A142, 628 (1933).

208. G.N. Lewis and M. Randall, J. Amer. Chem. Soc., 36, 1969 (1914).

209. F. Haber and F. Fleischmann, Z. Elektrochem., 12, 415 (1906); Z. Anorg. Chem., 51, 245, 289, 356 (1906).

210. D.A.J. Rand and R. Woods, J. Electroanal. Chem., 47, 353 (1973).

211. J.O'M. Bockris and A.K.M.S. Huq, Proc. Roy. Soc., A237, 277 (1956).

212. N. Watanabe and M.A.V. Devanathan, J. Electrochem. Soc., 111, 615 (1964).

213. R.K. Burshtein, M.R. Tarasevich and V.A. Bogdanovskaya, Elektrokhimiya, 8, 1542 (1972).

214. S. Schuldiner, T.B. Warner and B.J. Piersma, J. Electrochem. Soc., 114, 343 (1967).

215. P.R. Nadebaum and T.Z. Fahidy, Electrochim. Acta, 17, 1659 (1972).

216. N. Cabrera and N.F. Mott, Rep. Prog. Phys., 12, 163 (1948-9).

217. K.J. Vetter and J.W. Schultze, J. Electroanal. Chem., 34, 131 (1972).

218. J.L. Ord and F.C. Ho, J. Electrochem. Soc., 118, 46 (1971).

219. M.R. Tarasevich and V.A. Bogdanovskaya, Elektrokhimiya, 7, 1519 (1971).

220. K.J. Vetter and J.W. Schultze, J. Electroanal. Chem., 34, 141 (1972).

221. B.V. Tilak, B.E. Conway and H. Angerstein-Kozlowska, J. Electroanal. Chem., 48, 1 (1973).

222. S. Gilman, Electrochim. Acta, 9, 1025 (1964).

223. S.Y. Elovich and G.M. Zhabrova, Zh. Fiz. Khim., 13,1755, 1761 (1939).

224. M. Temkin, Russ. J. Phys. Chem., 15, 296 (1941).

225. J. Llopis and F. Colum, in Proc. Intern. Comm. on Electrochem., Thermod. and Kinetics, Eighth Meeting, Butterworths, London (1958).

226. J. Giner and E. Lange, Naturwiss, 40, 506 (1953).

227. V.S. Bagotskii and V.I. Veselovskii, Electrochim. Acta, 9, 869 (1964).

228. O.A. Khazova, Y.B. Vasiliev and V.S. Bagotskii, Izv. Akad. Nauk. S.S.S.R. Sr. Khim., 9, 1531, 1778 (1965).

229. H. Angerstein-Kozlowska, B.E. Conway and W.B.A. Sharp, J. Electroanal. Chem., 43, 9 (1973).

230. B.E. Conway and S. Gottesfeld, J.C.S. Faraday Trans., I, 69, 1190 (1973).

231. M.A.H. Lanyon and B.M.W. Trapnell, Proc. Roy. Soc., A227, 387 (1955).

232. N. Sato and M. Cohen, J. Electrochem. Soc., 111, 624 (1964).

233. D.H. Everett and W.I. Whitton, Trans. Faraday Soc., 48, 749 (1952).

234. D.H. Everett and F.W. Smith, Trans. Faraday Soc., 50, 187 (1954).

235. D.H. Everett, Trans. Faraday Soc., 50, 1077 (1954); 51, 1551 (1955).

236. A.N. Frumkin, Phys. Z. Sowjet., 4, 239 (1933).

237. V.E. Kazarinov and N.A. Balashova, Doklady Akad. Nauk. S.S.S.R., 157, 1174 (1964).

238. I.I. Labovskaya, V.I. Lukyanycheva and V.S. Bagotskii, Elektrokhimiya, 5, 580 (1969).

239. S.Y. Vasina and O.A. Petrii, Elektrokhimiya, 6, 242 (1970).

240. G. Horanyi and E.M. Rizmayer, J. Electroanal. Chem., 36, 496 (1972).

241. M.W. Breiter, Electrochim. Acta, 8, 925 (1963).

242. S. Gilman, J. Phys. Chem., 68, 2098 (1964).

243. J. Weber, D. Pirtskhalava, Y.B. Vasiliev and V.S. Bagotskii, Elektrokhimiya, 5, 1037 (1969).

244. Y.M. Tyurin, G.F. Volodin, L.A. Smirnova and Y.V. Battalova, Elektrokhimiya, 9, 532 (1973).

245. B.V. Ershler, G. Deborin and A.N. Frumkin, Bull. Acad. Sci. U.R.S.S., Classe sci. math. nat., Ser. chim. (1937) 1065.

246. S. Gilman, in "Electroanalytical Chemistry" ed. A.J. Bard, 2, 111, Arnold,N.Y. (1967).

247. V.I. Lukyanycheva, A.V. Yuzhanina, B.I. Lentsner, L.L. Knots, N.A. Shumilova and V.S. Bagotskii, Elektrokhimiya, 7, 1287 (1971).

248. I.I. Pyshnograeva, A.M. Skundin, Y.B. Vasiliev and V.S. Bagotskii, Elektrokhimiya, 6, 142, 204 (1970).

249. V.S. Bagotskii, Y.B. Vasiliev and I.I. Pyshnograeva, Electrochim. Acta, 16, 2141 (1971).

250. T. Biegler, J. Electrochem. Soc., 116, 1130 (1969).

251. S. Schuldiner, M. Rosen and D.R. Flinn, J. Electrochem. Soc., 117, 1251 (1970).

252. M.R. Tarasevich and V.S. Vilinskaya, Elektrokhimiya, 7, 710 (1971).

253. C.W. Tucker, J. Appl. Phys., 35, 1897 (1964).

254. C.W. Tucker, J. Appl. Phys., 37, 3013 (1966).

255. J.G. Aston, J. Amer. Chem. Soc., 67, 2042 (1963).

256. R. Lewis and R. Gomer, work cited in reference 137.

257. B. Lang, R.W. Joyner, and G.A. Somorjai, Surface Sci., 30, 454 (1972).

258. G.A. Somorjai, in "Catalysis Reviews" ed. M. Heinemann, 7, Arnold, London (1973).

259. Y.Y. Vinnikov, V.A. Shepelin and V.I. Veselovskii, Elektrokhimiya, 9, 552 (1973).

260. M. Becker and M. Breiter, Z. Elektrochem., 60, 1080 (1956).

261. S. Shibata, Bull. Chem. Soc. Japan, 36, 525 (1963); 37, 410 (1964).

262. S. Gilman, Electrochim. Acta, 9, 1025 (1964).

263. A. Kozawa, J. Electroanal. Chem., 8, 20 (1964).

264. M. Fleichmann, J.R. Mansfield and Lord Wynne-Jones, J. Electroanal. Chem., 10, 511 (1965).

265. J.S. Mayell and S.H. Langer, J. Electrochem. Soc., 113, 385 (1966).

266. B.E. Conway and D. Gilroy, Can. J. Chem., 46, 875 (1968).

267. S.D. James, J. Electrochem. Soc., 116, 1681 (1969).

268. J.W. Schultze, Z. Phys. Chem., NF73, 29 (1970).

269. Y.M. Tyurin and G.F. Volodin, Elektrokhimiya, 6, 1186 (1970).

270. S. Shibata and M.P. Sumino, Electrochim. Acta, 16, 1089, 1511, (1971).

271. V.I. Naumov and Y.M. Tyurin, Elektrokhimiya, 9, 1011 (1973).

272. R.I. Kaganovich, M.A. Gerovich and E.K. Enikeev, Doklady Akad. Nauk. S.S.S.R., 108, 107 (1956).

273. R.I. Kaganovich and Le Min Lap, Zh. Fiz. Khim., 38, 1656 (1964).

274. Y.M. Tyurin and G.F. Volodin, Elektrokhimiya, 5, 1203 (1969).

275. Y.Y. Vinnikov, V.A. Shepelin and V.I. Veselovskii, Elektrokhimiya, 9, 649 (1973).

276. J. Wojtowicz, N. Marincic, and B.E. Conway, J. Chem. Phys., 48, 4333 (1968).

277. J.W. Schultze, Ber. Bunsenges., 73, 483 (1969).

278. L.A. Khanova, E.V. Kasatkin and V.I. Veselovskii, Elektrokhimiya, 10, 800 (1974).

279. K.S. Kim, N. Winograd and R.E. Davis, J. Amer. Chem. Soc., 93, 6396 (1971).

280. W.C. Johnson and L.A. Heldt, J. Electrochem. Soc., 121, 34 (1974).

281. L.A. Khanova, E.V. Kasatkin and V.I. Veselovskii, Elektrokhimiya, 9, 562 (1973).

282. K.I. Rosenthal and V.I. Veselovskii, Dokl. Akad. Nauk. S.S.S.R., 111, 637 (1956).

283. T. Biegler and R. Woods, J. Electroanal. Chem., 20, 73 (1969).

284. T. Biegler, D.A.J. Rand and R. Woods, J. Electroanal. Chem., 29, 269 (1971).

285. R. Parsons and W.M.H. Visscher, J. Electroanal. Chem., 36, 329 (1972).

286. V.E. Kazarinov, Elektrokhimiya, 2, 776 (1970).

287. J. Balej and O. Spalek, Coll. Czech. Chem. Commun., 37, 499 (1972).

288. S. Shibata, Bull. Chem. Soc., Japan, 40, 696 (1969).

289. J.P. Hoare, J. Electrochem. Soc., 116, 612 (1969).

290. W.M.H. Visscher and M. Blijlevens, Electrochim. Acta, 19, 387 (1974).

291. S. Shibata and M.P. Sumino, Electrochim. Acta, 17, 2215 (1972).

292. Y.M. Tyurin, G.I. Afonshin, G.F. Volodin and V.E. Goncharuk, Elektrokhimiya, 6, 1854 (1970).

293. L.A. Khanova, E.V. Kasatkin and V.I. Veselovskii, Elektrokhimiya, 8, 451 (1972).

294. A.N. Frumkin, Electrochim. Acta, 5, 265 (1961).

295. A.A. Yakovleya and V.I. Veselovskii, Elektrokhimiya, 7, 683 (1971).

296. W.W. Lossev, M.A. Dembrovski, A.I. Molodow and W.W. Gorodezk, Electrochim. Acta, 8, 387 (1963).

297. L. Stuchlik, Ber. der Deutch. Chem. Gesellschaft, 37, 2913 (1904).

298. G. Senter, Trans. Faraday Soc., 2, 142 (1906).

299. A.N. Cherndanov, Y.M. Kolotyrkin and M.A. Dembrovskii, Elektrokhimiya, 6, 450 (1970).

300. D.A.J. Rand and R. Woods, J. Electroanal. Chem., 35, 209 (1972).

301. W. de la Rue, Pogg. Ann. (Ann. der Phys.), 46, 439 (1839).

302. M. Margules, Ann. Phys. u. Chem. (Wied. Ann.), 65, 629 (1898).

303. M. Margules, Ann. Phys. u. Chem. (Wied. Ann.), 66, 54 (1898).

304. K. Ohasi, K. Sasaki and S. Nagura, Denki Kagaku, 32, 515 (1964).

305. L. Müller and L. Nekrassov, Electrochim. Acta, 9, 1015 (1964).

306. A.N. Frumkin, E.I. Khruscheva, M.R. Tarasevich and N.A. Shumilova, Elektrokhimiya, 1, 17 (1965).

307. D.C. Johnson, D.T. Napp and S. Bruckenstein, Electrochim. Acta, 15, 1493 (1970).

308. T. Biegler, J. Electrochem. Soc., 114, 1261 (1967).

309. K. Kinoshita, J.T. Lundquist and P. Stonehart, J. Electroanal. Chem., 48, 157 (1973).

310. H.T. Beans and L.P. Hammett, J. Amer. Chem. Soc., 47, 1215 (1925).

311. S. Gilman, J. Phys. Chem., 67, 78 (1963).

312. O.A. Khazova, Y.B. Vasiliev and V.S. Bagotskii, Elektrokhimiya, 1, 439 (1965).

313. S.D. James, J. Electrochem. Soc., 114, 1113 (1967).

314. S. Shibata, Nippon Kagaku Zassi, 79, 239 (1958); 80, 453 (1959).

315. F. Chao, M. Costa and A. Tadjeddine, C.R. Acad. Sci. (Paris), 272C, 821 (1971); 274C, 1613 (1972).

316. W.G. Mixter, J. Amer. Chem. Soc., 33, 688 (1911).

317. F. Jirsa and J. Jelinek, Chem. Listy, 18, 1 (1924); Z. Elektrochem. 30, 286 (1924).

318. F.F. Faizullin and N.P. Nikandrov, Elektrokhimiya, 3, 988 (1967).

319. F.H. Jeffery, Trans. Faraday Soc., 11, 172 (1915).

320. W.B. Pollard, J. Chem. Soc., (1926), 1347.

321. F. Jirsa and O. Buryanek, Chem. Listy, 16, 299 (1922).

322. A. Hickling, Trans. Faraday Soc., 42, 518 (1946).

323. W.J. Shutt and A. Walton, Trans. Faraday Soc., 28, 740 (1932).

324. A. Rundespaden, Ann. der Chemie, 151, 306, 339 (1869).

325. S. Barnartt, J. Electrochem. Soc., 106, 722, 991 (1959).

326. F. Jirsa and O. Buryanek, Z. Elektrochem., 29, 126 (1923).

327. S.E.S. El Wakkad and A.M. Shams El Din, J. Chem. Soc., (1954) 3098.

328. G. Deborin and B. Ershler, Acta Physicochim. U.R.S.S., 13, 347 (1940).

329. G. Schmid and R.N. O'Brien, J. Electrochem. Soc., 111, 832 (1964).

330. H.A. Laitinen and M.S. Chao, J. Electrochem. Soc., 108, 726 (1961).

331. J.P. Hoare, Electrochim. Acta, 9, 1289 (1964).

332. R.H. Gerke and M.D. Rourke, J. Amer. Chem. Soc., 49, 1855 (1927).

333. T.E. Buehrer and W.E. Roseveare, J. Amer. Chem. Soc., 49, 1989 (1927).

334. J.W. Schultze, Electrochim. Acta, 17, 451 (1972).

335. R.S. Sirohi and M.A. Genshaw, J. Electrochem. Soc., 116, 910 (1969).

336. C.M. Ferro, A.J. Calandra and A.J. Arvia, J. Electroanal. Chem., 55, 291 (1974).

337. B.E. Conway, L.H. Laliberté, S. Gottesfeld and H.A. Kozlowska, in Proc. Symp. Oxide-Electrolyte Interfaces, Princeton, U.S.A., Electrochemical Society, N.Y. (1973).

338. A.J. Allmand and V.S. Puri, Trans. Faraday Soc., 21, 1 (1925).

339. J.P. Hoare, J. Electrochem. Soc., 110, 245 (1963).

340. K. Ogura, S. Haruyama and K. Nagasaki, J. Electrochem. Soc., 118, 531 (1971).

341. S.B. Brummer, J. Electrochem. Soc., 112, 633 (1965).

342. M.D. Goldstein, T.S. Zalkind and V.I. Veselovskii, Elektrokhimiya, 8, 606 (1972); 9, 699 (1973).

343. S.B. Brummer and A.C. Makrides, J. Electrochem. Soc., 111, 1122 (1964).

344. W.E. Reid and J. Kruger, Nature, 203, 403 (1964).

345. J.W. Schultze and K.J. Vetter, Ber. Bunsenges., 75, 470 (1971).

346. J. Clavilier and T. Nguyen Van Huong, C.R. Acad. Sci. (Paris), 269C, 736 (1969).

347. K.I. Noninski and E.M. Lazarova, Elektrokhimiya, 9, 673 (1973).

348. J.P. Carr and N.A. Hampson, J. Electrochem. Soc., 119, 325 (1972),

349. A. Hamelin and J.P. Bellier, J. Electroanal. Chem., 41, 179 (1973).

350. F. Chao, M. Costa and A. Tadjeddine, Surface Sci., 46, 265 (1974).

351. J.N. Gaur and G.M. Schmid, J. Electroanal. Chem., 24, 279 (1970).

352. K. Ogaru, S. Haruyama and K. Nagasaki, J. Electrochem. Soc., 118, 531, (1971).

353. M. Sotto, C.R. Acad. Sci. (Paris), 274C, 1776 (1972); 276C, 141 (1973).

354. D. Dickertmann, J.W. Schultze and K.J. Vetter, J. Electroanal. Chem., 55, 429 (1974).

355. A. Hamelin and J. Lecoeur, Coll. Czech. Chem. Commun., 36, 714 (1971).

356. R.A. Bonewitz and G.M. Schmid, J. Electrochem. Soc., 117, 1367 (1970).

357. Y.Y. Vinnikov, V.A. Shepelin and V.I. Veselovskii, Elektrokhimiya, 8, 1229, 1384 (1972).

358. T. Takamura, K. Takamura, W. Nippe and E. Yeager, J. Electrochem. Soc., 117, 626 (1970).

359. Grotthus, (1806),(cited in reference 316).

360. Bunsen, cited in reference 361.

361. J. Spiller, Chem. News, 10, 88 (1866).

362. V. Lehner, J. Amer. Chem. Soc., 26, 550 (1904).

363. S.H. Cadle and S. Bruckenstein, Anal. Chem., 46, 16 (1974).

364. K. Moslavac, B. Lovreček and R. Radeka, Electrochim. Acta, 17, 415 (1972).

365. M.L. Nichols, J. Amer. Chem. Soc., 57, 267 (1935).

366. M. Haissinsky, "Electrochimie des substances radioactives et des substances extremement diluees", Hermann, Paris (1946).

367. L.B. Rogers, Record Chem. Progr., 16, 197 (1955).

368. R.C. Degeiso and L.B. Rogers, J. Electrochem. Soc., 106, 433 (1959).

369. E. Barendrecht in "Electroanalytical Chemistry", ed. A.J. Bard, 2, 53, Dekker, N.Y. (1967).

370. K.Z. Brainina, Talanta, 18, 513 (1971).

371. W.D. Ellis, J. Chem. Educ., 50, A131 (1973).

372. G.W. Tindall and S. Bruckenstein, Anal. Chem., 40, 1051 (1968).

373. T. Yoshida, T. Takeshita and O. Yoshioka, Denki Kagaku, 40, 853 (1972).

374. T. Yoshida, I. Matsuda, S. Nomoto and O. Yoshioka, Denki Kagaku, 41, 603 (1973).

375. B.H. Vassos and H.B. Mark, J. Electroanal. Chem., 13, 1 (1967).

376. M. Stulikova and F. Vydra, J. Electroanal. Chem., 44, 117 (1973).

377. L.N. Nekrasov and N.P. Berezina, Doklady Akad. Nauk. S.S.S.R., 142, 855 (1962).

378. A.R. Nisbet and A.J. Bard, J. Electroanal. Chem., 6, 332 (1963).

379. M.W. Breiter, J. Electrochem. Soc., 114, 1125 (1967).

380. M.W. Breiter, J. Phys. Chem., 68, 2249 (1964).

381. B.J. Bowles, Electrochim. Acta, 15, 589 (1970).

382. K.J. Vetter and J.W. Schultze, Ber. Bunsenges. Phys. Chem., 76, 920, 927 (1972).

383. K.J. Vetter and J.W. Schultze, J. Electroanal. Chem., 44, 63 (1973); 53, 67 (1974).

384. A.N. Frumkin, B. Damaskin and O.A. Petrii, J. Electroanal. Chem., 53, 57 (1974).

385. B.E. Conway, H. Angerstein-Kozlowska and W.B.A. Sharp, J. Electroanal. Chem., accepted for publication (1975).

386. J.W. Schultze, Ber. Bunsenges. Phys. Chem., 74, 705 (1970).

387. S.H. Cadle and S. Bruckenstein, Anal. Chem., 43, 932 (1971).

388. D.T. Napp and S. Bruckenstein, Anal. Chem., 40, 1036 (1968).

389. M.W. Breiter, Trans. Faraday Soc., 65, 2197 (1969).

390. S.H. Cadle and S. Bruckenstein, Anal. Chem., 43, 1858 (1971).

391. G. Horanyi, J. Electroanal. Chem., 55, 45 (1974).

392. J.T. Byrnes and L.B. Rogers, J. Electrochem. Soc., 98, 457 (1951).

393. G.W. Tindall and S. Bruckenstein, Anal. Chem., 40, 1637 (1968).

394. C.T. Horng and R.W. Vook, J. Vac. Sci. Technol., 11, 140 (1974).

395. V.V. Mikhailov, Zh. Fiz. Khim., 28, 1067 (1954).

396. M. LeBlanc and K. Schick, Z. Phys. Chem., 46, 213 (1903).

397. M. Pourbaix, "Thermodynamics of dilute aqueous solutions", Arnold, London (1949).

398. P.J. Hillson, Trans. Faraday Soc., 50, 385 (1954).

399. E. Mattson and J.O'M. Bockris, Trans. Faraday Soc., 55, 1586 (1959).

400. J.O'M. Bockris and M. Enyo, Trans. Faraday Soc., 58, 1187 (1962).

401. J.O'M. Bockris and H. Kita, J. Electrochem. Soc., 109, 928 (1962).

402. U. Bertocci, Electrochim. Acta, 11, 1261 (1966).

403. G. Eichkorn, H. Fischer and H.R. Mache, Ber. Bunsenges. Phys. Chem., 75, 482 (1971).

404. D. Postl, E. Eichkorn and H. Fischer, Z. Phys. Chem. (Frankfurt), 77, 138 (1972).

405. H.C. Albaya and W.J. Lorenz, Z. Phys. Chem. (Frankfurt), 81, 294 (1972).

406. M. Stackelberg and H. Freyhold, Z. Elektrochem., 46, 120 (1940).

407. D.T. Napp, D.C. Johnson and S. Bruckenstein, Anal. Chem., 39, 481 (1967).

408. G.W. Tindall and S. Bruckenstein, Anal. Chem., 40, 1402 (1968).

409. J.W. Bixler and W.F. Stafford, Anal. Chem., 40, 425 (1968).

410. I.C. Raducanu and W.J. Lorenz, Electrochim. Acta, 16, 1143 (1971).

411. W.J. Lorenz, I. Moumtzis and E. Schmidt, J. Electroanal. Chem., 33, 121 (1971).

412. T. Takamura, Y. Sato and K. Takamura, J. Electroanal. Chem., 41, 31 (1973).

413. E. Schmidt, P. Beutler and W.J. Lorenz, Ber. Bunsenges. Phys. Chem., 75, 71 (1971).

414. E. Schmidt and H.R. Gygax, Chimia, 16, 165 (1962); Helv. Chim. Acta, 48, 1178 (1965).

415. W.J. Lorenz, Chem.-Ing.-Tech., 45, 175 (1973).

416. W.J. Lorenz, H.D. Hermann, N. Wüthrich and F. Hilbert, J. Electrochem. Soc., 121, 1167 (1974).

417. H.D. Hermann, Diplomarbeit, Universität Karlsruhe, Germany (1971).

418. A. Coche, Compt. Rend. Acad. Sci. (Paris), 225C, 61 (1947).

419. T. Mills and G.M. Willis, J. Electrochem. Soc., 100, 452 (1953).

420. E. Schmidt, P. Moser and W. Riesen, Helv. Chim. Acta, 46, 2285 (1963).

421. E. Schmidt and H.R. Gygax, J. Electroanal. Chem., 13, 378 (1967).

422. E. Schmidt and N. Wüthrich, J. Electroanal. Chem., 34, 377 (1972).

423. R. Adzic, E. Yeager, and B.D. Cahan, J. Electrochem. Soc., 121, 474 (1974).

424. T. Takamura and M. Sakamoto, J. Electroanal. Chem., 56, 249 (1974).

425. V.A. Vi cente and S. Bruckenstein, Anal. Chem., 45, 2036 (1973).

426. T. Takamura, F. Watanabe and K. Takamura, Electrochimica Acta, 19, 933 (1974).

427. W. Conrad, "Beiträge zum elektrochemischen Verhalten des Bleis", Diss., Universität Göttingen, Germany (1903).

428. E. Schmidt and H.R. Gygax, J. Electroanal. Chem., 14, 126 (1967).

429. J.R. Sams, Prog. Surf. and Membrane Sci., 8, 1, (1974).

430. S. Ross, Prog. Surf. and Membrane Sci., 4, 377 (1971).

431. J.J. Lander and J. Morrison, Surface Sci., 6, 1, (1967).

432. A. Thomy and X. Duval, J. Chim. Phys., 67, 1101 (1970).

433. F. Tsien and G.D. Halsey, J. Phys. Chem., 32, 1279 (1960).

434. T.L. Hill, J. Chem. Phys., 14, 441 (1946).

435. J.H. de Boer, "The dynamic character of adsorption", Oxford University Press, (Clarendon), London, (1953).

436. R.A. Pierotti, Chem. Phys. Lett., 2, 385 (1968).

437. R.A. Pierotti and H.E. Thomas, in "Surface and Colloid Science" ed. F.R. Matijevic, 4, 93, Wiley-Interscience, New York (1971).

438. O. Sinanoglu and K.S. Pitzer, J. Chem. Phys., 32, 1279 (1960).

439. J.E. Lennard-Jones, Trans. Faraday Soc., 28, 333 (1932).

440. S. Ross and J.P. Oliver, "On physical adsorption", Wiley-Interscience, New York (1964).

441. J. Müller, Surface Sci., 42, 525 (1974).

442. R. Smoluchowski, Phys. Rev., 60, 661 (1941).

443. L. Pauling, J. Amer. Chem. Soc., 54, 3570 (1932).

444. D.D. Eley, Disc. Faraday Soc., 8, 34 (1950).

445. J.C.P. Mignolet, Disc. Faraday Soc., 8, 105, 326 (1950).

446. M. Malone, J. Chem. Phys., 1, 197 (1933).

447. A. Clark, "The chemisorptive bond-basic concepts", Academic Press, New York (1974).

448. D.P. Stevenson, J. Chem. Phys., 23, 203 (1955).

449. D.A. Dowden in "Chemisorption", ed. W.E. Garner, Butterworths, London, (1964).

450. G. Erlich, J. Chem. Phys., 34, 39 (1961).

451. P.A. Redhead, Trans. Faraday Soc., 57, 641 (1961).

452. G.C. Bond, "Catalysis by metals", Academic Press, New York (1962).

453. P. Mark, Catal. Revs., 1, 165 (1967); J. Phys. Chem. Solids, 29, 689 (1968).

454. M. Tomasek and J. Koutecky, Int. J. Quantum Chem., 3, 249 (1969).

455. M. Boudart, J. Amer. Chem. Soc., 74, 3556 (1952).

456. J.C. Mignolet, Bull. Soc. Chim. Belg., 64, 126 (1955).

457. I. Higuchi, T. Ree and H. Eyring, J. Amer. Chem. Soc., 77, 4969 (1955); 79, 1330 (1957).

458. T. Ree and N. Murayama, Proc. Imp. Acad. Tokyo, 20, 93 (1944).

459. J.D. Levine and E.P. Gyftopoulos, Surface Sci., 1, 171 (1964).

460. L.D. Schmidt and R. Gomer, J. Chem. Phys., 45, 1605 (1966).

461. H. Utsugi and R. Gomer, J. Chem. Phys., 37, 1720 (1962).

462. M. Scherer and P. Phariseau, Z. Phys., 233, 368 (1970).

463. R.A. Collins and B.H. Blott, J. Appl. Phys., 40, 5390 (1969).

464. P.M. Gundry and F.C. Tomkins, Quart. Revs., 14, 257 (1960).

465. A.U. MacRae, Surface Sci., 1, 319 (1964).

466. H. Gerischer, D.M. Kolb and M. Przasnyski, Surface Sci., 43, 662 (1974).

467. D.M. Kolb, M. Przasnyski and H. Gerischer, J. Electroanal. Chem., 54, 25 (1974).

468. P. Drude, Ann. Phys., 1, 566 (1898); 3, 369 (1900).

469. H.A. Lorentz, "Theory of electrons", Teubner, Leipzig (1906).

470. W. Pauli, Z. Phys., 31, 765 (1925).

471. C.J. Davisson and L.H. Germer, Nature, 119, 558 (1927); Phys. Rev., 30, 705 (1927); Proc. Natl. Acad. Sci., U.S.A., 14, 317, 619 (1928).

472. G.P. Thompson and A. Reid, Nature, 119, 890 (1927).

473. G.P. Thompson, Nature, 120, 802 (1927); Proc. Roy. Soc., A117, 600 (1928).

474. L. de Broglie, Phil. Mag., 47, 446 (1924); Ann. Phys., 3, 22 (1925).

475. S. Sommerfeld, Naturwiss., 15, 824 (1927); 16, 374 (1928); Z. Phys., 47, 1 (1928).

476. F. Bloch, Z. Phys., 52, 555 (1928); 53, 216 (1929); 59, 208 (1930).

477. L. Brillouin, "Quantenstatistik", Springer, Berlin (1931).

478. H. Jones, Proc. Roy. Soc., A144, 225 (1934); A147, 396 (1934); Proc. Phys. Soc. (London), A49, 250 (1937); Phil. Mag., 43, 105 (1952).

479. N.F. Mott and H. Jones, "The theory of the properties of metals and alloys", Oxford University Press, England (1936).

480. W. Hume-Rothery, J. Inst. Metals, 35, 309 (1926).

481. W. Hume-Rothery and G.V. Raynor, "The structure of metals and alloys", 3rd edition, Institute of Metals, London (1954).

482. C. Herring, Phys. Rev., 57, 1169 (1940).

483. L. Landau, Soviet Phys. J.E.T.P., 3, 920 (1956); 5, 101 (1957); 8, 70 (1959).

484. M.H. Cohen and V. Heine, Adv. in Phys., 7, 395 (1958).

485. W.A. Harrison and M.B. Webb, eds, "The Fermi surface", Wiley, New York (1960).

486. A.B. Migdal, Soviet Phys. J.E.T.P., 5, 333 (1957); 7, 96 (1958).

487. E. Daniel and S.H. Vosko, Phys. Rev., 120, 2041 (1960).

488. J.M. Luttinger, in "The Fermi Surface", eds. W.A. Harrison and M.B. Webb, Wiley, New York (1960).

489. J.M. Ziman, "Electrons and Phonons", Clarendon Press, Oxford, England (1960).

490. A.B. Pippard, Phil. Trans. Roy. Soc., A250, 325 (1957).

491. H. Brooks, in "Theory of Alloy Phases", American Society for Metals, Cleveland, Ohio (1956).

492. N.F. Mott, Prog. Met. Phys., 3, 76 (1952).

493. W. Hume-Rothery, G.W. Mabbott and K.M. Channel-Evans, Phil. Trans. Roy. Soc., London, A233, 1 (1934).

494. F.C. Nix and W. Shockley, Revs. Mod. Phys., 10, 1 (1938).

495. H. Lipson, Prog. Met. Phys., 2, 1 (1950).

496. C.S. Barrett and T.B. Massalski, "Structure of Metals", 3rd edn., McGraw-Hill, New York (1966).

497. O. Kubaschewski and J.A. Catterall, "Thermochemical Data of Alloys", Pergamon Press, London (1956).

498. O. Kubaschewski, E.L. Evans and C.B. Alcock, "Metallurgical Thermochemistry", 4th edn., Pergamon Press, London (1967).

499. W. Hume-Rothery, J. Inst. Metals, 35, 309 (1926).

500. S.T. Konobejewski, Ann. Phys., 26, 97 (1936).

501. N.F. Mott, Proc. Phys. Soc., 47, 571 (1935).

502. A. Blandin, in "Alloying behaviour and effects in concentrated solid solutions", ed. T.B. Massalski, Gordon and Breach, New York (1965).

503. R.W. Morse, A. Myers and C.T. Walker, Phys. Rev. Letts., 4, 605 (1960).

504. A.P. Cracknell, "The Fermi Surfaces of Metals", Taylor and Francis, London, (1971).

505. W. Hume-Rothery and D.J. Roaf, Phil. Mag., 6, 55 (1961).

506. J. Freidel, Adv. in Phys., 3, 446 (1954).

507. N.F. Mott, Rep. Prog. Phys., 25, 218 (1962).

508. K. Schubert, in "Symposium on physical chemistry of metallic solutions and intermetallic compounds", Vol. 1, Chemical Publishing Co., New York (1960).

509. W. Hume-Rothery, J. Less-common metals, 7, 152 (1964).

510. P.A. Flinn, Phys. Rev., 104, 350 (1956).

511. J.W. Gadzuk and E.W. Plummer, Revs. Mod. Phys., 45, 487 (1973).

512. T.B. Massalski and H.W. King, Prog. Mats. Sci., 10, 1 (1961).

513. G.V. Raynor, J. Inst. Metals, 71, 553 (1945).

514. K. Schubert, Naturwiss., 39, 159 (1952).

515. E.A. Owen and E.A. O'D. Roberts, J. Inst. Metals, 73, 471 (1947).

516. G.V. Raynor, Prog. Met. Phys., 1, 1 (1949).

517. I. Tamm, Phys. Z. Sowjet, 1, 732 (1932); Z. Phys., 76, 849 (1932).

518. R.H. Fowler, Proc. Roy. Soc., A141, 56 (1933).

519. A.W. Maue, Naturwiss., 38, 648 (1934); Z. Phys., 94, 717 (1935).

520. S. Ryzhanov, Z. Phys., 89, 806 (1934).

521. E.T. Goodwin, Proc. Cambridge Phil. Soc., 35, 205, 221, 232, 245 (1939).

522. S.G. Davison and J.D. Levine, in "Solid State Physics", 25, eds. H. Ehrenreich, F. Seitz and D. Turnbull, Academic Press, New York (1970).

523. C.W. Deutche, Phys. Rev., B7, 1524 (1973).

524. W. Shockley, Phys. Rev., 56, 212,317 (1939).

525. K. Artmann, Z. Phys., 131, 224 (1952).

526. G.E. Smith, in "The Fermi Surface", ed. W.A. Harrison and M.B. Webb, Wiley, New York (1960).

527. J. Koutecky, Phys. Rev., 108, 13 (1957); Adv. Chem. Phys., 9, 85 (1965).

528. T.B. Grimley, Adv. in Catal., 12, 1 (1960).

529. J.R. Smith and J.G. Gay, J. Vac. Sci. Technol., 11, 272 (1974); Phys. Rev. Letts., 32, 774 (1974).

530. D. Kalkenstein and P. Soven, Surface Sci., 26, 85 (1971).

531. P. Mark, Catal. Revs., 1, 165 (1967).

532. R. Haydock, V. Heine, M.J. Kelly and J.B. Pendry, Phys. Rev. Letts., 29, 868 (1972).

533. R. Haydock and M.J. Kelly, Surface Sci., 38, 139 (1973).

534. N.D. Lang, Solid State Phys., 28, 225 (1973).

535. P.M. Marcus, J.F. Janak and A.R. Williams, eds., "Pseudopotentials in the theory of metals", Benjamin, New York (1966).

536. F.F. Volkenstein, Zh. Fiz. Khim., 21, 1317 (1947); 22, 163 (1947); Adv. in Catal., 9, 807 (1957).

537. T.B. Grimley, Proc. Phys. Soc., 72, 103 (1958).

538. S.G. Davison and J. Koutecky, Proc. Phys. Soc., 89, 237 (1966).

539. G. Blyholder and C.A. Coulson, Trans. Faraday Soc., 63, 1782 (1967).

540. C.A. Coulson and G.R. Baldock, Disc. Faraday Soc., 8, 27 (1950).

541. G.R. Baldock, Proc. Cambridge Phil Soc., 48, 457 (1952).

542. T.L. Einstein, Surface Sci., 45, 713 (1974).

543. E.W. Plummer, B.J. Waclawski and T. Vorburger, Surface Sci., (1975), in press, cited in reference 542.

544. J. Koutecky, Trans. Faraday Soc., 54, 1038 (1958).

545. D.R. Olander, J. Phys. Chem. Solids, 32, 2499 (1971).

546. T.B. Grimley, in "Molecular processes on solid surfaces", 3rd Battelle Inst. Mater. Sci. Colloq., E. Drauglis, R.D. Gretz and R.I. Jaffee, eds., McGraw-Hill, New York (1968).

547. R.R. Ford, Adv. in Catal., 21, 51 (1970).

548. G. Blyholder, J. Phys. Chem., 68, 2772 (1964).

549. G. Doyen and G. Ertl, Surface Sci., 43, 197 (1974).

550. D. Brennan and F.H. Hayes, Phil. Trans., A258, 347 (1965).

551. L. Jansen, in "Molecular processes on solid surfaces", 3rd Batelle Inst. Mater. Sci. Colloq., E. Drauglis, R.D. Gretz and R.I. Jaffee, eds., McGraw-Hill, New York (1968).

552. D.A.J. Rand and R. Woods, J. Electroanal. Chem., 36, 57 (1972); 44, 83 (1973); Surface Sci., 41, 611 (1974).

553. E. Greenhalgh, N. Slack and B.M.W. Trapnell, Trans. Faraday Soc., 52, 865 (1956).

554. L. Orgel, "An introduction to transition metal chemistry: ligand field theory", Methuen, London (1960).

555. D.A. Dowden and D. Wells, in "Actes du 2me Congres Int. Catalyse, Editions Technip, Paris (1961).

556. D.A. Dowden, Catal. Revs., 5, 1 (1971).

557. J. Haber and F.S. Stone, Trans. Faraday Soc., 59, 192 (1963).

558. V.A. Shvets and V.B. Kazanskii, J. Catal., 25, 123 (1972).

559. W.R. Trost, Can. J. Chem., 37, 460 (1959).

560. J.B. Goodenough, "Magnetism and the chemical bond", Wiley-Interscience, New York (1963).

561. D.A. Dowden, in "Coloquio sobre quimica fisica de processes en superficies solidas", Libreria Cientifica Medinaceli, Madrid (1965).

562. S. Carra and R. Ugo, Inorg. Chem. Acta Revs., (1967), 49.

563. W.H. Weinberg and R.P. Merrill, Surface Sci., 39, 206 (1973).

564. M.J. Kelly, Surface Sci., 43,587 (1974).

565. T.B. Grimley, in "Chemisorption", ed. W.E. Garner, Butterworths, London (1957).

566. D.M. Newns, Phys. Rev., 178, 1123 (1969).

567. R.V. Culver, J. Pritchard and F.C. Tompkins, in "Proc. 2nd Intern. Congr. on Surface Activity", 2, Butterworths, London (1957).

568. T.B. Grimley, Proc. Phys. Soc., 92, 776 (1967).

569. N.D. Lang and W. Kohn, Phys. Rev., B7, 3541 (1973).

570. N.D. Lang, Phys. Rev., B4, 4234 (1971).

571. A.P. Ovchinnikov and B.M. Tsarev, Soviet Phys. Solid State, 9, 1519 (1968).

572. A.M. Feltham and M. Spiro, Chem. Revs., 71, 177 (1971).

573. B.E. Conway, H. Angerstein-Kozlowska, W.B.A. Shapp and E.E. Criddle, Anal. Chem., 45, 1331 (1973).

574. J.I. Konikoff (to G.E., Schenectady, N.Y., U.S.A.), U.S. Patent 3,127,243 (Cl.23-204), Mar. 31st, 1964; Canadian Patent 675,829 (Cl.202-29), Dec. 10th, 1963.

575. E.E. Criddle, Defence Research Board, Ottawa, private communication (1971).

576. E.K. Rideal and O.H. Wansborough-Jones, Proc. Roy. Soc., A123, 202 (1929).

577. C.B. Alcock and G.W. Hooper, Proc. Roy. Soc., A254, 555 (1960).

578. G.C. Fryburg and H.M. Petrus, J. Electrochem. Soc., 108, 496 (1961).

579. N.P. Berezina and N.V. Nikolaeva-Fedorovich, Elektrokhimiya, 3, 255 (1967).

580. M.Z. Hassan and S. Bruckenstein, Anal. Chem., 46, 1962 (1974).

581. J. Horkans, B.D. Cahan and E. Yeager, Surface Sci., 46, 1 (1974).

582. H. Angerstein-Kozlowska, University of Ottawa, unpublished results (1973).

583. B.E. Conway, Proc. Roy. Soc., A256, 128 (1960).

584. B.E. Conway, H. Angerstein-Kozlowska, F.C. Ho, J. Klinger, B. MacDougall and S. Gottesfeld, Faraday Discs. of the Chem. Soc., 56, 199 (1973).

585. A.A. Michri, A.G. Pshchenichnikov and R.K. Burshtein, Elektrokhimiya, 8, 364 (1972).

586. A.N. Frumkin and O.A. Petrii, Electrochim. Acta, 15, 391 (1970).

587. V.E. Kazarinov and N.A. Balashova, Coll. Czech. Chem. Commun., 30, 4184 (1965).

588. N.A. Balashova, V.E. Kazarinov and M.I. Kulezneva, Elektrokhimiya, 6, 398 (1970).

589. V.E. Kazarinov, O.A. Petrii, V.V. Topolev and A.V. Losev, Elektrokhimiya, 7, 1365 (1971).

590. B. Dandapani, B.E. Conway and H. Angerstein-Kozlowska, University of Ottawa, unpublished work (1973).

591. L. Pauling, "The nature of the chemical bond: an introduction to modern structural chemistry", 3rd Edn., Cornell Univ. Press, (1960).

592. R.T. Sanderson, "Inorganic Chemistry", Van Nostrand-Reinhold, (1967).

593. A. Damjanovic, A.T. Ward and M. O'Jea, J. Electrochem. Soc., 121, 1186 (1974).

594. G. Czartoryska, H. Angerstein-Kozlowska and B.E. Conway, University of Ottawa, unpublished work (1975).

595. A.N. Frumkin, Zh. Fiz. Khim., 34, 391 (1960).

596. R.K. Burshtein, M.R. Tarasevich and V.S. Vilinskaya, "Liquid Phase Catalytic Reactions," p.315, pub. Nauk, Alma-Ata (1967), (in Russian).

597. S.B. Brummer, J. Ford and M.J. Turner, J. Phys. Chem., 69, 3424 (1965).

598. J.W. Schultze and K.J. Vetter, Electrochim. Acta, 18, 889 (1973).

599. C.M. Ferro, A.J. Calandra and A.J. Arvia, J. Electroanal. Chem., 59, 239 (1975).

600. J.W. Gadzuk, Surface Sci., 6, 133, 159 (1967).

601. J.W. Gadzuk, Surface Sci., 43, 44 (1974).

602. J.P. Hoare, J. Phys. Chem., 79, 2175 (1975).

603. A. Damjanovic, A.T. Ward, B. Ulrick and M. O'Jea, J. Electrochem. Soc., 122, 471 (1975).

604. L.B. Harris and A. Damjanovic, J. Electrochem. Soc., 122, 593 (1975).

605. C. Pariset and J.P. Chauvineau, Surface Sci., 47, 543 (1975).

606. N.R. de Tacconi, A.J. Calandra and A.J. Arvia, J. Electroanal. Chem., 57, 325 (1974).

607. S. Schuldiner and T.B. Warner, J. Phys. Chem., 68, 1223 (1964).

608. M. Pourbaix, "Atlas of electrochemical equilibria in aqueous solutions", Pergamon, London (1966).

609. Z. Szlarska-Smialowska and M. Smialowski, Bull. Acad. Polon. Sci., 6, 187, 427 (1958).

610. B. Barnowski and M. Smialowski, Bull. Acad. Polon. Sci., 7, 663 (1959).

611. B. Barnowski and M. Smialowski, Phys. Chem. Solids, 12, 206 (1960).

612. J.M. Blakely, Prog. Mats. Sci., 10, 395 (1963).

613. B.V. Tilak, B.E. Conway and H. Angerstein-Kozlowska, University of Ottawa, unpublished work (1970).

614. A.L. Allred, J. Inorg. Nucl. Chem., 5, 264 (1958); 17, 215 (1961).

615. E. Schmidt and S. Stucki, J. Electroanal.Chem., 39, 63 (1972).

616. B.D. Kutnikov and Y.B. Vassiliev, Elektrokhimiya, 9, 1203, 1845 (1973); 10, 77 (1974).

617. J.M. Otten and W. Visscher, J. Electroanal. Chem., 55, 1, 13 (1974).

618. D.A.J. Rand and R. Woods, J. Electroanal. Chem., 55, 375 (1974)

619. S.H. Cadle and S. Bruckenstein, Anal. Chem., 44, 2225 (1972).

620. J.D.E. McIntyre, Bell Laboratories, Murray Hill, N.J., private communication to H. Angerstein-Kozlowska, University of Ottawa (1975).

621. A. Hamelin and E. Lecoeur, Coll. Czech. Chem. Commun., 36, 714 (1971).

622. F.C. Ho, H. Angerstein-Kozlowska and B.E. Conway, University of Ottawa, unpublished work (1975).

623. D.M. Kolb, D. Leutloff and M. Przasnyski, Surface Sci., 47, 622 (1975).

624. R.D. Gretz in "Vapour Deposition", C.F. Powell, J.H. Oxley and J.M. Blocher, eds., Wiley, N.Y. (1967).

625. J.H. Van der Merwe and F.C. Frank, Proc. Roy. Soc., A198, 205 (1949).

626. J. Horkans, B.D. Cahan and E. Yeager, J. Electrochem. Soc., 122, 1585 (1975).

627. L. Schmidt and R. Gomer, J. Chem. Phys., 42, 3573 (1965).

628. P.W. Palmberg and T.N. Rhodin, Phys. Rev., 161, 586 (1967).

629. R.S. Wagner and R.J.H. Voorhoeve, J. Appl. Phys., 42, 3948 (1971).

630. C.M. Lo and J.B. Hudson, Thin Solid Films, 12, 261 (1972).

631. B.J. Hopkins and G.D. Watts, Surface Sci., 45, 77 (1974).

632. G. Wedler, D. Borgmann and K.P. Geuss, Surface Sci., 47, 592 (1975).

633. C.M. Comrie and W.H. Weinberg, J. Chem. Phys., 64, 250 (1976).

634. D.R. Penn, Surface Sci., 39, 333 (1973).

635. T.B. Grimley, Proc. Phys. Soc., 90, 751 (1967).

636. T.B. Grimley and S.M. Walker, Surface Sci., 14, 395 (1969).

637. T.L. Einstein and J.R. Schreiffer, Phys. Rev., B7, 3629 (1973).

638. B.J. Bowles and T.E. Cranshaw, Phys. Rev. Letts., 17, 258 (1965).

639. D.M. Kolb, Faraday Discs. of the Chem. Soc., 56, 138 (1973).

640. E. Schmidt and H.R. Gygax, J. Electroanal. Chem., 12, 300 (1966).

641. E. Schmidt, H.R. Gygax and Y. Cramer, Helv. Chim. Acta, 53, 649 (1970).

642. V.A. Vicente and S. Bruckenstein, Anal. Chem., 44, 297 (1972).

643. J.W. Schultze, F.D. Koppitz and M.M. Lohrengel, Ber. der Bunsenges., 78, 693 (1974).

644. E. Schmidt and H.R. Gygax, Helv. Chim. Acta, 50, 2058 (1967).

645. E. Schmidt and N. Wüthrich, Helv. Chim. Acta, 49, 1105 (1966).

646. H. Angerstein-Kozlowska, B. MacDougall and B.E. Conway, J. Electrochem. Soc., 120, 756 (1973).

647. B.J. Bowles, Nature, 212, 1456 (1966).

648. A.J. Vijh, J. Phys. Chem., 78, 2240 (1974).

649. S. Trasatti, J. Chem. Soc. Faraday Trans. I. 68, 229 (1972).

650. B.E. Conway and J.O'M. Bockris, Proc. Roy. Soc., A248, 394 (1958).

651. B.E. Conway and J.O'M. Bockris, Electrochim. Acta, 3, 340 (1961).

652. W.A. Welsh, T.B. Brill, P.T. Thompson, R.H. Wood and R.C. Gearhart, Inorg. Chem. 13, 1797 (1974).

653. M. Webster and P.H. Collins, J. Chem. Soc. Dalton Trans. (1973), 588.

654. R.F. Lane and A.T. Hubbard, J. Phys. Chem., 79, 808 (1975).

655. S. Gottesfeld and B.E. Conway, J. Chem. Soc. Faraday Trans. I, 70 1793 (1974).

656. M.Z. Hassan, D.F. Untereker and S. Bruckenstein, J. Electroanal. Chem., 42, 161 (1973).

657. R.W.Andrews, J.H. Larochelle and D.C. Johnson, Anal. Chem., 48, 212 (1976).

658. H.H. Uhlig, J.S. MacNairn, D.A. Vaughn, Acta Met. 3, 302 (1955).

659. M.J. Stowell, Thin Solid Films, 12, 341 (1972).

660. D.W. Bassett and M.J. Parsley, Nature, 221, 1046 (1969).

661. J. Panitz, J. Vac. Sci. Technol., 11, 206 (1974).

662. W. Graham and G. Ehrlich, J. Vac. Sci. Technol., 11, 211 (1974).

663. W. Graham and G. Ehrlich, Surface Sci., 45, 530 (1974).

664. J. O'M. Bockris and B.E. Conway, J. Sci. Instrum., 25, 283 (1948).

665. N. Pentland, J. O'M. Bockris and B.E. Conway, J. Electrochem. Soc., 104, 182 (1957).